

Investigation of Explosion Characteristics of Multiphase Fuel Mixtures with Air

Dissertation
for the award of the degree
Doktoringenieur
(Dr.-Ing.)

By:
M.Sc. Emmanuel Kwasi Addai
Date of birth: 2nd August, 1987
In: Mim-B/A, Ghana

Accepted by the Faculty of Process and Systems Engineering of the Otto-von-Guericke-University of Magdeburg

Graduation Committee:

Prof. Frank Beyrau (Chairman)
Prof. Ulrich Krause (Reviewer)
Prof. Paul Amyotte (Reviewer)
Dr. Michael Beyer (Reviewer)

Submitted on: 11th August, 2016

Graduation Colloquium on: 7th October, 2016

Copyright © 2016
Emmanuel Kwasi Addai

All rights reserved. No part of this book may be reproduced in any form, except for the inclusion of a brief quotation in review, without permission in writing from author/publisher.

ISBN 978-0-9913782-2-7

Published by Western Engineering, Inc., Powell, Wyoming

Printed in the USA by Instantpublisher.com

Acknowledgement

I am very grateful to the almighty God for giving me life, understanding, wisdom, knowledge and the spirit of perseverance to complete this thesis successfully.

The work presented in this thesis would not have been possible without my close association with many people who were always there when I needed them the most. I take this opportunity to acknowledge them and extend my sincere gratitude for helping me make this Ph.D. thesis a possibility.

First of all, I would like thank my mentor, advisor and "doctor father" Prof Ulrich Krause whose support and guidance made my thesis work possible. He has been actively interested in my work and has always been available to advise me. I am very grateful for his patience, motivation, enthusiasm and immense knowledge in the field of fire and explosion prevention and protection. Without his encouragement, support and continuous optimism this thesis would hardly have been completed.

I would also like to thank my second and third supervisors Professor Paul Amyotte (Dalhousie University, Canada) and Dr Michael Beyer (Physikalisch- Technische Bundesanstalt) for guidance and support throughout the course of this research work.

I express my heart-felt gratitude to Dr. Dieter Gabel for his constant motivation and support during the course of my thesis. His conceptual and technical inputs throughout the project have been very fruitful.

My sincere thanks to Mr. Michael Schmidt, Ms. Sabine Schlüsselburg, Ms. Marlies Kupfernagel, Mr. Lutz Herbst and Mr. Thomas Moog for their help in the laboratory work.

I thank my parents Mr. and Mrs. Awuku, who are the kindest and most loving people I know. The unconditional love and inexplicable confidence they have on me remains to be the greatest mystery I ponder upon. They have given me the most valuable property called Education, which can never perish nor be taken away from me.

It is my pleasure to make a special mention of my lovely wife Agnes Fosuah Addai, who has been the woman behind my success and happiness. Her motivation, encouragement, cheerful smile and devoted love have been the greatest source of human inspiration to me.

I am grateful to my siblings especially my brother Mr. Daniel Awuku Twumasi and the wife for their support and encouragement.

I would also like to acknowledge the support of the Dr. Samuel Tulashie, Prof Francis Acquah, Mr. Zaheer Abbas, Mr. Okyere Galahad, Dr. Kristin Hecht, Mrs. Ruth Martey, Mr. Isaac Yeboah, Mr. Lartey Joseph, Mr. Emmanuel Antwi Adjei, Mr. Kwadwo Afreh, Ms. Francisca Yeboah, Mr. Kwaku Brempong, Mr. Jesse Balogun Roberts, Mr. Saquib Siddiqui and Mr. Vitor Gabriel.

I am grateful to German Academic Exchange Service (DAAD) for providing funding for this project. Finally, I would like to appreciate all my friends and well-wishers around the globe whose expertise and resources aided me in producing this work.

Dedicated to

my lovely wife (Agnes Fosuah Addai), my dear parents (Isaac Awuku and Grace Adobah), my dear brother and the wife (Daniel Awuku Twumasi and Margret Darkoa Awuku) and my entire family.

Abstract

Explosion hazards involving mixtures of different states of aggregation continue to occur in facilities where dusts, gases or solvents are handled or processed. In order to prevent or mitigate the risk associated with these mixtures, more knowledge of the explosion behavior of hybrid mixtures is required. The aim of this study is to undertake an extensive investigation on the explosion phenomenon of hybrid mixtures to obtain insight into the driving mechanisms and the explosion features affecting the course of hybrid mixture explosions. This was accomplished by performing an extensive experimental and theoretical investigation on the various explosion parameters such as: minimum ignition temperature, minimum ignition energy, limiting oxygen concentration, lower explosion limits and explosion severity. Mixtures of twenty combustible dusts ranging from food substances, metals, plastics, natural products, fuels and artificial materials; three gases; and six solvents were used to carry out this study. Three different standard equipments: the 20-liter sphere (for testing lower explosion limits, limiting oxygen concentration and explosion severity), the modified Hartmann apparatus (for testing minimum ignition energy) and the modified Godbert–Greenwald (GG) furnace (for testing minimum ignition temperature) were used. The test protocols were in accordance with the European standard procedures for dust testing for each parameter. However, modifications were made on each equipment in order to test the explosion properties of gases, solvents, and hybrid mixtures. The experimental results demonstrated a significant decrease of the minimum ignition temperature, minimum ignition energy and limiting oxygen concentration of gas or solvent and increase in the likelihood of explosion when a small amount of dust, which was either below the minimum explosion concentration or not ignitable by itself, was mixed with gas or solvent and vice versa. For example, methane with minimum ignition temperature of 600 °C decreased to 530 °C when 30 g/m³ of toner dust, which is 50 % below its minimum explosible concentration was, added. A similar explosion behavior was observed for minimum ignition energy and limiting oxygen concentration. Furthermore, it was generally observed that the addition of a non-explosible concentration of flammable gas or spray to a dust-air mixture increases the maximum explosion pressure to some extent and significantly increases the maximum rate of pressure rise of the dust mixture, even

though the added concentrations of gases or vapor are below its lower explosion limit. Finally, it could be said that, one cannot rely on the explosion properties of a single substance to ensure full protection of an equipment or a process if substances with different states of aggregate are present.

Table of Contents

Acknowledgement	V
Dedication	VII
Abstract.....	vi
Table of Content	x
Table of Figures	xvi
List of Tables	xxii
Abbreviation	xxiv
Nomenclature.....	xxiv
Chapter One	1
1 Introduction.....	1
1.1 Thesis outline.....	3
2 Theoretical Background	5
2.1 General overview of explosions	5
2.2 Gas / vapor explosion	6
2.3 Spray explosion.....	7
2.4 Dust explosion	10
2.4.1 Mechanism of dust explosion	11
2.4.2 Prevention and mitigation of dust explosion	14
2.5 Hybrid mixture explosion	15
3 Safety Characteristics	21
3.1 Explosion relevant parameters.....	21
3.2 Lower explosion limit / minimum explosible concentration.....	22
3.2.1 Models to estimate the lower explosion limit of dusts, gases and hybrid mixtures	

3.2.1.1	Models to estimate the minimum explosible concentration (MEC) of dusts	24
3.2.1.1.1	Schönewald Model [98]	24
3.2.1.1.2	Shevchuk et al. Model [99]	24
3.2.1.1.3	Buksowicz and Wolanski Model [100]	25
3.2.1.2	Models to estimate the lower explosion limit (LEL) of Gases	25
3.2.1.2.1	Zabetakis model [26].....	25
3.2.1.2.2	Shebeko et al. model [101]	26
3.2.1.2.3	Spakowski model [102]	26
3.2.1.3	Models to estimate the lower explosion limit of hybrid mixtures.....	27
3.2.1.3.1	Le Chatelier’s model [103]	27
3.2.1.3.2	Bartknecht model [104]	27
3.2.1.3.3	Mannan et al. model [74]	28
3.3	Limiting oxygen concentration	28
3.4	Minimum ignition energy	30
3.5	Minimum ignition temperature.....	32
3.5.1	Mathematical models to estimate the minimum ignition temperature of dusts ...	34
3.5.1.1	Cassel and Liebman model [134].....	35
3.5.1.2	Nagy and Surincik model [135].....	35
3.5.1.3	Mitsui and Tanaka model [136].....	36
3.5.1.4	Mittal and Guha model [137]	36
3.5.1.5	Krishna and Berlad model [138]	36
3.5.1.6	Zhang and Wall model [139]	37
3.6	Explosion severity: maximum overpressure P_{max} and the maximum rate of pressure rise (dP/dt) _{max}	37
4	Material properties and preliminary analysis.....	39

4.1	Dusts	39
4.1.1	Moisture content.....	39
4.1.2	Volatile Content.....	39
4.1.1	Elemental analysis	40
4.1.2	Particle size distribution	40
4.1.3	Heat of combustion	42
4.1.4	Microscopic images.....	42
4.2	Choice and properties of gases and solvents	44
5	Experimental Methods and Procedures	46
5.1	Tests in the 20-liter sphere.....	46
5.1.1	Experimental procedure for single substances.....	49
5.1.1.1	Dusts	49
5.1.1.2	Gases.....	50
5.1.1.3	Vapors.....	50
5.1.1.4	Sprays.....	50
5.1.2	Experimental procedure for two-phase hybrid mixtures	52
5.1.3	Experimental procedure for three-phase hybrid mixtures.....	52
5.2	Explosibility parameters test	52
5.2.1	Lower explosible limit / minimum explosible concentration	52
5.2.2	Limiting oxygen concentration.....	53
5.2.3	Maximum explosion overpressure, (P_{max}) and maximum rate of pressure rise (dP/dt) _{max}	53
5.3	Experimental procedure for testing the MIT and LEL modified Godbert-Greenwald (GG) furnace.....	54
5.3.1	Godbert-Greenwald Furnace	54

5.3.2	Minimum ignition temperature test procedures in the GG-furnace.....	56
5.3.2.1	Experimental procedure for the MIT of a single component.....	56
5.3.2.1.1	Dusts.....	57
5.3.2.1.2	Gases.....	57
5.3.2.1.3	Solvent Vapors.....	57
5.3.2.2	Experimental procedure for the MIT of two-phase hybrid mixture.....	58
5.3.2.3	Experimental procedure for the MIT of three Component hybrid mixtures.....	59
5.3.3	The lower explosible (LEL) and the minimum explosible concentration (MEC) tests in the GG furnace.....	59
5.3.3.1	Experimental procedure for LEL/MEC of single component.....	59
5.3.3.2	Experimental procedure for MEC/LEL of two component hybrid mixture.....	60
5.3.3.3	Experimental procedure for MEC/LEL of three component hybrid mixtures.....	61
5.4	Minimum ignition energy test in the Hartmann apparatus.....	61
5.4.1	Experimental procedure of the minimum ignition energy of dusts.....	63
5.4.2	Experimental procedure of the minimum ignition energy of hybrid mixtures.....	64
6	Results and Discussions.....	65
6.1	Lower explosion limits and minimum explosible concentrations.....	65
6.1.1	Lower explosion limits in the standard 20-liter sphere.....	66
6.1.1.1	Lower explosion limits of single substances.....	66
6.1.1.2	Lower explosion limits of two-phase hybrid mixtures.....	68
6.1.1.3	Lower explosion limits of three-phase hybrid mixtures.....	75
6.1.2	Representation of the lower explosion limits of three-phase hybrid mixtures in ternary phase diagrams.....	77
6.1.3	Lower explosion limits in the Godbert-Greenwald (GG) furnace.....	84
6.1.3.1	Lower explosion limits of single substances.....	85

6.1.3.2	Lower explosion limits of two-phase hybrid mixtures	86
6.1.3.3	Lower explosion limits of three component hybrid mixtures	90
6.1.4	Mathematical models to estimate the lower explosion limits of dusts, gases and hybrid mixtures	94
6.1.4.1	Comparison of single dusts and gases models with experimental results.....	94
6.1.4.2	Comparisons of hybrid mixture models and the experimental results.....	96
6.2	Limiting oxygen concentration	100
6.2.1	Limiting oxygen concentration of single substances	101
6.2.2	Limiting oxygen concentration of hybrid mixtures	104
6.2.3	Models to estimate the limiting oxygen concentration of dust	109
6.2.4	Model to estimate the limiting oxygen concentration of gases	114
6.2.5	Model to estimate the limiting oxygen concentration of hybrid mixtures.....	115
6.3	Minimum ignition energy	120
6.3.1	Minimum ignition energy of single substances	121
6.3.2	Minimum ignition energy of hybrid mixtures	122
6.3.3	Empirical model to estimate the minimum ignition energy	131
6.4	Minimum ignition temperature.....	132
6.4.1	Minimum ignition temperature single substances	133
6.4.2	Minimum ignition temperature of two-phase hybrid mixtures	135
6.4.3	Minimum ignition temperature of three component hybrid mixtures	139
6.4.4	Models to predict the minimum ignition temperature of dusts.....	144
6.4.4.1	Proposed model to estimate the minimum ignition temperature of hybrid mixtures	145
6.5	Explosion severity	152
6.5.1	Explosion severity of single substances	153

6.5.2	Explosion severity of two-phase hybrid mixtures.....	156
6.5.3	Explosion severity for three-phase hybrid mixtures.....	163
7	Conclusion and Recommendations.....	167
7.1	Conclusion.....	167
7.2	Recommendations.....	172
8	Appendixes.....	188
8.1	A. Detail process diagram for test in the GG furnace.....	188
8.2	Appendix B: Test results.....	193
	B Experimental results for dust and gas hybrid mixtures.....	193
	B: Experimental results for dust and spray hybrid mixture.....	195
	B.3 Experimental results for gas and spray hybrid mixture.....	200
	B.4 Three-phase hybrid mixtures test results.....	205
	B.5 Comparisons between hybrid mixture models and the experimental results.....	212
	B.6 Diagrams to estimate Limiting oxygen concentration of dusts and hybrid mixtures.....	216
8.3	Appendixes C Error and uncertainty analyses.....	220
	C.1 Error and uncertainty analyses in the 20-liters sphere.....	220
	C.2 Uncertainty and error analysis for the minimum ignition energy test for hybrid mixtures in the Hartmann apparatus.....	221
	C.3: Uncertainty and error analysis for both the minimum ignition temperature of hybrid mixture and single dust test.....	224
8.4	Appendixes D: derivation of equations.....	226

List of Figures

Figure 2.1: Relationships between the different types of explosions.	6
Figure 2.2: Understanding of atomization [37].	8
Figure 2.3: Dust explosion pentagon[22].	10
Figure 2.4: Comparison of TG-DTG traces between sweet potato powders and Magnesium dust in N ₂ and air atmosphere [59].	13
Figure 2.5: Schematic representation of the paths occurring during dust explosion [61].	13
Figure 3.1: Safety characteristics.	21
Figure 3.2: Influence of inert gas on the explosion limits of methane [26].	29
Figure 3.3: Temperature influence on the limiting oxygen concentration of different dusts [112].	30
Figure 3.4: Dust explosibility characteristics: effect of particle size on some principal parameters for atomized aluminium [121]. (1) minimum ignition energy; (2) minimum explosive concentration; (3) maximum explosion pressure; and (4) maximum rate of pressure rise.	32
Figure 3.5: The MIT of hydrocarbon-air mixtures as a function of the average carbon chain length [26].	34
Figure 4.1: Particle size distributions of the dust samples.	41
Figure 4.2: Particle size distributions of the dust samples.	41
Figure 4.3: SEM images of dusts.	43
Figure 5.1: Technical diagram of the 20-liter sphere apparatus.	47
Figure 5.2: (A) spray system, (B) spray control system, (C) timer (D) nozzle.	47
Figure 5.3: Experimental arrangement of the 20-liter sphere.	48
Figure 5.4: (A) electrical ignition assembly (B) chemical ignition assembly.	49
Figure 5.5: High speed photographs of the nozzle spray pattern with time.	51
Figure 5.6: Dimensions of the spray.	51
Figure 5.7: Pressure/time-diagram of a fuel explosion.	54
Figure 5.8: Schematic sketch of Godbert-Greenwald furnace.	55
Figure 5.9: A photo of the Godbert-Greenwald furnace experimental setup.	56

Figure 5.10: A representation of how the MIT of both single dust, gas and hybrid mixtures were obtained.	58
Figure 5.11: A photo of the Hartmann apparatus experimental set-up.	62
Figure 5.12: Technical diagram of the Hartmann apparatus.....	62
Figure 5.13: The development of an explosion in the Hartmann apparatus.	63
Figure 6.1: Lower explosion limits of solvents as spray.....	67
Figure 6.2: Maximum explosion pressure and rate of pressure rise of a mixture of methane and lycopodium in dependence on the lycopodium concentration.	69
Figure 6.3: Maximum explosion pressure and rate of pressure rise of a mixture of methane and brown coal in dependence on the brown coal concentration.	69
Figure 6.4: Maximum explosion pressure and rate of pressure rise of a mixture of ethanol spray and lycopodium in dependence on the lycopodium concentration.	70
Figure 6.5: Maximum explosion pressure and rate of pressure rise of a mixture of ethanol spray and brown coal in dependence on the brown coal concentration.	71
Figure 6.6: Maximum explosion pressure and rate of pressure rise of a mixture of methane and isopropanol spray in dependence on the isopropanol concentration.	74
Figure 6.7: Maximum explosion pressure and rate of pressure rise of a mixture of hydrogen and isopropanol spray in dependence on the isopropanol concentration.	74
Figure 6.8: Maximum explosion pressure and rate of pressure rise of mixtures of lycopodium, methane and 50 g/m ³ of isopropanol spray in dependence on lycopodium concentration.....	75
Figure 6.9: Maximum explosion pressure and rate of pressure rise of mixtures of brown coal, methane and 50 g/m ³ of isopropanol spray in dependence on the dust concentration.	76
Figure 6.10: A representation on how to obtain each point from the diagram.....	78
Figure 6.11: Ternary phase diagram for the lower explosion limits of mixtures of lycopodium, methane and ethanol.....	79
Figure 6.12: Ternary phase diagram for the lower explosion limits of mixtures of lycopodium, methane and isopropanol.	79
Figure 6.13: Ternary phase diagram for the lower explosion limits of mixtures of brown coal, methane and ethanol.....	80
Figure 6.14: Ternary phase diagram for the lower explosion limits of mixtures of brown coal,	

methane and isopropanol.	81
Figure 6.15: Ternary phase diagram for the lower explosion limits of mixtures of brown coal, hydrogen and ethanol.	82
Figure 6.16: Ternary phase diagram for the lower explosion limits of mixtures of brown coal, hydrogen and isopropanol.	82
Figure 6.17: Ternary phase diagram for the lower explosion limits of mixtures of lycopodium, hydrogen and isopropanol.	83
Figure 6.18: Ternary phase diagram for the lower explosion limits of mixtures of lycopodium, hydrogen and ethanol.	83
Figure 6.19: LEL of two-phase hybrid mixture of dusts and gases or solvent- vapor (effect of admixture of dust on the LEL of gas).....	87
Figure 6.20: MEC of two-phase hybrid mixture of dusts and gases or solvents- vapor (effect of admixture of gas on the MEC of dust).....	88
Figure 6.21: LEL of hybrid mixture of solvents and gases (effect of admixture of solvent on the LEL of gas).	89
Figure 6.22: LEL of hybrid mixture of solvents and gases (effect of admixture of gas on the LEL of solvent).....	90
Figure 6.23: Comparison between experimental results for the MEC of dusts and the three models.	95
Figure 6.24: Comparison between experimental results for LEL of gases and solvents for the three models.	95
Figure 6.25: Diagram showing a comparison between experimental results and three models: (A) brown coal-methane, (B) lycopodium-methane, (C) brown coal-hydrogen, (D) lycopodium-hydrogen.....	97
Figure 6.26: Diagram showing a comparison between experimental results and three models: (A) lycopodium-isopropanol, (B) lycopodium-ethanol, (C) brown coal-isopropanol, (D) brown coal-ethanol.	98
Figure 6.27: Diagram showing a comparison between experimental results and three models: (A) methane-isopropanol, (B) methane-ethanol, (C) hydrogen-isopropanol, (D) hydrogen-ethanol.	99
Figure 6.28: Limiting oxygen concentration of dusts with different ignition energies.	102

Figure 6.29: Limiting oxygen concentration of gases with different ignition energies.104

Figure 6.30: Limiting oxygen concentration of hybrid mixtures of isopropanol spray and dusts with different ignition energies.105

Figure 6.31: Limiting oxygen concentration of hybrid mixtures of acetone (left) / methane (right) and dusts with different ignition energies.105

Figure 6.32: Limiting oxygen concentration of hybrid mixtures with 10 J electrical igniter.106

Figure 6.33: limiting oxygen concentration of hybrid mixtures with 2 kJ (left), 10 kJ (right) chemical igniters.107

Figure 6.34: A comparison between computational and experimental results for the LOC of dusts with different ignition energies.113

Figure 6.35: A diagram to estimate the LOC of dust-air mixtures in dependence on MEC and the fuel number.113

Figure 6.36: A comparison between computational and experimental results for the LOC of hybrid mixture of methane and dusts with different ignition energies.116

Figure 6.37: A comparison between computational and experimental results for the LOC of hybrid mixture of acetone and dusts with different ignition energies.117

Figure 6.38: A comparison between computational and experimental results for the LOC of hybrid mixture of isopropanol and dusts with different ignition energies.117

Figure 6.39: A diagram to estimate the LOC of hybrid mixture of methane and dusts in dependence on $LEL_{\text{-hybrid}}$ and the fuel number with 2 kJ chemical igniter.119

Figure 6.40: A diagram to estimate the LOC of hybrid mixture of acetone and dusts in dependence on $LEL_{\text{-hybrid}}$ and the fuel number with 2 kJ chemical igniter.119

Figure 6.41: A diagram to estimate the LOC of hybrid mixture of isopropanol and dusts in dependence on $LEL_{\text{-hybrid}}$ and the fuel parameter fuel number with 2 kJ chemical igniter.120

Figure 6.42: Experimental results for the minimum ignition energy of dusts.121

Figure 6.43: Ignition energy of hybrid mixture of starch with propane and methane in dependence on gases concentration and its comparison with empirical model.123

Figure 6.44: Ignition energy of hybrid mixture of wheat flour with propane and methane in dependence on gases concentration and its comparison with empirical model.125

Figure 6.45: Ignition energy of hybrid mixture of protein with propane and methane in

dependence on gases concentration and its comparison with empirical model.	125
Figure 6.46: Ignition energy of hybrid mixture of polypropylene with propane and methane in dependence on gases concentration and its comparison with empirical model.	126
Figure 6.47: Ignition energy of hybrid mixture of dextrin with propane and methane in dependence on gases concentration and its comparison with empirical model.	126
Figure 6.48: Ignition energy of hybrid mixture of peat with propane and methane in dependence on gases concentration and its comparison with empirical model.	128
Figure 6.49: Ignition energy of hybrid mixture of charcoal with propane and methane in dependence on gases concentration and its comparison with empirical model.	128
Figure 6.50: Ignition energy of hybrid mixture of brown coal with propane and methane in dependence on gases concentration and its comparison with empirical model.	129
Figure 6.51: The trend of MIE of hybrid mixture of polypropylene and propane.	131
Figure 6.52: MIT of the dust materials.	133
Figure 6.53: MIT for the gases and solvents used.	134
Figure 6.54: Comparison of experimental MIT values of gases and solvent-vapor obtained with the GG furnace and according to standard procedure by Brandes et al.	135
Figure 6.55: MIT of two-phase hybrid mixture of dust and gas: effect of admixture of dust on the MIT of gases.	137
Figure 6.56: MIT of two-phase hybrid mixture of dust and gas: effect of admixture of gas on the MIT of dusts.	138
Figure 6.57: MIT of two component mixture of solvent-vapor and gas: effect of admixture of solvent on the MIT of gases	139
Figure 6.58: Comparing the MIT of the various dust models with the experimental results.	145
Figure 6.59: A comparison between the model and the experimental result for hybrid mixtures of various dusts and methane gas.	147
Figure 6.60: A comparison between the model and the experimental result for hybrid mixtures of propane gas and various dusts.	148
Figure 6.61: A comparison between the model and the experimental results for hybrid mixtures of hydrogen gas and various dusts.	149
Figure 6.62: A comparison between the model and the experimental results for hybrid mixtures	

of toluene vapor and various dusts.....	149
Figure 6.63: A comparison between the model and the experimental results for hybrid mixtures of ethanol vapor and various dusts.....	150
Figure 6.64: A comparison between the model and the experimental results for hybrid mixtures of isopropanol vapor and various dusts.....	151
Figure 6.65: Maximum explosion pressure and rate of pressure rise of solvents.	154
Figure 6.66: Maximum explosion pressure and rate of pressure rise of methane and hydrogen.	155
Figure 6.67: Maximum explosion pressure and rate of pressure rise of lycopodium and brown coal.	156
Figure 6.68: Maximum explosion pressure and rate of pressure rise of a mixtures of methane and lycopodium in dependence on the lycopodium concentration.	157
Figure 6.69: Maximum explosion pressure and rate of pressure rise of a mixtures of methane and brown coal in dependence on the brown coal concentration.	158
Figure 6.70: Maximum explosion pressure and rate of pressure rise of a mixtures of isopropanol and lycopodium in dependence on the lycopodium concentration.	159
Figure 6.71: Maximum explosion pressure and rate of pressure rise of a mixtures of isopropanol and lycopodium in dependence on the lycopodium concentration.	159
Figure 6.72: Maximum explosion pressure and rate of pressure rise of a mixtures of methane and isopropanol spray in dependence on the isopropanol concentration.	161
Figure 6.73: Maximum explosion pressure and rate of pressure rise of a mixtures of hydrogen and isopropanol spray in dependence on the isopropanol concentration.	162
Figure 6.74: Maximum explosion pressure and rate of pressure rise of mixtures of lycopodium, methane and 50 g/m ³ of isopropanol spray in dependence on lycopodium concentration.	163
Figure 6.75: Maximum explosion pressure and rate of pressure rise of mixtures of brown coal, methane and 50 g/m ³ of isopropanol spray in dependence on the dust concentration.	164

List of Tables

Table 2.1:Composition of the gases obtained from starch pyrolysis [61].	14
Table 3.1: Explosibility parameters [79].	22
Table 3.2: Constants for Schönewald model [98].	24
Table 3.3: Summary of the MIT of alkane-air mixture [83].	33
Table 4.1: Physical and chemical properties of dusts.	42
Table 4.2:Properties of gases [83, 150].	44
Table 4.3: Properties of solvents [83, 150, 151].	45
Table 5.1: The volume fractions or masses of fuels used for the tests.	56
Table 6.1: A summary of results for the lower explosion limits of mixtures of dusts and gases as well as dusts and solvents (spray).	72
Table 6.2: A summary of results for the lower explosion limits of mixtures of gases and solvents (spray).	73
Table 6.3: A summary of results for the lower explosion limits of three-phase hybrid mixtures.	77
Table 6.4: LEL and MIT of gases, the furnace temperature used in the individual and hybrid mixtures tests as well as a comparison between the LEL according to Brandes et al. [83] and the experimental results.	86
Table 6.5: MEC and MIT of dusts as well as the density of dusts and the furnace temperature used for single substances and hybrid mixtures tests.	86
Table 6.6: Effect of an admixture of gases and solvents on the MEC of dust, (dust concentrations in g/m ³).	91
Table 6.7: Effect of an admixture of dusts and solvents on the LEL of gases, (gas concentrations in vol %).	92
Table 6.8: Effect of an admixture of dusts and gases on the LEL of solvents, (solvent concentrations in vol%).	93
Table 6.9: Summary results for the LOC of dusts and concentrations with different ignition energies.	107
Table 6.10: Summary results for the LOC of hybrid mixtures of methane and dusts as well as concentrations with different ignition energies.	108
Table 6.11: Summary results for the LOC of hybrid mixtures of acetone vapor and dusts as well as	

concentrations with different ignition energies.....	108
Table 6.12: Summary results for the LOC of hybrid mixtures of isopropanol spray and dusts as well as concentrations with different ignition energies.	109
Table 6.13: Mass fractions of elements, MEC, heat of reaction and estimated fuel numbers for the fifteen dusts.....	111
Table 6.14: Mass fractions of elements, LEL, and the estimated fuel number for methane, acetone and isopropanol.....	114
Table 6.15: LEL and MEC of gases and dusts.	136
Table 6.16: Effect of admixture of solvents and gases on the MIT of dusts, (all in °C).	140
Table 6.17: Effect of admixture of dusts and gases on the MIT of solvents, (all in °C).	141
Table 6.18: Effect of admixture of dusts and solvents on the MIT of gases, (all in °C).	142
Table 6.19: Parameters used in model calculation.....	144
Table 6.20: Comparison between the MIT of the various dust models and the experimental results.	145
Table 6.21: Summary for comparison of the models with experimental results for hybrid mixtures of flammable gases and various dusts.	152
Table 6.22: Summary of results for the explosion severity of dust- gas as well as dusts-spray mixtures.....	160
Table 6.23: Summary of results for the explosion severity of gas-spray mixtures.....	162
Table 6.24: Maximum explosion pressure and rate of pressure rise for three-phase hybrid mixtures	165

Abbreviations

AC	Acetone
ASTM	America Standard testing method
Conc	Concentration
BS	British standard
DIN	German institute for Standardization
$(dP/dt)_{\max}$	Maximum rate of pressure rise
EN	European standard
ET	Ethanol
eq.	Equation
HX	Hexane
HP	Heptane
HY	Hydrogen
IS	Isopropanol
ISO	International standardization organization
K_{st}	Specific gas constant
K_G	Specific dust constant
LEL	Lower explosion limit
LEL-hybrid	Lower explosion limit of hybrid mixture
LOC	Limiting oxygen concentration
ME	Methane
MEC	Minimum explosible concentration

MIE	Minimum ignition energy
MIT	Minimum ignition temperature
P_{\max}	Maximum explosion overpressure
NFPA	National Fire Protection Association
SEM	Scanning electron image
TL	Toluene
UEL	Upper explosion limit
VDI	Association of German Engineers

Nomenclature

Symbol	Description	Units
c	Specific heat capacity	[J/g K]
c_{air}	Specific heat of air	[J/g K]
C_d	Initial dust concentration,	[g/cm ³]
C_s	Specific heat capacity of the dusts	[kJ/kg K]
C_l	Minimum explosible concentration of dust	[g/m ³]
d	Diameter of the dust particle	[m]
E	Activation energy	[J/mol]
f	Frequency factor,	[cm/s]
h	Heat transfer coefficient	[J/m ² s K]
Δhr	heat of reaction	[J/g]
H_d	Heat of combustion of dust	[J/g]
H_g	Heat of combustion of gas	[J/g]
ΔH_{comb}	Combustion enthalpy	[J/g]
k	Thermal conductivity,	[W/m K]
k_c	Coefficient of heat transfer	[1/s]
K_{st}	Specific gas constant	[bar m/s]
K_G	Specific dust constant	[bar m/s]
LEL	Lower explosion limit of gas	[vol%],
LEL _{hybrid}	Lower explosible limit of hybrid mixture	[g/m ³]
\dot{m}_c	Mass combustion rate of particle,	[g/s]
M_d	Mass of dust,	[g]

M_{dt}	Molecular weight of dust	[g/mol]
M_g	Mass of gas,	[g]
MEC	Minimum Explosive Concentration,	[g/cm ³]
MIE_{dust}	Minimum ignition energy of dust	[mJ]
MIE_{gas}	Minimum ignition energy of gas	[mJ]
M_{ot}	Molecular weight of oxygen	[g/mol]
M_p	Mass of dust particle	[g]
n_p	Number of dust particles in the furnace or in an elemental dust cloud	
q''	Heat flux	[W/m ²]
R	Gas constant	[J/mol K]
S	Surface area of dust cloud	[cm ²]
S_p	Effective surface area of dust	[cm ²]
T	Temperature	[K]
T_0	Ambient temperature	[K]
T_i	Ignition temperature	[K]
T_i	Minimum ignition temperature	[K]
$T_{i,d}$	Minimum ignition temperature of particles,	[K]
$T_{i,g}$	Minimum ignition temperature of gas,	[K]
$T_{i,hybrid}$	Minimum ignition temperature of hybrid mixture	[K]
T_0	Initial temperature of dust cloud	[K]
T_s	Temperature of particle surface	[K]

$X_{\text{gas}}, X_{\text{dust}}$ Fractional content of gas and dust in the fuel mixture,

Y Concentration of gas in the mixture [vol%]

Greek Symbols

ρ Density of the gas-air mixture [g/m³]

ρ_{air} Density of air [g/cm³]

ρ_{d} Density of dust [g/cm³]

ρ_{g} Density of gas [g/cm³]

ρ_s Density of the dust [kg/m³]

σ Stefan-Boltzmann constant [J/cm²K⁴s]

τ Combustion time [s]

τ_{b} The time a material to reach ignition temperature [s]

σ_{fu-g} Fuel number of gas [mol/g]

σ_{fu-d} Fuel number of dust [mol/g]

β_g Mass fraction of gas in the mixture

β_d Mass fraction of dust in the mixture

Chapter One

1 Introduction

Dust, gas and hybrid mixture explosions pose serious and widespread hazards in process industries such as chemical factories, refineries, enameling plants, paint workshops, cleaning equipment, mills or stores for milled products and other combustible dusts, as well as in tank facilities, loading areas for flammable gases, liquids and solids etc. [1]. The accidents involving these types of explosions can cause failure to equipment, injuries and damages to people as well as the surrounding environment, plant shut-down and sometimes destruction of the factory resulting in fatalities and huge financial losses. Starting from the early days of the process industries, continuous efforts have been made to develop and improve measures to prevent or mitigate these types of explosions [1, 2]. However, despite an extensive research and advancement of technology in combustible dust or flammable gas hazards, these types of explosions still occur in this modern era. For example, the US Chemical Safety Board (CSB) [3] in 2006 stated that 281 dust explosions were reported between 1980 and 2005 in the USA alone, killing 119 workers and injuring 718. In the process industries, approximately 70% of the dusts used are combustible. Most of the reported dust explosions were organic products from industries such as agricultural, food, fuel and pharmaceuticals. Metal dusts have also been reported in a growing number of explosions in the last decades due to their increased use in the process industries like automotive, aeronautics and electronics [3].

In process industries, not only dust, gas and vapor are present, but also much more complex mixtures such as mixtures of two or more materials of different state of aggregates (hybrid

mixtures). These kinds of mixtures are usually not considered in the various hazard and risk assessments even though combustible dusts are dispersed in industrial equipment containing flammable gas or solvents. Hybrid mixtures are usually encountered in facilities that either handle or process combustible dust and flammable gases or vapors. For example, paint factories (pigments and solvents), mining (coal and methane), grain elevators (small grains and fermentation gases), pharmaceutical industries (incipient and solvents) etc. Some examples of industrial accidents involving hybrid mixture explosion include: (1) Westray Mine, 1992, Nova Scotia, Canada: methane gas and coal dust mixture explosion, twenty- six workers were killed [4], (2) BPS Inc., 1997, Arkansas, USA: Azinphos methyl pesticide powder and devolatilized gas mixture explosion, three firefighters were killed [5], (3) SEMABLA Blaye, 1997, France: grain dust and devolatilized gas mixture explosion, 11 workers were killed [6], (4) Upper Big Branch Mine disaster, 2010, Raleigh County, USA: coal dust and methane gas explosion, 38 miners were killed [7], (5) AL Solutions, 2010, West Virginia, USA: zirconium metal dust and hydrogen gas mixture explosion, three employees were killed and a contractor was injured [8] and (6) Soma Mine Disaster, 2014, West Turkey: coal dust and methane gas explosion, 301 workers were killed [9].

Unlike solitary dust, gas or solvent explosions, which have been widely studied in the past decades, data on explosion characteristics of hybrid mixtures are comparatively sparse. Most of the research on hybrid mixtures concentrates only on dust and gas or vapor mixtures [10-21]. However, mixtures of spray-dusts, spray-gases, vapor-gases are generally not considered. Moreover, the explosion behavior of complex systems such as three-component mixtures (dust, gas and vapor) as well as three-phase mixtures (dust, gas and spray) have not been studied yet. Furthermore, most research on hybrid mixtures use weak electric spark or chemical igniters as an ignition source. None of the available research on hybrid mixtures considered hot surface as an ignition source, even though, hot surfaces are considered as one of the leading sources of ignition in industrial explosions [22]. As a result of the aforementioned reasons, the present study seeks to undertake an investigation on the explosion phenomenon of hybrid mixtures to obtain insight into the driving mechanisms and the explosions features affecting the course of hybrid mixture explosion by considering the following scopes:

1. Experimental investigation and theoretical modeling of the minimum ignition temperature of two-phase (dust-gas, dust-vapor), two components (gas-vapor) and three-components (dust-gas-vapor) hybrid mixtures.
2. Experimental investigation and theoretical modeling of the limiting oxygen concentration of two-phase (dust-gas, dust-vapor as well as dust-spray) hybrid mixtures with different ignition energies.
3. Experimental and theoretical modeling of the minimum ignition energy of two-phase (dust-gas) hybrid mixtures.
4. Experimental investigation and theoretical modeling of the lower explosion limits of two-phase (dust-gas, dust-spray, dust-vapor as well as gas-spray), three-components (gas-vapor-gas) and three-phase (dust-gas-spray) hybrid mixtures.
5. Experimental investigation of the maximum explosion pressure and maximum rate of pressure rise of two-phase (dust-gas, dust-spray as well as gas-spray) and three-phase (dust-gas-spray) hybrid mixtures.

1.1 Thesis outline

This thesis describes several contributions with regard to hybrid mixture explosion. All experimental tests were performed at the University of Magdeburg, Department of Plant Design and Process Safety, fire and explosion laboratory. In addition to this *introduction (Chapter 1)*, the thesis is structured as follows:

Chapter 2 (*Theoretical Background and Literature reviews*) outlines an overview of explosions. Background information as well as a detailed literature review of previous work related to gas, dust, spray and hybrid mixtures explosion are discussed.

Chapter 3 (*Explosion Characteristics*) discusses the relevant explosion parameters considered in this thesis such as minimum ignition temperature, minimum ignition energy, limiting oxygen concentration, lower explosion limit and explosion severity. Standard methods of determination as well as the relevant factors influencing the determination of each of the parameters are discussed. Moreover, mathematical models to estimate these parameters are also presented.

Chapter 4 (*Material Properties and Preliminary Analysis*) presents a brief description of the properties of the investigated materials. The materials used include twenty combustible dusts, three gases and six solvents. All twenty dust samples were analyzed for: particle size distribution, volatile content, heat of combustion and elemental analysis. Moreover, physical, chemical and thermodynamic properties of both the solvent and the gas samples are also reported.

Chapter 5 (*Experimental Methods and Procedure*) explains in detail the experimental procedure used to determine the explosion parameters of hybrid mixtures. These experiments include: (1) the determination of the lower explosion limit, explosion overpressure, rate of pressure rise and limiting oxygen concentration for the ignition of dusts, gases, solvents (spray) and their mixtures in the standard 20-liter sphere, (2) the determination of the minimum ignition temperature of dusts, gases, solvents (vapor) and their mixtures in the modified Godbert-Greenwald furnace and (3) the determination of the minimum ignition energy of dusts and hybrid mixtures in the modified Hartmann apparatus.

Chapter 6 (*Results and Discussions*) presents detailed discussion of the results obtained from this study. The presentation of the results for each of the considered parameters is done separately. The following are the hierarchy on how the results are presented. (1) lower explosion limit, (2) limiting oxygen concentration, (3) minimum ignition energy, (4) minimum ignition temperature and (5) explosion severity. In all cases, the results from single materials are initially presented, followed by double-phase and triple-phase. The results from mathematical models presented in Chapter 3 are also compared with the experimental results.

Chapter 7 (*Conclusion and Recommendations*) closes the thesis with a summary of the presented research topic and results. Some recommendations and perspectives regarding future research on hybrid mixture explosion are stated.

Chapter Two

2 Theoretical Background

2.1 General overview of explosions

The term “explosion” has many definitions in literature, however, they are mainly divided into two categories; one focusing on the noise due to sudden release of a strong pressure wave, and the other considering the sudden release of chemical energy. **Eckhoff [22]** defined an explosion as “an exothermal chemical/physical process that, when occurring at constant volume, gives a sudden and significant pressure rise”. The types of explosions usually encountered in process industries are physical and chemical explosions **[23]**. Subcategories of physical and chemical explosions are presented in Figure 2.1. Only the highlighted portion of this diagram is considered in this study.

Chemical explosions are associated with the sudden release of chemical energy, which is generated from chemical reactions. These reactions may include rapid combustion processes, decompositions or other rapid exothermic reactions. In chemical explosions, reactions can occur in either the vapor, liquid or solid phase **[24]**. A *propagating reaction* is a reaction which propagates spatially through the reaction mass, such as the combustion of a flammable vapor in a pipeline, a vapor cloud explosion, or the decomposition of an unstable solid. In *deflagration* the combustion or reaction wave propagates at a velocity less than the speed of sound **[25]**. Deflagration reactions involving combustion of various types of material such as gases, dusts, sprays and hybrid mixtures are considered in this study. For this reaction

to occur, three main components need to come together in the right proportion, which include the fuel (it could be any combustible material such as gas, dust, mist and their mixtures), oxidants (for example, oxygen, halogen etc.) and effective ignition source (for example, mechanical sparks, heating, smouldering spot, electrostatic discharge, hot surface, welding, electrical equipment etc.).

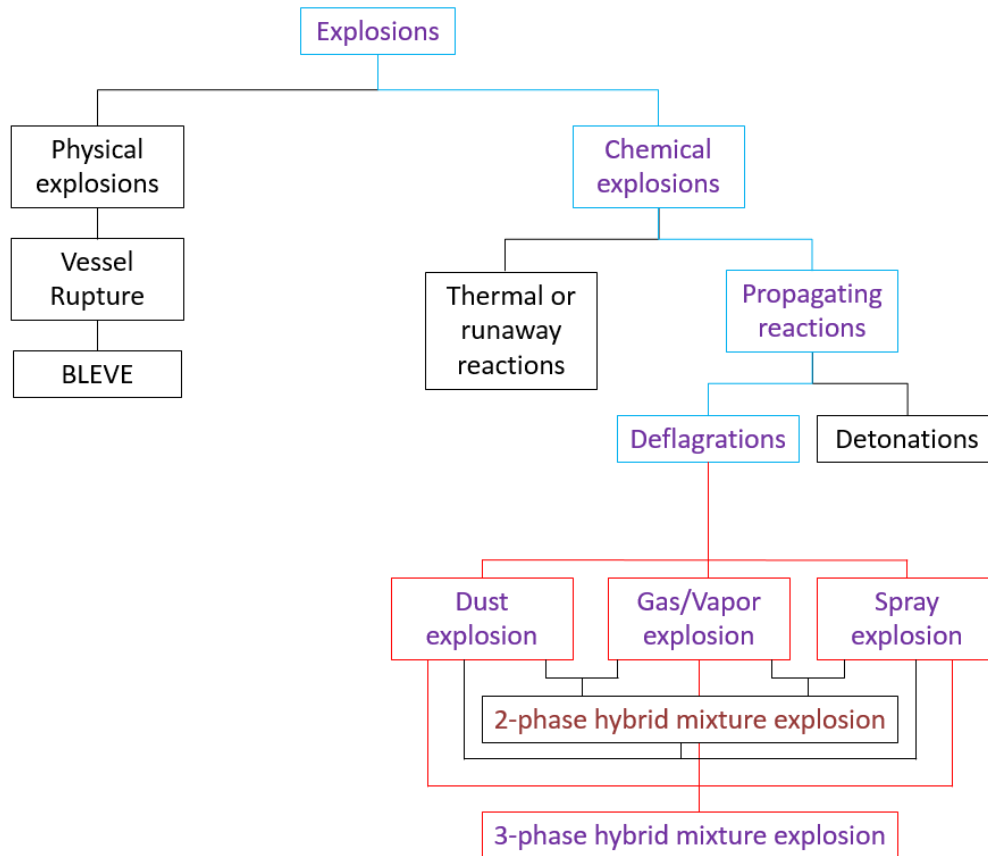


Figure 2.1: Relationships between the different types of explosions.

2.2 Gas / vapor explosion

Gas is defined as the state of matter characterized by complete molecular mobility and unlimited expansion [26]. Gas explosion phenomena depend strongly on the conditions and structure of the system where the explosion occurs [27, 28]. Most gas explosions happen when combustible gas from accidental releases, mixes with air in the atmosphere and generates an explosible cloud. If the fuel-air ratio in the cloud is within the explosible range, and there is the presence of an ignition source an explosion would occur. The consequences of a gas explosion depend on the environment in which the gas cloud is contained [29].

Therefore, the environment where the explosion takes place can be classified as: Confined Gas Explosion, Partly Confined Gas Explosion and Unconfined Gas Explosion [30]. A *confined Gas Explosion* [31] occurs within physical enclosures, e.g. tanks, process equipment, pipes, culverts, sewage systems, closed rooms and in underground installations. Pressure build-up in a confined explosion can be analysed by knowing the gas cloud size. These types of explosion may result in loss of containment and a subsequent event could be strong blast waves from high pressure reservoirs, fires or toxic releases [31]. *Partly Confined Gas Explosion* results when a fuel is accidentally released inside a building which is partly open such as compressor rooms and offshore modules. The consequences of such explosions depend on several parameters such as the type of fuel, size and concentration of the gas cloud, ignition and geometrical layout. *Unconfined Gas Explosions* are usually the result of a flammable gas release which occur within an unconfined area [24]. Gas or vapor explosion could be prevented or mitigated by measures such as: combustible gases leak prevention and control, installation of venting system to release the gas and reduce the explosible atmosphere, elimination of ignition sources and blast fire barrier installation etc. More information on the prevention of gas or vapor explosion could be referred to [24, 32-35].

2.3 Spray explosion

According to ASTM [36], “a spray is defined as a dynamic collection of drops dispersed in a gas”. It is a momentum driven collection of droplets usually produced by atomization (generation of small droplets) of liquid through mechanical forces for example, a pressurized release through a nozzle. In this process, liquid is forced through a nozzle which converts it into fine drops. The geometry of the nozzle and the potential energy of the liquid causes the liquid to appear as small ligaments. Ligaments formed from the previous process then break into smaller units, which are usually called droplets or liquid particles. Figure 2.2 shows the formation of droplets [37]. Droplets are easier to ignite than the bulk liquid due to their higher surface to volume ratio of the liquid. Thus, droplets are more sensitive to heat input from potential ignition sources and more surface get into contact with oxygen in the air.

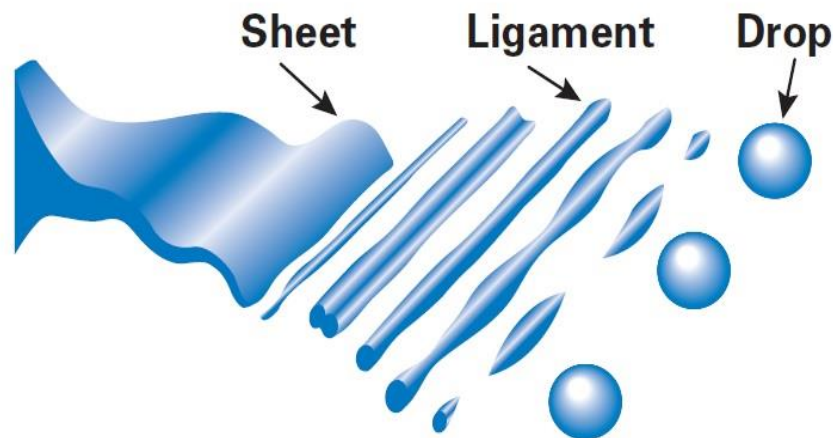


Figure 2.2: Understanding of atomization [37].

According to **Eckhoff [22]**, sprays of combustible liquids, for example, hydrocarbons in air at atmospheric pressure and normal temperature, with a droplet size $< 100 \mu\text{m}$ and a droplet mass concentration in the range of $100\text{-}500 \text{ g/m}^3$ are explosible. This is so regardless of whether the liquid is of a low or a high boiling point. In the case of a low boiling point liquid, the droplets will evaporate readily and the cloud becomes a mixture of combustible vapor and air. If the boiling point of the liquid is high, i.e. the vapor pressure at normal ambient conditions is low, the droplets will, with regard to the combustion process, behave similarly to solid particles of an organic material. **Zehr [38]** explained that a spray and a cloud of solid particles (dust) have common features, in that, both consist of a finely divided dense fuel phase suspended in an oxidizing gas. However, explosible spray clouds are less stable than explosible dust clouds because of the collisions between droplets which give rise to coalescence and transformation to fewer and larger droplets. When the droplet size gets sufficiently large, the droplet sedimentation velocity in the gas becomes significant and the droplets settle out of the cloud. A similar finding was observed by **Williams [39]** when he undertook a wide range of studies on spray explosions by considering various properties of liquid fuels such as characteristics of sprays in terms of drop size and drop velocity distributions, processes for atomization of liquid fuels and combustion of single droplet and droplet clouds. Moreover, **Forster [40]** also provided very important information on generation, ignition and combustion of sprays. The author mentioned that the mechanism of flame propagation is strongly influenced by the droplet size. Below $10 \mu\text{m}$, the droplets evaporate completely before combustion and behave more like a premixed gas; on the other hand, droplets

size of over 50 μm burn individually and ignite further droplets around them, spreading the combustion.

Furthermore, **Gant et al. [41]** undertook a comprehensive literature survey on the explosibility of flammable solvents as spray. They discussed the following safety parameters: lower explosion limit, minimum ignition energy and minimum ignition temperature. The authors observed that droplet size influences the explosibility of spray. They explained that when the spray droplets are very small (with a diameter less than 10 μm), as the flame propagates through the spray, the droplets vaporise ahead of the flame front and the flame travels through essentially as a vapor-air mixture. The lower explosion limit of spray in this case is therefore similar to that of the corresponding vapor-air mixture [26, 42, 43]. However, with regards to larger droplets, there is insufficient time for the droplets to vaporise completely before becoming engulfed in the advancing flame front. Each droplet burns with its own diffusion flame, rather than as a homogeneous gas mixture. With respect to droplets with a median diameter greater than 40 μm , the heat transfer from one burning droplet to its neighbours becomes the principal mechanism for flame propagation through the spray [42]. In the cases of the minimum ignition energy of the spray, droplet size, fuel concentration, air velocity and the presence of any fuel vapor (in addition to the droplets) are the predominant factors to consider. These factors have been studied in detail by [44-47]. Decreasing the droplet size, increases the required energy for ignition to prevail. Moreover, increase in the fuel concentration also decreases the minimum ignition energy until a point where the fuel is too rich to support combustion. With respect to minimum ignition temperature, it is considered that the hot surface initially vaporises a sufficient quantity of fuel to produce flammable concentrations of vapor and, the temperature of the flammable vapor to be sustained for a period longer than the chemical ignition delay time. The effectiveness of hot surface ignition, therefore, depends on many factors which includes the physical properties of the liquid, the concentration of fuel in the air, the droplet size and the shape and extent of the heated surface. Detailed information on the effect of these factors on the minimum ignition temperature of sprays could be found in the following articles [41, 48-51]. Similar preventive and protective measures discussed in the previous section (gas / vapor explosion) could also be used in this case where as more detailed discussions could be referred to the appropriate articles cited above.

2.4 Dust explosion

The American National Fire Protection Association (NFPA) [52] defined combustible dust as a solid which has the ability to explode and cause a fire or deflagration hazard when suspended in air or some other oxidizing medium over a range of concentrations, regardless of particle size and shape. Dust explosion can be defined as the rapid combustion of a combustible dust cloud, resulting in a sudden increase in temperature and pressure. Figure 2.3 illustrates the five indispensable elements that must be present in order for a dust explosion to occur. These include: combustible dust [e.g. natural organic materials (grain, linen, sugar, etc.), synthetic organic materials (plastics, organic pigments, pesticides, etc.), fuel materials (wood, coal and peat etc.) and metals (aluminium, magnesium, zinc, iron, etc.)], the availability of an oxidant (e.g. oxygen, halogens, nitrous oxide etc.), presence of an ignition source (e.g. hot surface, sparks etc.), confinement (to develop overpressure) and dispersion (mixing of the dust and air) [22].

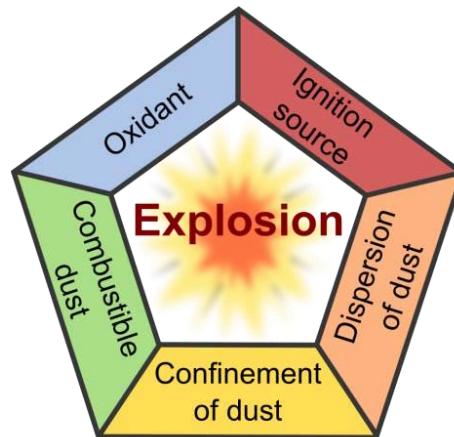


Figure 2.3: Dust explosion pentagon[22].

Both the explosion severity and ignition sensitivity of a dust cloud depend on a number of variables such as chemical composition, moisture content, initial temperature of the dust, particle size and shape distribution of the dust, the degree of dispersion and dust concentration in the cloud [22]. In general, the combustion rate increases as the size of dust particles decreases. The higher the degree of sub-division the more rapid would be the burning, until a limiting stage is reached where the particles become too fine in size and tend to agglomerate together. If the ignited dust cloud is unconstrained, it would only produce a

flash fire [22]. But if the ignited dust cloud is confined, the heat from the burning may result in rapid development of pressure to flame propagation across the dust cloud. Moreover, the strength of an explosion also depends on the rate at which energy is being released due to combustion relative to the degree of confinement and heat losses [53]. Dust explosions can be subdivided into two types which include: primary and secondary dust explosions [22, 54]. *Primary dust explosion* is the first explosion. It occurs when a dust is suspended in an atmosphere with sufficient amount of oxygen for combustion, in the presence of an appropriate ignition source. If the equipment in which primary explosion occurs is of light material, as is often the case, the burning dust particles, flames and hot gases produce pressure capable of rupturing the enclosure. A *secondary dust explosion* can be initiated due to the entrainment of dust layers by the blast wave arising from primary explosions. The primary event might be a dust explosion originating in a process unit, or could be any disturbance energetic enough to disperse the combustible dust layered on the floor and other surfaces. This airborne dust in the presence of an ignition source (original source of ignition or combustion products of the primary explosion) can result in a secondary explosion [22, 55].

2.4.1 Mechanism of dust explosion

Research into dust explosions has found that volatile matter in dust plays an important role in dust explosion mechanism. The volatile matter determines the quantity of gaseous product that the dust releases when heated. **Medard [56]** explained that when a cloud of dust burns, each unburned particle is heated by radiation from particles already burning and undergoes pyrolysis, which creates a small sphere around it, in which the atmosphere is a mixture of air and combustible gases (H, CO, hydrocarbon, etc.). An experimental study by **Gomez et al. [57]** on ignition and combustion of single coal particle concluded that two chemical reactions compete for the oxygen surrounding the coal particle, in which; one involving the carbon surface (heterogeneous) and the other involving the volatile gases (homogenous). The authors further stressed that when the coal particles are ignited homogeneously, gas phase combustion of the volatile matter burns most of the carbon to produce carbon dioxide. This finding was confirmed by **Di Benedetto et al. [58]** of which

they explained that dust explosion occurs via two main paths: the heterogeneous and the homogenous combustion. Heterogeneous combustion is where the oxidation taking place at the surface of solid particle is responsible for ignition and flame propagation (low volatile matter content like metals) whereas, in homogeneous combustion, oxidation of volatiles evolved from dust particles prior to ignition is responsible for ignition and flame propagation (high volatile matter content like organics and gas).

The latter (pyrolysis with the release of volatile gases) cannot occur with combustible substances, such as certain metals with very high boiling point, where the particles will certainly melt but will not release combustible vapor [56]. In addition, in metals, low melting point material may oxidize in solid phase, but due to an oxide film around each particle, this does not result in a homogenous metal vapor/air flame. Consequently, the metal dust particle may react directly with oxygen diffusing towards the particles itself. **Bing Du et al. [59]** studied the homogenous and heterogeneous deflagration mechanism of magnesium dust and sweet potato powder using Thermo-Gravimetric–Analysis (TGA) as shown in Figure 2.4. The magnesium dust sample was heated with a linear rate of 15 K/min from room temperature to 800°C under nitrogen and air atmosphere respectively. In this case, the thermogravimetric trace presented no obvious variation under nitrogen atmosphere, whereas, under air atmosphere, a pronounced weight increment of 43 % was identified at temperature 520°C to 547°C, which corresponds to the surface heterogeneous oxidation of MgO solution in the molten particles. In contrast to sweet potato dust, where weight loss can be divided into 4 stages. The first stage is associated with the loss of physically absorbed water. In stage two significant weight loss was attributed to starch depolymerisation and decomposition. Stage three is the decomposition of cellulose and stage four decomposition of lignin.

Similarly, in the case of organic dust, the explosion (homogenous combustion) occurs in three steps (in order and very quick succession) which includes: heating (particle heating), pyrolysis and devolatilization and oxidation of pyrolysis gases as shown in Figure 2.5.

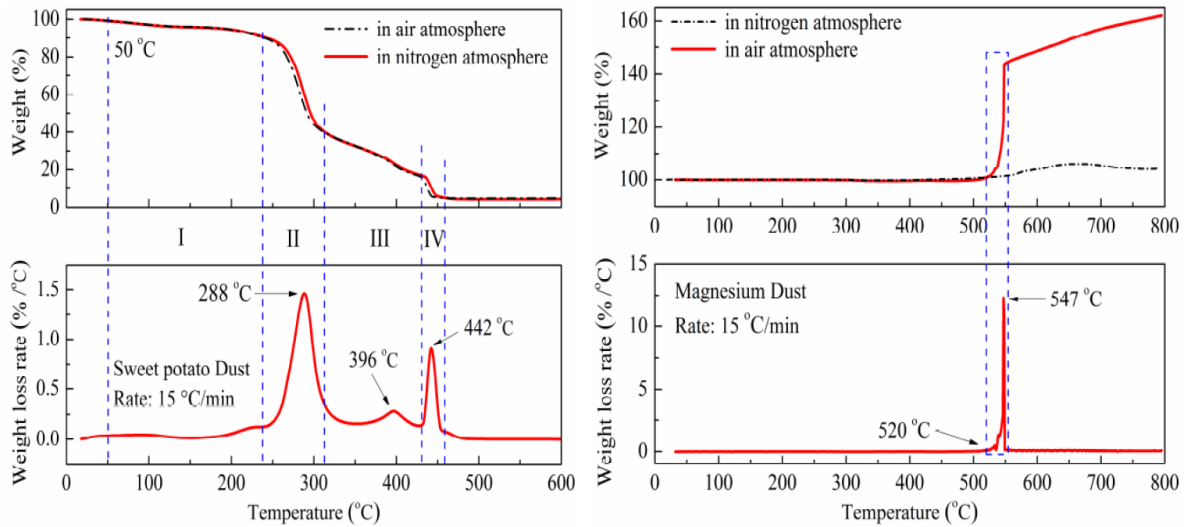


Figure 2.4: Comparison of TG-DTG traces between sweet potato powders and Magnesium dust in N_2 and air atmosphere [59].

During the pre-heating stage, the moisture or water content in the substance is vaporised. Hence, dust with high moisture content requires high minimum ignition energy or higher ignition temperature because evaporation and heating of water serve as an inert heat sink [22, 60]. Eckhoff [22] further added that the water vapor is mixed with the pyrolysis gases in the preheating zone of the combustion wave and makes the gas mixture less reactive.

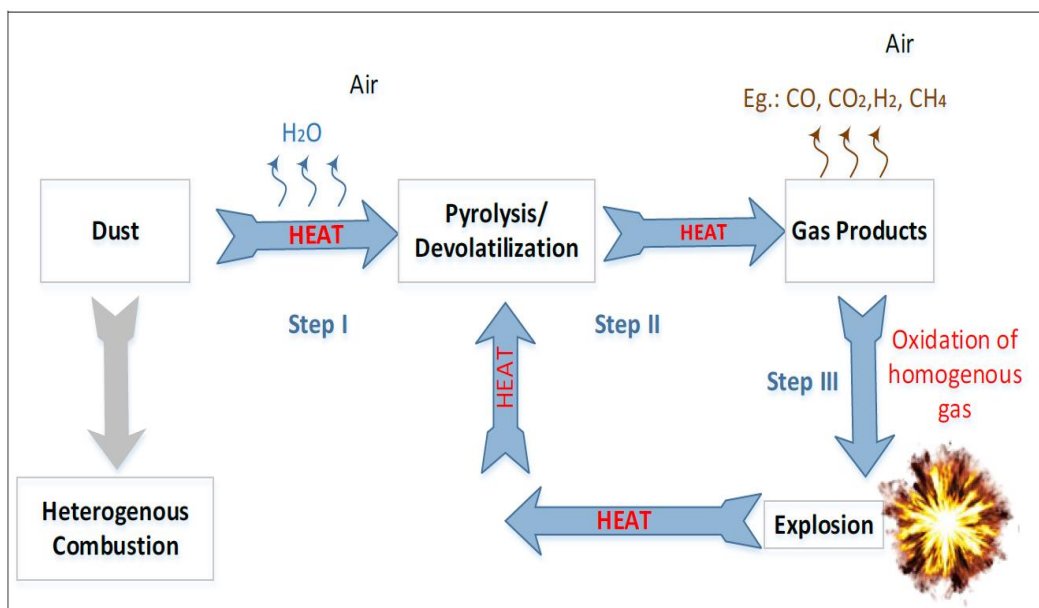


Figure 2.5: Schematic representation of the paths occurring during dust explosion [61].

The next stage is the pyrolysis and devolatilization step. This step is considered as the first step in the combustion process. During this stage, the organic particle is further heated, producing volatile matter or combustible gases. The combustible gases are then mixed with air in the space between the particle. **Dufaud et al.[61]** analysed the pyrolysis gas of starch at various reactor temperatures, but always greater than 550°C. The authors stated that the main pyrolysis products of starch are carbon monoxide and carbon dioxide and a few percent of methane, hydrogen, ethylene and propylene as shown in Table 2.1.

Table 2.1:Composition of the gases obtained from starch pyrolysis [61].

Pyrolysis Gas	Composition (wt%)
Carbon monoxide	60
Carbon dioxide	30
Methane	3.0
Ethylene	3.0
Propylene	2.0
Hydrogen	1.0
Ethane	0.7
Acetylene	0.3

The final stage is the oxidation of pyrolysis gases, where the gas phase combustion of premixed volatile-air takes place or in other words, the oxidation of homogeneous gas takes place. These steps are mutually dependent and are strongly affected by the particle size in which for small particle size typically below 50 µm, the oxidation in homogeneous gas phase is the step controlling the dust combustion and the heating and pyrolysis steps are very fast [60]. This finding has been confirmed by [22, 62, 63] but with varied critical particle size diameter, which typically have different value for each dust. In contrast, the pyrolysis and devolatilization of the solid particles become rate-controlling at high dust loadings and larger particle size [61].

2.4.2 Prevention and mitigation of dust explosion

In order to prevent or protect dust explosion, the following measures are to be taken into consideration. (1) *preventive measures*: elimination of the dust by cleaning of working environment, elimination of oxidant by means of suitable inerting procedures, elimination of

ignition sources by avoiding free flames, hot surfaces, sparks and also installing appropriate electrical systems for hazardous areas [22]. (2) *protective measures*: containment of explosion that is, the employment of equipment appropriately dimensioned to withstand the maximum explosion overpressure; separation of equipment that is, installation of different apparatus in different places; physical division of the operations with higher explosion risk, explosion suppression by using appropriate extinguishing substances, and venting (which consists of a surface that can be broken against an unacceptable pressure increase). More information on the prevention of dust explosion could be referred to [64-66].

2.5 Hybrid mixture explosion

Hybrid mixture explosions are the type of explosion that involves at least two combustible materials of different state of aggregation, for example mixtures of combustible dust with a flammable gas, vapor or spray. They are usually found in industrial processes that handle combustible mixtures of different state. It has long been known that the explosion severity and ignition sensitivity of hybrid mixtures significantly differ from that of the single substances [10, 67-73]. Unlike single substance (i.e. dust, gas or solvent) explosions, which have been widely studied in the past decades (see sections 2.2 to 2.4 for more information on single substance explosion), data on explosion characteristics of hybrid mixtures are relatively few. However, these kinds of mixtures are usually encountered at facilities where gases, solvents and dusts are either handled or processed. As a results, several studies has been done throughout the world with the aim of preventing the occurrences and mitigating the consequences.

More than a century ago, **Engler [67]** observed that mixtures of coal dust and methane at a concentration lower than the lower explosion limit of methane and minimum explosible concentration of coal dust could be flammable thus producing unexpected hazardous conditions. Since Engler's observation, many studies have been focused on the explosion behavior of hybrid mixture of dusts and gases.

Cardillo et al. [68] determined an empirical correlation between the content of combustible gas (propane) in air and the minimum explosible concentration of polypropylene, polyethylene, and iron. They observed that iron responded to the propane addition in the

same systematic way as the organic dusts. The minimum explosible concentration of iron dust was found to be 200 g/m^3 . This concentration, then decreases to 100 g/m^3 when 1 vol% of propane which is below the lower explosion limit was added.

Pellmont [69] investigated the influence of combustible gas in air on the minimum explosible concentration of polyvinyl chloride dust cloud. Pellmont found that the concentration of the dusts decreased almost linearly with increasing content of propane in the air. For example, for $20 \mu\text{m}$ particle size of polyvinyl chloride in air, the minimum explosible concentration was 500 g/m^3 , whereas with 1 vol% propane in the air, it was 250 g/m^3 .

Franke [70] reported that adding 3 vol% methane to the coal dust-air mixture can reduce the minimum ignition energy required to ignite coal dusts clouds by factors of the order of 100.

Bartknecht [71] studied the explosibility of cellulose by adding non-explosible concentrations of methane, butane and propane. He found that a hybrid mixture constituted of dust and gas concentration, which is not explosible can turn into an explosible one. Bartknecht also emphasized that when gas is added to a dust-air mixture, the maximum explosion pressure was found to have consistent increase, whereas a more dramatic effect was observed on the hybrid deflagration index (Kst).

Cashdollar [72] studied the explosion behavior of coal dust and methane mixtures in the 20-liter sphere using 2500 J igniters as an ignition source. Low-volatile Pocahontas coal and high-volatile Pittsburgh coal were tested. Cashdollar found that both coal dusts became explosible when methane was added even though the added concentration of methane was below the lower explosion limit.

Siwek [73] undertook a comprehensive investigation on the deflagration parameters of organic dust and propane-air mixtures in the 20-liter sphere. He gave the following conclusion: (1) hybrid mixtures are easier to ignite and explode with greater severity than the corresponding pure dust-air mixtures, (2) non-explosible concentration of dust-air mixtures and non-explosible flammable gas-air mixtures can form explosible hybrid dust-gas-air mixtures and (3) the addition of a flammable gas to a dust-air mixture increases the maximum explosion pressure to some extent and significantly increases the maximum rate of pressure rise of the dust mixture, even though the concentration of the flammable gas is below its lower explosion limit.

Pilao et al. [10] also investigated the behavior of the hybrid mixture of methane and cork. They observed that the presence of methane at concentrations below the lower explosion limit affects the explosion severity (maximum explosion pressure and maximum rate of pressure rise) for lower dust concentration (40 g/m^3), whereas both parameters are slightly affected in the case of higher dust concentration (450 g/m^3).

Denkevits [11, 12] experimentally evaluated the deflagration severity of graphite-hydrogen as well as aluminum-hydrogen hybrid mixture with air by measuring the maximum explosion pressure and maximum rate of pressure rise using the 20-liter explosion sphere. In Denkevits' tests, hydrogen gas concentration was varied from 4 to 18 vol%; which is below the stoichiometric hydrogen-air mixture concentration and the fine graphite dust concentrations were in the range of 25 to 300 g/m^3 . The author performed the test with two different ignition energies; 10 kJ chemical igniter and 10 J electric sparks. Denkevits observed that adding hydrogen to graphite dust made the mixture explosible at any of the tested dust concentration. He also found that the explosion involving graphite-hydrogen-air mixtures produced higher overpressure than hydrogen-air mixtures of the same hydrogen concentration. With respect to hydrogen-aluminium-air mixture, he observed that both the explosion overpressure and the rate of pressure rise were noticeably higher than those of pure hydrogen-air mixtures and pure aluminium dust-air mixtures. At lower hybrid fuel concentrations, the mixture exploded in two steps: first hydrogen explosion followed by a clearly separated aluminium dust explosion. With increasing concentrations, the two-phase explosion regime transits to a single-phase regime where the two fuel component exploded together as a single fuel. In this regime, both the hybrid explosion pressure and rate of pressure rise were higher than either hydrogen or aluminium alone.

Dufaud et al. [13, 14, 63] studied the influence of pharmaceutical dusts such as: excipients, vitamins, and their associated solvent (ethanol, di-isopropyl ether, toluene) concentrations on the maximum explosion pressure and maximum rate of pressure rise. They investigated three cases: (1) magnesium stearate and ethanol, (2) niacin and di-isopropyl ether (3) antibiotic and toluene by using the 20-liter sphere with 10 kJ chemical igniters as an ignition source. They observed that the deflagration index for dust-vapor-air mixtures were significantly greater than those of the pure fuels (dust-air or vapor-air). They also noted that

the evolution of maximum rate of pressure rise and the combustion kinetics were not linear and discounted the notion that most flammable compound imposes its combustion kinetics. A significant enhancement of the combustion kinetics of the hybrid mixture (magnesium stearate-ethanol-air mixture) was observed for concentrations pairs for magnesium stearate and ethanol ranging from 200 g/m³, 1.0 vol% to 600 g/m³, 2.0 vol%.

Chatrathi [16] also evaluated the explosibility of hybrid mixture of cornstarch and propane in the 1m³ spherical explosion chamber. The author measured the lower explosion limit of hybrid mixtures. Chatrathi observed that the presence of propane concentrations below the lower explosion limits decrease the minimum explosible concentration of cornstarch. Similarly, the presence of cornstarch decreased the lower explosion limit of propane. Additionally, Chatrathi further observed that the violence of hybrid mixture is higher than that of single fuel under turbulent condition.

Sanchirico et al. [17] studied the explosion severity of hybrid mixture explosions with niacin and acetone in the 20-liter sphere using 10 J electric spark as an ignition source. The authors found that the dust and gas or vapor mixtures, both at concentrations below the lower explosion limits can form an explosible mixture when combined.

Amyotte et al. [18, 19] undertook an experimental investigation on the explosion parameters of polyethylene admixed with propane, ethylene and hexane at the standard test conditions for dusts (in the 20-liter sphere, ignition source by 10 kJ chemical igniters and ignition delay time of 60 ms). The authors performed the experiments by adding low gas concentrations (1-5 vol %) of ethylene, propane and hexane (in vapor state) to polyethylene dust by changing the dust concentration. They observed a significant increase in the deflagration index by adding ethylene at concentrations higher than its lower explosion limit with respect to the dust alone.

Garcia et al. [20] experimentally studied mixtures of niacin dust and methane in the 20-liter sphere by using a weak electric spark ignition source. They concluded that the addition of methane can intensely decrease the minimum explosible concentration of niacin.

Khalili et al. [21] undertook an experimental study on the ignition sensitivity of various gas or vapor-dust mixtures (e.g. starch-methane, starch-hexane) in the 20-liter sphere. Their results showed that a concentration of gas or vapor as low as 1.0 vol% causes a significant

decrease in the minimum explosible concentration of starch and induces changes in the rate limiting step of the combustion reaction from boundary diffusion to homogeneous gas phase reaction.

Jiaojun et al. [74, 75] also undertook both experimental and theoretical investigations on the explosibility of hybrid mixture of ethane-niacin, methane-cornstarch and ethylene-niacin in air in the 36-liter explosion chamber using 2500 J igniter as an ignition source. They observed that the deflagration index of flammable gas was found to be significantly higher than the results from literature due to the high turbulence inside the vessel established by the ignition delay time. The authors also noted that the lower explosion limits of hybrid mixtures are lower than that of individual substances. Based on the authors' experimental results, an empirical model to predict the lower explosion limit of hybrid mixtures was proposed, which seems to fit well with their own experimental results.

Kosinski et al. [76] undertook experimental investigation on carbon black and propane hybrid mixtures in the standard 20-liter explosion vessel with 1-kJ chemical igniter as an ignition source. They observed that it is possible to obtain flame propagation even when the concentration of gaseous fuel is below the lower explosion limit. They also mentioned that for the case when the content of volatiles is high, the flame propagation in such a system resembles combustion of multi-component gas.

Sanchirico et al. [77] experimentally investigated hybrid mixtures of lycopodium-nicotinic acid and methane complex in the standard 20-liter sphere with 10 J electrical spark as an ignition source. An exceptional behavior (in terms of unexpected values of the rate of pressure rise and pressure) was found in the complex mixtures containing lycopodium and nicotinic acid in equal amounts. This mixture was found to be much more reactive than all the other dust mixtures, no matter what the dust and methane concentrations were.

Li et al. [78] undertook an experimental study on the explosion characteristics of hydrogen-methane-air and methane-coal dust-air mixtures in the standard 20-liter vessel using 2.5 kJ chemical igniter as an ignition source. The authors observed that the presence of hydrogen in the coal dust significantly increases the maximum explosion pressure and rate of pressure rise. With an increase of hydrogen content in the mixture, the minimum explosible concentration of coal dust decreased correspondingly.

The main conclusions from the discussion of the above literatures on the explosion parameters of hybrid mixtures could be summarized non-exhaustively by the following assertions that: (1) the ignition sensitivity of the dust can be strongly increased by the addition of a few percent of combustible gases or vapor, even with concentrations lower than the respective lower explosion limits, (2) hybrid mixtures can be explosible when the concentrations of the dust and the gas or vapor are both below their respective lower explosion limits, (3) the explosion severities of hybrid mixtures dust and gas are higher than single dust explosion.

From the analysis of the available literatures, it appears that the effect of hybrid mixture explosions cannot be predicted by simply overlapping the effects of the single substance explosion. Also, it can be deduced that the research on hybrid mixture explosions is complicated because of the large number of complex physical processes that occur during the explosion and the high number of parameters that should be considered during the explosion. Some parameters related to the hybrid mixture explosions include: ignition source, the enclosure, the initial conditions, response or output flammable parameters, combustion dynamics, available energy, heat transfer and turbulence effects. As already mentioned in Chapter one, the research literatures discussed above concentrate on only dusts and gases or vapor mixtures which focused on the maximum explosion pressure, maximum rate of pressure rise, lower explosion limit and only few data on minimum ignition energy. However, hybrid mixtures of spray-dusts, spray-gases, vapor-gases are generally not considered. The explosion behavior of complex systems such as three-component mixtures (dust, gas and vapor) as well as three-phase mixture (dust, gas and spray) are not considered. Furthermore, the discussed literature used either weak electric spark or chemical igniters as an ignition source for hybrid mixtures test. However, none of these studies applied hot surface as an ignition source, even though, hot surfaces are considered as one of the leading sources of ignition in industrial explosions [22]. Based on the aforementioned reasons, this present study seeks to fill these research gaps in hybrid mixtures by performing an extensive theoretical and experimental investigation on the explosion characteristics such as: minimum ignition temperature, minimum ignition energy, lower explosion limits, limiting oxygen concentration and explosion severity.

Chapter Three

3 Safety Characteristics

3.1 Explosion relevant parameters

Explosion prevention and protection measures are very vital for the reduction of the risks associated with dusts, gases/vapor, spray and hybrid mixture explosions. The preventive measures are concerned with the reduction of the explosion likelihood, whereas the protective measures are adequate to reduce the effects of the explosions. Figure 3.1 provides the safety relevant parameters considered in this study while Table 3.1 provides a brief description of each parameter and their industrial applications.

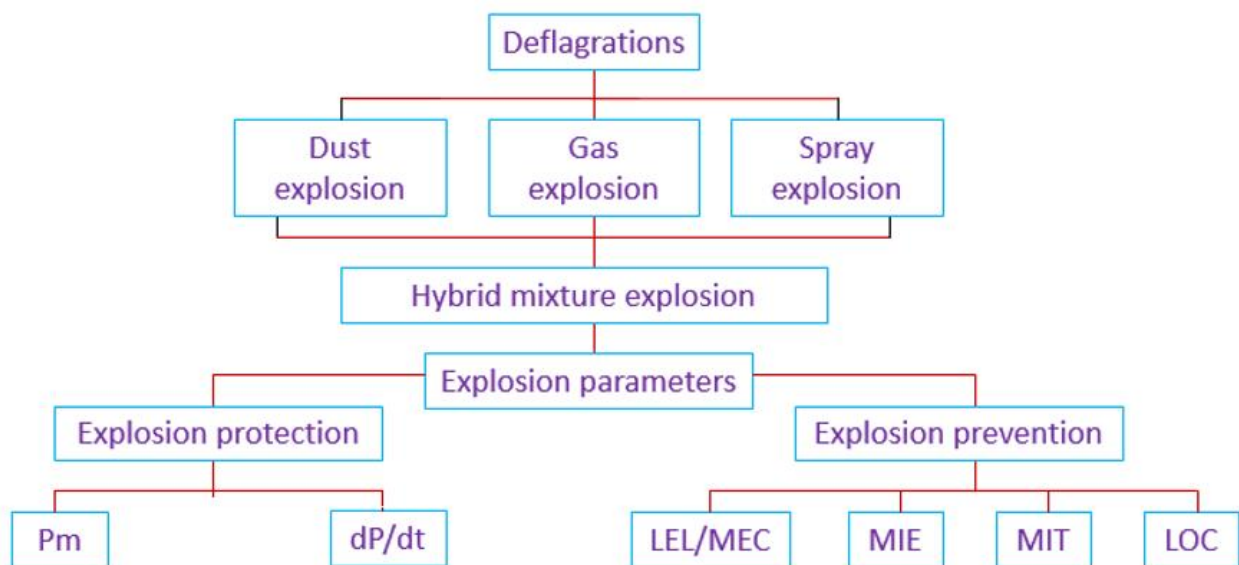


Figure 3.1: Safety characteristics.

Table 3.1: Explosibility parameters [79].

Explosion Parameters	Typical units	Description	Examples of industrial applications
P_{max}	bar (g)	Maximum explosion pressure in constant-volume explosion	Isolation, partial inerting, pressure-resistant design
$(dP/dt)_{max}$	bar/s	Maximum rate of pressure rise in constant-volume explosion	Venting, suppression
MEC	g/m ³	Minimum explosible concentration of dust	Control of fuel concentrations
LEL	Vol %	Lower explosion limits of gas or vapor	Control of fuel concentrations
MIE	mJ	Minimum ignition energy of dust cloud (electric spark)	Removal of ignition sources, grounding and bonding
MIT	°C	Minimum ignition temperature	Control of process and surface temperatures
LOC	Vol%	Minimum (or limiting) oxygen concentration in the atmosphere for flame propagation.	Inerting

3.2 Lower explosion limit / minimum explosible concentration

Oxidant-fuel mixtures will only ignite within a specified range of fuel concentration. If the fuel concentration of the mixture decreases below a certain point, the mixture becomes too lean for combustion to happen. This point is called the lower explosion limit. As the fuel concentration increases, the upper explosion limit is reached. Beyond the upper explosion limit, the fuel concentration becomes too rich to support combustion [80]. These limits may be used to determine guidelines for the safe handling of combustible materials [1, 34, 81]. With regards to this present study, LEL is used as an abbreviation for lower explosion limits of gases and vapor (unit, vol%), while MEC represents the minimum explosible concentration of dusts (unit, g/m³). With respect to gases or vapors, the explosion limits are influenced by parameters such as

pressure, temperature, oxygen concentration, ignition energy etc. Detailed discussion of these parameters could be referred to [82-89].

In the case of dusts, the MEC is influenced by particle size, temperature, volatile matter, oxygen content and moisture content as discussed in [90-93]. For example, the MEC values increase with the increase in particle sizes until a size is reached that cannot be ignited. The increase in particle size leads to the reduction of the particle specific surface area, and therefore the effective heating and reaction area of particles decrease. Moreover, the MEC decreases with the increase of initial temperature. This is because at higher temperature more volatile matters are vaporized contributing to the gas phase combustion. Encinar et al. [94] undertook an experimental study on the pyrolysis of maize and observed that an increase in temperature resulted in an increase of methane concentration produced from the maize. The authors added that the higher the temperature the higher the maximum gas concentration obtained and the lower the reaction time needed to reach it. MEC is also increased by the increase of moisture content, as higher moisture content leads to particle agglomeration, and hence reduces the particle surface area [95]. Higher moisture content also serves as a heat sink during a combustion process. Determination of the explosion limits for both gases and dusts are in accordance with EN 1839 [96] and EN 14034-3 [97], respectively.

The lower explosion limit of hybrid mixture is considered as the lowest concentration of fuel mixtures of different state of aggregate with air, below which self-sustaining flame propagation is not possible. For instance, a dust with a concentration below the minimum explosible concentration could form an explosible atmosphere by the admixture of small amount of gas or vapor which is below the lower explosion limits. These effects of the lower explosion limits of hybrid mixtures have already been discussed in section 2.5.

3.2.1 Models to estimate the lower explosion limit of dusts, gases and hybrid mixtures

Experimental determination of the explosion limits is time consuming and expensive as a result of the cost of equipment and labour. Due to this, different mathematical models to estimate the lower explosion limits of gases, dusts and hybrid mixtures are presented. Comparisons between

calculated results from these models and the experimental results are presented in section 6.1.4. It must be mentioned that only models relevant to this studies are presented in this section.

3.2.1.1 Models to estimate the minimum explosible concentration (MEC) of dusts

Different dusts models proposed by different authors based on different assumptions and conditions to predict the MEC of dusts are presented. Detailed discussion of each of the models could be obtained from the original source as cited appropriately.

3.2.1.1.1 Schönewald Model [98]

According to Schönewald, the MEC is the minimum amount of fuel necessary to shift the reactive system from initial to a “flame” temperature. Schönewald used this assumption to propose a semi-empirical model where constants were fitted to a wide range of dusts.

$$MEC = \frac{a}{\Delta h_r} - b \quad (3.2.1)$$

Where; MEC represent the minimum explosible concentration of dusts [g/m³], the values for “a and b” are given in Table 3.2. Δh_r indicates heat of reaction [J/g]. Schönewald supposed a “flame” temperature of 1000 °C.

Table 3.2: Constants for Schönewald model [98].

Constants	Coating Powder	Industrial Dusts	Fuel Dusts	Metal Dusts
a in J/g	1.235*10 ⁶	1.194*10 ⁶	1.390*10 ⁶	1.132*10 ⁶
b in g/m ³	2.532	0.604	7.952	1.540

3.2.1.1.2 Shevchuk et al. Model [99]

Shevchuk et al. used a discrete approach by considering individual particle behavior and interaction to develop a model to estimate the MEC of dust based on the following assumptions:

- The attainment of the ignition temperature of the suspension T_i controlled the moment of ignition of the heated particles;
- The combustion of the single particles occurs under diffusion conditions.

Shevchuk et al. proposed the following model based on the first law of thermodynamic and the assumption mentioned above as shown in eq. (3.2.2).

$$\text{MEC} = \frac{(T_i - T_0)c_g \rho_g}{FQ - c_d(T_i - T_0)} \quad (3.2.2)$$

Where; MEC represents the minimum explosible concentration of dust [g/m³], T₀ is the ambient temperature [K], T_i indicates the ignition temperature [K], Q indicates the heat of combustion of the particles [[kJ/kg], c_g and c_d are heat capacities of gas and dust material, respectively [(kJ/kg K)], ρ_g is the gas density [g/cm³], F is the special particle distribution factor resulting from this particular analysis (in the range of 0.5 to 0.75).

3.2.1.1.3 Buksowicz and Wolanski Model [100]

Buksowicz and Wolanski expressed an empirical correlation between the heat of combustion of the dust and the minimum explosible concentration. Eq. (3.2.2) presents a summary of the model proposed by Buksowicz and Wolanski.

$$\text{MEC} = 1.55 \times 10^7 Q^{-1.21} \quad (3.2.3)$$

Where; MEC is the minimum explosible concentration of dust [g/m³], Q is the heat of combustion [kJ/kg].

3.2.1.2 Models to estimate the lower explosion limit (LEL) of Gases

Mathematical models proposed by different authors based on different assumptions and conditions to predict the LEL of gases/ vapors are presented in this section. Detailed discussions of each of the model can be obtained from the original source and cited in the appropriate model.

3.2.1.2.1 Zabetakis model [26]

Zabetakis developed a semi-empirical model to estimate the lower explosion limit of flammable gases in air based on the stoichiometric concentration of paraffin hydrocarbon.

$$\text{LEL} = 0.55 \frac{100}{1 + 1.193k} \quad (3.2.4)$$

$$k = 4C + H + 4S - 2O - N - 2Cl - 3F - 5Br \quad (3.2.5)$$

Where; LEL is lower explosion limit of gas [vol%], C, H, S, O, N, Cl, F, Br are number of atoms of carbon, hydrogen, sulphur, oxygen, nitrogen, chlorine, fluorine and bromine in the molecule.

3.2.1.2.2 Shebeko et al. model [101]

Shebeko et al. considered a balance of energy in the chemical reaction of combustion. The heat losses were neglected and CO₂ and H₂O were the only combustion products. The equation below allows LEL to be determined from the data of the minimum number of moles required for a flame propagation reaction.

$$\text{LEL} = \frac{100}{1+n_a} \quad (3.2.6)$$

Where; LEL= lower explosion limit of gas [vol%], n_a is the number of moles of air per mole of fuel in the mixture at LEL.

$$n_a = g_f \Delta H_f + g_C n_C + g_H n_H + g_O n_O + g_N n_N \quad (3.2.7)$$

n_C, n_H, n_O and n_N are the number of moles of carbon, hydrogen, oxygen and nitrogen in the fuel respectively.

H_a, *H_{CO₂}*, *H_{H₂O}*, *H_{N₂}* and *H_{O₂}* are absolute mole enthalpies of air, carbon dioxide, steam, nitrogen and oxygen respectively while Δ*H_f* is the mole enthalpy of formation of the fuel.

where the values g_f, g_C, g_H, g_O, g_N are described by formulas below

$$\begin{aligned} g_f &= 1/(H_a^0 - H'_a) \\ g_C &= g_f(H'_C - H_{CO_2}^0 + H_{O_2}^0) \\ g_H &= 0.5g_f(H'_{H_2} - H_{H_2O}^0 + 0.5H_{O_2}^0) \\ g_O &= -0.5g_f(H_{O_2}^0 - H'_{O_2}) \\ g_N &= -0.5g_f(H_{N_2}^0 - H'_{N_2}) \end{aligned}$$

The superscript (' and ⁰) correspond to initial temperature and the adiabatic temperature respectively.

3.2.1.2.3 Spakowski model [102]

Spakowski proposed an empirical model to estimate the LEL of flammable gases based on the combustion enthalpy as presented in eq. (3.2.8)

$$\text{LEL} = -\frac{43.54}{\Delta H_{comb}} \cdot 100 \quad (3.2.8)$$

Where; LEL represents the lower explosion limit of gas [vol%], ΔH_{comb} is the combustion enthalpy [J/g]

3.2.1.3 Models to estimate the lower explosion limit of hybrid mixtures

Three different mathematical models to estimate the lower explosion limits of hybrid mixtures proposed by **Le Chatelier [103]**, **Bartknecht [104]** and **Mannan et al. [74]** are presented. These models are based on different assumptions and conditions with detailed discussions found in the original article.

3.2.1.3.1 Le Chatelier's model [103]

This model takes into account a homogeneous mixture by considering a constant flame temperature. It shows a linear relationship between the LEL of gas and the MEC of dust, and the weighted factor for each fuel in the fractional content in the mixture as represented in eq. (3.2.8).

$$LEL_{\text{hybrid}} = \frac{100}{\frac{Y_{\text{gas}}}{LEL_{\text{gas}}} + \frac{X_{\text{dust}}}{MEC_{\text{dust}}}} \quad (3.2.8)$$

Where; Y_{gas} and X_{dust} are the gas and dust concentrations in the fuel mixture, respectively, MEC_{dust} represents the minimum explosible concentration of dust [g/m³], LEL_{gas} is the lower explosion limit of gas [vol%] and LEL_{hybrid} indicates lower explosible limit [g/m³]

3.2.1.3.2 Bartknecht model [104]

The empirical formula below was derived from measurements by Bartknecht to estimate the lower explosion limits of hybrid mixtures. The LEL of hybrid mixtures decreases with an increase of gas concentration by a second order as represented in eq. (3.2.9).

$$LEL_{\text{hybrid}} = MEC_{\text{dust}} \left(\frac{Y}{LEL_{\text{gas}}} - 1 \right)^2 \quad (3.2.9)$$

Where; Y is the concentration of gas in the mixture [vol%], MEC_{dust} indicates minimum explosible concentration of dust [g/m³], LEL_{gas} represents lower explosion limit of gas [vol%] and LEL_{hybrid} is the lower explosible limit [g/m³]

3.2.1.3.3 Mannan et al. model [74]

This empirical model is an extension of both Le Chatelier equation and the Bartknecht equation by incorporating the deflagration index for both dust and gas as presented in eq. (3.2.10)

$$LEL_{\text{hybrid}} = MEC_{\text{dust}} \left[1 - \frac{Y}{LEL_{\text{gas}}} \right]^{(1.12 \pm 0.03) \frac{K_{St}}{K_G}} \quad (3.2.10)$$

Where; Y is the concentration of gas in the mixture [vol%], MEC_{dust} represents minimum explosible concentration of dust [g/m^3], LEL_{gas} indicates lower explosion limit of gas [vol%], LEL_{hybrid} is the lower explosible limit [g/m^3], K_{St} is the specific gas constant in [bar m/s] and K_G represents specific dust constant in [bar m/s]

3.3 Limiting oxygen concentration

The Limiting Oxygen Concentration (LOC) is the maximum content of oxygen in a mixture of combustible materials with air and inert gas, at which the mixture will just not allow an explosion. Below this limit adding any amount of combustible substances would not form an explosible mixture [105]. The LOC value is usually determined in accordance with **EN 14034-4** [106] and **ASTM-E2079-07** [107] for dust and gas respectively. Thus, in order to prevent hazards associated with explosions, the oxygen content in the system is decreased by mixing the fuel–air mixture with an inert substance so that self-sustained flame propagation could not occur [72]. The most commonly used inert gases are nitrogen, carbon dioxide, steam, flue gases and noble gases [108] however, as far as the scope of this study is concerned, nitrogen is considered as an inert gas. The LOC depends on the type of inert gas used, the temperature, and the pressure of the system. Figure 3.2 shows the effect of various inert gases on methane [26].

Moreover, an increase in the initial pressure may also lead to a decrease in the maximum allowable oxygen concentration. For example, a rise in pressure from 1 to 4 bar resulted in a decrease of the limiting oxygen concentration of 2 vol% for brown coal [109].

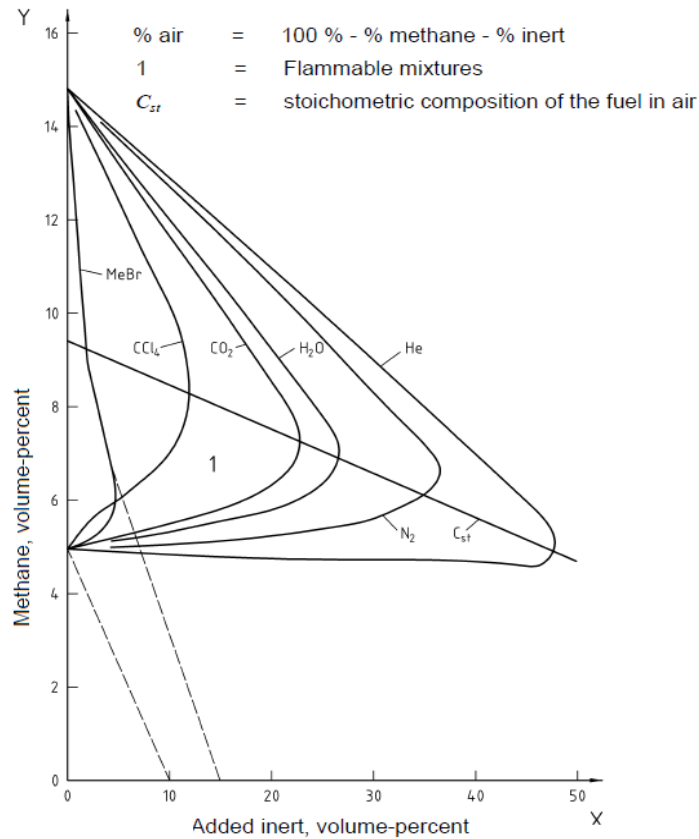


Figure 3.2: Influence of inert gas on the explosion limits of methane [26].

Furthermore, both the explosion violence and ignition sensitivity of dust clouds decrease with decreasing oxygen content of the gas in which the dust is suspended. **Wiemann [110]** investigated the influence of the oxygen content on the maximum pressure and maximum rate of pressure rise of coal dust explosions in the 1m³ vessel and observed that both the explosion pressure and the rate of pressure rise decreased with decreasing oxygen content.

Also, the LOC increases with increasing particle size of the dust. **Sweiss et al. [111]** investigated the influence of particle size of synthetic organic dusts on the LOC for flame propagation through dust clouds. The results from the study indicated that the LOC decreased with decreasing particle size down to 100 μm. Below 100 μm, the LOC was practically independent on the particle size. However, the addition of only 5% by mass of a fine dust (60 μm) to a coarse main dust (200-1000 μm) reduced the LOC by at least 60% of the difference between the values of the coarse dust only [79].

Furthermore, the initial temperature of the combustible mixtures affects the LOC of the dust cloud. **White et al. [112]** investigated the influence of temperature on the LOC of seven different combustible dusts. It was observed that, increasing the temperature of the reaction mixture decreases the LOC of the dusts as shown in Figure 3.3.

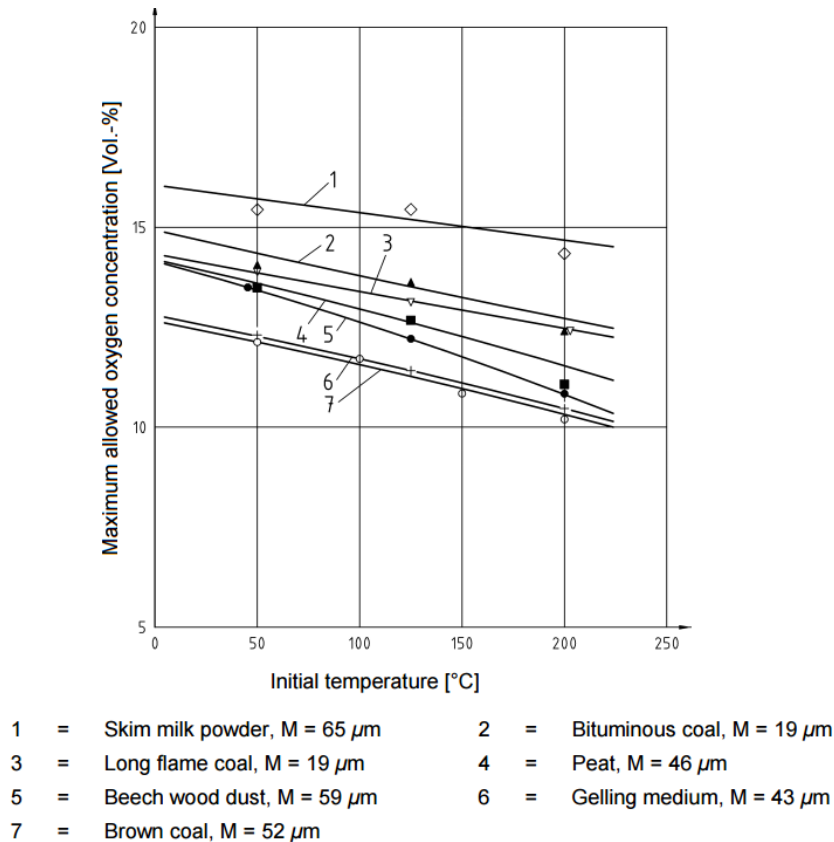


Figure 3.3: Temperature influence on the limiting oxygen concentration of different dusts [112].

3.4 Minimum ignition energy

The minimum ignition energy refers to the smallest amount of energy that an electric spark discharge must have to cause an ignition of a given fuel-air mixture at given test conditions [113]. The experimental determination of minimum ignition energy is done using different types of electric sparks [114]. Detailed information on spark energy as well as spark generation could be referred to [114-116]. The term electric spark is defined as a disruptive discharge through a single ionization channel that bridges the gap between two conductive electrodes [23]. Experimentally, the minimum ignition energy is determined using MIKE 3 apparatus and Hartmann MIE III in accordance with **EN 13821 [117]** for dust and **ASTM-E582 [118]** for gases.

The MIE values depend on the composition of the mixtures, the method of the spark generation and properties of the electric circuit [116]. Moreover, other parameters such as pressure, temperature, flow characteristics, spark gap length, and discharge duration also influence the MIE. With respect to dust, particle size and the moisture content are also considered. For example, an increase in the particle size of a dust decreases the surface area available for an ignition to prevail and consequently, largely increases minimum ignition energy [119]. Thus, dust particles with smaller median value are easy to ignite as compared to the one with coarser size [22]. Kalkert [120] presented a model for the theoretical calculation of MIE of a dust cloud based on particle size.

$$E_{min} = (4\pi k)^{\frac{3}{2}} \rho c \left[\frac{\ln 2 \rho_s c_s}{\lambda} \right]^{\frac{3}{2}} \cdot T_{fl} d^3 \quad (3.4.1)$$

Where; $k = \frac{\lambda}{\rho_s c_s}$ is the “temperature conductivity” of air, C represent the concentration [g/m³], λ is the thermal conductivity of the dust [W/m.K], T_{fl} indicates the adiabatic flame temperature [K], d is the diameter of the dust particle [m], ρ_s represent the density of the dust [kg/m³] and C_s indicates specific heat capacity of the dusts [kJ/kg K]

The validation of this model only holds, if the dust particles are considered to be of spherical shape and uniform diameter. It is also assumed that the dispersion of dust particles in the air is homogeneous. According to Kalkert’s model, MIE of a dust cloud increases to third power of the particle diameter [120]. This signifies the fact that particle size greatly influences the MIE value of a dust cloud. Moreover, Nagy et al. [121] studied the explosibility of aluminium dust and observed that the MIE increases with increasing particle size as shown in line 1 in Figure 3.4.

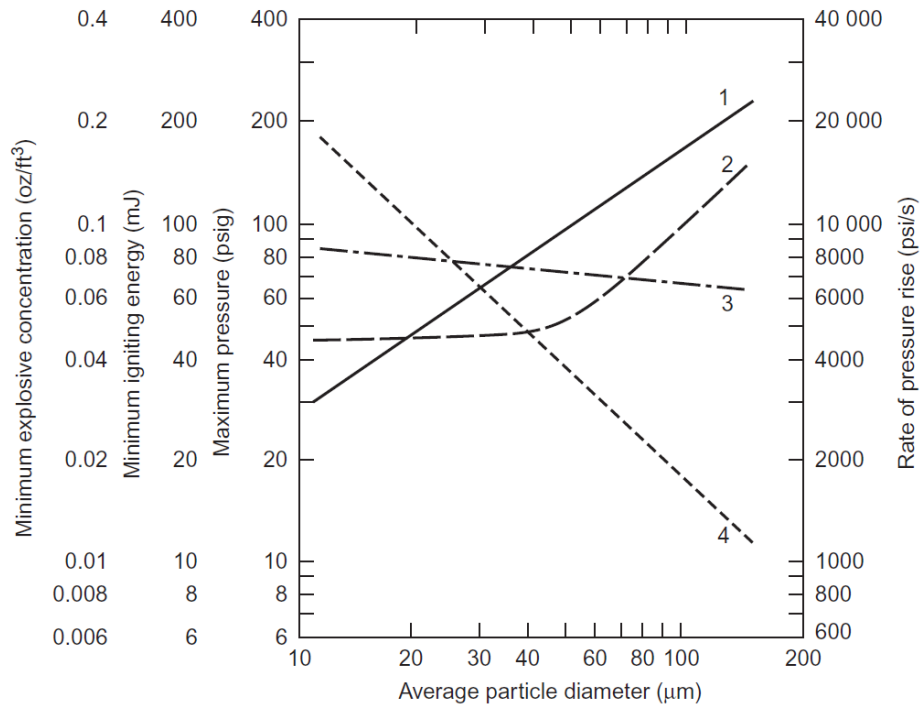


Figure 3.4: Dust explosibility characteristics: effect of particle size on some principal parameters for atomized aluminium [121]. (1) minimum ignition energy; (2) minimum explosive concentration; (3) maximum explosion pressure; and (4) maximum rate of pressure rise.

Other parameters which influence the MIE determination are explained in detail in the following articles: spark generation and properties of the electric circuit [122], pressure [123], temperature [124], turbulence [125], spark gap length [126], and discharge duration [127], oxygen concentration [126] and the moisture content of dusts particle [22].

3.5 Minimum ignition temperature

According to ASTM E1491 [128], the minimum ignition temperature (MIT) is defined as the lowest temperature of a heated surface which can ignite a fuel oxidizer mixture within the explosible range under the specified test condition. Experimentally, the MIT of dusts cloud is determined using Godbert-Greenwald furnace or the BAM oven in accordance with the European standard procedure [129] while for gases or vapors the MIT is determined in the Erlenmeyer flask [130].

With respect to gases, the MIT is influenced by parameters such as pressure, fuel type, fuel concentration, and oxidiser. An increase in pressure generally decreases the ignition temperature

of a gas mixture. The eq. (3.5.1) from **Zabetakis [26]** shows the dependency of pressure and the ignition temperature. It could be observed that the ignition temperature is inversely proportional to the pressure.

$$\ln\left(\frac{P_c}{T_0}\right) = \frac{E_a}{2RT_0} + C \quad (3.5.1)$$

where; P_c and T_0 are the initial pressure and temperature at the critical condition, E_a is the activation energy of the applied Arrhenius reaction, R is the universal gas constant and C is a constant depending on different factors including the surface/volume ratio of the vessel and the heat transfer coefficient.

The ignition temperature is also strongly dependent on the fuel type. As shown in Table 3.3 and Figure 3.5, the ignition temperature for hydrocarbon-air mixtures decreases with increasing molecular weight and the chain length.

Table 3.3: Summary of the MIT of alkane-air mixture [83].

MIT (K)	Fuel
868	Methane
788	Ethane
743	Propane
733	i-butane
638	n-butane
533	pentane
503	hexane

With respect to the dust cloud, the MIT is influenced by parameters such as moisture content, inert materials, volatile matter, oxygen concentration and dust particle size.

For instance, the influence of moisture content on the MIT of dust clouds is more predominant. The specific role of moisture in reducing both the ignition sensitivity and the explosion violence of clouds of organic dusts is complex. First, evaporation and heating of water represents an inert heat sink. Second, the water vapor mixes with the pyrolysis gases in the preheating zone of the combustion wave and makes the gas mixture less reactive.

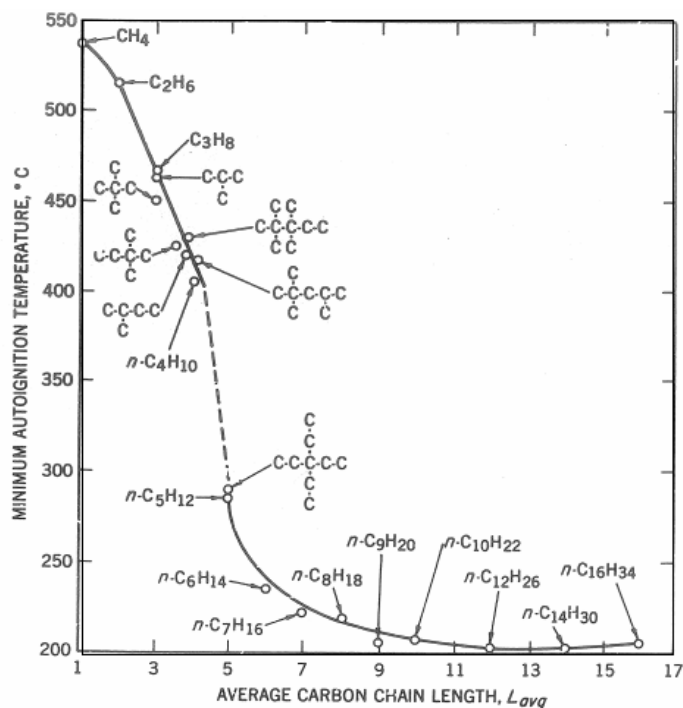


Figure 3.5: The MIT of hydrocarbon-air mixtures as a function of the average carbon chain length [26].

Third, moisture increases the antiparticle cohesion of the dust and prevents dispersion into primary particles [22]. For example, van Laar et al. [131] reported that wheat flour of 14 wt% moisture had MIT of 470°C, whereas dry flour had 440°C. For starch, the values were 400°C for the dry powder and 460°C with 13% moisture. The detailed information on the effect of other parameters on the MIT of dust cloud could be referred to following: inert dust content [132], volatile matter [79, 133], oxygen concentration and dust particle size [22].

3.5.1 Mathematical models to estimate the minimum ignition temperature of dusts

Mathematical models proposed by different authors based on different assumptions and conditions to estimate the MIT of dusts are presented in this section. Detailed discussion of each of the models can be obtained from the original source, which are cited in the appropriate model. It must be mentioned that only models relevant to this research study as well as availability of the input data will be considered for comparisons with the experimental results.

Available models for the ignition of dust particles on hot surfaces refer to two types of reaction mechanisms: (1) Heterogeneous reaction, this involves oxidation taking place at the surface of

solid particles. (2) Homogeneous reaction, it also involves the oxidation of volatiles evolved from dust particles prior to ignition. Six different models developed by different authors are summarized below.

3.5.1.1 Cassel and Liebman model [134]

This model is based on single particle to dusts cloud combustion. A heterogeneous oxidation reaction at the surface of an individual particle leads to its ignition. Conduction and radiation are the form of heat transfer from the particle surface to the ambient. The final form of this model presented in eq. (3.5.2) below could be used to predict the MIT of dust.

$$T_i = T_s \left(1 - \frac{RT_s}{E}\right) \quad (3.5.2)$$

Where; T_i is the minimum ignition temperature [K], T_s represents the temperature of particle surface [K] E indicates the activation energy of fuel, [J/mol] and R is the gas constant, [J/mol K].

3.5.1.2 Nagy and Surincik model [135]

According to this model, a heterogeneous oxidation of solid particles is responsible for the ignition process. Heat conduction and convection both exist as heat transfer processes. This model is based on the ignition criterion that the rates of heat generation and heat removal are equal. The MIT of dust can be calculated from eq. (3.5.3) below.

$$C_{gF} f * \exp(-S_d E / RT_F) = K' T_i^2 \quad (3.5.3)$$

$$K' = \frac{k_c R M_{ot}}{S_d k_r H E} \quad (3.5.4)$$

Where; T_i indicates the minimum ignition temperature [K], C_{gF} represents concentration of oxygen at reaction or furnace temperature [g mol/cm³], S_d is the factor accounting for the specific surface area of dust [-], T_F is the furnace temperature [K] E indicates the activation energy of fuel, [J/mol] and R is the gas constant, [J/mol K], k_c = coefficient of heat transfer [1/s], H is the heat of reaction [J/mol], k_r indicates the reaction rate constant [J/mol s], M_{ot} is the molecular weight of oxygen [g/mol] and f indicates the frequency factor [cm/s].

3.5.1.3 Mitsui and Tanaka model [136]

In this model a spherical cloud of particles is ignited with the assumption that the oxidation and reaction of dust particle are a surface phenomenon. The ignition temperature of dust could be calculated from eq. (3.5.5) below.

$$T_i = \frac{ET_s - 2RT_s^2}{E - RT_s} \quad (3.5.5)$$

Where; T_i is the minimum ignition temperature [K], T_s indicates the temperature of particle surface [K], E is the activation energy of fuel [J/mol] and R indicates the gas constant [J/mol K].

3.5.1.4 Mittal and Guha model [137]

Mittal and Guha proposed this model to estimate the ignition temperature of organic dusts by applying the thermal balance criteria for ignition. The final form of this model presented in eq. (3.5.6) below could be used to predict the MIT of dust.

$$T_i = T_s \left(1 - \frac{RT_s}{E}\right) \quad (3.5.6)$$

Where; T_i indicates the minimum ignition temperature [K], T_s is the temperature of particle surface [K] E represents the activation energy of fuel [J/mol] and R indicates the gas constant [J/mol K].

3.5.1.5 Krishna and Berlad model [138]

This model considers the ignition of a cloud of solid particles uniformly dispersed in a gas. A heterogeneous reaction at the surface of the particles controls the ignition process. The particle is heated by the gas/solid reaction. Heat transfer takes place from the particle to the surrounding gas. The gas in the cloud loses heat to the ambience at the cloud/vessel boundary. A steady state condition is assumed when both the gas and the particle temperature gradients become zero. The ignition temperature of dust cloud could be calculated from eq. (3.5.7) below.

$$T_i = T_s \left(1 - \frac{RT_s}{E}\right) \quad (3.5.7)$$

T_s could be obtained from eq. (3.5.8) below

$$\frac{1}{T_s^2} \exp\left(\frac{-E}{RT_s}\right) = \frac{h_g R}{S_p^{1/2} E A_c \rho_g Y_{0H}} \quad (3.5.8)$$

Where; T_i is the minimum ignition temperature [K], T_s represents the temperature of particle surface [K] E indicates the activation energy of fuel [J/mol] and R is the gas constant [J/mol K].

3.5.1.6 Zhang and Wall model [139]

This model defines a dust ignition of spherical particles dispersed in oxygen. The model made the assumption that the particles undergo devolatilization and heterogeneous surface oxidations. Heat convection and radiation are considered as heat loss from the dust cloud to the surroundings. The ignition temperature of dust could be calculated from eq. (3.5.9) below.

$$T_i = T_g - \frac{Q_v + n_p Q_p}{h_s S} \quad (3.5.9)$$

n_p could be calculated from (3.5.10) below

$$n_p = \frac{6C_d V_f}{\pi D_p^3 \rho_d} \quad (3.5.10)$$

Where; T_i indicates the minimum ignition temperature [K], $T_{i, g}$ is the minimum ignition temperature of gas [K], Q_v is the total rate of heat generation due to volatile matter, n_p is the number of dust particles in the furnace or in an elemental dust cloud, h_s is the coefficient for heat exchange between cloud and surroundings [J/cm² s K], S is the surface area of dust cloud [cm²], Q_p represents total rate of heat generation per particle [J/s], D_p represents initial diameter of dust particle [cm], and ρ_d is the density of dust, [g/cm³].

3.6 Explosion severity: maximum overpressure P_{max} and the maximum rate of pressure rise $(dP/dt)_{max}$

The P_{max} indicates the highest pressure an explosion at the optimum concentration can produce in a closed vessel while the $(dP/dt)_{max}$ represents the steepest slope of a tangent line at the pressure-time curve at the optimum concentration. They describe the violence of reaction of fuel-air mixtures of optimum concentration after ignition in a closed vessel [22]. They are essential for any type of equipment design for handling combustible materials; in particular, these values are

used by manufacturers to validate the design of protection systems (such as spark detection, explosion venting, explosion suppression and explosion containment). The violence of an explosion is dependent on the rate of energy release from a chemical reaction. The rate of pressure rise is defined as the slope of a tangent, laid through the point of inflection in the rising part of the pressure/time curve as shown in Figure 5.7 in section 5.23. The term $(dP/dt)_{\max}$ depends on the volume of the vessel in which the explosion occurs. In order to take into account, the influence of the volume on the course of explosion, the deflagration index, K_{st} for dust and K_G for gas, Cubic relationship is taken into consideration, as:

$$K_{st} \text{ or } K_G = \left(\frac{dP}{dt}\right)_{\max} * V^{\frac{1}{3}} \quad (3.6.1)$$

Determinations of the explosion severities are done in the standard 20-liter sphere in accordance with the standard similar to the European standard **EN 14034-1 [140]** for P_{\max} and $(dp/dt)_{\max}$ and **EN 14034-2[141]** for dust and gases/vapor respectively. The determination of both P_{\max} and $(dp/dt)_{\max}$ are generally influenced by initial temperature, oxygen concentration, turbulence and volatile content. For dusts testing the particle size and moisture content are additionally considered. For example, the explosion severity decreases with an increase in moisture content. As the dust becomes dry, it becomes more easily ignitable and burns with greater intensity. The dust having greater moisture content is more difficult to ignite and will burn more slowly due to the moisture within the dust absorbing the heat during evaporation. **Eckhoff [22]** investigated the effect of moisture content on the $(dP/dt)_{\max}$ of starch at different turbulence levels and concluded that the $(dP/dt)_{\max}$ decreases sharply as the moisture content increases. More information on the influence of other parameters on the explosion severities could be referred to: initial temperature [142], oxygen concentration [110, 143], turbulence [143], volatile content [144] and particle size [121].

Chapter Four

4 Material properties and preliminary analysis

4.1 Dusts

In order to obtain a general understanding of dust and hybrid mixture explosion, a wide variety of materials with different properties and reaction mechanisms were chosen. For the dusts, materials as diverse as food substances, metals, plastics, natural products, fuels and artificial materials were chosen. The raw dust samples were received in different forms and conditions. For this reason, both physical and chemical analyses were performed on each dust sample. The results of these analyses are explained below.

4.1.1 Moisture content

The moisture content is the quantity of water contained in a dust sample. It can be determined from the weight loss registered during drying. It is usually expressed as a mass fraction (% mass of water in the material). The moisture content was determined using a thermogravimetric moisture analyser according to **ISO 5071:1996 [145]**. The results are presented in in Table 4.1. The moisture content of all dust samples was below 2 wt%.

4.1.2 Volatile Content

In the context of dust explosions, materials with a high of volatile content ignite easily and produce explosions of high severity. The reason for this phenomenon can be explained as dusts

with a higher volatile content produce more combustible gas at the same conditions, which contributes to the gas phase combustion [146]. The determination of volatile content was performed in accordance with **ISO 5071: 1996 [145]**. The content of volatile material in the dust samples varied between 14 wt% and 99.98 wt%. The content of volatile material determined for each dust sample is presented in Table 4.1. Notably, materials with high carbon and low hydrogen contents, such as CN4 (a mixture of activated carbon and lignite coal) and charcoal, had volatile contents below 20 wt%.

4.1.1 Elemental analysis

The elemental analysis for all the dust samples were determined both quantitatively and qualitatively and the results are shown in Table 4.1. Based on the results of the quantitative elemental analysis, the molecular formula for the dust samples could be determined. Determinations were done according to **ISO 29541 and ISO 19579:2002 [147]** with CS230 (LECO®) for carbon and sulphur, and CHN628 (LECO®) for carbon, hydrogen and nitrogen respectively.

4.1.2 Particle size distribution

The particle size is one of the most important parameters that affects the explosion characteristics of dusts and hybrid mixtures. Because the particle size and shape varied widely in the dust samples, the samples were prepared by grinding (Retsch Ultra Centrifugal ZM1000). The particle size distribution of each sample was determined using a multi-wavelength laser diffraction particle size analyzer (Beckman Coulter LS 13320 CAMSIZER®) according to **ISO 13319:2007 [148]**. The measured particle size distributions are shown in Figure 4.1 and Figure 4.2. The values of d50 and d90 are summarized in Table 4.1. The median diameter d50 is the diameter where 50 % by weight of the sample is finer and 50 % is coarser. d (0.9) 90 % is a measure for the largest particle in the sample. Out of the twenty dust samples, corn-starch and toner samples had the finest particle sizes with a median particle size of 14 µm while char coal dust had the coarsest particle size with a median size of 79 µm.

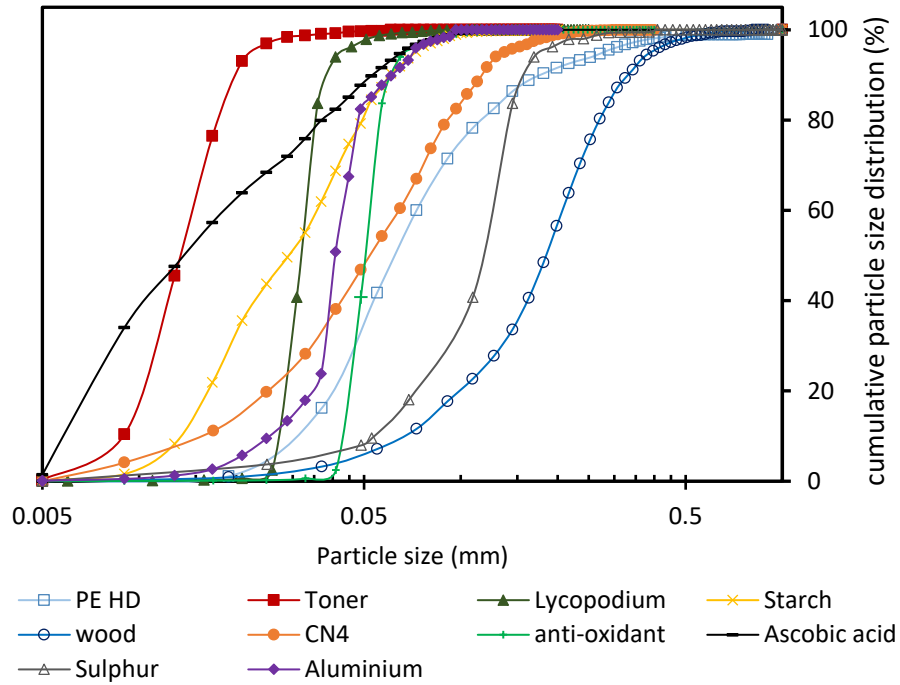


Figure 4.1: Particle size distributions of the dust samples.

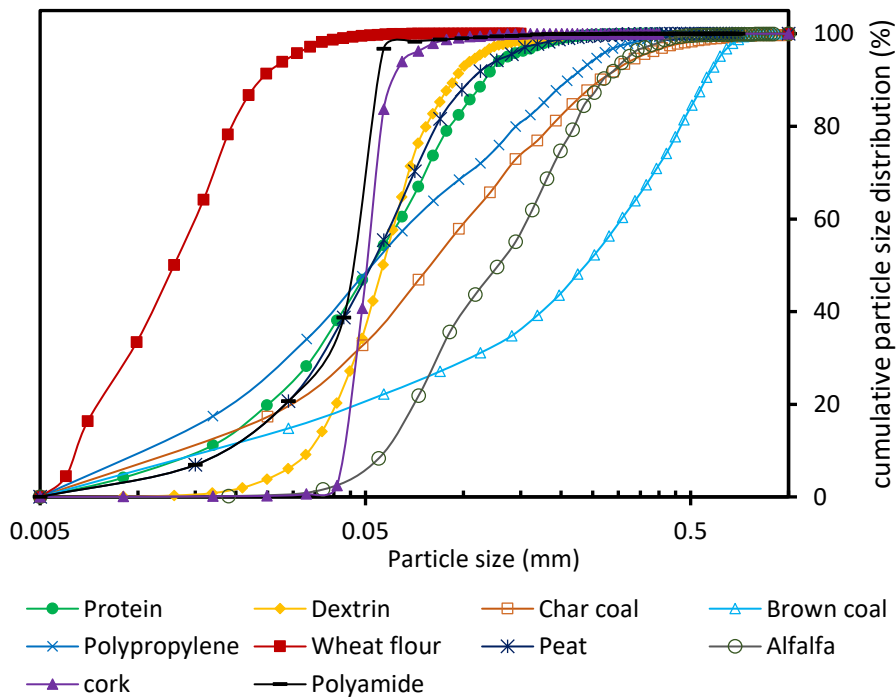


Figure 4.2: Particle size distributions of the dust samples.

Table 4.1: Physical and chemical properties of dusts.

Dust sample	Particle size (μm)		Volatile Content (% wt)	Moisture Content (% wt)	Heat of combustion (MJ/Kg)	Elemental analysis (% wt)				
	d50	d90				C	H	O	S	N
Starch	14	21	93.77	0.50	15.30	44.3	6.3	48.9	0.4	0
Lycopodium	32	38	91.06	0.35	28.44	69.3	9.6	19.6	0.4	1.3
Toner	14	21	90.18	0.92	35.79	86.1	7.7	5.2	1.0	0.0
HD-PE	61	165	99.78	0.01	42.74	84.8	14	1.36	0.1	0.0
Wood	61	201	84.38	0.20	16.44	50.3	6.3	43.2	0.1	0.0
CN4	52	115	17.08	0.23	26.63	80.4	1.3	14.0	3.0	0.4
Wheat flour	52	121	79.60	0.38	15.64	45.6	6.6	45.9	1.8	0.0
Protein	46	76	81.47	1.93	20.49	53.0	7.2	23.5	0.3	16
Polypropylene	34	84	98.67	0.68	39.68	86.0	14	0.0	0.0	0.0
Peat	45	176	68.76	1.43	17.46	57.4	5.8	35.3	1.1	0.6
Dextrin	56	93	99.17	1.08	13.35	43.8	6.4	49.1	0.7	0.0
Charcoal	79	264	14.99	0.77	29.36	90.2	2.8	6.7	0.2	0.2
Brown coal	37	55	55.12	1.56	21.52	69.1	6.7	5.6	0.6	1.3
Antioxidant	18	54	94.56	0.58	32.16	72.8	6.7	12.5	5.3	0.7
Cork	78	154	80.79	0.86	22.99	63.8	6.9	28.4	0.4	0.4
Polyamide	52	107	97.98	0.97	29.46	63.7	6.0	14.3	0.0	15
Alfalfa	32	158	76.00	1.96	16.27	50.6	6.6	39	0.2	3.5
Ascorbic acid	32	106	83.14	0.42	11.46	41.8	4.7	53.9	0.3	0.0
Aluminium	54	85	-	1.21	-	-	-	-	-	-
Sulphur	42	83	-	0.67	-	-	-	-	100	-

4.1.3 Heat of combustion

The heat of combustion of a substance is determined by measuring the heat produced by a complete combustion of the material. It is usually expressed in joules per kilogram. Heat of combustion were determined according to **ISO 1928:2009-06 [149]**. The heat of combustion of solid materials can be determined by the bomb calorimetric method (IKA®, C 200). The results obtained for the dust samples varied between 11 MJ/kg and 43 MJ/kg and are listed in Table 4.1.

4.1.4 Microscopic images

The microscopic images were obtained through scanning electron microscopy (SEM). In order to visualize the surface structure of the dust particles, (SEM) images of the dusts are presented in Figure 4.3. The images provide insight into the particle shape, agglomeration behavior and pore size of each dust sample. Starch, dextrin and polypropylene particles could be seen from the SEM

image to agglomerate, thereby increasing the individual particle size and the particle settling velocity. The coal dusts had smooth surfaces and hardly agglomerated.

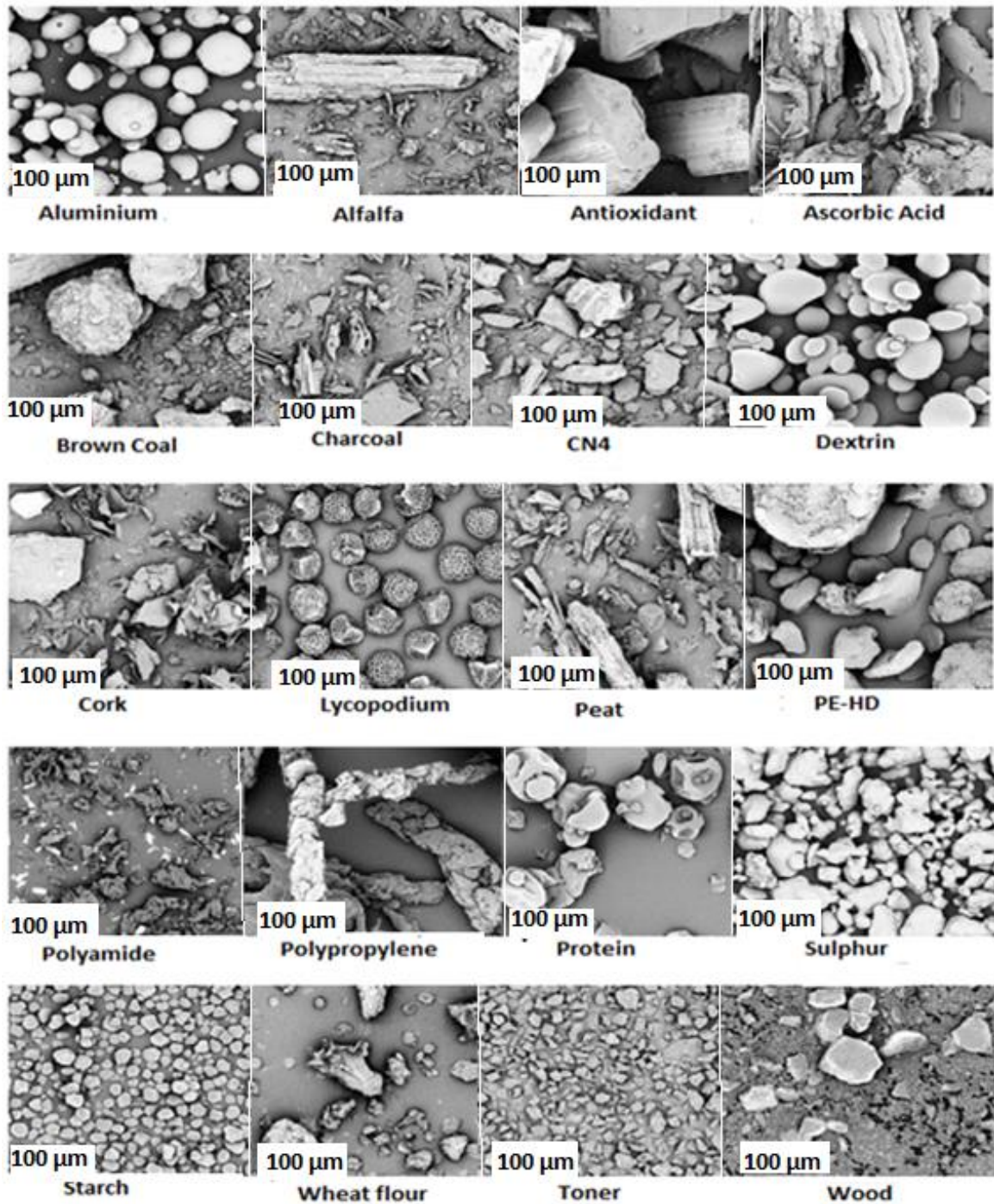


Figure 4.3: SEM images of dusts.

4.2 Choice and properties of gases and solvents

Three flammable gases; methane, propane and hydrogen (source: Air Liquide Technische Gase GmbH, Magdeburg) and six flammable solvents: ethanol (source: CVM Chemie-Vertrieb Magdeburg GmbH & Co. KG:), isopropanol (source: CVM Chemie-Vertrieb Magdeburg GmbH & Co. KG), toluene (source: Stockmeier Chemie Eilenburg GmbH & Co. KG), acetone (source: Carl Dicke Magdeburg GmbH & Co. KG), hexane (source: Carl Dicke Magdeburg GmbH & Co. KG) and heptane (source: Carl Dicke Magdeburg GmbH & Co. KG) were used. The choice of both solvents and gases were based on the behaviors and reaction mechanism such as burning velocity, heat of combustion etc. For example, burning velocity is high hydrogen (3.06 m/s), but is slower for propane (0.45 m/s) and methane (0.39 m/s) [150]. Selecting materials with different reaction behaviors helps to understand the parameters influencing the complex explosion behavior of hybrid mixtures. The most important (physical, chemical, ignition, thermodynamic) properties of investigated materials are listed in Table 4.2 for gases and Table 4.3 for solvents.

Table 4.2: Properties of gases [83, 150].

Properties	Methane	Propane	Hydrogen
Molecular formula	CH ₄	C ₃ H ₈	H ₂
Purity (%)	99.87	99.00	99.99
Density (g/cm ³)	6.6E-4	4.93E-4	8.99E-4
Molecular weight (g/mol)	16	44.1	2
Explosible range (vol. %)	4.4-17	1.7-10.8	4.0-77
Melting point (°C)	-161	-187	-259
Specific heat capacity (J/mol. K)	35.69	73.60	28.80
Boiling point (°C)	-182.5	-42.1	-253
Heat of vaporization (kJ/mol)	-74.87	-103.80	0.00
Max. explosion pressure (barg)	8.1	9.8	8.3
MESG (mm)	1.14	0.92	0.29
Temperature class	T1	T1	T1
Explosion Group	IIA	IIA	IIC
Heat of combustion: (MJ/kg)	55	50	141
: (kJ/mol)	-286	-890	-2220
Diffusivity (m ² /sec)	1.60	1.00	6.11
Adiabatic flame temperature (K)	2226	2267	2380
Burning velocity (cm/s)	39	45	306

Table 4.3: Properties of solvents [83, 150, 151].

Properties	Ethanol	Isopropanol	Toluene	Acetone	Hexane	Heptane
Molecular formula	C ₂ H ₆ O	C ₃ H ₈ O	C ₇ H ₈	C ₃ H ₆ O	C ₆ H ₁₄	C ₇ H ₁₆
Purity (%)	96.90	99.9	99.00	99.60	98.9	98.5
Density (g/cm ³)	0.79	0.78	0.87	0.79	0.65	0.684
Molecular weight (g/mol)	46.07	60.1	92.1	50.2	86.18	100.2
Explosible range (vol. %)	3.3–19	2.0-13.4	1.1-7.8	2.3- 14.0	1.2–7.7	1.1-7
Melting point (°C)	-114	-88	-95	-95	-96	-91
Specific heat capacity (J/mol K)	112	246	155	126	265	224
Boiling point (°C)	78.0	82	111	57	68.5	98
Heat of vaporization (kJ/mol)	38	44	38	28	41	37
Max. explosion pressure (barg)	8.4	8.2	7.7	9.7	9.5	9.4
MESG (mm)	0.89	0.99	1.06	1.04	0.93	0.97
Temperature class	T2	T2	T1	T1	T3	T3
Explosion Group	IIB	IIA	IIA	IIA	IIA	IIA
Burning velocity (cm/s)	47.0	41.0	41.0	54.0	38.5	38.6
Vapor pressure (barg) 20 °C	0.059	0.044	0.029	0.240	0.160	0.048
Solubility in H ₂ O (g/100g)	Miscible	Miscible	0.0500	Miscible	0.0014	0.0003
Eluent strength	0.880	0.820	0.290	0.560	0.010	0.011
Relative polarity	0.654	0.5646	0.099	0.355	0.009	0.012
Viscosity (kg m ⁻¹ s ⁻¹ at 20°C)	0.0011	0.0024	0.00059	0.00036	0.0003	0.00032
					1	
Surface tension @ 20 °C in mN/m	21	23	28	27	20	18
Heat of combustion (kJ/mol)	-1367	-2006	-3910	-1785	-4863	-4317

Chapter Five

5 Experimental Methods and Procedures

5.1 Tests in the 20-liter sphere

Experiments were performed in a 20-liter sphere (Siwek Apparatus) to determine the maximum explosion pressure (P_{\max}), maximum rate of pressure rise $(dP/dt)_{\max}$, lower explosion limit (LEL) and limiting oxygen concentration (LOC). Measurements were performed in accordance with **EN 14034 1-4 [152]**. A diagram of the 20-liter sphere apparatus is presented in Figure 5.1.

The commercially-available test apparatus consisted of a hollow sphere made of a stainless steel with an internal volume of 20-liter, a jacketed cooling system, a vacuum pump for evacuating the chamber, distribution systems for gases and dusts, an ignition source at the center of the sphere, pressure measurement, and a data recording system (Kuhner KSEP-Software). The apparatus was modified to include a distribution system for liquid sprays as well as vapors and gases. The system for introducing a liquid spray consisted of a solvent chamber (0.2-liter), a fuel injection nozzle (Mitsubishi E7T05071), and a spray control system (time controller and nozzle voltage regulator) as shown in Figure 5.2 and 5.3. The spray system (liquid chamber) was connected to the 20-liter sphere at point (#9) in Figure 5.3.

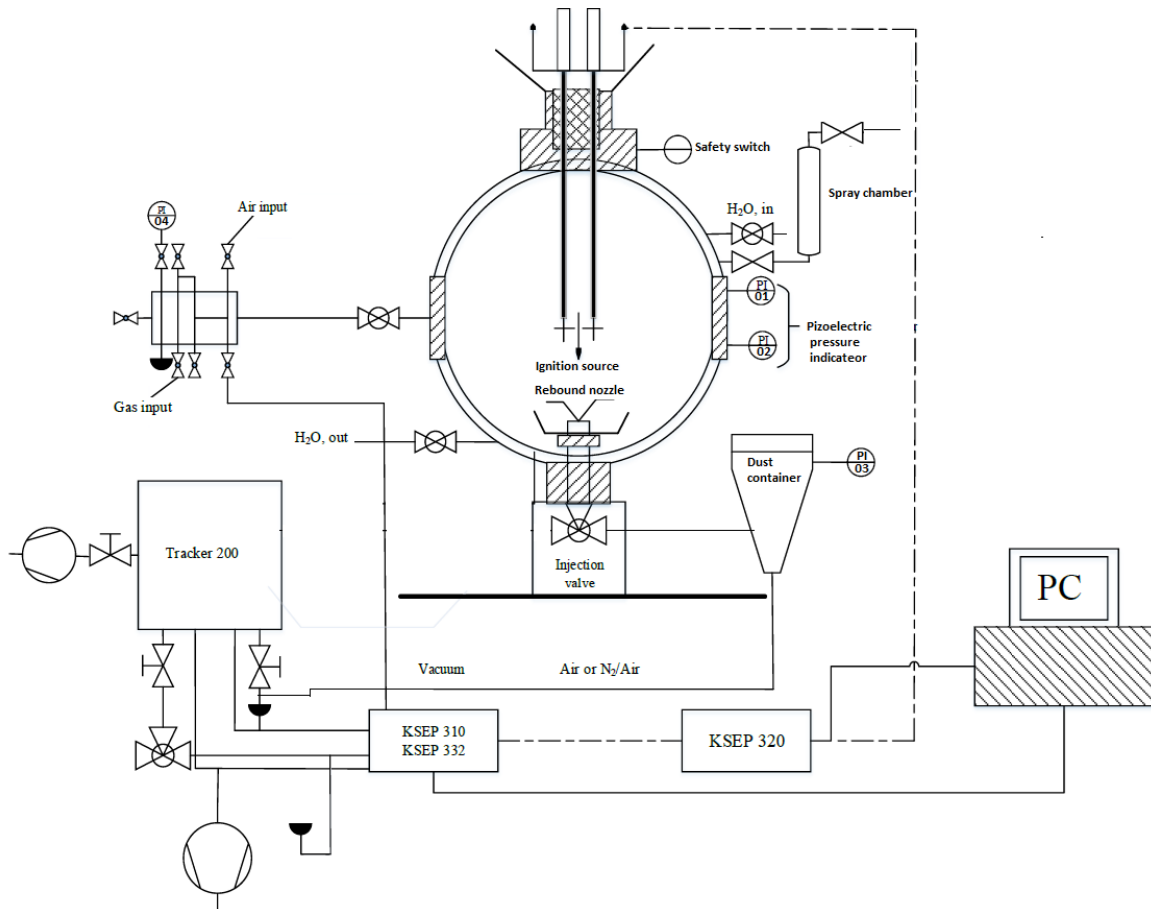


Figure 5.1: Technical diagram of the 20-liter sphere apparatus.

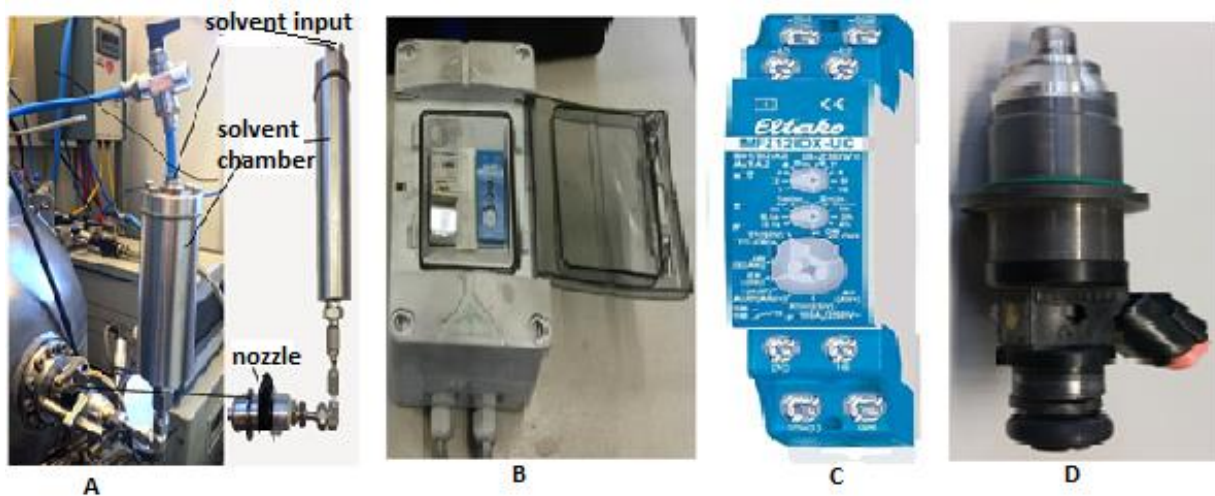
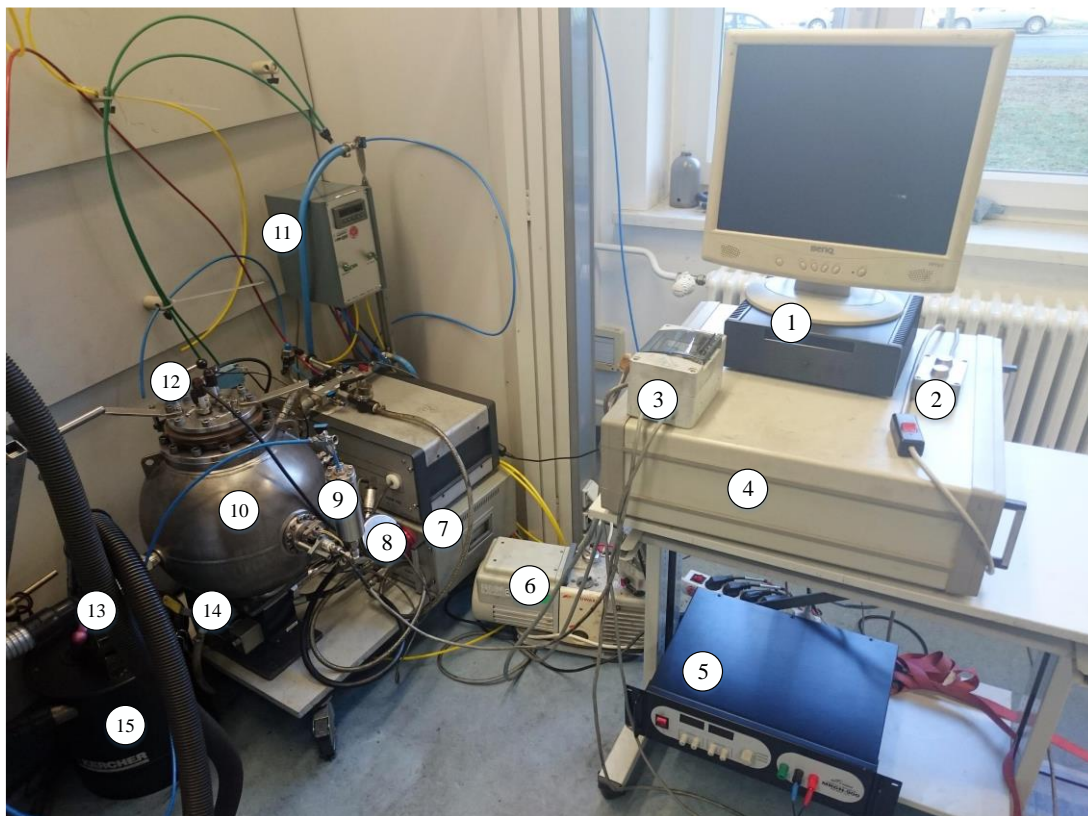


Figure 5.2: (A) spray system, (B) spray control system, (C) timer (D) nozzle.

An ignition source was placed at the center of the sphere through a flange located on the top of the combustion chamber. International standards [152] require ignition energies of 10 kJ (2 x 5 kJ) for testing dusts, 10 J for gases and 2 kJ (2 x 1 kJ) for hybrid mixtures. The igniter assemblies are shown in Figure 5.4. The electrical spark electrodes are two round tungsten rods with ends ground to a point whose tips are spaced 6 mm apart. They are supplied with power from a high voltage transformer (KSEP 320) and produce a permanent spark (15 kV, 30 mA) [153]. The chemical igniters (40 wt% zirconium, 30 wt% barium nitrate, 30 wt% barium peroxide) are activated electrically by a low-voltage source and provide a dense cloud of hot dispersed particles with very little gas by-product. The delay time (60 ms) was constant for all tests in the 20-liter sphere in this study.



- | | | |
|-----------------------------------|--------------------------|-------------------|
| ① Data processing unit | ⑥ Vacuum pump | ⑪ Gas mixing unit |
| ② Air in/out unit | ⑦ Control system | ⑫ Safety switch |
| ③ Time controller for spray input | ⑧ Dust storage container | ⑬ Relieve valve |
| ④ KSEP 310 | ⑨ Liquid chamber | ⑭ Water inlet |
| ⑤ Nozzle's voltage regulator | ⑩ 20 liter vessel | ⑮ Dust cleaner |

Figure 5.3: Experimental arrangement of the 20-liter sphere.

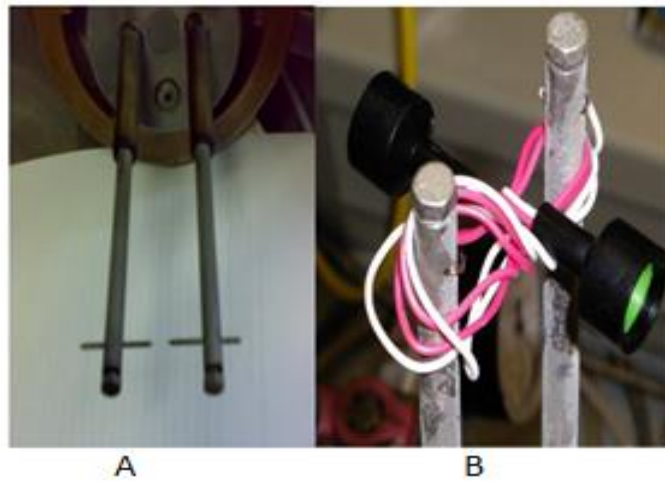


Figure 5.4: (A) electrical ignition assembly (B) chemical ignition assembly.

5.1.1 Experimental procedure for single substances

5.1.1.1 Dusts

Dust explosion testing was carried out using the apparatus and method specified in the European standard [152]. For dust explosion testing, a defined amount of combustible dust was placed into the dust container. The explosion chamber, which was initially filled with air at atmospheric pressure, was then evacuated to 0.4 bar absolute. An automatic test sequence was initiated to pressurize the dust container to 20 barg, and then the fast acting valve on the dust container outlet was opened to inject dust into the explosion chamber through a rebound nozzle. The rebound nozzle ensured an even distribution of dust within the explosion chamber. The control system activates the igniters at the center of the sphere 60 ms after the dust was dispersed. Explosion pressures were measured for a range of dust concentrations using two piezoelectric pressure transducers. Each test was repeated three times to ensure a reproducible investigation of the explosion properties. The arithmetic mean of the maximum values i.e. both maximum pressure and maximum rate of pressure rise for each measurement were obtained from three successive test. An explosion was assumed to occur when the recorded pressure for P_m was greater than 0.1 bar.

5.1.1.2 Gases

In the case of gas test, the same principle as explained in the dust test was followed with the only difference that the dust dispersion step inside the sphere was omitted. The pressure before adding the combustible gas had to be reduced to less than 0.4 bar to leave space for the gas. For example, for the use of methane concentrations of 5 vol % and 10 vol %, the partial pressures of methane were 0.05 bar and 0.10 bar respectively, and the evacuation pressures had to be 0.35 bar and 0.3 bar respectively.

5.1.1.3 Vapors

The explosions of vapors were performed similar to the dust explosion tests (see section 5.1.1.1). The sphere was evacuated below the vapor pressure of the respective solvent (See Table 4.3). A defined amount of solvent was placed into the solvent reservoir; the reservoir was closed, and the solvent was drawn into the sphere upon opening the solvent inlet valve. Since the pressure in the sphere was below the vapor pressure of the solvent, the solvent turned to vapor as soon as it entered the sphere.

5.1.1.4 Sprays

To investigate the explosion characteristics of liquid sprays, a defined amount of solvent was introduced into the solvent chamber with a pipette. After the introduction of solvent into the solvent chamber, the chamber was then filled with 10 bar compressed air. The sphere was evacuated to a pressure of 0.4 bar. Upon opening the valve connecting the liquid reservoir to the spray nozzle, the liquid was sprayed as a fine mist into the sphere. The injection of the spray was always between the opening of inlet valve and the initiation of ignition source i.e. within 1s, depending on the concentration of the spray.

In order to reveal the nature of the mist obtained for the nozzle used, high speed photograph (Redlake MotionProX4) was used to collect images at 1200 fps for 20 ml water sprayed from the nozzle into atmospheric conditions when the solvent chamber is filled with 10 bar compressed air. The images are shown in Figure 5.5. The dimensions of the spray are shown in Figure 5.6. The photographs reveal that the spray exits the nozzle as an 80° cone, which reaches a diameter of

257 mm at the center of the 20-liter sphere. The diameter of the sphere is 337 mm. Thus, the nozzle effectively distributes the liquid spray throughout the sphere with a focus at the center, around the ignition source. The average Sauter mean diameter of the liquid droplets based on the specification of the nozzles was within the range of 7 to 17 μm .

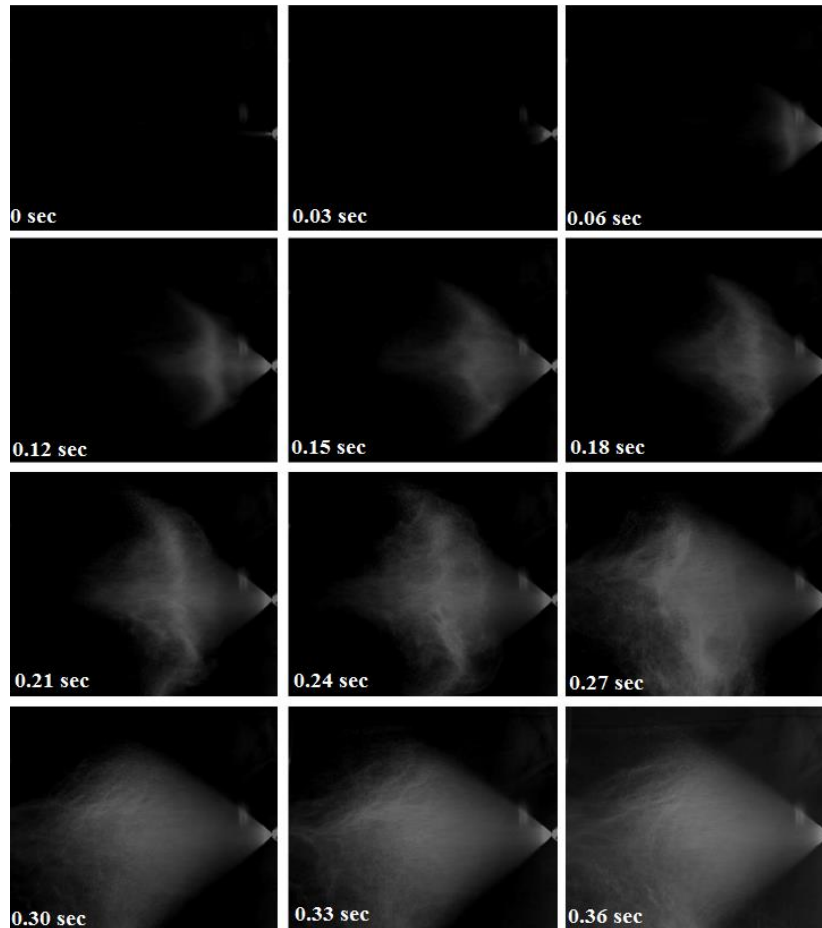


Figure 5.5: High speed photographs of the nozzle spray pattern with time.

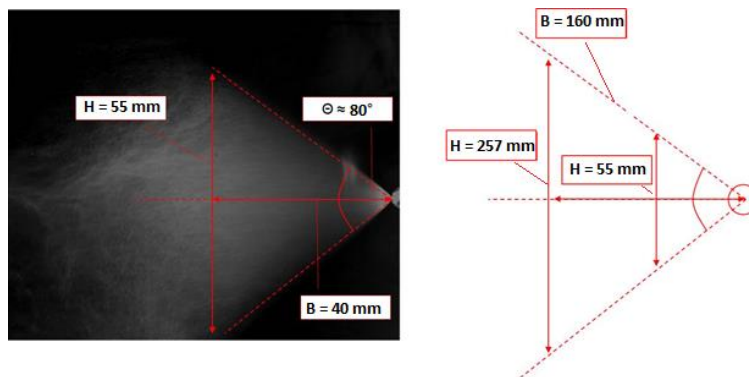


Figure 5.6: Dimensions of the spray.

5.1.2 Experimental procedure for two-phase hybrid mixtures

The explosion characteristics of hybrid mixtures of dusts and gases, dusts and vapor, dusts and sprays, gases and vapor, gases and sprays were investigated. The procedures for introducing the materials into the sphere were the same as for the individual substances. Gases and vapors were introduced into the sphere after evacuation. Dusts and sprays were injected into the sphere 60 ms prior to ignition. Hybrid mixtures were ignited using a 10 J electrical discharge

5.1.3 Experimental procedure for three-phase hybrid mixtures

The explosion characteristics of three-phase hybrid mixtures were investigated for mixtures of dust/gas/vapor and dust/gas/spray. The experimental procedure was the same as for two-phase hybrid mixtures with gases and vapors being introduced into the sphere following evacuation and dusts and sprays being rapidly injected 60 ms before ignition. Explosions occurring at concentrations below the LEL of the two-phase hybrid mixtures were investigated.

5.2 Explosibility parameters test

This section describes how the explosibility parameters tested in the 20-liter sphere: lower explosive limit (LEL), limiting oxygen concentration (LOC), explosion overpressure (p_m), and the rate of pressure rise (dp/dt) were obtained.

5.2.1 Lower explosible limit / minimum explosible concentration

The explosion limit tests for dusts, gases, sprays and their mixtures were performed in the 20-liter sphere in accordance with the European standard procedure **EN 14034-3 [97]**. With respect to dust testing, it involves dispersing the dust sample into a sphere and attempting to ignite the resulting dust cloud with an ignition source. At first, arbitrary concentration of the fuel was tested to check if ignition would be obtained or not. In case no ignition was observed, the concentration of the fuel was increased until an ignition was realized. The testing then continued and the concentration was further reduced until a point of which no ignition of the fuel/air mixture was observed in three successive tests. The least concentration where last ignition was obtained was considered to be the MEC /LEL of the fuel. An explosion over pressure value recorded by the

piezo-electric pressure transducers greater than 0.2 bar was considered as ignition. The same experimental principle was used to determine the lower explosible limit of gases, sprays and hybrid mixtures. It must be mentioned that the added concentration for hybrid mixtures test were all below the individual lower explosible limits. For the purpose of comparison 10 J electrical ignitors was used for all tests with the same initial and testing conditions.

5.2.2 Limiting oxygen concentration

The limiting oxygen concentration (LOC) testing was performed in the 20-liter sphere according to the procedure stated in the European standard **EN 14034-4 [106]**. Modification was done on the equipment for the input of nitrogen gas into the sphere. In order to test for the LOC of a specific fuel air mixture, the mixture was initially tested at 21 vol% oxygen. The test was then continued by systematic reduction of the oxygen concentration in the combustion atmosphere until ignition was no longer possible in three trials. The concentration of oxygen which will just not allow an explosion of the fuel/oxygen/inert gas mixture in three consecutive tests was considered as the limiting oxygen concentration. Different ignition energies such as electrical ignitor (10 J) and chemical ignitors (2 kJ and 10 kJ) were used for this study and the results were compared with each other. In order to assess an ignition, the explosion over pressure value recorded by the piezo-electric pressure transducers must be greater than 0.2 bar. The same testing procedure and testing conditions for dust, gas, spray and hybrid mixtures were considered.

5.2.3 Maximum explosion overpressure, (P_{\max}) and maximum rate of pressure rise (dP/dt)_{max}

A typical pressure evolution curve resulting from an experiment where the explosion occurred is shown in Figure 5.7. Gases and vapors are introduced into the sphere prior to starting of the experiment. The sprays and dust reservoirs are pressurized and ready for injection. At $t = 0$ s the experiment is initiated by the software. The injection of the dust occurs after a delay t_d (in the range of 30 to 50 ms), however, with respect to spray, t_d could be a bit longer depending on the concentration. A pressure rise P_d occurs due to the injection of dust or spray using pressurized air. An electrical or chemical energies discharge is initiated after a delay of $t_v = 60$ ms; which was

used in all the tests. If explosion occurs, a rapid increase in the pressure is observed. The determination of P_{max} and $(dP/dt)_{max}$ was performed in accordance with the standard similar to the European standard **EN 14034-1 & 2 [141]**, respectively.

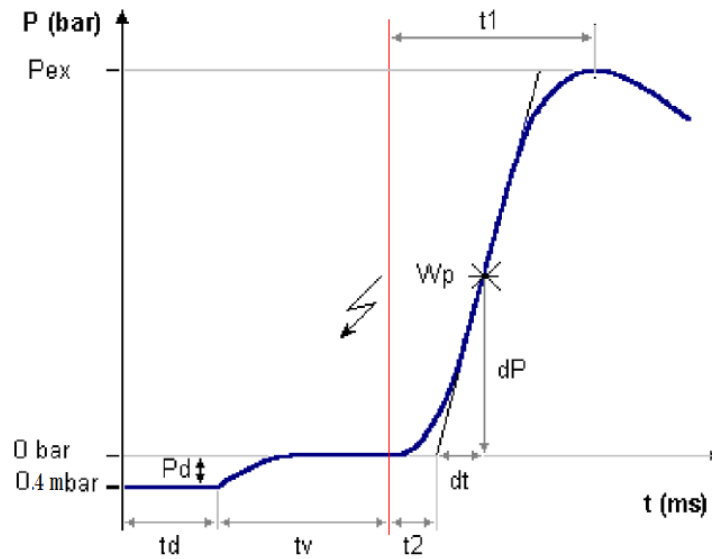


Figure 5.7: Pressure/time-diagram of a fuel explosion.

The time between ignition and the occurrence of P_{max} , t_1 , is considered as the duration of combustion. The induction time, t_2 , is the time between ignition and the intercept of a line drawn tangent to the pressure curve at $(dP/dt)_{max}$. The reproducibility of the maximum values was checked by performing the experiment at the concentration determined to produce the maximum values three times and the average values are presented.

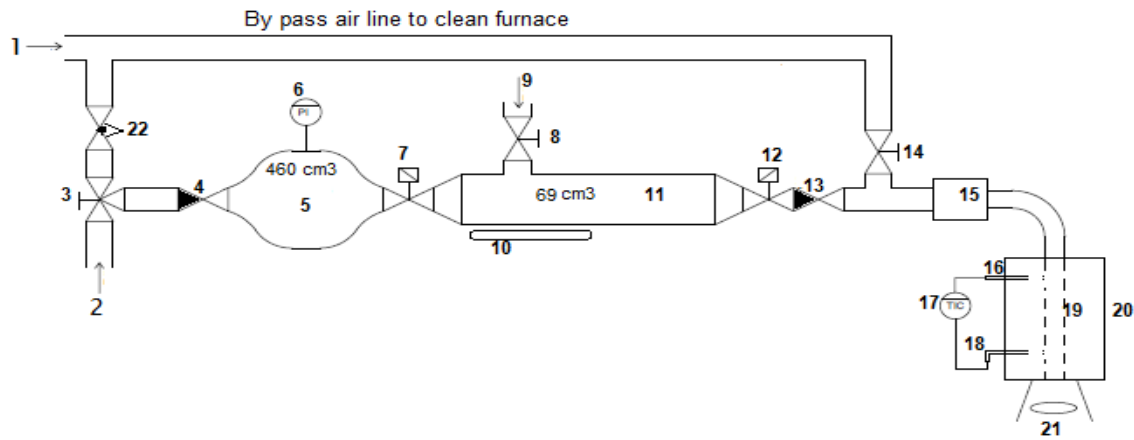
5.3 Experimental procedure for testing the MIT and LEL modified Godbert-Greenwald (GG) furnace

A modified Godbert-Greenwald (GG) furnace was used for the determination of the minimum ignition temperature (MIT) and lower explosible limit (LEL).

5.3.1 Godbert-Greenwald Furnace

A diagram of the modified GG apparatus is shown in Figure 5.8 and a photograph of the experimental installation is shown in Figure 5.9. The GG furnace consists of a heated steel tube, an air reservoir, a pressure regulator, dust chamber, and solvent chamber. The furnace tube is 42

cm long which is twice the length of the standard as described in EN 50281 [129] and 3.5 cm in diameter with internal volume of 460 cm³. It is heated by an electric coil with maximum set temperature of 700 °C. The furnace tube is mounted vertically on a steel case insulated with glass wool. The furnace tube is oriented vertically with an opening at the bottom with a mirror placed underneath the lower rim of the furnace. This mirror allows an observation of flame within and at the bottom of the furnace. A thermocouple is placed close to the inner wall of the furnace that is connected to a PID temperature controller to record the temperature of the furnace.



- | | |
|-----------------------------------|--|
| 1. Air supply | 12. Solenoid valve |
| 2. Gas supply | 13. Check valve |
| 3. T- shape ball valve | 14. L- shape ball valve |
| 4. Check valve | 15. Dust Chamber / reservoir |
| 5. Air / gas reservoir or gas. | 16. Thermocouple |
| 6. Digital pressure gauge | 17. Temperature controller |
| 7. Solenoid valve | 18. Electric power supply |
| 8. L- shape ball valve (two port) | 19. Steel furnace tube |
| 9. Solvent or liquid supply | 20. Furnace shell and insulation materials |
| 10. Heating filament. | 21. Mirror |
| 11. Solvent reservoir | 22. Air regulating valve |

Figure 5.8: Schematic sketch of Godbert-Greenwald furnace.

In order to measure the MIT or the LEL of hybrid mixtures, further modifications were done on the GG furnace to allow input of gases and solvents. A detailed technical diagram for this modification is shown in Figure 5.8. A flammable gas supply line was connected to the air chamber (#5). With respect to flammable vapor supply, a solvent chamber was installed between the air reservoir and the dust chamber which was heated up with an external heating filament at

a temperature above the boiling point of the respective solvent in order to ensure complete vaporization. Glass wool was wrapped around the solvent chamber as a thermal insulator to minimize heat loss. The solvent was introduced into the solvent chamber by a syringe or pipette. Two solenoid valves (#7) and (#12) were installed at the two edges of the solvent chamber to contain the vaporized solvent.

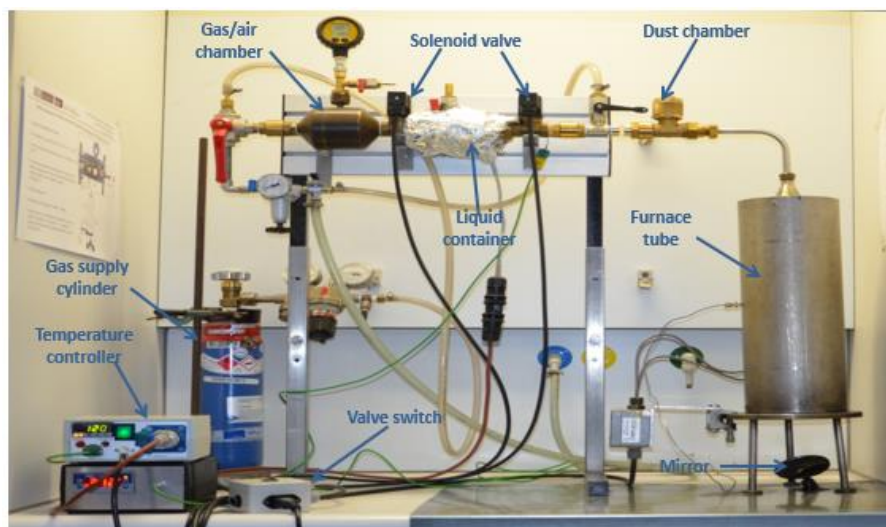


Figure 5.9: A photo of the Godbert-Greenwald furnace experimental setup.

5.3.2 Minimum ignition temperature test procedures in the GG-furnace

5.3.2.1 Experimental procedure for the MIT of a single component

In the Godbert-Greenwald furnace, a known amount of flammable gas, solvent vapor, dust, or mixture thereof was mixed with air and blown into a tube furnace heated to a specified temperature (depending of the tested material). Ignition of the mixture was determined visually. For an explosible mixture, the furnace temperature was decreased in 5 K steps and the mixture was classified as explosible if ignition occurred once within ten repeated experiments. The concentrations of materials investigated are listed in Table 5.1. Detailed flow diagrams for the experimental procedure for single substances and hybrid mixtures are presented in Figures A.1 to A.5 at Appendix A.

Table 5.1: The volume fractions or masses of fuels used for the tests.

Materials	Propane	Methane	Hexane	Isopropanol	Ethanol	Toluene	Dust
Concentration	2-10 vol%	4-15 vol%	1-8 vol%	2-14 vol%	3-18 vol%	1-7 vol%	0.1 to 0.5 g

5.3.2.1.1 Dusts

A known quantity of dust was placed into the dust chamber, and the chamber was closed. The air reservoir was filled with air to an absolute pressure of 1.2 to 1.7 bar. Upon activating the solenoid valves via a switch, the dust sample was then dispersed into the furnace tube by a blast of air. The presence of an explosion was determined visually from observation of a flame at the bottom of the furnace with the help of a mirror. Both the pressure (0.2 to 0.7 bar above atmospheric pressure) and the mass of dust (0.1 to 0.5 g) were varied until a definite explosion was obtained. The condition at which the vigorous explosion was obtained was taken as the “best” explosion condition (BEC). This condition was maintained and the furnace temperature was lowered and testing continued until no flame was observed in ten tests. The temperature of the oven was lowered in 5 K increments. For a given temperature, the process of injecting dust into the heated tube and observing the presence or absence of an explosion was repeated either until an explosion was observed or when no explosion occurred for ten repetitions. The minimum ignition temperature (MIT) was taken to be the lowest temperature at which ignition occurred.

5.3.2.1.2 Gases

The same experimental principle as explained for dust was used for the gas test. The only difference in this case was that, the air was premixed with the combustible gas in the air reservoir and the dust chamber was left empty. The composition of the gas mixtures was determined based on partial pressures. For example, in considering 5 vol% of combustible gas and a total absolute pressure of 0.5 bar is required. At first the reservoir is filled with 0.475 bar of air followed by 0.025 bar of combustible gas to make a total pressure of 0.5 bar. The concentrations of gases investigated are summarized in Table 5.1.

5.3.2.1.3 Solvent Vapors

The solvent chamber was heated to a temperature above the boiling point of individual solvents with a heating filament to allow the solvent to vaporize before being dispersed into the furnace. A given volume of solvent was measured with a syringe, placed in the solvent chamber, and allowed to completely vaporize. The air reservoir was filled with pressurized air, and the valve to

the air supply was closed. Upon opening of the two solenoid valves (connected in series) the pressurized air pushes the vaporized solvent into the hot furnace. If the concentration of the air–solvent mixture was within the explosible range and the temperature was either at the MIT or above, explosion would be obtained. For an explosible mixture, the furnace temperature was decreased in 5 K steps and the mixture was classified as explosible if ignition occurred once within ten repeated experiments. The MIT for an explosible mixture was determined as the lowest temperature at which a flame was observed. Figure 5.10 provides a representation of how the MIT of both single substance and hybrid mixtures was obtained.

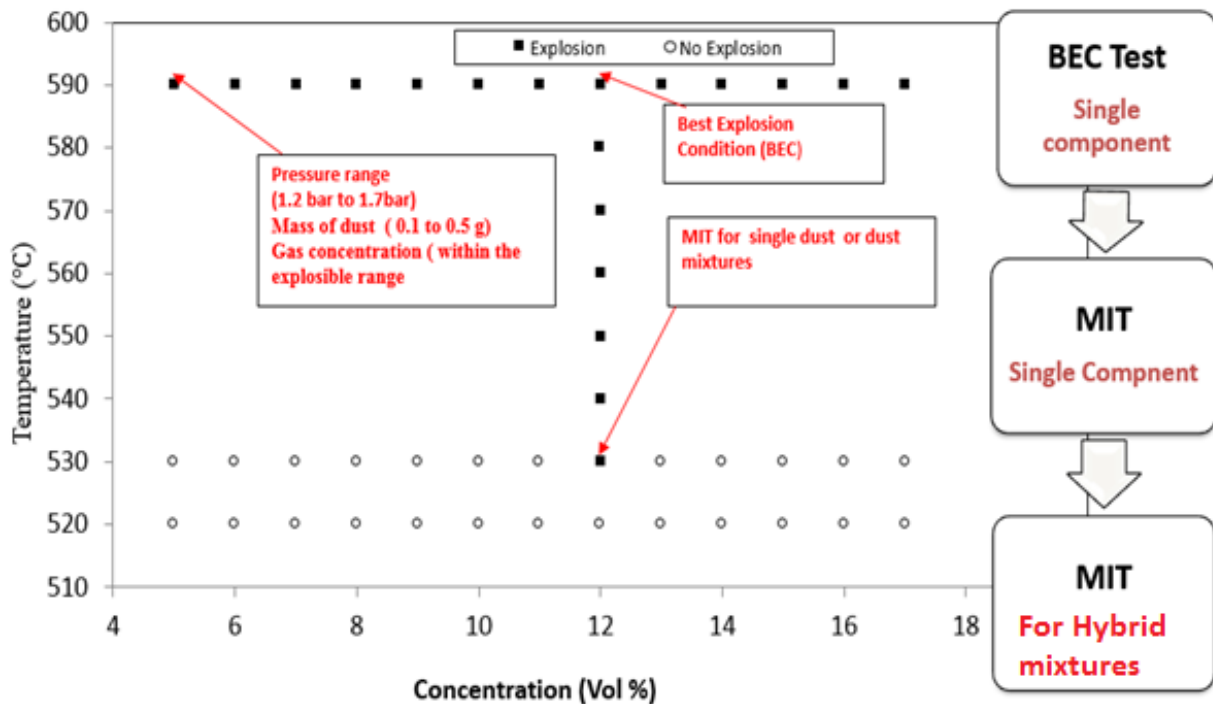


Figure 5.10: A representation of how the MIT of both single dust, gas and hybrid mixtures were obtained.

5.3.2.2 Experimental procedure for the MIT of two-phase hybrid mixture

For the test with hybrid mixtures (two phase), the same experimental principle as explained for the single component test was used. In this case, it was just the combination of the test method with pure dust and pure gas or solvent. The preceding steps follow the same test principle for pure dust. As soon as the MIT is obtained further tests were performed at 5 K below the MIT by varying both pressure and concentration to check if ignition will occur. Two main testing cases were

considered, which includes: the effect of dust on the MIT of gases as well as the effect of gases on the MIT of dusts. With respect to the first test case, the LEL of the single gas or vapor was initially tested at a temperature equivalent to the MIT of dust. Then a concentration lower than the already determined LEL was added to the dust below its MIT. The test procedure for the second test case i.e. effect of adding a non-explosible concentration of dust on the MIT of gas or vapor is just the vice versa of the first test case.

5.3.2.3 Experimental procedure for the MIT of three Component hybrid mixtures

The three component hybrid mixture tests follow the same principle as the two-phase hybrid mixture test. It involves the combinations of the various test of dusts, gases and solvents. Three main testing cases were considered, which included: the effect of adding non-explosible concentrations of gas and vapor on the MIT of dust, the effect of adding non-explosible concentrations of dust and gas on MIT of vapor and the effect of adding non-explosible concentrations of dust and vapor on the MIT gas. For the sake of simplicity, the main component is the component (whether a vapor, gas, or dust) on which various effects are tested. With regards to the first test case (i.e. the effect of adding a non-explosible concentration of gas and vapor on the MIT of dust), the LEL of the gas and vapor at a temperature equivalent to MIT of dust was initially determined. Then, a concentration of gas and vapor, below the LEL was added to the dust at its non-explosible temperature. It was ensured that the concentration of gas and vapor combination does not themselves ignite at the MIT of the dust. The test procedures for the other test cases are similar to the first test case as explained above.

5.3.3 The lower explosible (LEL) and the minimum explosible concentration (MEC) tests in the GG furnace

5.3.3.1 Experimental procedure for LEL/MEC of single component

A similar experimental procedure used in the determination of MIT of single component was also used for the determination of MEC/LEL. The initial testing conditions (dispersion pressure and concentration) were based on the best explosion condition as already described in section 5.3.3.1. The furnace temperature was fixed at 20 °C to 40 °C (depending on the material) above the MIT of the individual substances obtained from the MIT of the single component test. It must be

mention that the explosion limit is influenced by the temperature of the furnace, as a result of this the effect of temperature on the explosion limits were initially tested (see Figure C.1 in appendix C). Using the same temperature and dispersion pressure at the best explosion condition, further tests were carried out by reducing the fuel concentration until no further ignition was obtained. At the point where no ignition was obtained, the concentration was kept constant and testing continued using lower and higher air dispersion pressure as presented in Table 5.1. In case no ignition occurred at any combination of concentrations and dispersion pressures, the lowest concentration at which last ignition occurred was taken as the MEC/LEL of the sample. The concentration of the dust was estimated by dividing the mass of dusts used by the total volume of the furnace (460 cm³).

5.3.3.2 Experimental procedure for MEC/LEL of two component hybrid mixture

For the test with hybrid mixtures, a similar experimental principle as explained for the single component test was used. It was just the combination of the test methods with pure dust and pure gas or solvent. The preceding steps followed the same test principle for the pure substance. After obtaining the MEC/LEL of single components, further tests were performed below the concentration by varying the pressure to check if ignition could be obtained. Two testing cases were considered i.e. the effect of adding a non-explosible concentration of gas or vapor on the MEC of dust and the effect of adding a non-explosible concentration of dust on the LEL of gas or vapor. With respect to the first test case i.e. the effect of adding a non-explosible concentration of gas or vapor on the MEC of dust, the LEL of gas/vapor was initially tested at the temperature where the MEC of dust was obtained. Then, a non-explosible concentration of gas/solvent lower than the respective LEL was added to the dust below its MEC. In case no ignition occurred, the concentration of the mixture was kept constant and the pressure was varied. The last concentration where ignition happens was considered as the MEC of the mixture. The second test case i.e. the effect of adding a non-explosible concentration of dust on the LEL of gas or vapor is just the vice versa of the first test case as explained above.

5.3.3.3 Experimental procedure for MEC/LEL of three component hybrid mixtures

A similar procedure as explained for the two-phase or two-component hybrid mixtures was used for the three component hybrid mixture tests. Holding the concentration of two substances constant, the concentration of the third substance was systematically reduced until ignition did not occur in 10 attempts.

5.4 Minimum ignition energy test in the Hartmann apparatus

The minimum ignition energy (MIE) for dusts, flammable gases, and hybrid mixtures of dusts and gases was investigated in a Hartmann apparatus (Chilworth CTL04 MIE III Apparatus). The experimental setup is shown in Figure 5.11 and Figure 5.12. The experimental protocol was in accordance with that defined in European standard **EN 13821 [117]**. The combustion chamber consists of a plastic tube with a volume of 1.2-liters, diameter of 7 cm and a height of 31 cm. A cloud of dust suspended in air is produced by forcing air through a mushroom-shaped nozzle at the bottom of the tube. Electrodes placed at a height of 12 cm from the bottom of the combustion chamber were used to provide an ignition source for the mixtures. The electrodes were connected to an energy storage unit (# 13 of Figure 12) which provides and regulates the spark ignition energy essential for dust and hybrid mixture explosion as well as a chart recorder to accurately monitor the breakdown voltage of the discharged energy. A blast of compressed air at 7 bar is used to disperse the dust into the glass cylinder which is ignited by a spark between two electrodes. In order to perform hybrid mixture tests, a minor modification was added to the equipment by introducing a flammable gas feed line.

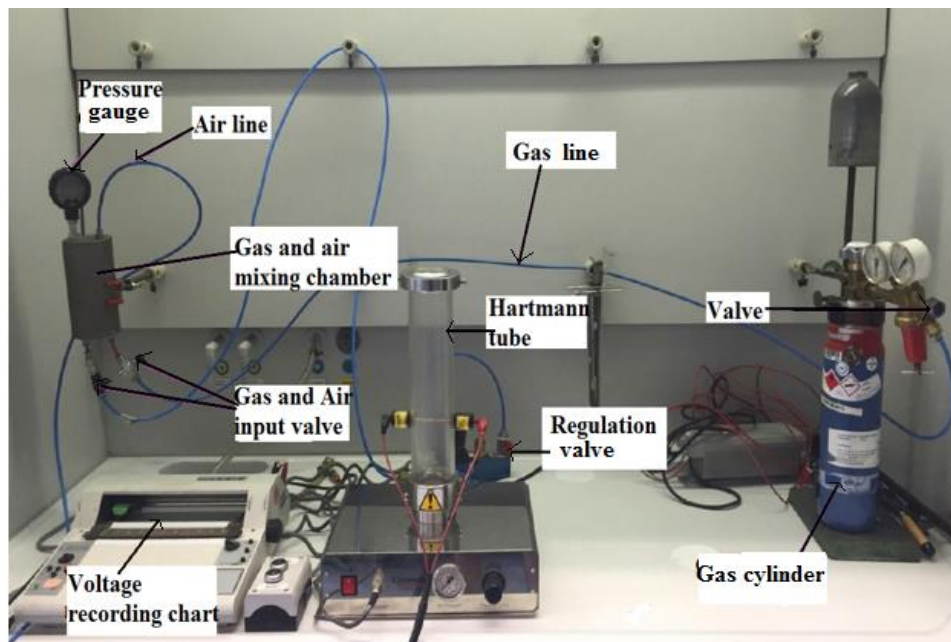
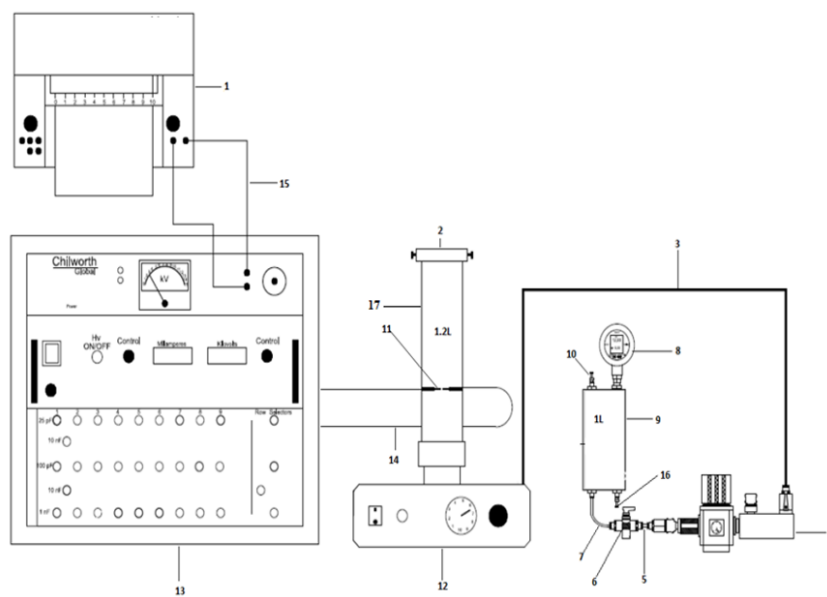


Figure 5.11: A photo of the Hartmann apparatus experimental set-up.



- | | | |
|--|-------------------------------------|---|
| 1: Line recorder | 7: Connecting hose from gas chamber | 13: Capacitor assembly system |
| 2: Bursting disc (filter paper) | 8: Digital pressure gauge | 14: High voltage cable |
| 3: Gas feed line to Hartmann apparatus | 9: Gas-air mixing chamber | 15: connecting cable between the line recorder and the capacitor system |
| 4: Pressure regulator | 10: Gas input line | 16: Air input line |
| 5: Connecting hose to the pressure regulator | 11: electrode assembly | 17: Hartman 1.2-liter chamber |
| 6: Gas air mixture outlet valve | 12: Hartmann tube control system | |

Figure 5.12: Technical diagram of the Hartmann apparatus.

5.4.1 Experimental procedure of the minimum ignition energy of dusts

A known amount of dust was placed into the mushroom (bottom) part of the combustion chamber. The dust dispersion was triggered by a compressed air blast at 7 bar. The air blast generated considerable turbulence and resulted in the creation of a dust cloud. The spark was drawn between two electrodes with spark gaps between 2- 6 mm. Ignition was observed visually as shown in Figure 5.13. The minimum ignition energy lies between the highest energy at which ignition fails to occur (E1) for twenty successive attempts and the lowest energy at which ignition occurs (E2) within up to twelve successive attempts.

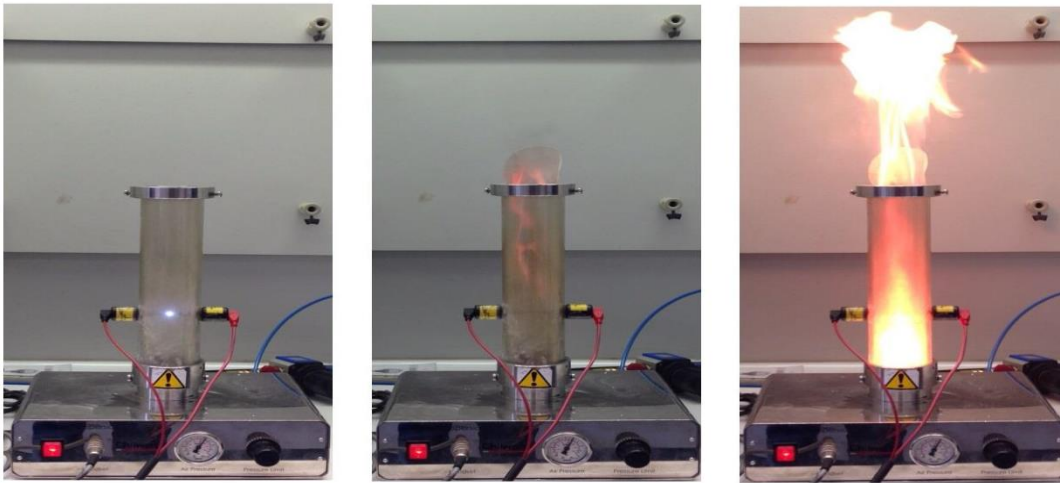


Figure 5.13: The development of an explosion in the Hartmann apparatus.

For the purpose of comparison between different combustible mixtures, instead of using energy range, only one single value estimated by the use of the probability of ignition as specified in EN 13821 standards was used:

$$\log \text{MIE} = \log E2 - I[E2] \cdot \frac{(\log E2 - \log E1)}{(NI+I) \cdot [E2]+1} \quad (5.1)$$

$I [E2]$ is the number of tests with successful ignition at energy level $E2$ and $(NI + I) [E2]$ stands for the total number of tests at the energy level of $E2$. The values obtained using the above formula has a maximum deviation of 1 mJ.

5.4.2 Experimental procedure of the minimum ignition energy of hybrid mixtures

For testing hybrid mixtures containing both dusts and flammable gases, the flammable gas was combined with air in the gas chamber. Initially the gas chamber was filled with air at atmospheric pressure. Flammable gas was then introduced into the chamber and the pressure was increased to P_{gas} , depending on the desired concentration. The gas inlet valve was then closed. The valve to the air inlet was then opened and the container was filled with air up to a pressure of 7 bar. The air inlet valve was then closed. The concentration of the flammable gas is related to its partial pressure in the mixture:

$$y_{gas} = \frac{P_{gas} - P_i}{P_{end}} \quad (5.2)$$

Where P_{gas} is the pressure of flammable gas, P_i is the initial pressure in the vessel ($P_i = 1\text{bar}$) and P_{end} is the set pressure to disperse the dust. The dust was then dispersed by a blast of flammable gas- air mixture. It must be noted that the flammable gases were tested at concentrations lower than the lower explosion limits in air.

Chapter Six

6 Results and Discussions

6.1 Lower explosion limits and minimum explosible concentrations

The lower explosion limit of gas (LEL) or minimum explosible concentration of dust (MEC) is the concentration of fuel-air mixture below which self-sustained propagation of flame is not possible at a specific test condition. In order to prevent the risks associated with gas, dust or hybrid mixture explosions, it is very important to know the lowest concentration of these mixtures at which explosion can occur. Knowing these limits can help set a margin for a system so that the concentration could always stay below these limits. Contrarily to the lower explosion limits of solitary dust, gas or solvent which have been widely investigated in the past decades, data on explosion limits of hybrid mixtures are comparatively sparse. Most of the studies on hybrid mixtures focus on dust and gas mixtures, for example, coal dust and methane [154], graphite and hydrogen [11], niacin and methane [155] etc. However, mixtures such as: sprays/vapors with either dusts or gases have not been investigated in detail. As a result of the aforementioned reasons, this section presents detailed results on the lower explosion limits of different combinations of mixtures such as: spray-gas, spray-dust, gas/vapor, dust-vapor-gas as well as spray-gas-dust. Experiments were performed in two different laboratory equipments i.e. the standard 20-liter sphere and the Godbert-Greenwald (GG) furnace with six solvents (ethanol,

isopropanol, acetone, toluene, heptane, and hexane), three gases (methane, propane and hydrogen) and five dusts (corn-starch, lycopodium, brown coal, HDPE and toner). Experimental procedures for these tests are discussed in Section 5.2.1 and 5.3.4 for the standard 20-liter sphere and the Godbert-Greenwald (GG) furnace, respectively.

Furthermore, accurate estimation of the explosion limits is necessary for safe handling of combustible mixtures in industries. Theoretically, these estimations could be done through experimental measurements but the tests are usually time and money consuming, and sometimes impossible for the emergent requirements. Therefore, different mathematical models to estimate explosion limits of dusts, gases and hybrid mixtures proposed by different authors are presented and compared with the experimental results

6.1.1 Lower explosion limits in the standard 20-liter sphere.

The standard 20-liter sphere is an alternative standard test apparatus to the 1 m³ combustion chamber. It is usually used to determine explosion data for dusts alone. In order to use this equipment for gases, spray and hybrid mixtures testing, modifications were made on the sphere to allow the input of gas and spray.

6.1.1.1 Lower explosion limits of single substances

To begin with, the lower explosion limits of single substances were tested. Figure 6.1 presents the results obtained for the LEL of solvents (as spray). It was observed that the alcohols (ethanol and isopropanol) recorded higher LEL compared to other solvents. Ignition of spray is strongly influenced by the droplet size [156]: the smaller the droplet size, the easier it is to ignite. Although, the determination of the droplet size distribution for all solvents was not performed in the experimental capacity of this research work, the average droplet size according to the Sauter mean diameter based on the specification of the nozzle was found to be in the range of 7 to 17 μm.

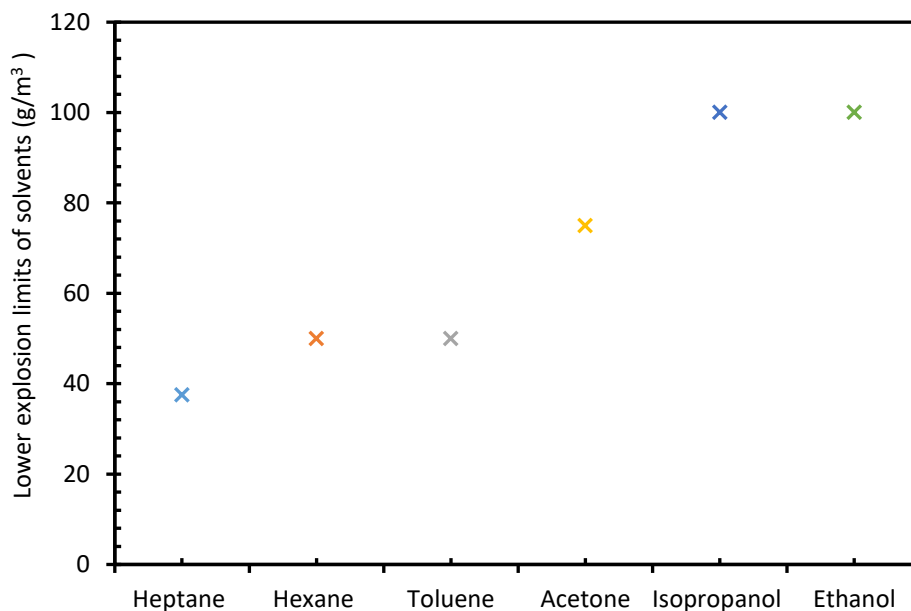


Figure 6.1: Lower explosion limits of solvents as spray.

Parameters such as density, surface tension, viscosity, flow rate and spraying pressure have a direct effect on the droplet size of the spray. Droplet size increased as the spraying pressure decreased and decreased, as the pressure increased. An increase in flow rate will increase the pressure drop and decrease the drop size, while, a decrease in flow rate will decrease the pressure drop. Increasing the viscosity and surface tension increases the amount of energy required to atomize the spray and hence, increases the drop size [157]. A general trend was noticed with regards to the LEL of sprays that is, increasing parameters such as viscosity, density, relative polarity, surface tension and eluent strength, increases the LEL. For example, heptane with viscosity and density of $3.1 \times 10^{-4} \text{ kg m}^{-1} \text{ s}^{-1}$ and 0.01 g/cm^3 respectively recorded the lowest LEL of 37.5 g/m^3 compared to isopropanol with viscosity and density of $0.0024 \text{ kg m}^{-1} \text{ s}^{-1}$ and 0.78 g/cm^3 which recorded a LEL of 100 g/m^3 (see Table 4.3 for properties of solvents).

With respect to flammable gases, the recorded LELs are 5 vol% for both methane and hydrogen respectively (see Table 6.1). These values are comparable to literature values obtained from the standard procedure [83] (methane = 4.4 vol% and hydrogen = 4.6 vol%). It must be mentioned here that, only the experimental LEL obtained from this research is used throughout the discussion. Furthermore, the MEC recorded for lycopodium and brown coal are 125 g/m^3 and 250 g/m^3 respectively (see Table 6.1). The particle size and the volatile content of the dusts played an

important role in the determination of the MEC of dusts. Decreasing the particle size increase, the number of particles under the same dust concentration which in turn increases the surface area available for ignition to take place.

6.1.1.2 Lower explosion limits of two-phase hybrid mixtures

Based on the results obtained from single substances, the lower explosion limits of hybrid mixtures were investigated. Three different combinations were considered: mixtures of combustible dust with combustible gas and air, mixtures of combustible dust with solvent (spray) and air as well as mixtures of combustible gas with a combustible solvent (spray) and air. As it is well known from literature (see section 2.5) that the LEL of hybrid mixtures could lie below the individual LEL of the single component, the combustible materials were mixed at concentrations below their individual LEL. Concentrations were varied systematically in order to obtain the LEL of the hybrid mixtures.

With respect to the first tested combination, that is: mixtures of combustible dusts (lycopodium and brown coal) with combustible gases (methane and hydrogen) and air, different concentrations of gases were added to the dust. Figure 6.2 presents the results obtained for lycopodium and methane mixtures. It could be seen that the explosion limit of hybrid mixtures decreases when the concentration of methane is increased. With the exception of 1 vol% of methane, all other concentrations made an impact on the explosion limits of hybrid mixture. For example, the explosion limit of hybrid mixtures with lycopodium decreased from 125 g/m³ to 100 g/m³ and 60 g/m³ when 2 vol% and 4 vol% of methane was respectively added.

Similar explosion behavior was seen when methane was added to brown coal as shown in Figure 6.3. It was also noticed that the explosion limit of hybrid mixtures with brown coal decreased when a non explosible concentration of methane was added. For example, the explosion limit of brown coal decreased from 250 g/m³ to 60 g/m³ when 4 vol% of methane was added. These results confirm the findings reported by [13, 14, 19, 158-160], of which they concluded that the explosion limits of hybrid mixture could decrease when a non-explosible concentration of gas is added. The results from other mixtures showed a similar explosion behavior and are presented in Table 6.1 and Figures B.1 and B.2 at Appendix B.

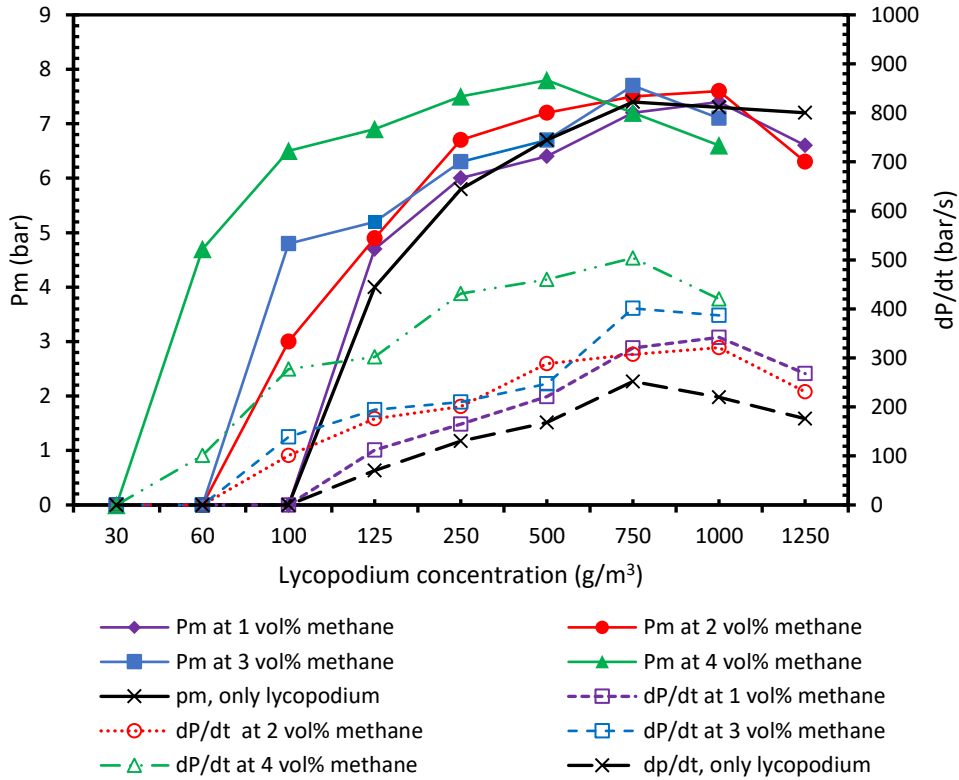


Figure 6.2: Maximum explosion pressure and rate of pressure rise of a mixture of methane and lycopodium in dependence on the lycopodium concentration.

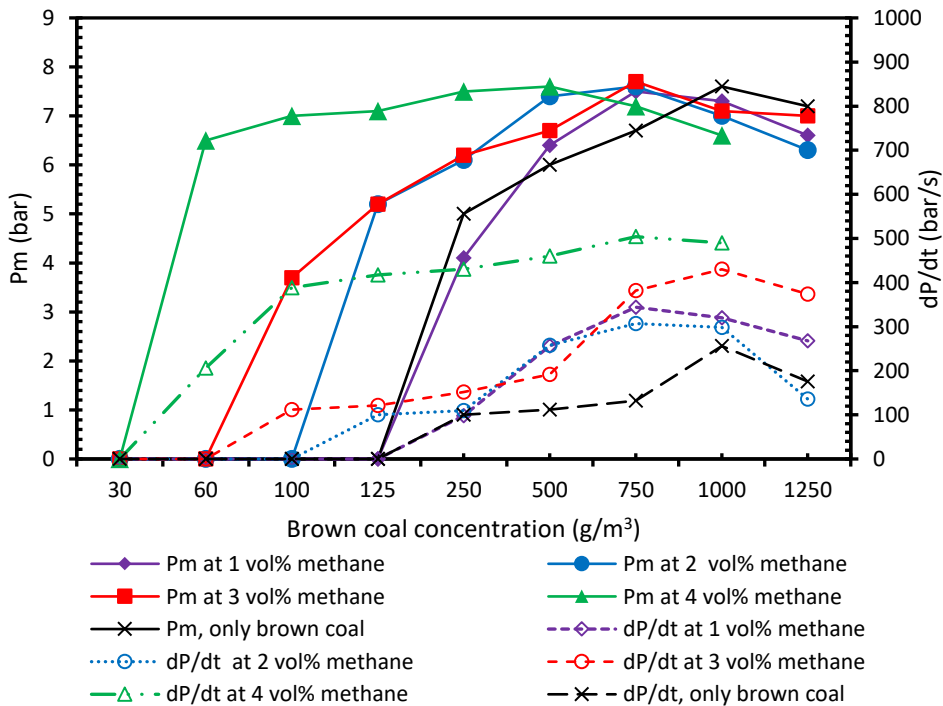


Figure 6.3: Maximum explosion pressure and rate of pressure rise of a mixture of methane and brown coal in dependence on the brown coal concentration.

Furthermore, Figures 6.4 and 6.5 present the results obtained for hybrid mixtures of dusts (lycopodium and brown coal) and solvents (ethanol, isopropanol, acetone, toluene, hexane and heptane). Different concentrations of the solvents below their lower explosion limits were added to the dusts at its non-explorable concentration (below the MEC). This was done to verify if the addition of a non-explorable concentration of the solvent (spray) together with a non-explorable dust concentration could give an explorable hybrid mixture. From Figure 6.4, it could be seen that the explosion limits of hybrid mixture of lycopodium and ethanol drastically decreased when ethanol concentrations which, themselves do not form an explorable atmosphere, were added. For example, the explosion limit of hybrid mixtures of lycopodium drops from 125 g/m³ to 60 g/m³ when a concentration of isopropanol which is 50% below the LEL was added.

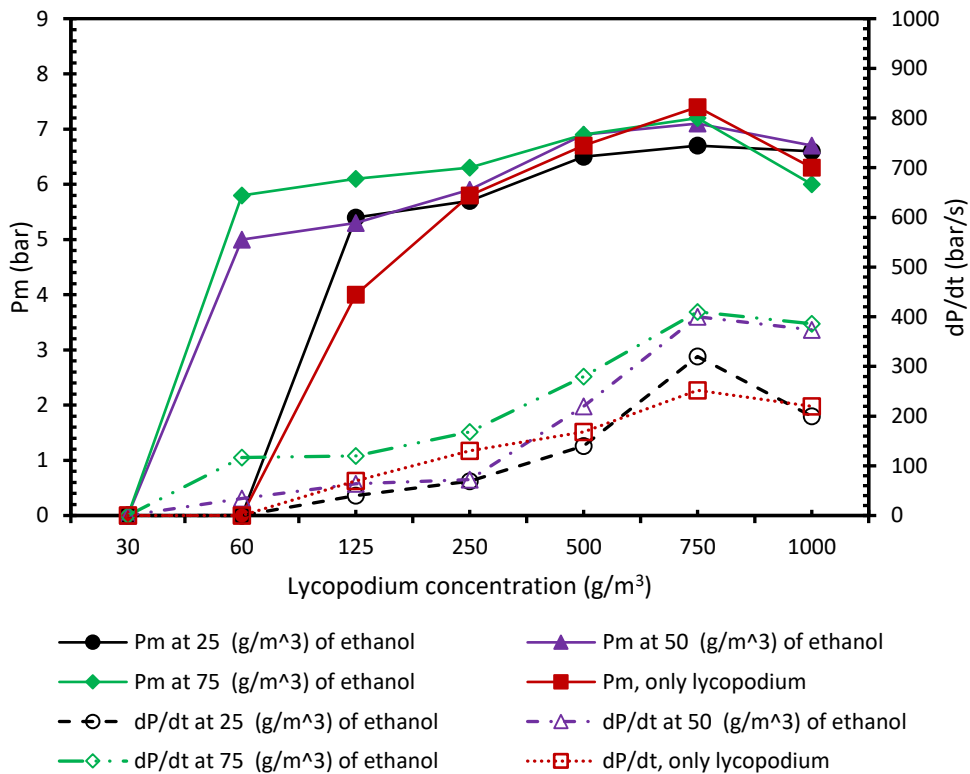


Figure 6.4: Maximum explosion pressure and rate of pressure rise of a mixture of ethanol spray and lycopodium in dependence on the lycopodium concentration.

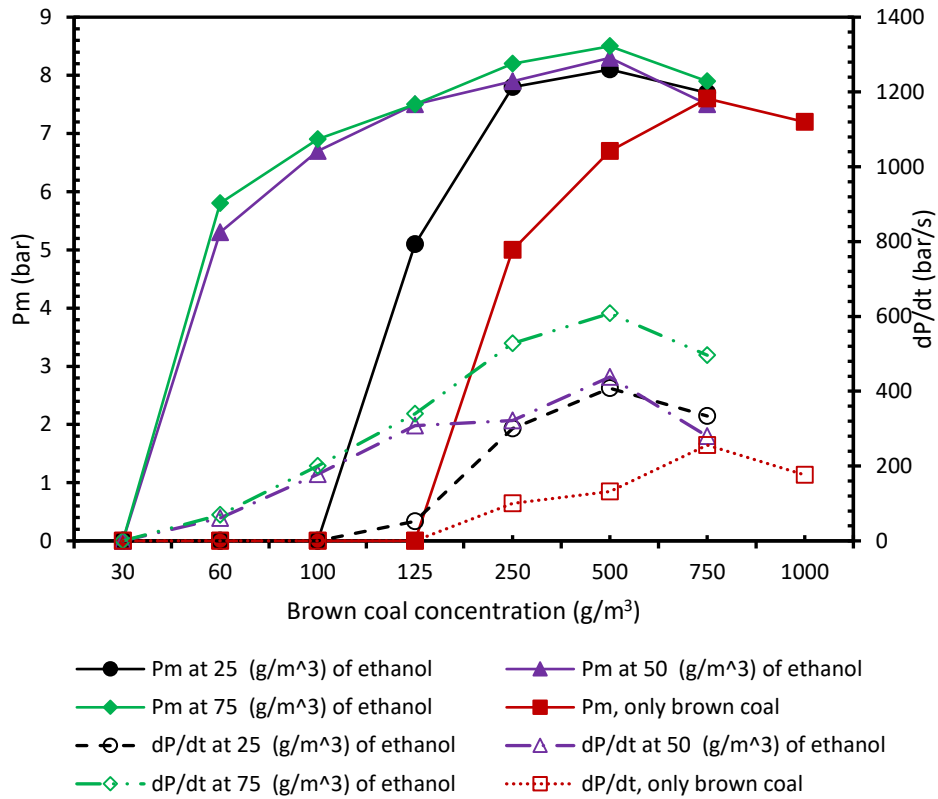


Figure 6.5: Maximum explosion pressure and rate of pressure rise of a mixture of ethanol spray and brown coal in dependence on the brown coal concentration.

A similar explosion behavior was also observed when non-explosible concentrations of ethanol were added to brown coal. The explosion limits of hybrid mixture of brown coal and ethanol decreased when ethanol concentration increased. For example, the explosion limit of hybrid mixtures with brown coal decreased from 250 g/m³ to 60 g/m³ when a non-explosible concentration of ethanol (75 g/m³), was added. The results from other mixtures showed similar explosion behavior and are presented in Table 6.1 and Figures B.3 to B.11 at Appendix B.

Table 6.1: A summary of results for the lower explosion limits of mixtures of dusts and gases as well as dusts and solvents (spray).

Single substances	symbols	MEC of single substances (g/m ³ /vol%)	Hybrid combinations	LEL of hybrid mixtures (g/m ³)	Hybrid combinations	LEL of hybrid mixtures (g/m ³)
Lycopodium	LY	125	LY + 25 g/m ³ ET	125	BC + 25 g/m ³ ET	125
Brown coal	BC	250	LY+ 50 g/m ³ ET	60	BC + 50 g/m ³ ET	60
			LY+75 g/m ³ ET	60	BC + 75 g/m ³ ET	60
Ethanol	ET	100				
Isopropanol	IS	100	LY + 25 g/m ³ IS	125	BC + 25 g/m ³ IS	250
Acetone	AC	75	LY + 50 g/m ³ IS	60	BC + 50 g/m ³ IS	125
Toluene	TL	50	LY + 75 g/m ³ IS	60	BC + 75 g/m ³ IS	60
Hexane	HX	50				
Heptane	HP	37.5	LY + 12.5 g/m ³ AC	125	BC + 12 g/m ³ AC	125
			LY + 25 g/m ³ AC	60	BC + 25 g/m ³ AC	60
Methane	ME	5.0	LY +3 7.5 g/m ³ AC	60	BC + 37.5 g/m ³ AC	60
Hydrogen	HY	5.0				
			LY + 12.5 g/m ³ TL	125	BC + 12.5 g/m ³ TL	125
			LY + 2 5 g/m ³ TL	125	BC + 25 g/m ³ TL	60
			LY + 37.5 g/m ³ TL	60	BC + 37.5 g/m ³ TL	60
			LY + 12.5 g/m ³ HX	60	BC + 12.5 g/m ³ HX	125
			LY + 25 g/m ³ HX	30	BC + 25 g/m ³ HX	60
			LY + 37.5 g/m ³ HX	30	BC + 37.5 g/m ³ HX	60
			LY + 12.5 g/m ³ HP	60	BC + 12 g/m ³ HP	125
			LY + 25 g/m ³ HP	30	BC + 25 g/m ³ HP	125
			LY + 37.5 g/m ³ HP	30	BC + 37.5 g/m ³ HP	60
			LY + 1 vol % ME	125	BC + 1 vol % ME	250
			LY + 2 vol % ME	100	BC + 2 vol % ME	125
			LY + 3 vol % ME	100	BC + 3 vol % ME	100
			LY + 4 vol % ME	60	BC + 4 vol % ME	60
			LY + 1 vol % HY	125	BC + 1 vol % HY	250
			LY + 2 vol % HY	125	BC + 2 vol % HY	250
			LY + 3 vol % HY	100	BC + 3 vol % HY	125
			LY + 4 vol % HY	60	BC + 4 vol % HY	100

Furthermore, mixtures of two gases (methane and hydrogen) and six solvents (ethanol, isopropanol, acetone, toluene, hexane and heptane) were tested. For this purpose, the concentration of gas was kept constant for a particular series of tests and the concentration of solvent was varied. Gases below their LEL were added to the solvents at their non-explosible concentration. It was noticed that the explosion limits of hybrid mixture of solvents decreased drastically, when a small percentage of gas was added. This was seen when methane concentrations which do not form explosible atmosphere was added to isopropanol as shown in Figure 6.6. For example, while the LEL of isopropanol alone was 100 g/m³, when adding 3 vol % of methane ignition could be achieved at 6.25 g/m³.

A similar explosion behavior as already discussed for methane and isopropanol was also observed when a non-explosible concentration of hydrogen was added to isopropanol spray. With the exception of 1 vol% of hydrogen gas, all the other concentrations had an effect on the explosion limits of hybrid mixture of isopropanol as presented in Figure 6.7. The explosion limit of hybrid mixtures of isopropanol decreased from 100 g/m³ to 75 g/m³, 50 g/m³ and 25 g/m³ when hydrogen concentrations of 2 vol%, 3 vol% and 4 vol% were added respectively. Similar explosion behavior was also observed for other combinations of gases and solvents as presented in Table 6.2 and Figures B.12 to B.21 at Appendix B.

Table 6.2: A summary of results for the lower explosion limits of mixtures of gases and solvents (spray).

single substance	symbols	MEC/LEL of single substance (g/m ³ /vol%)	Hybrid combinations	LEL of hybrid mixtures (g/m ³)	Hybrid combinations	LEL of hybrid mixtures (g/m ³)
Methane	ME	5.0	ET + 1 vol% ME	75	ET + 1 vol% HY	100
Hydrogen	HY	5.0	ET + 2 vol% ME	75	ET + 2 vol% HY	75
			ET + 3 vol% ME	50	ET + 3 vol% HY	50
			ET + 4 vol% ME	50	ET + 4 vol% HY	25
Ethanol	ET	100				
Isopropanol	IS	100	IS + 1 vol% ME	75	IS + 1 vol% HY	100
Acetone	AC	75	IS + 2 vol% ME	25	IS + 2 vol% HY	75
Toluene	TL	50	IS + 3 vol% ME	12.5	IS + 3 vol% HY	50
Hexane	HX	50	IS + 4 vol% ME	12.5	IS + 4 vol% HY	25
Heptane	HP	37.5				
			AC + 1 vol% ME	75	AC + 1 vol% HY	75
			AC + 2 vol% ME	50	AC + 2 vol% HY	50
			AC + 3 vol% ME	50	AC + 3 vol% HY	50
			AC + 4 vol% ME	25	AC + 4 vol% HY	25
			TL + 1 vol% ME	50	TL + 1 vol% HY	75
			TL + 2 vol% ME	50	TL + 2 vol% HY	50
			TL + 3 vol% ME	25	TL + 3 vol% HY	25
			TL + 4 vol% ME	25	TL + 4 vol% HY	25
			HX + 1 vol% ME	37.5	HX + 1 vol% HY	37.5
			HX + 2 vol% ME	37.5	HX + 2 vol% HY	37.5
			HX + 3 vol% ME	25	HX + 3 vol% HY	25
			HX + 4 vol% ME	25	HX + 4 vol% HY	25
			HX + 1 vol% ME	37.5	HX + 1 vol% HY	37.5
			HX + 2 vol% ME	37.5	HX + 2 vol% HY	37.5
			HX + 3 vol% ME	25	HX + 3 vol% HY	25
			HX + 4 vol% ME	12.5	HX + 4 vol% HY	12.5

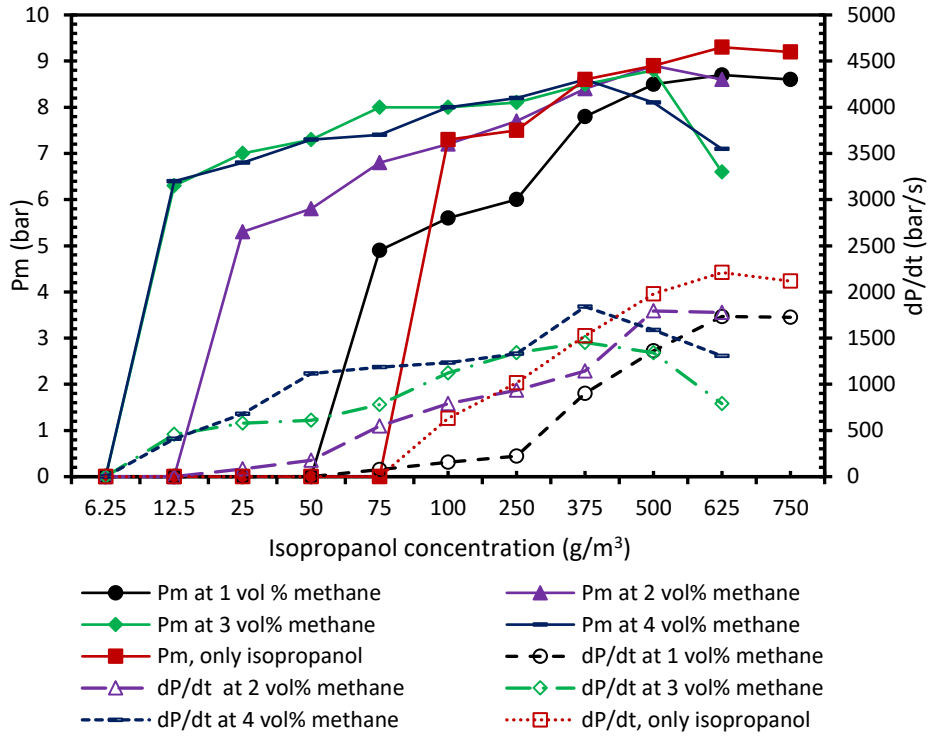


Figure 6.6: Maximum explosion pressure and rate of pressure rise of a mixture of methane and isopropanol spray in dependence on the isopropanol concentration.

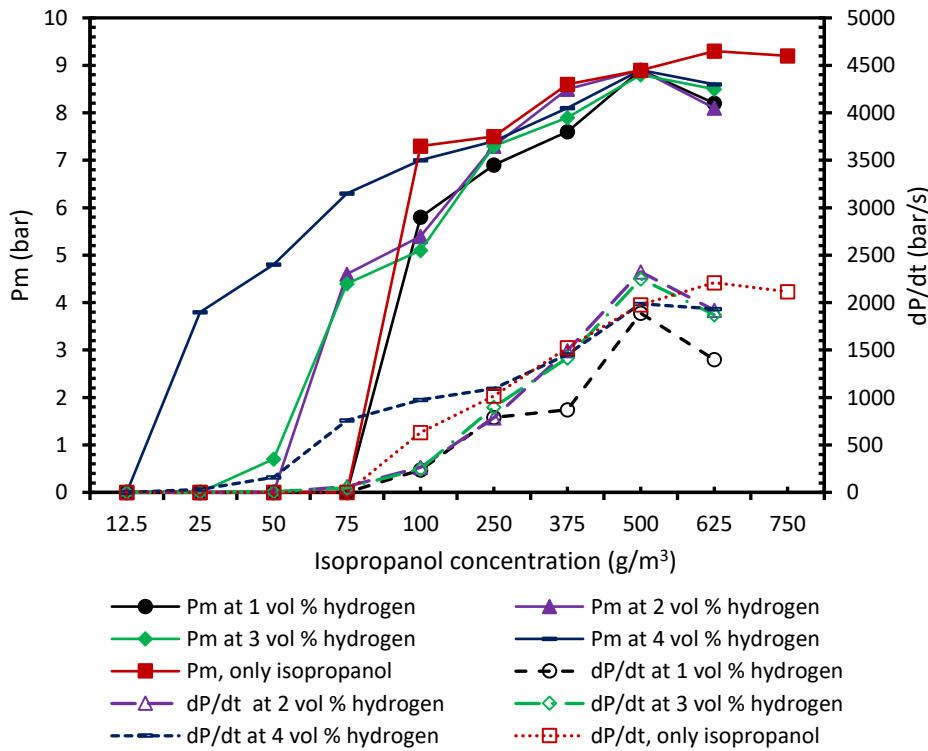


Figure 6.7: Maximum explosion pressure and rate of pressure rise of a mixture of hydrogen and isopropanol spray in dependence on the isopropanol concentration.

6.1.1.3 Lower explosion limits of three-phase hybrid mixtures

Based on the results obtained from single and two-phase mixtures, the lower explosion limits of three-phase hybrid mixtures were investigated. This was achieved by adding non-explosible concentrations of solvent (spray) and gas to a dust at its non-explosible concentration. Figures 6.8 and 6.9 have a fixed isopropanol concentration (50 g/m^3) and show the pressure development for different methane concentrations with increasing dust concentration. Figure 6.8 shows the results for 50 g/m^3 of isopropanol with varying concentrations of methane and lycopodium. The results revealed that increasing the methane concentration up to 4 vol% at 50 g/m^3 isopropanol, lowered the hybrid mixture at which ignition could be observed down to 10 g/m^3 . The special aspect of this result is that, various combinations of two-phase hybrid mixtures where explosions were not obtained became ignitable when just a small amount of the third phase was added. For example, mixtures of 1 vol% methane and 60 g/m^3 lycopodium, 2 vol% methane and 30 g/m^3 lycopodium, which initially were not ignitable became ignitable when a concentration of isopropanol which was 50 % lower than its LEL was added.

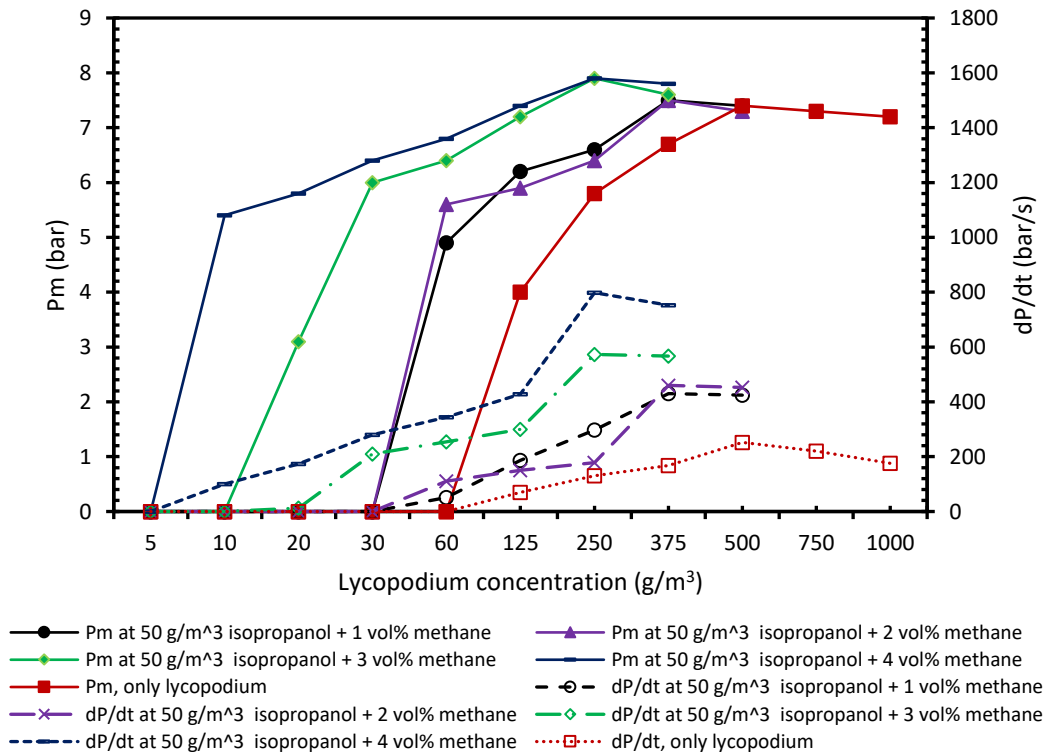


Figure 6.8: Maximum explosion pressure and rate of pressure rise of mixtures of lycopodium, methane and 50 g/m^3 of isopropanol spray in dependence on lycopodium concentration.

Moreover, Figure 6.9 presents the results obtained for 50 g/m³ of isopropanol with respect to various concentrations of methane and brown coal. A similar explosion behavior as explained above was noticed. Adding non-explosible concentrations of isopropanol and methane drastically decreased the explosion limit of hybrid mixtures of brown coal. For example, brown coal with a concentration of 60 g/m³ and 1 vol% of methane, which was originally not ignitable became ignitable when isopropanol concentration (50 % below the LEL) which does not itself form explosible atmosphere was added. Similar explosion behavior was also observed for other tested combinations as presented in Table 6.3 and Figures B.22 to B.35 at Appendix B. It must be noticed that the zero LEL in Table 6.3 indicates that, the addition of solvent and gas alone can explosion without the dust.

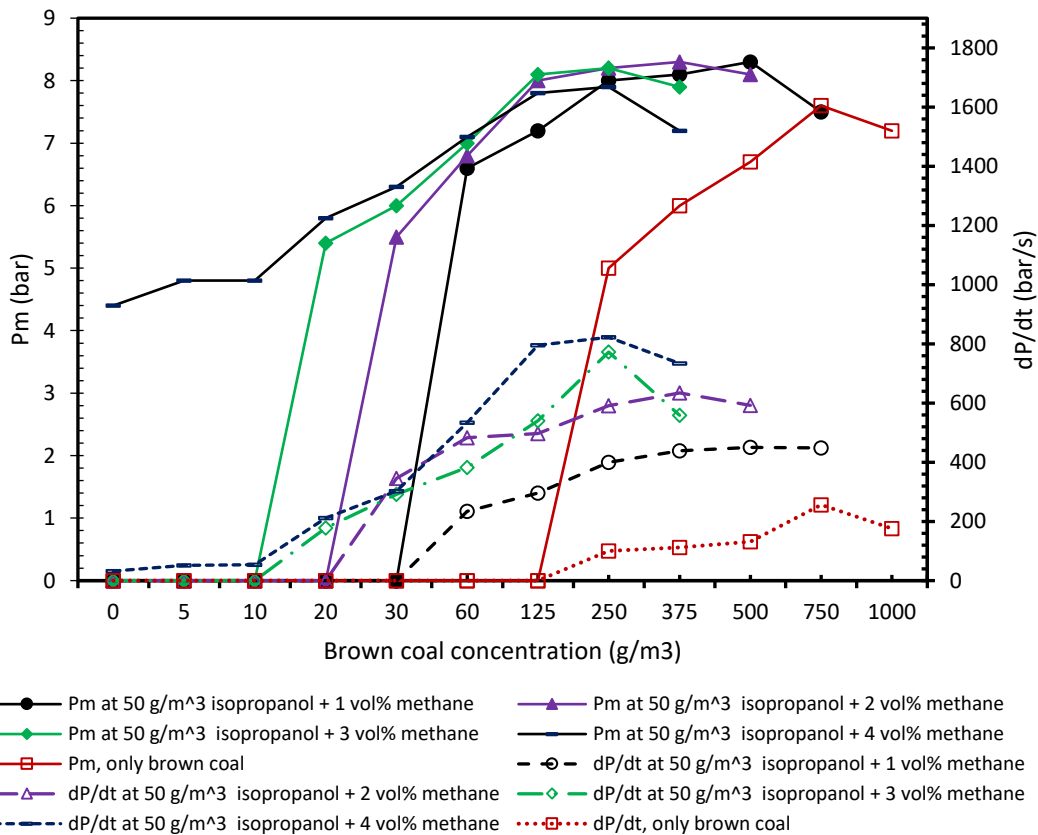


Figure 6.9: Maximum explosion pressure and rate of pressure rise of mixtures of brown coal, methane and 50 g/m³ of isopropanol spray in dependence on the dust concentration.

Table 6.3: A summary of results for the lower explosion limits of three-phase hybrid mixtures.

Hybrid combination	LEL of hybrid mixtures (g/m ³)	Hybrid combinations	LEL of hybrid mixtures (g/m ³)	Hybrid combinations	LEL of hybrid mixtures (g/m ³)	Hybrid combinations	LEL of hybrid mixtures (g/m ³)
LY + 25 g/m ³ IS + 1vol% ME	60	BC + 25 g/m ³ IS + 1vol% ME	250	LY + 25g/m ³ IS+1vol%HY	60	BC + 25g/m ³ IS+1vol% HY	125
LY + 25 g/m ³ IS + 2 vol% ME	60	BC + 25 g/m ³ IS + 2 vol% ME	125	LY + 25g/m ³ IS+2vol%HY	60	BC + 25g/m ³ IS+2vol% HY	125
LY + 25 g/m ³ IS + 3 vol% ME	30	BC + 25 g/m ³ IS + 3 vol% ME	125	LY + 25g/m ³ IS+3vol%HY	30	BC + 25g/m ³ IS+3vol% HY	60
LY + 25 g/m ³ IS + 4 vol% ME	20	BC + 25 g/m ³ IS + 4 vol% ME	60	LY + 25g/m ³ IS+4vol%HY	20	BC + 25g/m ³ IS+4vol% HY	60
LY + 50 g/m ³ IS + 1vol% ME	60	BC + 50 g/m ³ IS + 1vol% ME	125	LY + 50g/m ³ IS+1vol%HY	30	BC + 50g/m ³ IS+1vol% HY	125
LY + 50 g/m ³ IS + 2 vol% ME	60	BC + 50 g/m ³ IS + 2 vol% ME	60	LY + 50g/m ³ IS+2vol%HY	30	BC + 50g/m ³ IS+2vol% HY	125
LY + 50 g/m ³ IS + 3 vol% ME	20	BC + 50 g/m ³ IS + 3 vol% ME	60	LY + 50g/m ³ IS+3vol%HY	20	BC + 50g/m ³ IS+3vol% HY	60
LY + 50 g/m ³ IS + 4 vol% ME	10	BC + 50 g/m ³ IS + 4 vol% ME	0	LY + 50g/m ³ IS+4vol%HY	10	BC + 50g/m ³ IS+4vol% HY	60
LY + 75 g/m ³ IS + 1vol% ME	30	BC + 75 g/m ³ IS + 1vol% ME	125	LY + 75g/m ³ IS+1vol% HY	30	BC + 75g/m ³ IS+1vol% HY	125
LY + 75 g/m ³ IS + 2 vol% ME	20	BC + 75 g/m ³ IS + 2 vol% ME	30	LY + 75g/m ³ IS+2vol% HY	20	BC + 75g/m ³ IS+2vol% HY	125
LY + 75 g/m ³ IS + 3 vol% ME	10	BC + 75 g/m ³ IS + 3 vol% ME	20	LY + 75g/m ³ IS+3vol% HY	20	BC + 75g/m ³ IS+3vol% HY	20
LY + 75 g/m ³ IS + 4 vol% ME	5	BC + 75 g/m ³ IS + 4 vol% ME	0	LY + 75g/m ³ IS+4vol% HY	10	BC + 75g/m ³ IS+4vol% HY	0

6.1.2 Representation of the lower explosion limits of three-phase hybrid mixtures in ternary phase diagrams

In this section, the lower explosion limits of three-phase hybrid mixtures are presented using a ternary phase diagram. A ternary diagram is drawn in the form of a triangle and each side represents one of the phases. The phases of LEL being considered are dusts, gases and solvents. The left side of each diagram represents the gas concentration, while the right side represents the solvent (as spray) concentration and the horizontal axis represents the dust concentration. Each point in the diagram represents a mixture consisting of a specific composition of the three components, while each of the individual concentrations of these components lies between zero and its LEL or MEC, respectively. The summation of components (dust + gas + solvent) must be 100 %. The edges of each diagram indicate the point where gas, dust or solvent is at (100 %), meaning that the substance alone can ignite without the influence of the other component. These points are the lower explosion limits of individual component, e.g. (methane = 5 vol%, hydrogen = 5 vol%, ethanol = 100 g/m³, isopropanol = 100 g/m³, lycopodium = 125 g/m³ and brown coal =

250 g/m³). It must be mentioned that the LEL of the gases are value from experimental results in the 20-litre sphere but not from literature. Figure 6.10 provides a representation on how to obtain each point from the diagram. For example, the percentages of each component presented in Figure 6.10 are: dust = 60 % of MEC, gas = 20 % of LEL and solvent = 20 % of LEL. In order to obtain the total concentration of fuel used for the hybrid mixtures test, the percentages are multiplied by the lower explosion limits of the respective substance. Note, that the concentration of the oxidizer and possibly of inert gases is not represented in this kind of triangle diagrams, but would have to be considered to calculate total concentrations. For instance, if ethanol is considered as a solvent while lycopodium and methane are considered dust and gas respectively, and by applying the point shown in Figure 6.10, the concentration of each component can be obtained by multiplying the fractional percentage by the lower explosion limits. Hence, the concentration of each component could be obtained as: ethanol = 20 g/m³, methane = 1 vol% and lycopodium = 75 g/m³.

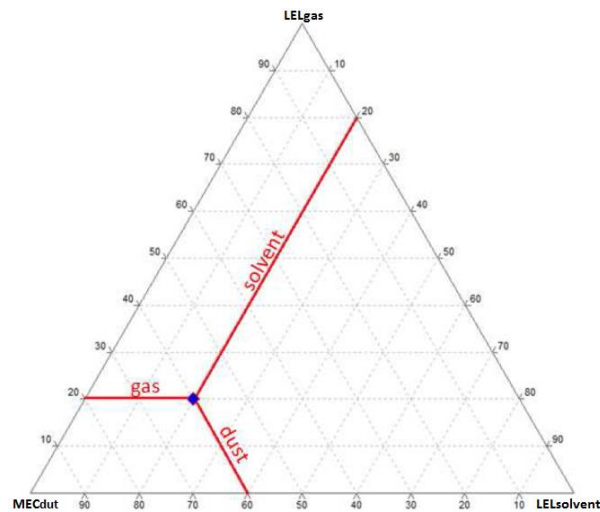


Figure 6.10: A representation on how to obtain each point from the diagram.

Figures 6.11 to 6.18 show ternary phase diagrams for the LELs of different combinations of dusts, gases and solvents (spray). The red “X” symbolizes non- ignition while the blue circle symbolizes ignition. Figure 6.11 presents the results obtained for the LEL of lycopodium, methane and ethanol mixture. Two different regions could be observed from the Figure 6.11, that is: the ignition located at the far left and the middle while the non-ignition portion located far right and the bottom. It could be seen that the influence of lycopodium and methane were more significant

as compared to the solvent. No ignition was observed at high concentration of ethanol (70 % of LEL or higher), lower concentration of lycopodium (10 % of MEC or lower) and lower concentrations of methane (10 % of LEL or lower). On the other hand, lycopodium concentrations at or above 20 % of MEC becomes more explosible when traces of methane and ethanol are added.

Similar explosion behavior was also observed when the solvent was changed to isopropanol as shown in Figure 6.12. However, in this case, ignition was observed at or above 65 % of MEC of lycopodium, 5 % of LEL of methane and 30 % of LEL of isopropanol.

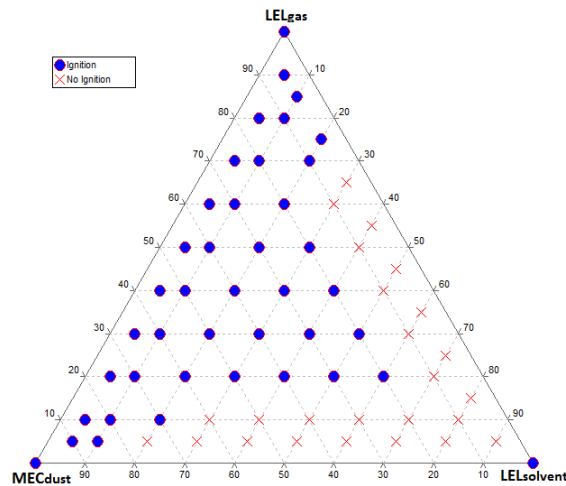


Figure 6.11: Ternary phase diagram for the lower explosion limits of mixtures of lycopodium, methane and ethanol.

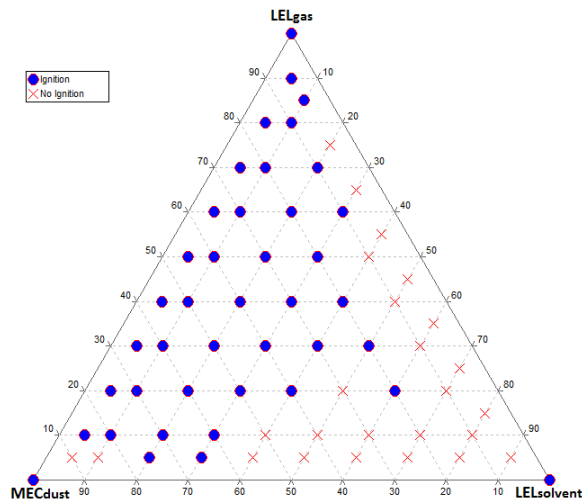


Figure 6.12: Ternary phase diagram for the lower explosion limits of mixtures of lycopodium, methane and isopropanol.

Figure 6.13 presents the results obtained for the LEL of mixtures of brown coal, methane and ethanol. Changing the dust from lycopodium to brown coal marginally changed the ignition behavior. A similar explosion behavior as already discussed for lycopodium, methane and ethanol could also be observed here. The only difference in this case was obtaining an ignition at 10 % of MEC of brown coal, 40 %, 50 % of LEL of methane and 40 %, 50 % of LEL of ethanol of which no ignition was observed when lycopodium was used [158].

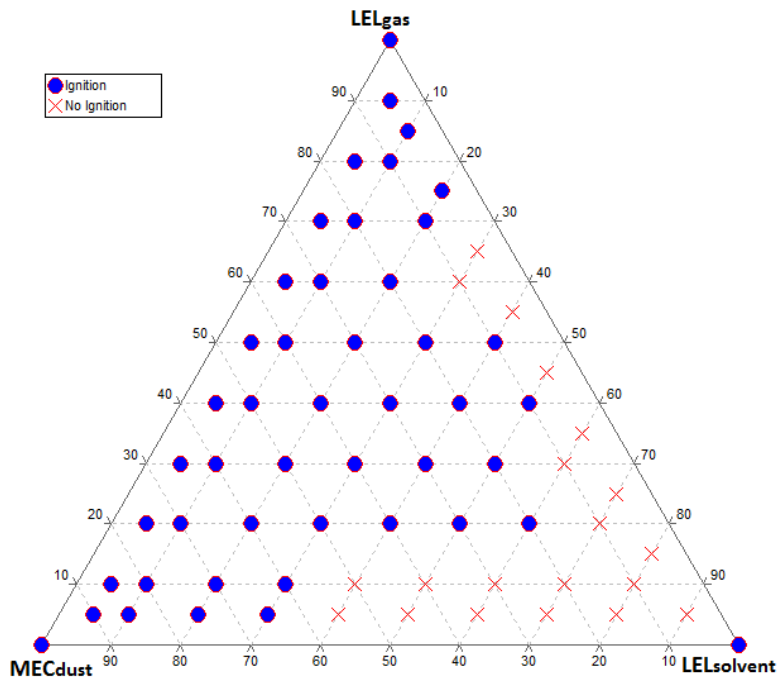


Figure 6.13: Ternary phase diagram for the lower explosion limits of mixtures of brown coal, methane and ethanol.

Furthermore, Figure 6.14 also shows the results obtained for the LEL of hybrid mixtures of brown coal, methane and isopropanol. Similar explosion behavior as already discussed for lycopodium, methane and isopropanol could also be seen here.

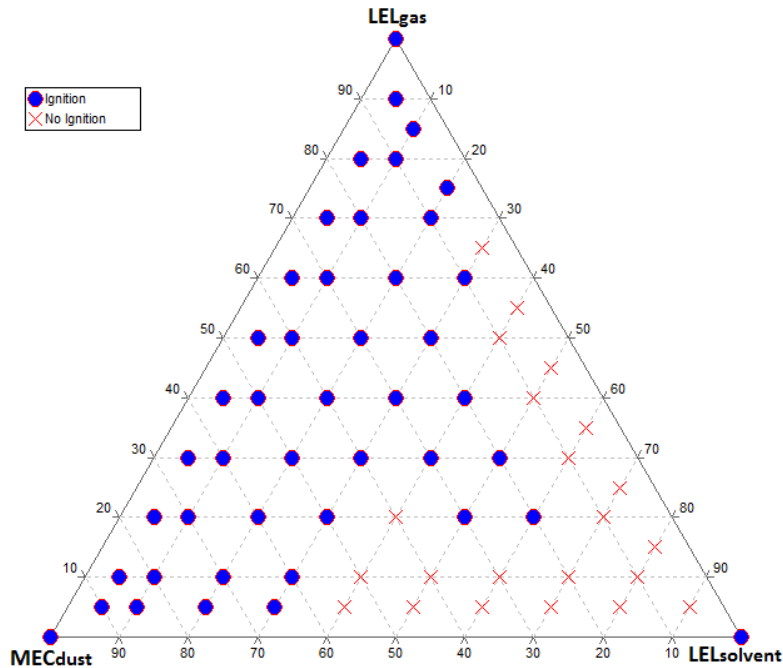


Figure 6.14: Ternary phase diagram for the lower explosion limits of mixtures of brown coal, methane and isopropanol.

Replacing methane with hydrogen showed different explosion behavior for the LEL of hybrid mixtures of gases, dusts and solvents as presented in Figures 6.15 to 6.18. With respect to hybrid mixtures of hydrogen, brown coal and ethanol as shown in Figure 6.15, three different regions could be observed for both ignition and non-ignition. Ignitions were observed in the middle, top and some parts of the left side of the diagram, while no ignition was noticed at low dust, gas and very high solvent concentrations. Moreover, no ignition was recorded at 5 %, 10 % of LEL of ethanol, 50 % to 70 % of LEL of hydrogen and 25 % to 45 % of MEC of brown coal. On the other hand, a different behavior was noticed when the solvent was changed to isopropanol as shown in Figure 6.16. Ignitions were obtained at 5 %, 10 % of LEL of ethanol, 50 % to 70 % of LEL of hydrogen and 25 % to 45 % of MEC of brown coal.

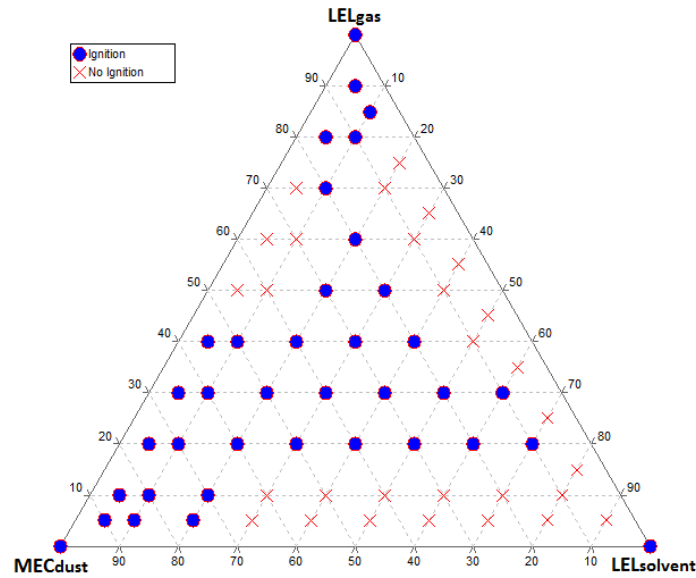


Figure 6.15: Ternary phase diagram for the lower explosion limits of mixtures of brown coal, hydrogen and ethanol.

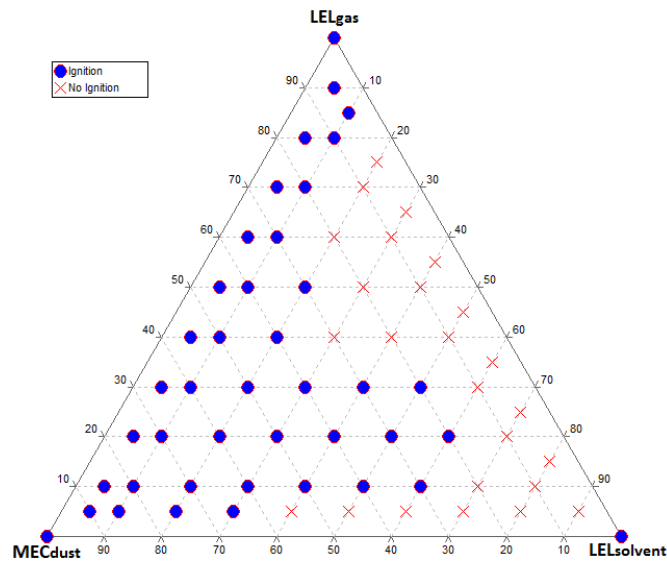


Figure 6.16: Ternary phase diagram for the lower explosion limits of mixtures of brown coal, hydrogen and isopropanol.

Moreover, Figure 6.17 presents the experimental results for the LEL of hybrid mixtures of hydrogen, lycopodium and isopropanol. Again, similar explosion behavior as discussed for brown coal, hydrogen and ethanol could be observed, but in this case, ignitions were obtained at 10 % of isopropanol, 50 % to 70 % of hydrogen and 25 % to 45 % of MEC of lycopodium as well as 10 % of LEL of hydrogen, 40 % to 60 % of LEL of isopropanol and 30 % to 50 % of brown coal. With respect to lycopodium, hydrogen and ethanol, ignitions were obtained for most combinations

with the exception of very low concentrations of lycopodium (5 % of MEC) as presented in Figure 6.18.

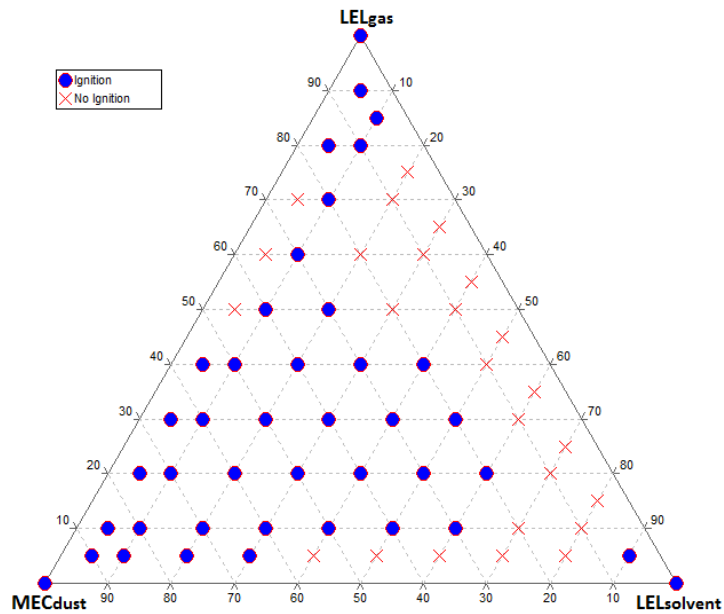


Figure 6.17: Ternary phase diagram for the lower explosion limits of mixtures of lycopodium, hydrogen and isopropanol.

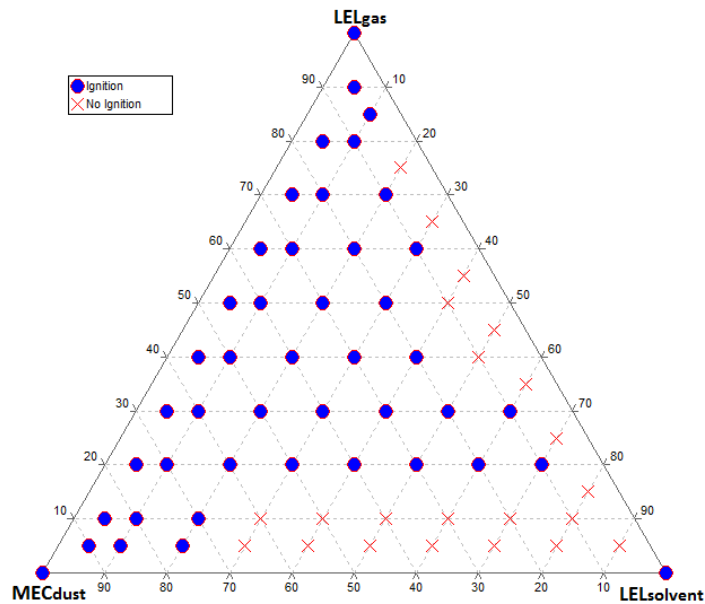


Figure 6.18: Ternary phase diagram for the lower explosion limits of mixtures of lycopodium, hydrogen and ethanol.

Based on the above discussion, it can clearly be deduced that the explosion behavior of hybrid mixtures cannot be predicted by simply overlapping the effects of the single substance

explosions. Mixtures of combustible substances with different states of aggregation increase the total concentration of combustibles in the system. With regard to hybrid mixture explosions, where the concentrations of the individual substances are below their respective LELs, not only the concentrations of the main substances are considered, but the summation of all combustible substances present in the mixtures are also valuable. For example, mixtures of 60 g/m³ brown coal, 25 g/m³ isopropanol and 2 vol% methane, formed an explosible atmosphere even though the added concentrations of the individual substances were far below the respective LELs. This could also be explained with the help of Le Chatelier's Law, which states that the total concentration of mixture has to be above a certain value for an explosion to occur (see section 3.2.1.3.1 on the discussion on the Le Chatelier's Law). When this value is reached, even if the concentration of the single substances below their LEL/MEC, ignition could occur [161].

6.1.3 Lower explosion limits in the Godbert-Greenwald (GG) furnace

Contrary to the standard 20-liter sphere which is normally used to determine the LEL or MEC of single substances and hybrid mixtures [96, 97] (as already discussed in Section 6.1.2), in this section, the Godbert-Greenwald (GG) furnace, an apparatus to determine the minimum ignition temperature of dusts, was used instead. The standard 20-liter sphere uses 10 J electrical spark ignition for gases LEL tests while 2 kJ chemical igniters are used for MEC tests of dusts.

Considering the factor of 200 between these two ignition energy values, the difficulty arises from which ignition energy could be an appropriate choice for hybrid mixtures in the 20-liter sphere. One might argue using instead a hot surface as an ignition source for which the differences in the ignition criteria for dusts and flammable gases are comparatively small. Moreover, the effect of ignitability is more visible when the mixture is exposed to a hot surface and, perhaps, the concentration at least of the dust is better defined in the GG furnace compared to the 20-liter sphere.

Furthermore, electric sparks and electrostatic discharges as well as hot surface are considered as one of the common sources of ignition for explosions occurring in the workplaces [22], therefore, one could use a hot surface to determine the explosion limits of dusts, gases and hybrid mixtures is justified.

Furthermore, the standard test method for minimum ignition temperatures of flammable gases, which is the Erlenmeyer flask does not allow for the dispersion of particles. Hence, this present section discusses experimental results from explosion limits of dusts, gases/vapor and hybrid mixtures using hot surface as an ignition source.

Three main testing cases are considered:

1. Testing for the LEL/MEC of single substances
2. Testing for the LEL/MEC of hybrid mixtures (two-phase and two component mixtures)
3. Testing for LEL/MEC of three component mixtures.

6.1.3.1 Lower explosion limits of single substances

In order to prove the validity of the experimental procedure used, the LEL for pure gases was initially tested and the results were compared with literature values obtained from the standard procedure according to [96]. From Table 6.4 it can be seen that the experimental results according to the method described in Section 5.3, were in agreement with the work done by **Brandes et al. [83]** with maximum deviations of 0.4 vol%. The deviations observed from the comparison of the experimental results and the values found in the literature were within the 6.3 % error margin obtained from the error and uncertainty analysis, discussed in detail in Appendix C.1. Moreover, with respect to the MEC of dust, a comparison was made between the results obtained from the GG furnace and the standard 20-liter sphere. The MEC for lycopodium obtained using the standard 20-liter sphere with 10 J electric sparks as ignition source was 125 g/m³, while the value obtained from the GG furnace was 108 g/m³, which was 17 g/m³ lower than the value obtained from the standard method. However, this deviation is within the experimental uncertainty. The concentration of the dusts was obtained by dividing the mass of dusts used by the total volume of the furnace. It should be noticed that the method used in this section (GG furnace) does not seek to replace the standard method for determination of LEL/MEC of dusts, gases or solvents, but could be used as an alternative method to determine the explosion limits of hybrid mixtures. As globally known that the explosion limits decrease by increasing temperature [162], a standard approach was considered by performing all the tests at a temperature 20 to 40 °C (depending on the material) above the minimum ignition temperature of the substance or mixtures. It must be mention that the explosion limit is influence by the temperature of the furnace, as a results of

this the effect of temperature on the explosion limits were initially tested (see Figure C.1 in appendix C) before selecting a specific temperature explosion limits testing.

*Table 6.4: LEL and MIT of gases, the furnace temperature used in the individual and hybrid mixtures tests as well as a comparison between the LEL according to **Brandes et al. [83]** and the experimental results.*

Gases	Experimental LEL (vol%)	LEL from Brandes et al. (vol%)	Deviations (vol%)	MIT (°C)	Furnace temperature used for LEL test (°C)
Methane	4.0	4.4	0.4	600	620
Propane	2.0	1.7	0.3	500	520
Hydrogen	5.0	4.6	0.4	530	550
Ethanol	3.0	3.3	0.3	410	430
Isopropanol	2.0	2.0	0	440	460
Toluene	1.1	1.1	0	540	560
Hexane	1.6	1.3	0.3	240	260

Table 6.5 presents experimentally determined MEC values of the dusts samples. It could be seen that toner recorded the lowest MEC, followed by lycopodium, starch and HDPE. This trend could be attributed to the particle size of the dust materials. Decreasing the particle size of the dusts increases the specific surface area available for ignition to prevail. This can be observed by comparing toner (median value = 14 µm) to HDPE (median value = 61 µm).

Table 6.5: MEC and MIT of dusts as well as the density of dusts and the furnace temperature used for single substances and hybrid mixtures tests.

Dust	MEC (g/m ³)	MIT (°C)	Furnace temperature used for the MEC test (°C)
Toner	87	460	490
Lycopodium	108	400	440
Starch	145	380	440
HDPE	185	340	370

6.1.3.2 Lower explosion limits of two-phase hybrid mixtures

In the next step, the LEL and MEC of hybrid mixtures of combustible dusts, gases or vapor were considered. This was done to verify if the addition of a combustible dust at a concentration below its MEC could decrease the LEL of gases and vice versa. Two main testing series were considered which include: the effect of addition of non-explosible concentrations of dusts on the LEL of gases and the effect of the addition of non-explosible concentrations of gases on the MEC of dusts.

Figure 6.19 presents the results of the addition of small concentrations (i.e. below its MEC) of dust, which itself does not form an explosible atmosphere to gases below their LEL. It could be seen that with the exception of hexane for which there was no influence of dust on its LEL of hybrid mixtures, the explosion limits of all other gases decreased upon the addition of a non-explosible concentration of dust. For example, the explosion limit of hybrid mixtures of methane and HDPE decreased from 4 vol% to 1 vol% when 87 g/m³ of high density polyethylene (HDPE) was added.

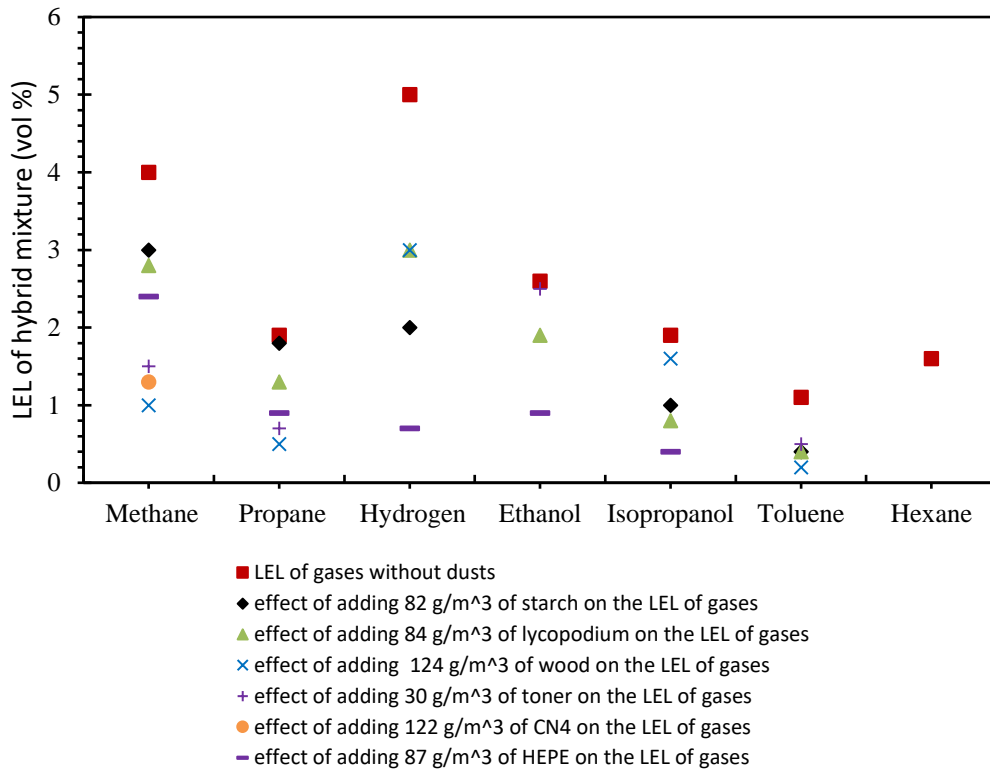


Figure 6.19: LEL of two-phase hybrid mixture of dusts and gases or solvent- vapor (effect of admixture of dust on the LEL of gas).

The reason why there was no effect of dusts on the MIT of hexane could be attributed to its low ignition temperature compared to the dust samples. With respect to the organic dusts ignition, the volatile matters in the dusts initially devolatilizes forming combustible gases (as already discussed in section 2.4.1). These volatile gases are then mixed with either the combustible gas or vapor to increase the gaseous fuel content which increases the ignitability of the mixture. However, in the case of hexane and dust mixtures, this devolatilization of the dust is not possible

since, the dust is introduced into the combustion chamber at a temperature which is far below its ignition temperature. Hence, no effect was seen when dust was added to hexane.

Furthermore, the effects of the addition of flammable gases on the explosion limits of hybrid mixtures (dust + gas) were also studied by adding volume fractions of the gases, which were below the LEL of the gases. Figure 6.20 presents the results of the addition of non-explosible concentrations of gases to different dusts below their MEC. It could be seen that the explosion limits of hybrid mixtures of dust and gas decreased when a non-explosible concentration of gas was added. For example, the explosion limits of hybrid mixture of toner decreased from 87 g/m³ to 21 g/m³ when 1.0 vol% of isopropanol vapor, which do not form explosible atmosphere, was added. These results confirmed the work done by [13, 19, 163] where it was concluded that the explosion limits of hybrid mixtures of dust and gas could decrease upon the addition of a non-explosible concentration of gas.

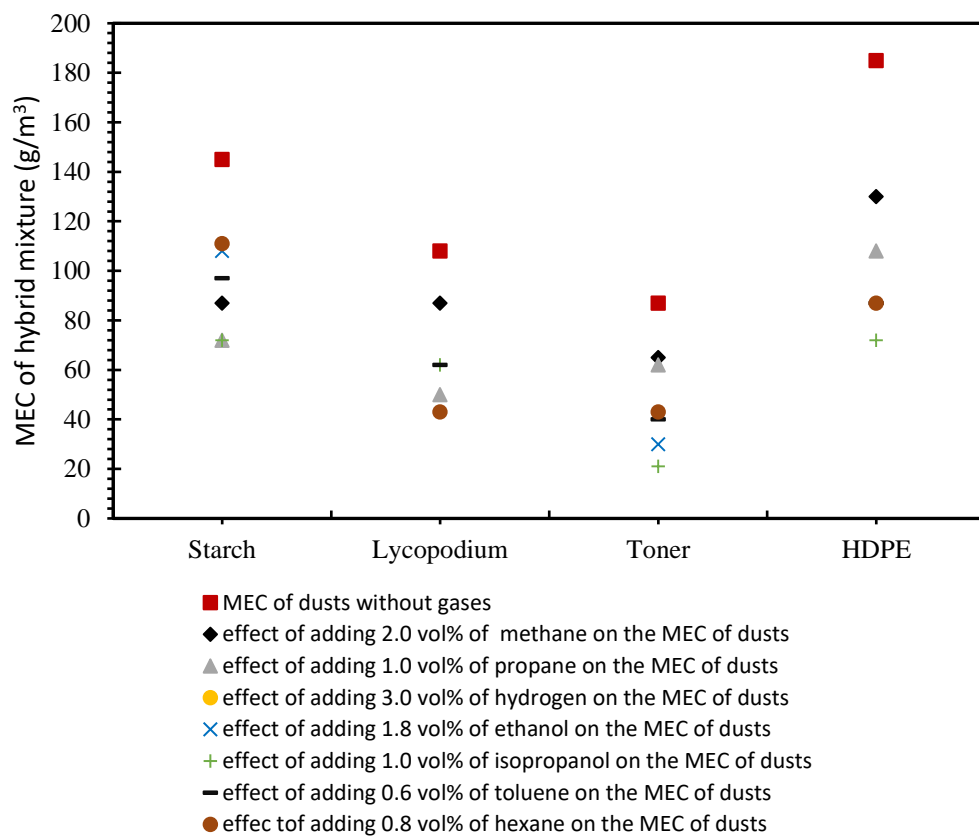


Figure 6.20: MEC of two-phase hybrid mixture of dusts and gases or solvents- vapor (effect of admixture of gas on the MEC of dust).

Furthermore, the LEL of two component mixtures – one being a gas and the other solvent vapor were also tested. Figures 6.21 and 6.22 present the results of the LEL tests of two component mixtures. It could be seen that the LELs of hybrid mixture generally decreased when a non-explosible concentration of one component was added to the other at its non-explosible concentration. For example, the explosion limit of hybrid mixtures of hydrogen and hexane decreased from 5 vol % to 0.5 vol % when 0.8 vol% of hexane was added.

A similar explosion behavior was also noticed when non-explosible concentrations of gases were added to solvent. No effects were observed when gases were added to hexane. This could be as a result of the low ignition temperature of hexane in comparison to the gases. Below the ignition temperature of gases, it is considered that irrespective of the concentration of gas used, ignition will not be obtained. Since, the effect of a gases on the LEL of hexane was tested at 260 °C which is 340°C, 270°C and 240°C below the MIT of methane, hydrogen and propane respectively. It could be said that no matter what the added amount of gas to hexane is, no ignition will be obtained. Hence, no effect of gases was seen on the LEL of hexane.

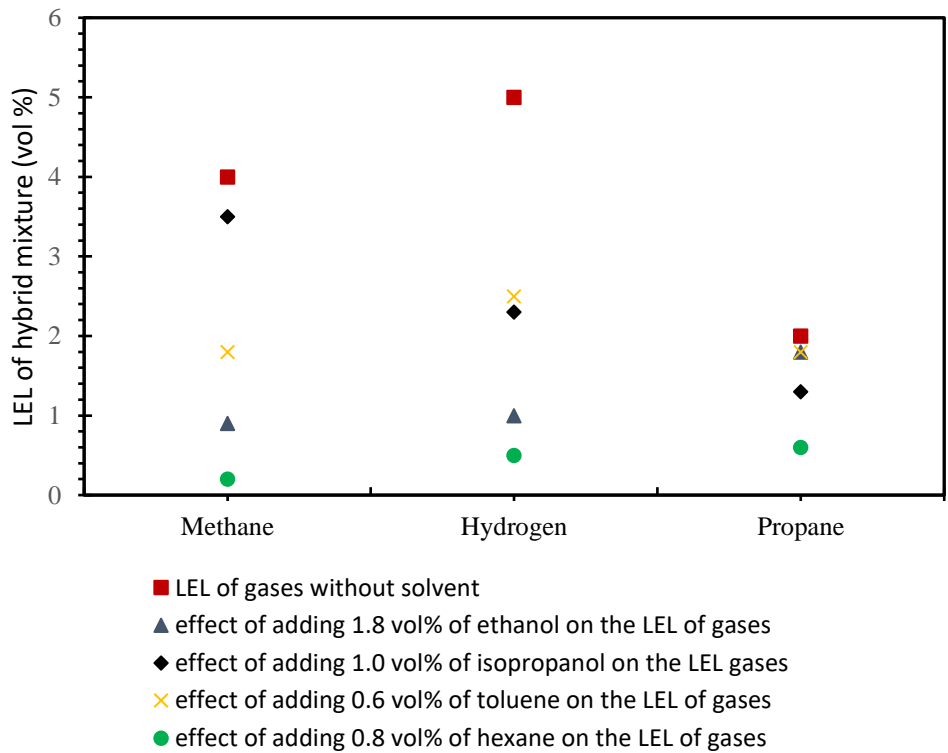


Figure 6.21: LEL of hybrid mixture of solvents and gases (effect of admixture of solvent on the LEL of gas).

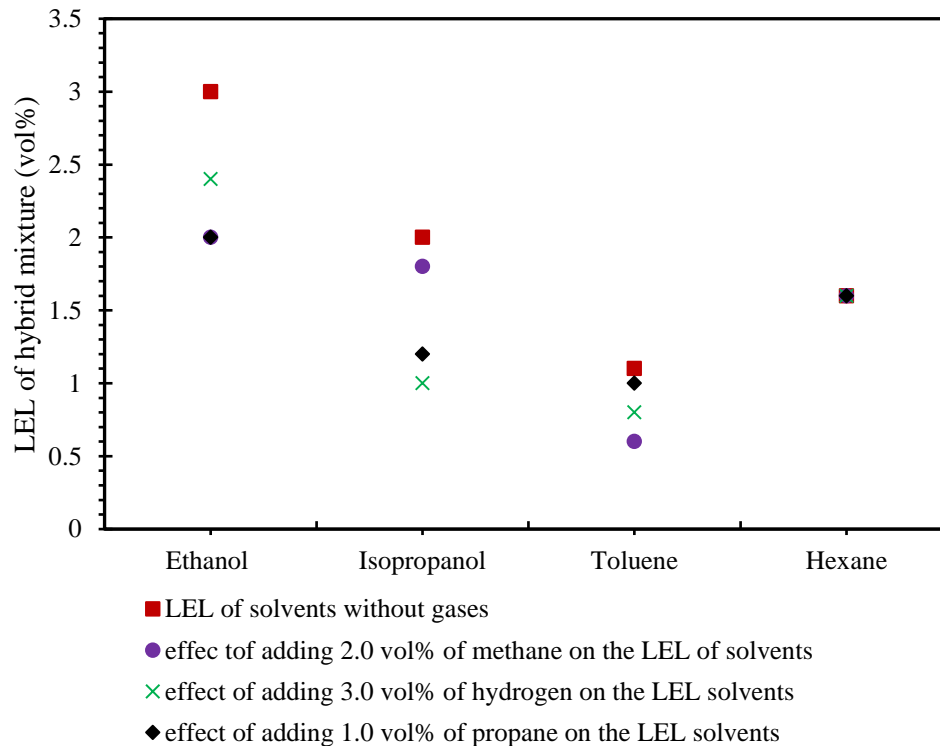


Figure 6.22: LEL of hybrid mixture of solvents and gases (effect of admixture of gas on the LEL of solvent).

6.1.3.3 Lower explosion limits of three component hybrid mixtures

Based on the results obtained from the single and double-phase or component mixtures, the LEL/MEC of mixtures of three-components were tested. In this case, three different groups of experimental tests were considered:

1. The effect of admixture of gases and solvents on the MEC of dusts
2. The effect of admixture of dusts and solvents on the LEL of gases
3. The effect of admixture of gases and dusts on the LEL of solvents.

For the first test case, both gases and solvents at concentrations below their respective LELs were added to the dusts at concentrations below their MEC. Table 6.6 shows the results of adding gas and solvent on the MEC of dust. It can be seen that, in comparison with the two-component hybrid mixtures the amount of dust for which a successful ignition was observed, further decreased. For example, HDPE with MEC of 185 g/m^3 decreased to 130 g/m^3 upon the addition of 2 vol% of methane which itself is not explosible (below the LEL). This concentration further decreased to 65 g/m^3 when 0.8 vol% of hexane were further added.

Table 6.6: Effect of an admixture of gases and solvents on the MEC of dust, (dust concentrations in g/m³).

Dust (g/m ³)	MEC of dusts	effect of admixture of 0.8 vol% hexane on the MEC of dusts	effect of admixture of 2.0 vol% methane on the MEC of dusts	effect of admixture of 2.0 vol% methane and 0.8 vol% hexane on the MEC of dusts	effect of admixture of 1.0 vol% propane on the MEC of dusts	effect of admixture of 1.0 vol% propane and 0.8 vol% hexane on the MEC of dusts	effect of admixture of 3.0 vol% hydrogen on the MEC of dusts	effect of admixture of 3.0 vol% hydrogen and 0.8 vol% hexane on the MEC of dusts
HDPE	185	87	130	65	108	87	170	119
Lycopodium	108	43	87	33	50	43	71	28
Starch	145	111	97	96	72	50	121	65
Toner	87	43	65	22	62	43	87	48
Dust (g/m ³)	MEC of dusts	effect of admixture of 1.0 vol% isopropanol on the MEC of dusts	effect of admixture of 2.0 vol% methane on the MEC of dusts	effect of admixture of 2.0 vol% methane and 1.0 vol% isopropanol on the MEC of dusts	effect of admixture of 1.0 vol% propane on the MEC of dusts	effect of admixture of 1.0 vol% propane and 1.0 vol% isopropanol on the MEC of dusts	effect of admixture of 3.0 vol% hydrogen on the MEC of dusts	effect of admixture of 3.0 vol% hydrogen and 1.0 vol% isopropanol on the MEC of dusts
HDPE	185	145	130	72	108	43	170	170
Lycopodium	108	87	87	62	50	43	71	71
Starch	145	145	97	72	72	62	121	121
Toner	87	62	65	21	62	40	87	87
Dust (g/m ³)	MEC of dusts	effect of admixture of 1.8 vol% ethanol on the MEC of dusts	effect of admixture of 2.0 vol% methane on the MEC of dusts	effect of admixture of 2.0 vol% methane and 1.8 vol% ethanol on the MEC of dusts	effect of admixture of 1.0 vol% propane on the MEC of dusts	effect of admixture of 1.0 vol% propane and 1.8 vol% ethanol on the MEC of dusts	effect of admixture of 3.0 vol% hydrogen on the MEC of dusts	effect of admixture of 3.0 vol% hydrogen and 1.8 vol% ethanol on the MEC of dusts
HDPE	185	133	130	92	108	63	170	163
Lycopodium	108	108	87	62	50	43	71	71
Starch	145	108	97	72	72	56	121	145
Toner	87	62	65	43	62	33	87	66
Dust (g/m ³)	MEC of dusts	effect of admixture of 0.6 vol% toluene on the MEC of dusts	effect of admixture of 2.0 vol% methane on the MEC of dusts	effect of admixture of 2.0 vol% methane and 0.6 vol% toluene on the MEC of dusts	effect of admixture of 1.0 vol% propane on the MEC of dusts	effect of admixture of 1.0 vol% propane and 0.6 vol% toluene on the MEC of dusts	effect of admixture of 3.0 vol% hydrogen on the MEC of dusts	effect of admixture of 3.0 vol% hydrogen and 0.6 vol% toluene on the MEC of dusts
HDPE	185	145	130	87	108	72	170	170
lycopodium	108	87	92	62	50	50	71	71
starch	145	111	97	97	72	41	121	121
toner	87	62	65	43	62	22	87	87

Furthermore, Table 6.7 presents the results of an admixture of dusts and solvents on the LEL of gases. Dust at a concentration below its MEC and solvent at a concentration below its LEL were added to the gas to check if an explosion could be obtained at a concentration below the LEL of the gas. Similar explosion behavior as explained above was also noticed. An explosion could be obtained at the concentrations, where both dusts and solvent mixtures did not ignite. The LEL of propane decreased from 1.9 vol% to 1.3 vol% when 84 g/m³ of lycopodium was added. This concentration further decreased to 0.8 vol % when 1.8 vol% of ethanol was added.

Table 6.7: Effect of an admixture of dusts and solvents on the LEL of gases, (gas concentrations in vol %).

Gases (Vol %)	LEL of only gases	effect of admixture of 0.8 vol% hexane on the LEL of gases	effect of admixture of 87 g/m ³ HDPE on the LEL of gases	effect of admixture of 87 g/m ³ HDPE and 0.8 vol% hexane on the LEL of gases	effect of admixture of 84 g/m ³ lycopodium on the LEL of gases	effect of admixture of 84 g/m ³ lycopodium and 0.8 vol% hexane on the LEL of gases	effect of admixture of 82 g/m ³ starch on the LEL of gases	effect of admixture of 82 g/m ³ starch and 0.8 vol% hexane on the LEL of gases	effect of admixture of 30 g/m ³ toner on the LEL of gases	effect of admixture of 30 g/m ³ toner and 0.8 vol% hexane on the LEL of gases
Methane	4.0	0.2	2.4	0.1	2.8	0.1	3.0	0.1	3.4	0.1
Propane	1.9	0.6	0.9	0.2	1.3	0.4	1.8	0.5	1.6	0.3
Hydrogen	5.0	0.5	2.3	0.2	3.1	0.5	3.3	0.3	3.0	0.3

Gases (Vol %)	LEL of only gases	effect of admixture of 1.0 vol% isopropanol on the LEL of gases	effect of admixture of 87 g/m ³ HDPE on the LEL of gases	effect of admixture of 87 g/m ³ HDPE and 1.0 vol% isopropanol on the LEL of gases	effect of admixture of 84 g/m ³ lycopodium on the LEL of gases	effect of admixture of 84 g/m ³ lycopodium and 1.0 vol% isopropanol on the LEL of gases	effect of admixture of 82 g/m ³ starch on the LEL of gases	effect of admixture of 82 g/m ³ starch and 1.0 vol% isopropanol on the LEL of gases	effect of admixture of 30 g/m ³ toner on the LEL of gases	effect of admixture of 30 g/m ³ toner and 1.0 vol% isopropanol on the LEL of gases
Methane	4.0	3.5	2.4	0.1	2.8	0.1	3.0	0.1	3.4	0.1
Propane	1.9	1.3	0.9	0.4	1.3	1.0	1.8	0.5	1.6	1.3
Hydrogen	5.0	2.3	2.3	0.7	3.1	1.3	3.3	1.7	3.0	1.5

Gases (Vol %)	LEL of only gases	effect of admixture of 1.8 vol% ethanol on the LEL of gases	effect of admixture of 87 g/m ³ HDPE on the LEL of gases	effect of admixture of 87 g/m ³ HDPE and 1.8 vol% ethanol on the LEL of gases	effect of admixture of 84 g/m ³ lycopodium on the LEL of gases	effect of admixture of 84 g/m ³ lycopodium and 1.8 vol% ethanol on the LEL of gases	effect of admixture of 82 g/m ³ starch on the LEL of gases	effect of admixture of 82 g/m ³ starch and 1.8 vol% ethanol on the LEL of gases	effect of admixture of 30 g/m ³ toner on the LEL of gases	effect of admixture of 30 g/m ³ toner and 1.8 vol% ethanol on the LEL of gases
Methane	4.0	0.9	2.4	0.1	2.8	0.1	3.0	0.1	3.4	0.1
Propane	1.9	0.9	0.9	0.05	1.3	0.8	1.8	0.5	1.6	0.8
Hydrogen	5.0	1.0	2.3	0.6	3.1	0.7	3.3	1.0	3.0	0.8

Gases (Vol %)	LEL of only gases	effect of admixture of 0.6 vol% toluene on the LEL of gases	effect of admixture of 87 g/m ³ HDPE on the LEL of gases	effect of admixture of 87 g/m ³ HDPE and 0.6 vol% toluene on the LEL of gases	effect of admixture of 84 g/m ³ lycopodium on the LEL of gases	effect of admixture of 84 g/m ³ lycopodium and 0.6 vol% toluene on the LEL of gases	effect of admixture of 82 g/m ³ starch on the LEL of gases	effect of admixture of 82 g/m ³ starch and 0.6 vol% toluene on the LEL of gases	effect of admixture of 30 g/m ³ toner on the LEL of gases	effect of admixture of 30 g/m ³ toner and 0.6 vol% toluene on the LEL of gases
Methane	4.0	1.8	2.4	0.1	2.8	0.1	3.0	0.1	3.4	0.1
Propane	1.9	1.8	0.9	0.5	1.3	0.8	1.8	0.5	1.6	0.9
Hydrogen	5.0	1.7	2.3	1.5	3.1	0.8	3.3	1.7	3.0	1.7

Finally, Table 6.8 provides the results of admixing dust and gas on the LEL of solvents. In this case, dust at a concentration below its MEC and gas at a concentration below its LEL were added to the solvents. It was observed that explosions were obtained at concentrations where both dust and gas mixtures alone could not explode. For example, toluene with LEL of 1.1 vol% decreased to 0.4 vol% when 82 g/m³ of starch was added. This concentration further decreased to 0.2 vol% when 2 vol% of methane was added to the mixture. In general, it was noticed that no effect on LEL was

observed when concentrations of both combustible dusts and flammable gases were added to hexane. This might be as a result of lower ignition temperature of hexane as explained in the previous section. Detailed discussion on these results could be referred to the discussion section of section 6.4.

Table 6.8: Effect of an admixture of dusts and gases on the LEL of solvents, (solvent concentrations in vol%).

Solvents (Vol %)	LEL of only gases	effect of admixture of 2.0 vol% methane on the LEL of gases	effect of admixture of 87 g/m ³ HDPE on the LEL of solvents	effect of admixture of 87 g/m ³ HDPE and 2.0 vol% methane on the LEL solvents	effect of admixture of 84 g/m ³ lycopodium on the LEL of solvents	effect of admixture of 84 g/m ³ lycopodium and 2.0 vol% methane on the LEL of solvents	effect of admixture of 82 g/m ³ starch on the LEL of solvents	effect of admixture of 82 g/m ³ starch and 2.0 vol% methane on the LEL of solvents	effect of admixture of 30 g/m ³ toner on the LEL of solvents	effect of admixture of 30 g/m ³ toner and 2.0 vol% methane on the LEL of solvents
Hexane	1.6	1.6	1.6	1.6	1.6	1.6	1.6	1.6	1.6	1.6
Isopropanol	1.9	1.5	0.9	0.6	0.8	0.7	1.0	1.0	0.6	0.6
Ethanol	2.6	2.0	0.7	0.7	1.9	1.5	0.7	0.7	2.6	2.6
Toluene	1.1	0.6	0.4	0.2	0.4	0.2	0.4	0.2	0.5	0.3

Solvents (Vol %)	LEL of only gases	effect of admixture of 1.0 vol% propane on the LEL of gases	effect of admixture of 87 g/m ³ HDPE on the LEL of solvents	effect of admixture of 87 g/m ³ HDPE and 1.0 vol% propane on the LEL solvents	effect of admixture of 84 g/m ³ lycopodium on the LEL of solvents	effect of admixture of 84 g/m ³ lycopodium and 1.0 vol% propane on the LEL of solvents	effect of admixture of 82 g/m ³ starch on the LEL of solvents	effect of admixture of 82 g/m ³ starch and 1.0 vol% propane on the LEL of solvents	effect of admixture of 30 g/m ³ toner on the LEL of solvents	effect of admixture of 30 g/m ³ toner and 1.0 vol% propane on the LEL of solvents
Hexane	1.6	1.6	1.6	1.6	1.6	1.6	1.6	1.6	1.6	1.6
Isopropanol	1.9	1.0	0.9	0.6	0.8	0.8	0.2	0.2	0.6	0.5
Ethanol	2.6	2.4	0.7	0.7	1.9	1.0	0.7	0.7	2.6	1.7
Toluene	1.1	0.8	0.4	0.1	0.4	0.05	0.4	0.05	0.5	0.2

Solvents (Vol %)	LEL of only gases	effect of admixture of 3.0 vol% hydrogen on the LEL of gases	effect of admixture of 87 g/m ³ HDPE on the LEL of solvents	effect of admixture of 87 g/m ³ HDPE and 3.0 vol% hydrogen on the LEL solvents	effect of admixture of 84 g/m ³ lycopodium on the LEL of solvents	effect of admixture of 84 g/m ³ lycopodium and 3.0 vol% hydrogen on the LEL of solvents	effect of admixture of 82 g/m ³ starch on the LEL of solvents	effect of admixture of 82 g/m ³ starch and 3.0 vol% hydrogen on the LEL of solvents	effect of admixture of 30 g/m ³ toner on the LEL of solvents	effect of admixture of 30 g/m ³ toner and 3.0 vol% hydrogen on the LEL of solvents
Hexane	1.6	1.6	1.6	1.6	1.6	1.6	1.6	1.6	1.6	1.6
Isopropanol	1.9	1.9	0.9	0.8	1.0	0.7	1.0	0.6	1.9	1.9
Ethanol	3.0	3.0	0.7	0.7	2.5	2.5	0.7	0.5	2.7	2.7
Toluene	1.1	1.1	0.4	0.1	0.3	0.3	0.4	0.4	0.5	0.3

6.1.4 Mathematical models to estimate the lower explosion limits of dusts, gases and hybrid mixtures

Different mathematical models proposed by different authors to estimate the lower explosion limits of dusts, gases and their mixtures are presented (see section 3.2.1). Moreover, comparisons between these models and the experimental results are presented in this section. Detailed parameters used in both dust and gas models can be found in Tables 4.1 to 4.3.

6.1.4.1 Comparison of single dusts and gases models with experimental results

With respect to dust samples, mathematical models proposed by Shevchuk et al. [99], Schonewald [98], and Buksowicz et al. [100] (see section 3.2.1.1 for detailed discussion of these models) to predict the minimum explosion concentration are compared with the experimental results as shown in Figure 6.23. The “X” symbolizes experimental results while, the rest of the symbols indicate the calculated MECs from the three models. An error bar based on the error and uncertainty analysis (7%) is plotted on the experimental results (see Appendix C.1 for detail discussion on the error and uncertainty analysis). It could be seen from Figure 6.23 that the calculated results from the models were all below the experimental values. The models under-predicted the MEC of dusts, this seems to be good from a safety point of view but the margins were too wide. For example, brown coal with the experimental value of 250 g/m³ gave calculated results of 145 g/m³, 79 g/m³ and 69 g/m³ when Buksowicz et al., Shevchuk et al. and Schönewald models were applied respectively. Moreover, it was generally noticed that the model according to Schönewald produced the lowest MEC values, which might be due to the assumptions and conditions based on which the model was derived. These models were formulated under the assumption of a homogeneous fuel-air mixture and a complete combustion. However, the experimental determination of the MEC is very complicated because of the difficulties to form homogenous dust dispersion. Local distributions of the dust concentration may cause considerable errors in the experiment and hence, the model results are far lower than the experimental results.

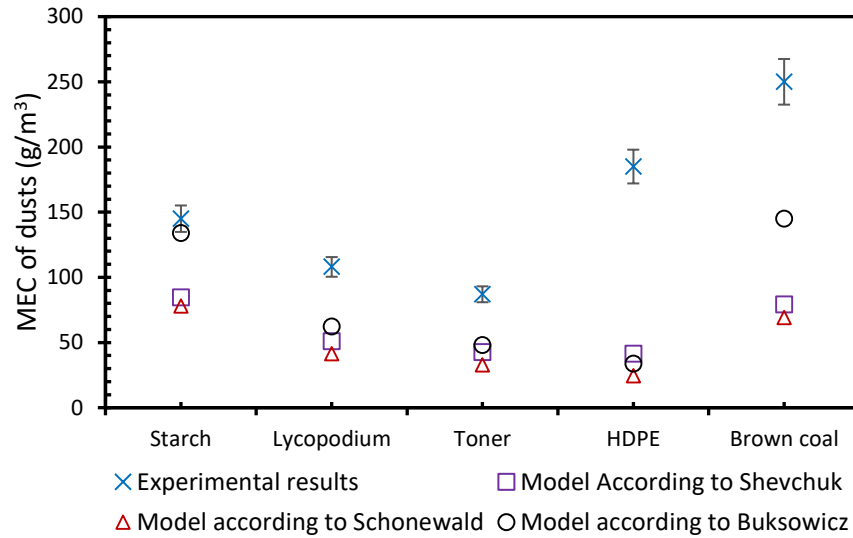


Figure 6.23: Comparison between experimental results for the MEC of dusts and the three models.

In the case of combustible gases Zabetakis [26], Shebeko et al. [101] and Spakowski [102] models (see section 3.2.1.2 for detailed discussion of these models) were compared with the experimental results as presented in Figure 6.24. The “X” symbolizes experimental results while the rest of the signs symbolize the calculated MECs from the three models. It can be seen that the results obtained from the computational models are almost the same as the experimental results with deviation within the measurement uncertainties.

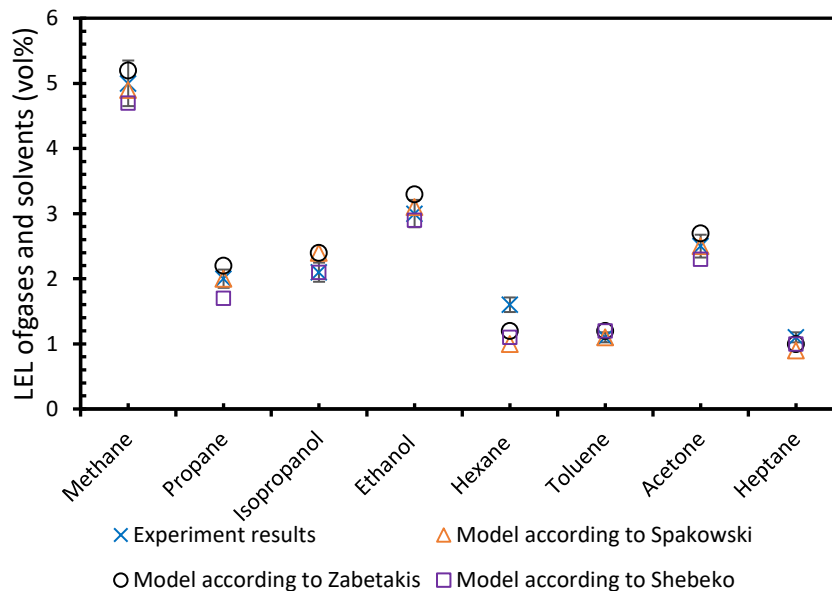


Figure 6.24: Comparison between experimental results for LEL of gases and solvents for the three models.

6.1.4.2 Comparisons of hybrid mixture models and the experimental results

Figures 6.25 to 6.27 present comparisons between the experimental results on the lower explosion limits of hybrid mixtures and mathematical models of Le Chatelier [161], Bartknecht [104], Mannan et al. [74] (see section 3.2.1.3 for detail discussion of these models). The diagrams have the relative concentration of gas and dust on both axes. The X-axis represents the gas concentration used in the experiment divided by the LEL of gas (y/LEL) and the Y-axis shows the dust concentration used in the experiment divided by the MEC of dust (c/MEC). The solid dots represent ignition, while the empty circle symbolizes no ignition. The Le Chatelier's equation is indicated by a green straight line, Bartknecht's equation is indicated by a red dashed curve below Le Chatelier's while, Mannan et al. equation is indicated by a violet dashed curve. These curves delimit the explosion region versus the non-explosible region. Figure 6.25 shows the comparison between experimental results and three models for dusts and gas mixtures. In all cases, a series of ignitions were obtained at the no-ignition zone for both Le Chatelier's and Mannan et al. equations. Only one ignition was obtained in the no-ignition area of the Bartknecht curve and the deviations for lycopodium-methane and lycopodium-hydrogen hybrid mixtures were within the measurement uncertainty.

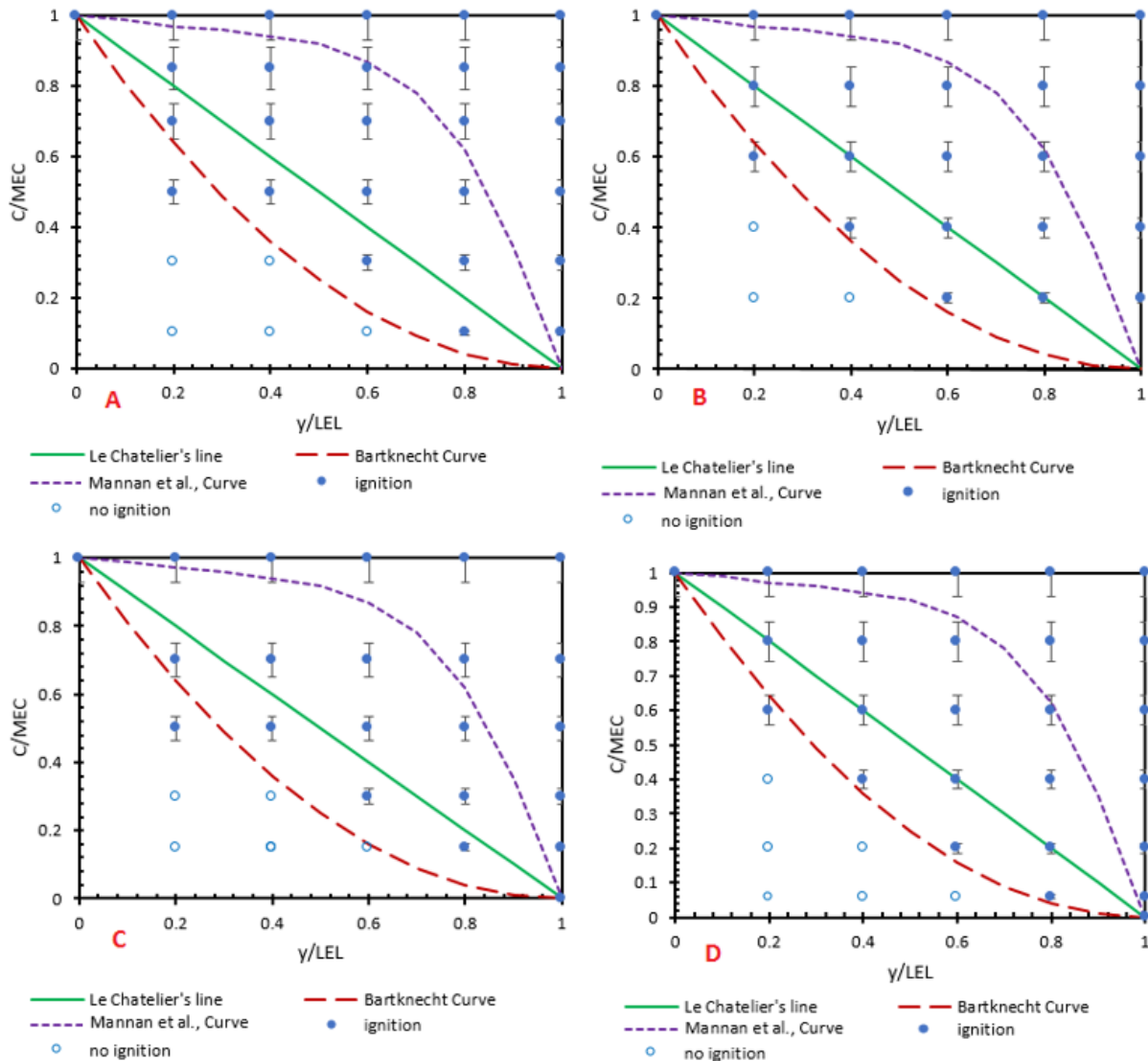


Figure 6.25: Diagram showing a comparison between experimental results and three models: (A) brown coal-methane, (B) lycopodium-methane, (C) brown coal-hydrogen, (D) lycopodium-hydrogen.

With respect to dusts and spray mixtures, Figure 6.26 presents comparisons between the three hybrid mixture models and the experimental results. Four different mixtures were considered: lycopodium- isopropanol, lycopodium-ethanol, brown coal-isopropanol and brown coal-methane. Series of ignitions were observed below the no ignition zone for both Le Chatelier's and Mannan et al. models for all the above mentioned combinations. With the exception of brown coal-ethanol and lycopodium-isopropanol mixtures, where only one ignition was recorded in the no ignition zone (25 %- 50 % spray and dust mixture), no ignition was observed below the Bartknecht curve for the other sprays and dust mixtures.

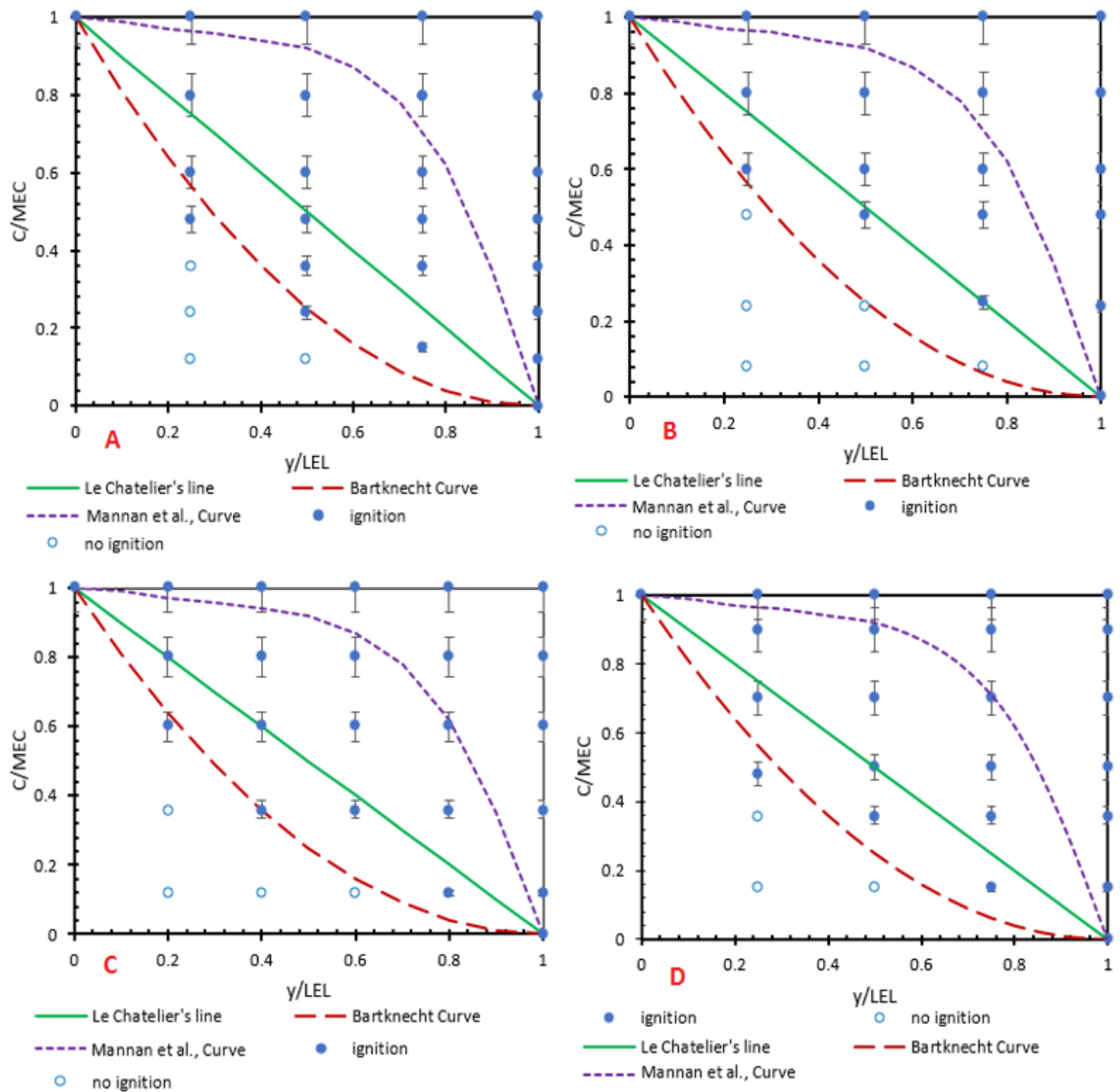


Figure 6.26: Diagram showing a comparison between experimental results and three models: (A) lycopodium-isopropanol, (B) lycopodium-ethanol, (C) brown coal-isopropanol, (D) brown coal-ethanol.

Finally, Figure 6.27 presents the comparisons between the experimental results and the mathematical models for spray and gas mixture. No ignition was observed below the Bartknecht curve within the measurement uncertainties. In all cases, series of ignitions were observed below both the Le Chatelier line and Mannan et al., curve. A similar behavior was observed when other experimental results were compared to the three hybrid mixture models, and hence are presented in Figures B.36 to B.39 at Appendix B.

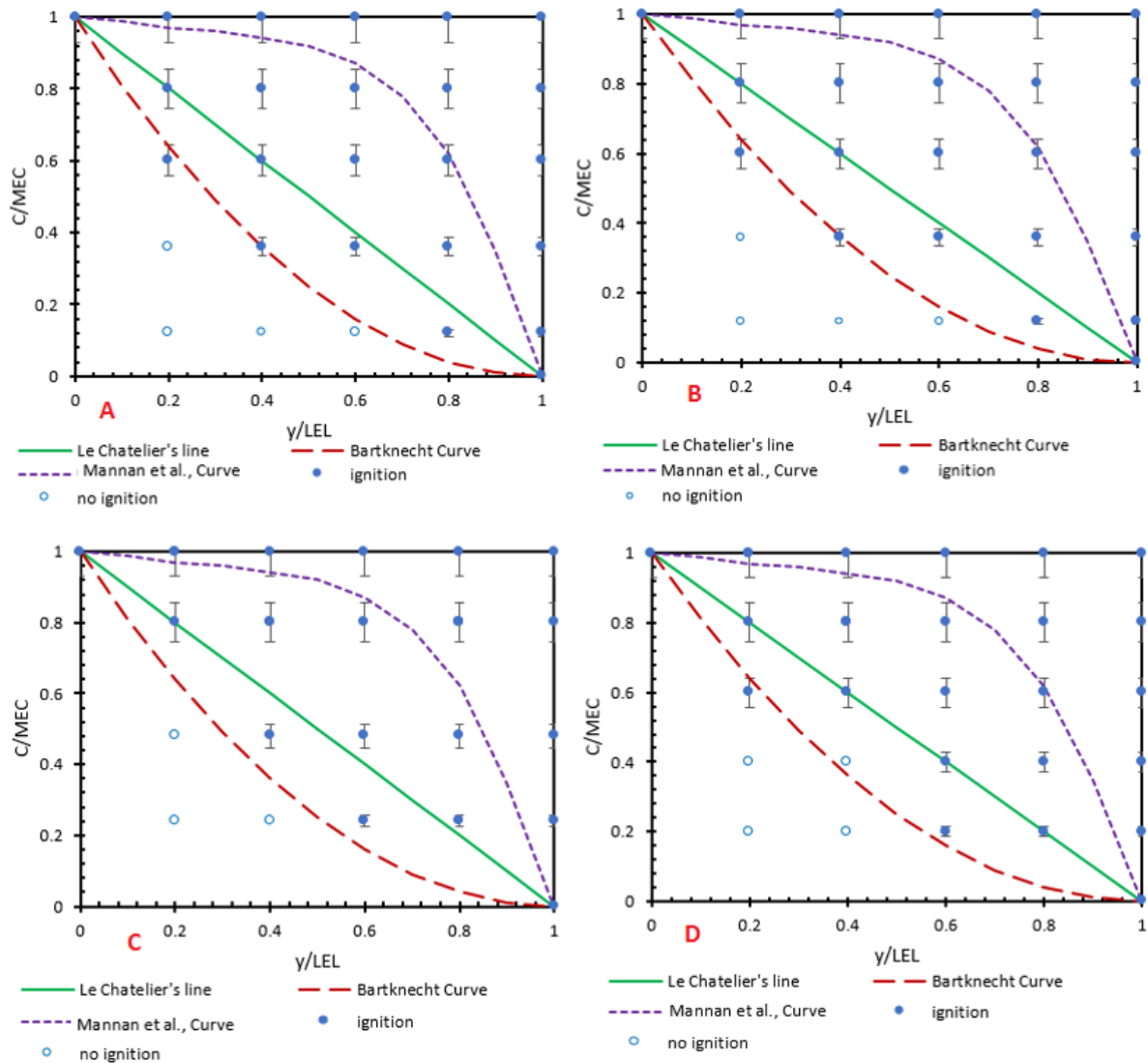


Figure 6.27: Diagram showing a comparison between experimental results and three models: (A) methane-isopropanol, (B) methane-ethanol, (C) hydrogen-isopropanol, (D) hydrogen-ethanol.

Based on the above comparison between hybrid mixture models and experimental results, it could be explained that the Bartknecht equation was able to give a satisfactory prediction of the lower explosion limit of hybrid mixtures as compared to Le Chatelier's and Mannan et al. In all cases, ignitions were observed at the no ignition zones of each model. This confirms the work done by **Cashdollar et al. [164]** of which they observed that more dust is required to render the system explosible which significantly deviates from either the linear relationship defined by Le Chatelier's Law or the second order curve defined by Bartknecht. Again, **Addai et al. [159]** also found a deviation in both Le Chatelier and Bartknecht equation when they applied methane and corn starch. Furthermore, **Pilao et al. [10]** observed deviations when they compared their results

to both Bartknecht and Le Chatelier's models. Moreover, based on the results it was noticed that the explosion of hybrid mixtures does not follow a linear trend, which implies that the Chatelier's equation could not be applied to heterogeneous mixtures. This also confirms the finding by Prugh [165] of which he summarized the lower explosion limits of different hybrid mixtures reported in the literature and compared to the heat capacity and the deflagration index of each fuel. Prugh concluded that the straight-line relationship applies only to mixtures where the ratio of the heat capacities of the dust and gas/vapor is similar, and where the deflagration indices are roughly equivalent. With respect to the model according Mannan et al., several deviations were observed. This could be as a result of the assumptions and the parameters used in the equation such as: deflagration index for both dusts (K_{st}) and gases (K_G). It has been well established that, the determination of deflagration index of dusts depends on several factors such as the particle size of the dusts, the turbulence level, the moisture content and the initial temperature. Moreover, the determination of the K_{st} of dusts is done under turbulence condition while K_G under quiescence environment therefore, combining these two parameters to estimate the LEL of hybrid mixtures could lead to deviations.

6.2 Limiting oxygen concentration

The limiting oxygen concentration (LOC) is usually expressed as the percentage of oxygen available in the fuel-oxygen- inert gas mixture. It is determined experimentally in the 20-liter sphere following the procedure discussed in section 5.2.2. The value of the oxygen concentration is decreased by a step of 1 vol% under the variation of fuel mixture concentration. If no ignition is obtained at any fuel mixture concentration, the oxygen concentration at that point is considered as the LOC. In order to protect process equipments, a safety margin of 2 vol% below the determined LOC is usually used. Numerous researches have been done to determine the LOC of single fuel air mixture by applying different inerting materials [72, 166-168] with the aim of diluting the oxygen concentration in the process facility or equipment in order to mitigate or prevent explosion hazards. Nevertheless, not only single fuel air mixtures are present in the process facilities, but also fuel mixtures of different state of aggregates (hybrid mixture). Research on hybrid mixtures, however, is limited as compared to the single substance especially for LOC. This research work investigates the LOC of hybrid mixtures using fifteen combustible dusts, one

flammable gas and two flammable solvents. Nitrogen gas is used as an inerting material in the standard 20-liter sphere under the same testing and initial conditions. The 2 kJ chemical igniter is used as a standard ignition source for the determination of LOC of dust; however, in this study three different ignition energies (10 J, 2 kJ, and 10 kJ) were employed to measure the LOC of dusts, gases and hybrid mixtures. Comparisons between these three igniters are done in order to estimate the effect of ignition energies on the LOC of different fuel mixtures. Moreover, mathematical models to estimate the LOC of dusts as well as hybrid mixtures are presented and comparisons between the models and the experimental results are performed. Furthermore, diagrams are presented which allow the determination of the LOC directly from the lower explosion limit (LEL) as well as the heat of combustion.

6.2.1 Limiting oxygen concentration of single substances

Initially, the LOC of individual materials were tested. With respect to dust testing, fifteen different materials including organics, polymers, metals, natural products and synthetic materials were investigated in order to obtain a wide range of results. Figure 6.28 presents experimentally determined LOC of dusts with different ignition energies. It can be seen that the ignition energy has a great influence on the LOC of dusts. The higher the ignition energy, the lower the LOC. The results obtained from 10 J electrical igniter are much higher than from the chemical igniters, which are in the range of 11 vol% to 17 vol% for aluminium and peat coal respectively. These LOC results decrease drastically when the ignition energy is increased to 2 kJ. A further decrease is also observed when the ignition energy is increased by a factor of five (10 kJ). For example, the LOC obtained for brown coal with 10 J ignition energy is 16 vol%. This oxygen concentration decreases to 8 vol% with an increase in ignition energy to 2 kJ, and to 7 vol% when the ignition energy is increased to 10 kJ. The reason for this huge effect of the ignition energy on the LOC of dusts could be attributed to the energy released from the ignition source during combustion. The chemical igniters provide a dense cloud of hot dispersed particles which occupy the entire volume of the combustion chamber. A complete combustion could be assumed since the entire fuel mixture ignites almost at the same time. Unlike chemical igniters, electrical igniters produce sparks only at a small region (center) of the combustion chamber and the materials in the close proximity to this region ignite first producing energy which is then transferred to the next

unburned materials. So, if the energy produced during the energy transfer process is not enough to burn the next particle, a complete combustion cannot be achieved.

These results confirm the findings of **Going et al. [169]**. They reported a reduction of the LOC with increasing ignition energy. They also explained that the LOC values obtained from the electrical igniter (10 J) appeared to be between 4 vol% and 8 vol% higher than the 2 kJ chemical igniter thus, indicating that the explosion may have been “underdriven” by the weak ignition source. Moreover, **(ASTM-E2931-13) [170]** indicates that LOC decreases with increasing ignition energy. For example, the LOC values obtained for pulverized Pittsburgh coal were 13.5 vol%, 11 vol% and 9.5 vol% when 1-kJ, 2.5 kJ and 5 kJ igniters, respectively were used.

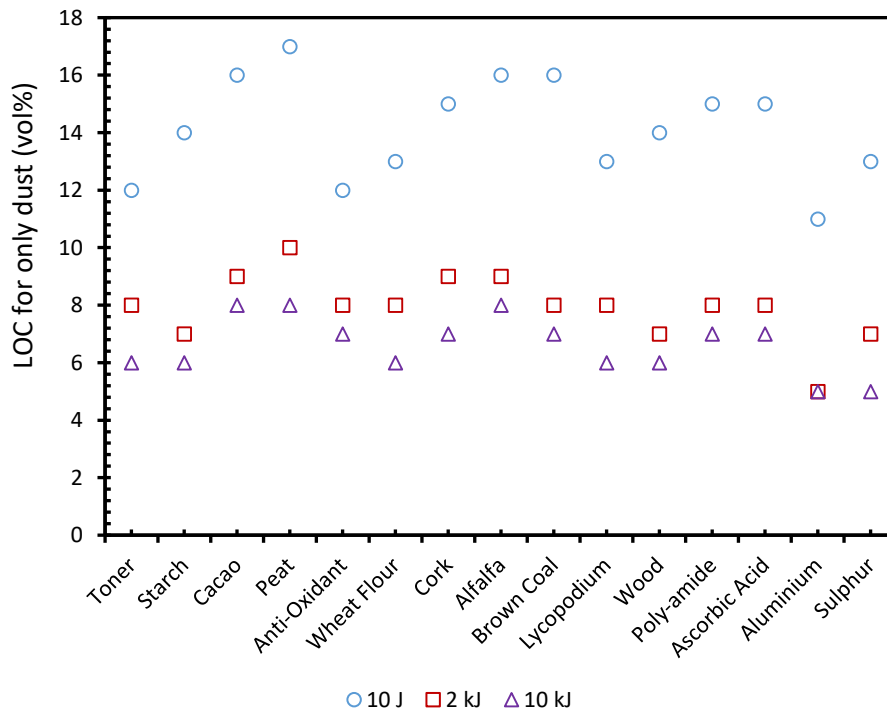


Figure 6.28: Limiting oxygen concentration of dusts with different ignition energies.

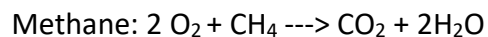
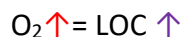
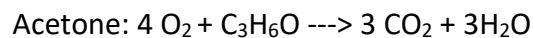
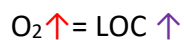
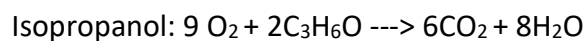
Furthermore, the differences in the LOC values obtained with ignition energies of 2 kJ and 10 kJ never exceeded 2 vol% of oxygen which suggests that, taking into account the effect of “overdriving” as reported by **Going et al. [169]** for the 10 kJ igniters, an ignition energy of 2 kJ would perhaps be the most appropriate choice for LOC tests in the 20-liter sphere.

Going et al. [169] also provided reasons to justify the lower value of LOC for 10 kJ igniter compared to 2kJ igniter, in the 20-liter sphere. They provided a comparison of LOC data obtained from ASTM 20-liter chamber and the 1 m³ explosion vessel, concluding that a 10 kJ ignition source

is appropriate for the 1 m³ vessel, but using the same ignition source for the 20-liter tests produced “overdriven” explosions. This means that the flame produced by the ignition source alone is able to fill the entire 20-liter explosion chamber.

Moreover, these results also confirm the work done by **Mittal [171]**. The author undertook experimental investigations of LOC of coal with different ignition energies and noticed that the LOC of the coal dust decreased from 11 vol% at 1 kJ to 7 vol% at 2.5 kJ, 6 vol% at 5 kJ and 5 vol% at 10 kJ.

Also, Figure 6.29 presents the results obtained for the LOC of methane, acetone vapor and isopropanol spray with different ignition energies. A similar explosion behavior as observed for the dust materials was also seen in the gases and solvents. Increasing the ignition energy decreased the LOCs of methane, acetone and isopropanol respectively. Out of tested gases and solvents, methane recorded the lowest LOC followed by acetone and isopropanol. This trend could be attributed to the stoichiometric concentration of oxygen required for a complete combustion, as explained by the balanced chemical equations below. It could be observed here that the higher the stoichiometric oxygen concentration, the higher the LOC will be. This implies that substances which require more oxygen for their complete combustion have higher LOC. This was confirmed by the LOC results obtained for isopropanol in comparison with acetone and methane.



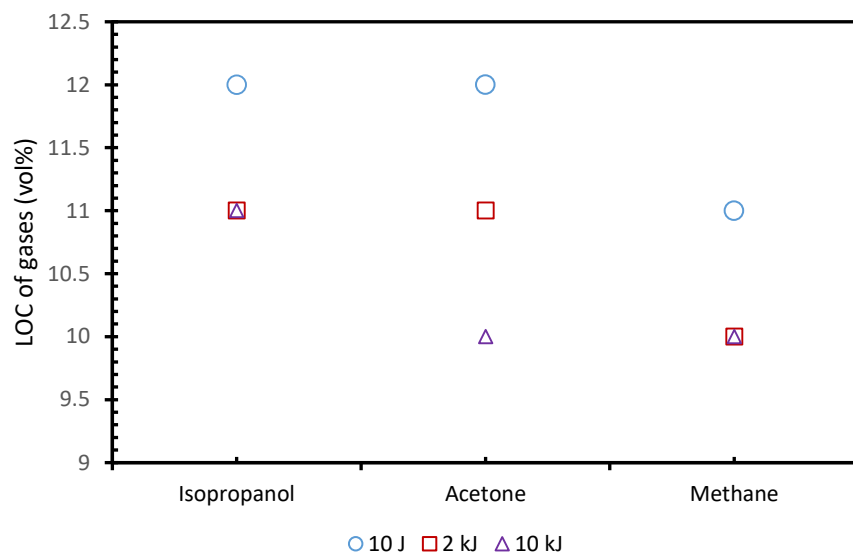


Figure 6.29: Limiting oxygen concentration of gases with different ignition energies.

6.2.2 Limiting oxygen concentration of hybrid mixtures

In the next step, the LOC of hybrid mixtures of fifteen dusts with methane, acetone vapor and isopropanol spray were investigated. Tests were performed with three different ignition energies which include: 10 J electrical igniter, 2 kJ and 10 kJ chemical igniters. Figures 6.30 and 6.31 present the results obtained for the LOC of hybrid mixtures of isopropanol spray, methane gas, acetone vapor and dusts with three ignition energies. It could be seen that the LOC of hybrid mixtures decreased as the ignition energy increased. For example, the LOC of hybrid mixture of isopropanol spray and sulphur dust decreased from 11 vol% at 10 J to 8 vol% at 2 kJ and 6 vol% at 10 kJ. A similar explanation, as provided for the effect of ignition energies on the LOC of single substance presented in the previous section, could be applied in this case. As explained for isopropanol and dust mixtures, a similar behavior was also seen in case of methane and dust as well as acetone vapor and dust mixtures as presented in Figure 6.31.

Figures 6.32 and 6.33 show the experimental results for the LOC of hybrid mixtures. In all cases, a comparison was done between dusts and the hybrid mixtures results. With regard to 10 J electrical igniter, the LOCs for hybrid mixtures were comparatively lower than for single dusts as shown in Figure 6.32. For example, the LOC of peat drops from 17 vol % to 12 vol% when 39 g/m³ of methane was added. No systematic trend could be seen for the hybrid mixtures results,

however, in most cases it appeared that hybrid mixtures with isopropanol recorded the highest LOC.

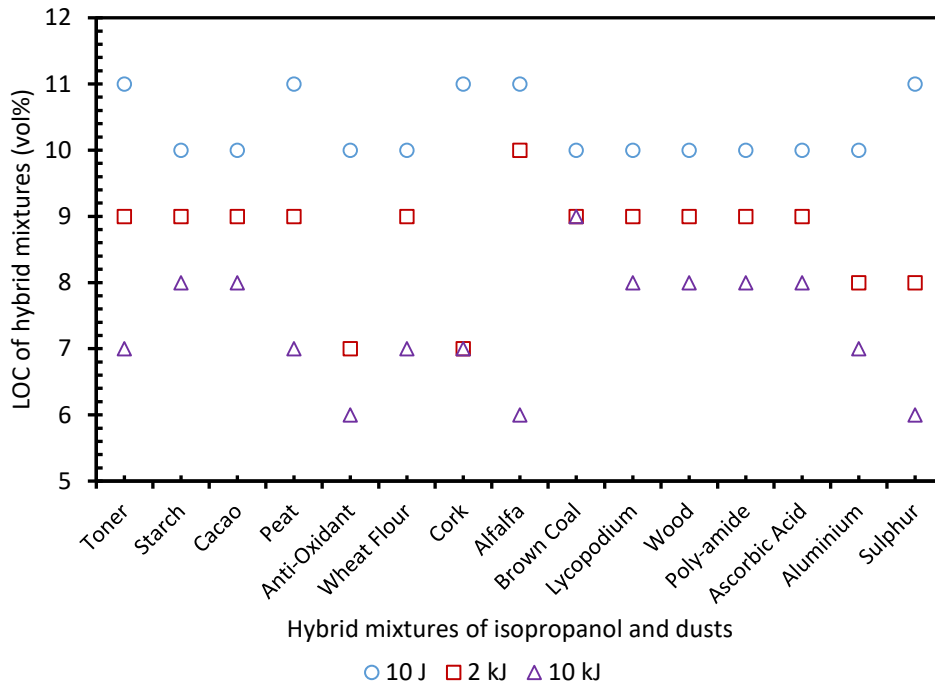


Figure 6.30: Limiting oxygen concentration of hybrid mixtures of isopropanol spray and dusts with different ignition energies.

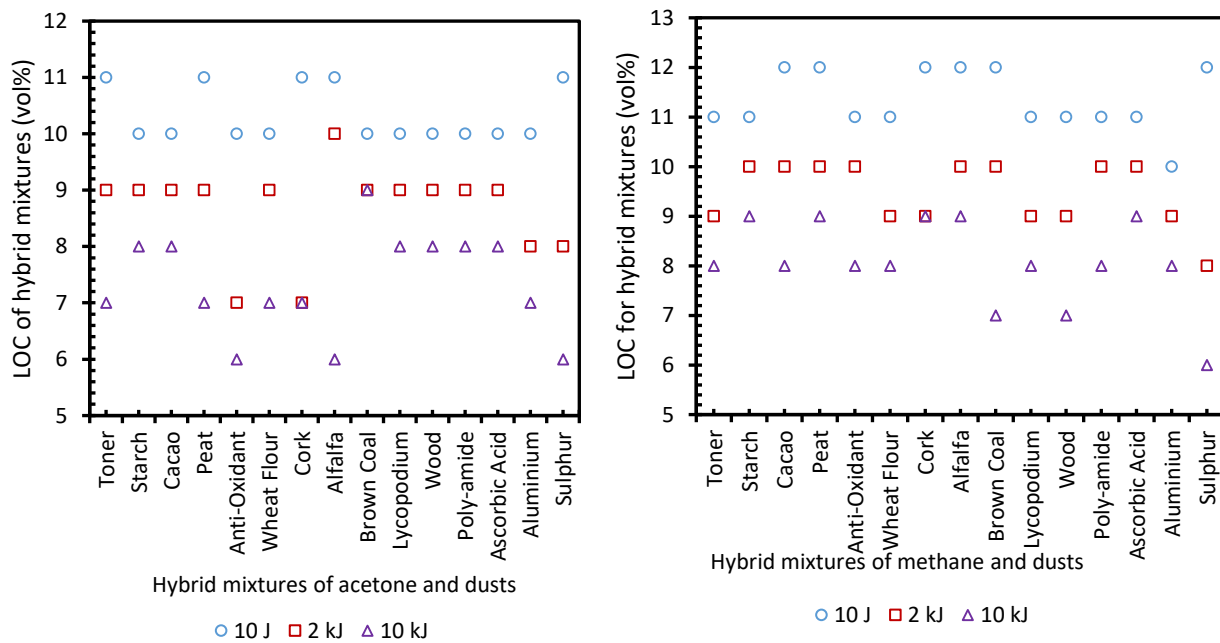


Figure 6.31: Limiting oxygen concentration of hybrid mixtures of acetone (left) / methane (right) and dusts with different ignition energies.

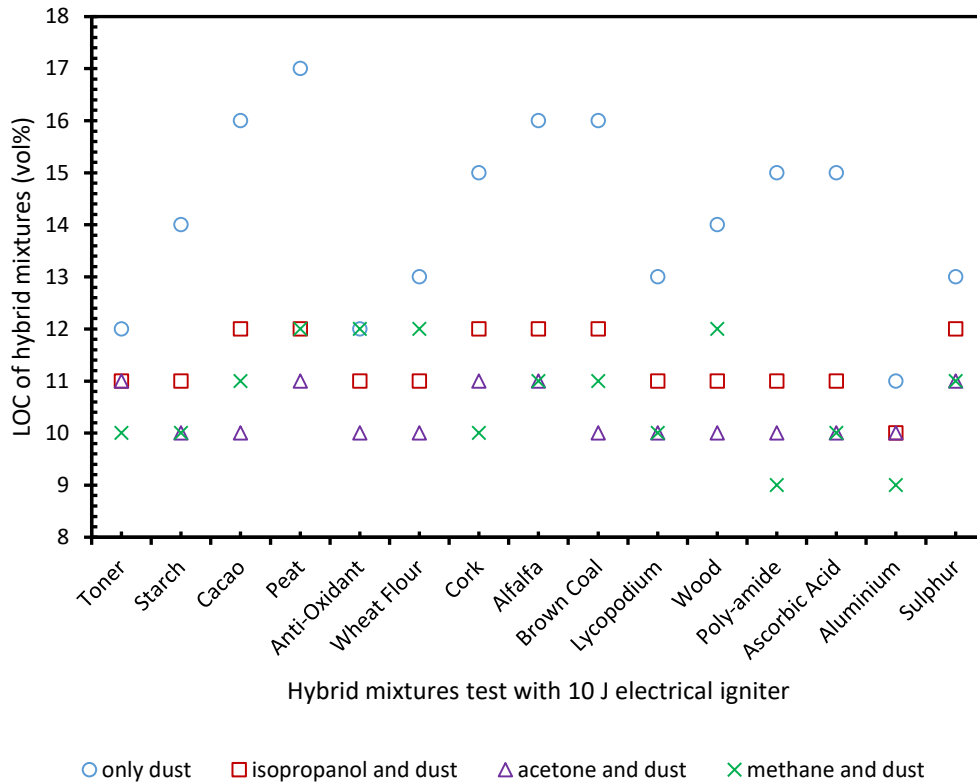


Figure 6.32: Limiting oxygen concentration of hybrid mixtures with 10 J electrical igniter.

Furthermore, Figure 6.33 presents experimentally determined LOC of hybrid mixtures using both 2 kJ and 10 kJ chemical igniter as ignition source. Unlike the 10 J electrical igniter for which the dusts recorded the highest LOC, in the case of 2 kJ chemical igniters, the dusts recorded the lowest LOC. A similar trend was noticed for the test with 10 kJ. Moreover, no systematic trend was also observed for hybrid mixture results, but in most cases, it was observed that isopropanol and dusts mixtures recorded the highest LOC values. This could also be explained with the reason that isopropanol requires a higher stoichiometric oxygen concentration as compared to methane and acetone. Tables 6.9 to 6.12 summarize the results obtained for the LOC of single dust, hybrid mixtures and the concentrations used with different ignition sources

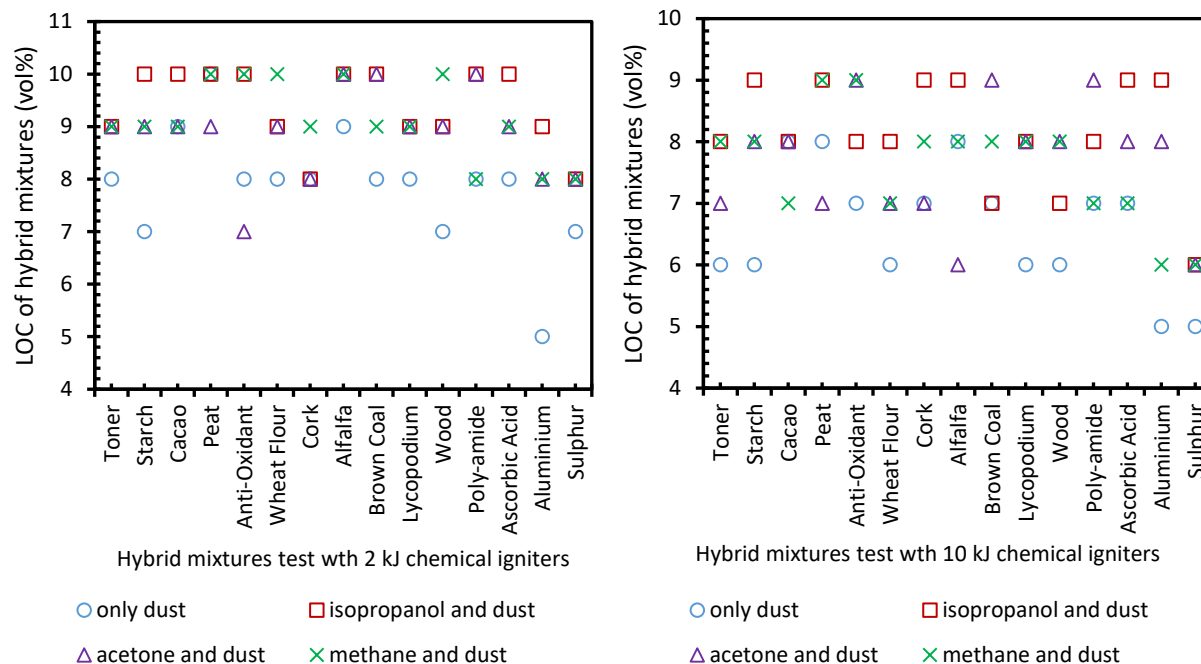


Figure 6.33: limiting oxygen concentration of hybrid mixtures with 2 kJ (left), 10 kJ (right) chemical igniters.

Table 6.9: Summary results for the LOC of dusts and concentrations with different ignition energies.

Dusts Samples	10 J		2 kJ		10 kJ	
	LOC (vol %)	Concentration (g/m ³)	LOC (vol %)	Concentration (g/m ³)	LOC (vol %)	Concentration (g/m ³)
Toner	12	750	8	500	6	500
Anti-Oxidant	14	500	7	500	6	500
Lycopodium	16	500	9	375	8	375
Starch	17	1000	10	500	8	250
Wheat Flour	12	1000	8	500	7	500
Wood	13	1250	8	750	6	500
Cocoa	15	1250	9	1000	7	750
Cork	16	1000	9	625	8	500
Polyamide	16	500	8	250	7	250
Peat	13	1250	8	750	6	500
Alfalfa	14	1500	7	1000	6	750
Ascorbic Acid	15	1250	8	750	7	750
Aluminium Powder	15	500	8	500	7	250
Brown Coal	11	750	5	500	5	500
Sulphur	13	500	7	500	5	500

Table 6.10: Summary results for the LOC of hybrid mixtures of methane and dusts as well as concentrations with different ignition energies.

Dusts Samples	10 J			2 kJ			10 kJ		
	LOC (vol %)	Gas conc. (g/m ³)	Dust conc. (g/m ³)	LOC (vol %)	Gas conc. (g/m ³)	Dust conc. (g/m ³)	LOC (vol %)	Gas conc. (g/m ³)	Dust conc. (g/m ³)
Toner	11	39	250	9	39	500	8	46	375
Anti-Oxidant	11	53	500	10	39	500	9		500
Lycopodium	12	46	250	10	33	250	8	39	250
Starch	12	33	500	10	33	250	9	33	200
Wheat Flour	11	39	500	10	33	500	8	33	500
Wood	11	33	750	9	39	250	8	33	250
Cocoa	12	59	500	9	39	500	9	33	375
Cork	12	46	750	10	39	500	9	33	500
Polyimide	12	53	500	10	33	375	7	33	375
Peat	11	46	375	9	39	250	8	33	250
Alfalfa	11	59	750	9	39	500	7	33	500
Ascorbic Acid	11	59	500	10	33	250	8	33	500
Aluminium Powder	11	39	375	10	33	375	9	33	375
Brown Coal	10	53	500	9	39	500	8	33	500
Sulphur	12	33	250	8	39	250	8	33	175

Table 6.11: Summary results for the LOC of hybrid mixtures of acetone vapor and dusts as well as concentrations with different ignition energies.

Dusts Samples	10 J			2 kJ			10 kJ		
	LOC (vol %)	Gas conc. (g/m ³)	Dust conc. (g/m ³)	LOC (vol %)	Gas conc. (g/m ³)	Dust conc. (g/m ³)	LOC (vol %)	Gas conc. (g/m ³)	Dust conc. (g/m ³)
Toner	10J	24	375	9	48	250	7	56	250
Anti-Oxidant	11	48	375	9	48	250	8	40	250
Lycopodium	10	32	750	9	40	500	8	48	500
Starch	10	24	750	9	48	500	7	40	500
Wheat Flour	11	24	750	7	48	750	9	6	500
Wood	10	32	250	9	40	750	7	40	500
Cocoa	10	32	375	7	40	500	7	56	250
Cork	11	40	750	10	40	500	6	48	125
Poly-imide	11	32	750	10	48	500	9	48	500
Peat	10	48	1000	9	48	250	8	40	250
Alfalfa	10	24	1000	9	48	250	8	40	250
Ascorbic Acid	10	40	500	10	48	250	9	40	250
Aluminium Powder	10	32	375	9	48	250	8	48	250
Brown Coal	10	48	750	8	40	500	8	40	250
Sulphur	10	24	375	8	48	250	6	40	125

Table 6.12: Summary results for the LOC of hybrid mixtures of isopropanol spray and dusts as well as concentrations with different ignition energies.

Dusts Samples	10 J			2 kJ			10 kJ		
	LOC (vol %)	Gas conc. (g/m ³)	Dust conc. (g/m ³)	LOC (vol %)	Gas conc. (g/m ³)	Dust conc. (g/m ³)	LOC (vol %)	Gas conc. (g/m ³)	Dust conc. (g/m ³)
Toner	10	150	375	9	125	50	8	125	250
Anti-Oxidant	10	150	500	9	125	500	8	250	250
Lycopodium	10	125	500	9	250	500	7	375	250
Starch	11	150	500	11	250	500	9	375	250
Wheat Flour	12	150	500	11	125	500	9	125	125
Wood	12	250	500	11	125	500	7	75	125
Cocoa	12	150	500	9	125	250	8	125	375
Cork	10	250	500	10	125	500	8	250	250
Poly-imide	11	250	500	9	250	375	8	250	250
Peat	11	250	500	9	250	500	8	250	250
Alfalfa	10	250	500	10	250	500	8	250	250
Ascorbic Acid	12	150	250	8	125	500	7	250	250
Aluminium Powder	9	250	125	9	150	250	7	75	125
Brown Coal	10	250	500	8	125	500	6	125	250
Sulphur	9	250	250	8	250	250	6	250	125

6.2.3 Models to estimate the limiting oxygen concentration of dust

In this section, mathematical estimations of the LOC of dust/air mixtures, as a function of the minimum explosion concentration of dusts, are discussed. The LOC is mostly measured experimentally according to the European standards (This experimental procedure has been discussed in section 5.2.2). A simple mathematical model proposed by Krause et al. [172] is presented and a comparison is made to the experimental results. This model is based on the assumption that the limiting oxygen concentration is equivalent to the stoichiometric concentration when the fuel concentration equals the lower explosion limit [173]. The LOC can then be calculated according to eq. (6.2.1).

$$\varphi_{LOC} = n_{O_2} \cdot \varphi_{LEL} \quad (6.2.1)$$

where n_{O_2} is the number of moles of oxygen needed to combust one mole of fuel and φ_{LEL} is the lower explosion limit of the fuel. φ_{LOC} and φ_{LEL} are given as volume fractions of oxygen and fuel, respectively. Moreover, an extended version of eq. (6.2.1) based on the stoichiometry of the

oxidizable elements contained in the fuel could be formulated, with μ_i being the mass fraction of the oxidizable element i and M_i being its molecular mass as shown in eq. (6.2.2).

$$\varphi_{\text{LOC}} = \left(\sum_{i=1}^N \nu_{\text{O}_2,i} \frac{\mu_i}{M_i} - \frac{\mu_{\text{O}_2}}{M_{\text{O}_2}} \right) \frac{M_{\text{O}_2}}{\rho_{\text{O}_2}} \cdot \varphi_{\text{LEL}} \quad (6.2.2)$$

Where; $\nu_{\text{O}_2,i}$ is the number of moles of oxygen required to burn one mole of the element i . The term $\mu_{\text{O}_2} / M_{\text{O}_2}$ describes the amount of oxygen contained in the fuel. φ_{LEL} represents the lower explosion limit of the gas-air mixture, but in case of dust-air-mixtures, this value is usually given as mass of the dust per unit volume of air in which the dust particles are dispersed. Therefore, to describe the limit for flame propagation in dust-air-mixtures the minimum explosible concentration MEC (g/m³) is used instead of LEL. MEC of dust could also be estimated under the assumption of a homogeneous fuel-air mixture of a given heat of reaction, specific heat capacity and complete combustion. The MEC is the minimum amount of fuel necessary to shift the reactive system from “initial” to a “flame” temperature. Schönewald, [98] used this assumption to propose the semi-empirical model as shown in eq. (6.2.3) where the constants were fitted to a wide range of hydrocarbons (see section 3.1.2.11 for detail discussion), where H_o is the heat of combustion of the dust while a and b are constant.

$$C_{\text{MEC}} = \frac{a}{H_o} - b \quad (6.2.3)$$

Based on eq. (6.2.2) and using the MEC instead of LEL, eq. (6.2.4) could be formulated

$$\varphi_{\text{LOC}} = \sigma_{\text{fu}} \cdot \frac{M_{\text{O}_2}}{\rho_{\text{O}_2}} \cdot C_{\text{MEC}} \quad (6.2.4)$$

Inserting the C_{MEC} model from eq. (6.2.3) into eq. (6.2.4), eq. (6.2.5) could be obtained

$$\varphi_{\text{LOC}} = \left(\sum_{i=1}^N \nu_{\text{O}_2,i} \frac{\mu_i}{M_i} - \frac{\mu_{\text{O}_2}}{M_{\text{O}_2}} \right) \cdot \frac{M_{\text{O}_2}}{\rho_{\text{O}_2}} \cdot \left(\frac{a}{H_o} - b \right) \quad (6.2.5)$$

In this case, a simple fuel consisting of carbon, hydrogen, oxygen and non-reacting component only that burns completely to carbon dioxide and water are considered, and based on eq. (6.2.2), the fuel number (σ_{fu}) could be estimated from eq. (6.2.6)

$$\sigma_{\text{fu-dust}} = \nu_{\text{O}_2,\text{C} \rightarrow \text{CO}_2} \frac{\mu_{\text{C}}}{M_{\text{C}}} + \nu_{\text{O}_2,\text{H} \rightarrow \text{H}_2\text{O}} \frac{\mu_{\text{H}}}{M_{\text{H}}} - \frac{\mu_{\text{O}_2}}{M_{\text{O}_2}} \quad (6.2.6)$$

If a complete combustion with only a few elementary reactions is assumed, the value of σ_{fu} will depend only on the chemical composition of the fuel. However, if incomplete combustion occurs, more elementary reactions have to be taken into account. It must be mentioned here that only complete combustion in a one-step oxidation process is considered.

For example, in case complete combustion of monomeric starch dust and air mixture is considered, and based on the chemical formula $C_6H_{10}O_5$ and the molecular masses of carbon, hydrogen and oxygen of 12 g/mol, 1 g/mol and 16 g/mol, the mass fractions of carbon, hydrogen and oxygen are $\mu_C=0.44$, $\mu_H=0.06$, $\mu_O=0.50$, respectively, the fuel number of starch $\sigma_{C_6H_{10}O_5}$ could be estimated. Two simple reactions for the conversion of the carbonaceous combustible dusts are assumed as presented in eq. (6.2.7) and eq. (6.2.8) [9].



With the molecular weights and the mass fractions of the elements presented in Table 6.13, the $\sigma_{C_6H_{10}O_5}$ could be obtained as presented in eq. (6.2.9)

$$\sigma_{C_6H_{10}O_5} = \left(\frac{0.44}{12} + \frac{1}{2} \cdot \frac{0.06}{1} \cdot \frac{0.5}{16} \right) \frac{mol}{g} = 0.0354 \frac{mol}{g} \quad (6.2.9)$$

Table 6.13: Mass fractions of elements, MEC, heat of reaction and estimated fuel numbers for the fifteen dusts.

Samples	μ_c	μ_H	μ_o	MEC (g/m ³)	σ_{fu} (mol/g)	H _o (J/g)
Wheat	0.42	0.061	0.476	64.7	0.035	18360
Starch	0.433	0.064	0.477	63.9	0.035	17310
Brown coal	0.69	0.060	0.22	69.5	0.066	17148
Wood	0.491	0.063	0.440	77.7	0.043	15395
Lycopodium	0.695	0.094	0.186	37.9	0.075	30554
Polyamide	0.637	0.097	0.142	46.4	0.073	29461
Cork	0.42	0.06	0.51	83.90	0.035	14230
Alfalfa	0.44	0.05	0.34	74.6	0.038	15990
Peat	0.50	0.05	0.3	64.8	0.044	18420
Antioxidant	0.72	0.08	0.12	37.35	0.076	31960
Ascorbic acid	0.40	0.04	0.53	104	0.024	11469
Toner	0.86	0.07	0.05	32.75	0.089	35792
Cacao	0.52	0.06	0.28	57.13	0.049	20678
Aluminium	-	-	-	-	-	-
Sulphur	-	-	-	-	-	-

Figure 6.34 presents a comparison between the experimental and computational LOC for dust samples with different ignition energies. The red star and green rectangle symbolize 10 kJ and 2 kJ chemical igniters respectively while the black circle symbolizes 10 J electrical igniters. An error bar based on the error and uncertainty analysis from the experimental procedure is also plotted on the results. The results presented in the figure are segregated into two regions, that is the results obtained from 10 J is distinct from the 2 kJ and 10 kJ. It could be seen that the computational values were far below the experimental results for the 10 J electrical igniters, which seems to be good from a safety point of view. Moreover, the experimental results from 2 kJ chemical igniter were also in good agreement with the computational results. With respect to 10 kJ chemical igniter, it was observed that two of the experimental results were 1 vol% higher than the computational values.

Furthermore, considering that the fuel number of dusts σ_{fu} presented in Table 6.14, is a constant for each dust under the conditions presumed in eq. (6.2.4) in section 6.2.3.1, it indicates a linear dependence of LOC on the MEC. Figure 6.35 shows a diagram where the LOC is given as a function of MEC with σ_{fu} as a parameter. If MEC and the chemical composition of the dust samples (mass fractions of essential elements) are known, the LOC can be obtained directly from this diagram. However, the determination of the MEC by experiments is complicated because of the well-known difficulties to achieve homogenous dust dispersion. Local distributions of the dust concentration appear and may cause considerable errors. Hence, the model proposed by **Schönewald [98]** shown in eq. (6.2.3) could be used to determine the MEC of dusts by knowing only the heat of combustion of the dusts being considered.

It must be noted that, there are many assumptions and idealisations in the model, which makes it to give a lower boundary for MEC rather than a "realistic" value. For example, polyamide with an estimated MEC of 46 g/m³ and heat of combustion of 0.073 mol/g, when traced from the Figure 6.35, gave a LOC value of 7 vol% which is the same as the experimental value.

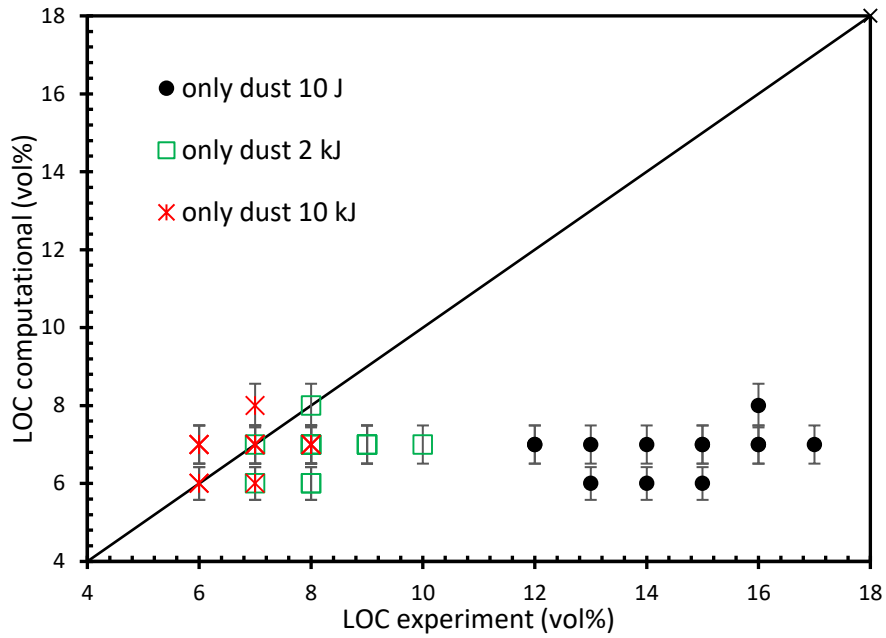


Figure 6.34: A comparison between computational and experimental results for the LOC of dusts with different ignition energies.

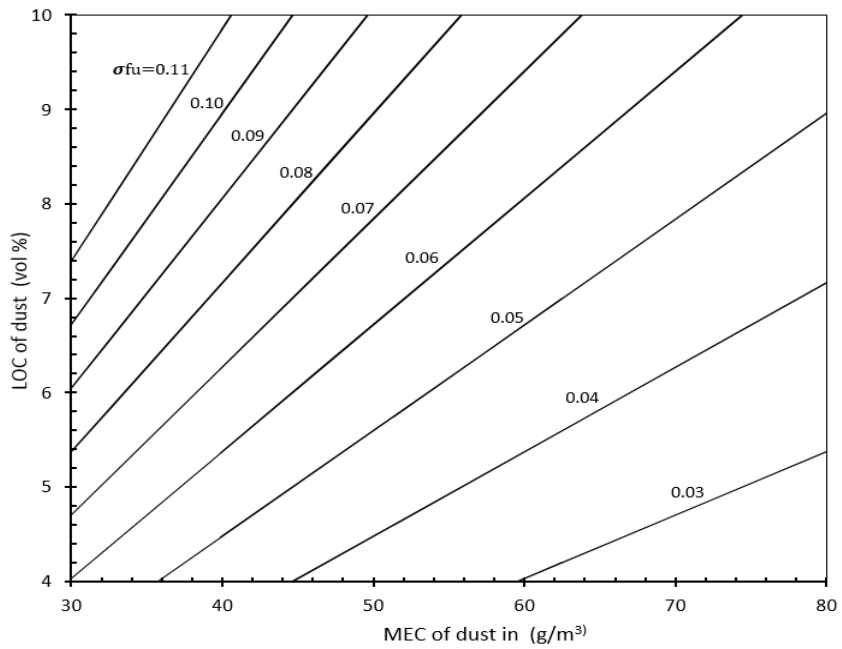


Figure 6.35: A diagram to estimate the LOC of dust-air mixtures in dependence on MEC and the fuel number.

6.2.4 Model to estimate the limiting oxygen concentration of gases

A similar approach used for the LOC of dusts estimation discussed in section 6.2.3.1 could also be applied for the determination of LOC of gases. From eq. (6.2.2), the LOC of gases could be rewritten to eq. (6.2.10)

$$\varphi_{\text{LOC}} = 100 \cdot \sigma_{\text{fu}} \cdot M_{\text{O}_2} \cdot \varphi_{\text{LEL}} \quad (6.2.10)$$

the fuel number of gases could be obtained from eq. (6.2.11) with the assumption of a complete combustion.

$$\sigma_{\text{fu-gas}} = \nu_{\text{O}_2, \text{C} \rightarrow \text{CO}_2} \frac{\mu_{\text{C}}}{M_{\text{C}}} + \nu_{\text{O}_2, \text{H} \rightarrow \text{H}_2\text{O}} \frac{\mu_{\text{H}}}{M_{\text{H}}} \frac{\mu_{\text{O}_2}}{M_{\text{O}_2}} \quad (6.2.11)$$

Moreover, the LEL of the gas could also be calculated from the model proposed by Zabetakis [26] shown in eq. (6.2.12) as already presented in eq. (3.2.4) with detail description.

$$\text{LEL} = 0.55 \frac{100}{1 + 1.193k} \quad (6.2.12)$$

By inserting eq. (6.2.11) and eq. (6.2.12) into eq. (6.2.10), eq. (6.2.13) could be obtained.

$$\varphi_{\text{LOC gas}} = 100 \cdot \left(\sum_{i=1}^N \nu_{\text{O}_2, i} \frac{\mu_i}{M_i} - \frac{\mu_{\text{O}_2}}{M_{\text{O}_2}} \right) \cdot M_{\text{O}_2} \cdot 0.55 \frac{100}{1 + 1.193k} \quad (6.2.13)$$

Table 6.14 presents a comparison between the estimated LOC of gases and the experimentally determined results using 10 J electrical igniter as an ignition source. It could be seen that the estimated LOC from the model was able to give a very good prediction for the LOC of methane, acetone and isopropanol.

Table 6.14: Mass fractions of elements, LEL, and the estimated fuel number for methane, acetone and isopropanol.

Samples	μ_{C}	μ_{H}	μ_{O}	σ_{fu}	LEL	LOC calculated (vol%)	LOC experimental (vol%) with 10 J ignition energy
Methane	0.75	0.25	0.00	0.116	33	8.4	11
Acetone	0.62	0.10	0.28	0.085	50	6.3	12
Isopropanol	0.6	0.13	0.27	0.101	49	6.5	12

6.2.5 Model to estimate the limiting oxygen concentration of hybrid mixtures

Based on presented models to estimate the φ_{LOC} of both dusts and gases discussed in sections 6.2.3.1 and 6.2.3.2, a model to estimate the φ_{LOC} of hybrid mixture could be derived by considering the assumption, that the φ_{LOC} of hybrid mixtures is the summation of the φ_{LOC} of dust and gas multiplied by the respective mass fractions of the individual component in the mixture, as shown in eq. (6.2.14).

$$\varphi_{\text{LOC_hybrid}} = \varphi_{\text{LOC_dust}} \cdot \beta_{\text{d}} + \varphi_{\text{LOC_gas}} \cdot \beta_{\text{g}} \quad (6.2.14)$$

Inserting eq. (6.2.2) and eq. (6.2.10) into eq. (6.2.14); eq. (6.1.15) could be obtained

$$\varphi_{\text{LOC_hybrid}} = (100 \cdot \sigma_{fu-g} \cdot M_{O_2} \cdot \varphi_{\text{LEL}} \cdot \beta_{\text{g}}) + (100 \cdot \sigma_{fu-d} \cdot \frac{M_{O_2}}{\rho_{O_2}} \cdot C_{\text{MEC}} \cdot \beta_{\text{d}}) \quad (6.2.15)$$

By inserting eq. (6.2.5) and eq. (6.2.13) into eq. (6.2.15), eq. (6.2.16) could be obtained

$$\varphi_{\text{LOC_hybrid}} = (100 \cdot \sigma_{fu-g} \cdot M_{O_2} \cdot 0.55 \frac{100}{1+1.193k} \cdot \beta_{\text{g}}) + (100 \cdot \sigma_{fu-d} \cdot \frac{M_{O_2}}{\rho_{O_2}} \cdot (\frac{a}{H_0} - b) \cdot \beta_{\text{d}}) \quad (6.2.16)$$

Moreover, eq. (6.2.16) could be rewritten to eq. (6.2.17)

$$\varphi_{\text{LOC_hybrid}} = 100 \cdot [(\sigma_{fu-g} \cdot M_{O_2} \cdot (0.55 \frac{100}{1+1.193k} \cdot \beta_{\text{g}})) + (\sigma_{fu-d} \cdot \frac{M_{O_2}}{\rho_{O_2}} \cdot (\frac{a}{H_0} - b) \cdot \beta_{\text{d}})] \quad (6.2.17)$$

In case, eq. (6.2.6) and eq. (6.2.11) are inserted into eq. (6.2.17), eq. (6.2.18) could be obtained.

$$\varphi_{\text{LOC_hybrid}} = 100 \cdot [(\sum_{i=1}^N v_{O_2,i} \frac{\mu_i}{M_i} - \frac{\mu_{O_2}}{M_{O_2}})_g \cdot M_{O_2} \cdot (0.55 \frac{100}{1+1.193k} \cdot \beta_{\text{g}}) + (\sum_{i=1}^N v_{O_2,i} \frac{\mu_i}{M_i} - \frac{\mu_{O_2}}{M_{O_2}})_d \cdot \frac{M_{O_2}}{\rho_{O_2}} \cdot (\frac{a}{H_0} - b) \cdot \beta_{\text{d}}] \quad (6.2.18)$$

Hence, the LOC of hybrid mixtures could be estimated from eq. (6.2.18).

Where, σ_{fu-g} is the fuel number of gas [mol/g], σ_{fu-d} indicates the fuel number of dust [mol/g], β_{g} represent the mass fraction of gas in the mixture, β_{d} is the mass fraction of dust in the mixture, g indicate gases and d indicate dusts.

Figures 6.36 to 6.38 present a comparison between the experimental and computational results for hybrid mixtures with different ignition energies. The red stars and green rectangles symbolize 10 kJ and 2 kJ chemical igniters, respectively, while the black circles symbolize 10 J electrical

igniters. An error bar based on the uncertainty analysis from the experimental procedure is also plotted on the experimental results. With respect to the results obtained for methane and dust mixtures with different ignition energies as presented in Figure 6.36, it could be seen that the computed values were always lower than or equal to the experimental ones for both 10 J and 2 kJ ignition energies. However, for 10 kJ chemical igniters, the computed values were below the experimental values with only one deviation, where the experimental value was 1 vol% higher than the computed one. For industrial applications, in order to protect process equipment, usually safety a margin of 2 vol% below the determined LOC is used.

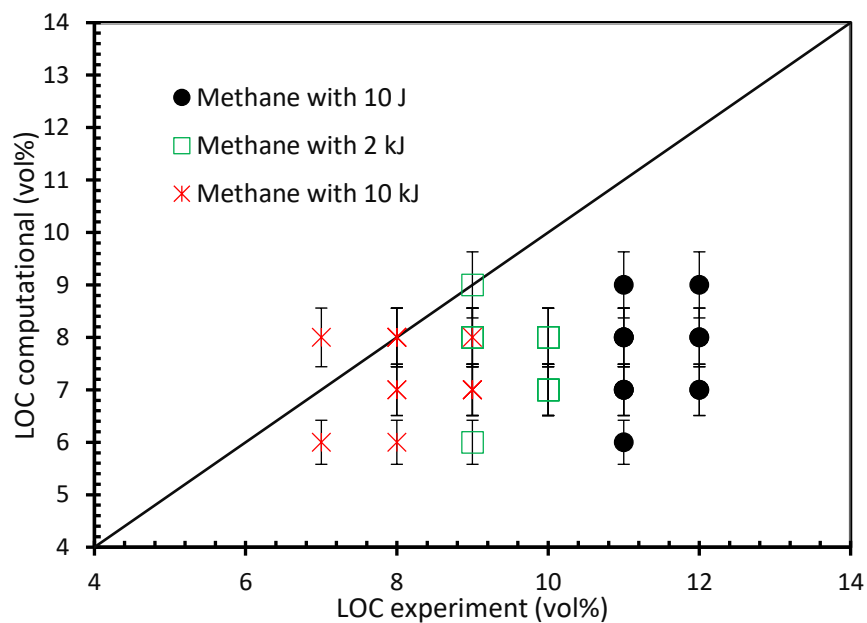


Figure 6.36: A comparison between computational and experimental results for the LOC of hybrid mixture of methane and dusts with different ignition energies.

Furthermore, Figure 6.37 shows the comparison between computational and experimental results for the LOC of hybrid mixtures of acetone and dusts with respect to different ignition energies. Explosion behaviors, similar to that of methane and dusts mixtures was also observed in this case, for both 10 J and 2 kJ energies. It was noticed that the computed results were either lower or the same as the experimental results. However, for the 10 kJ igniter, two deviations i.e. 1 vol% higher than the experimental values were observed. A similar trend was also noticed for isopropanol and dusts mixtures as shown in Figure 6.38.

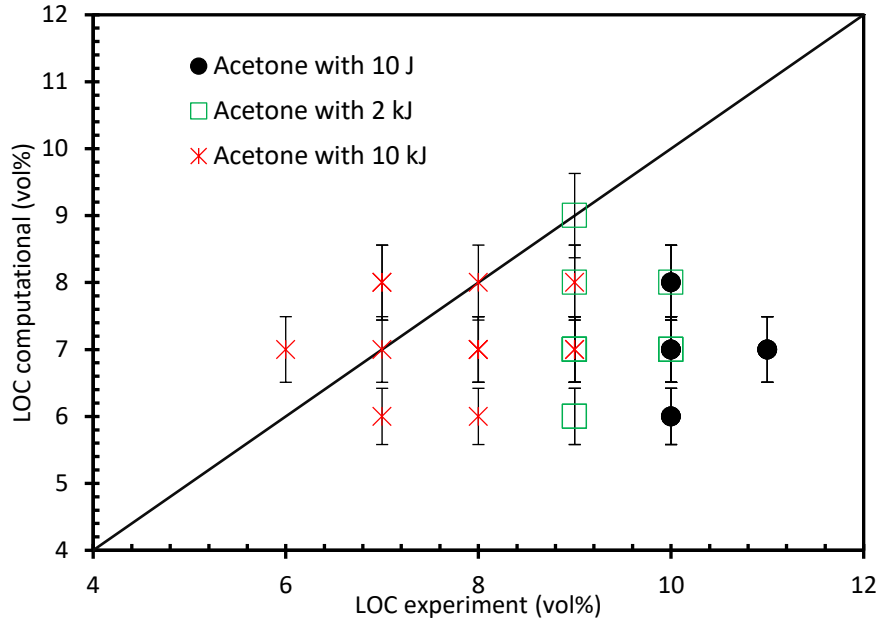


Figure 6.37: A comparison between computational and experimental results for the LOC of hybrid mixture of acetone and dusts with different ignition energies.

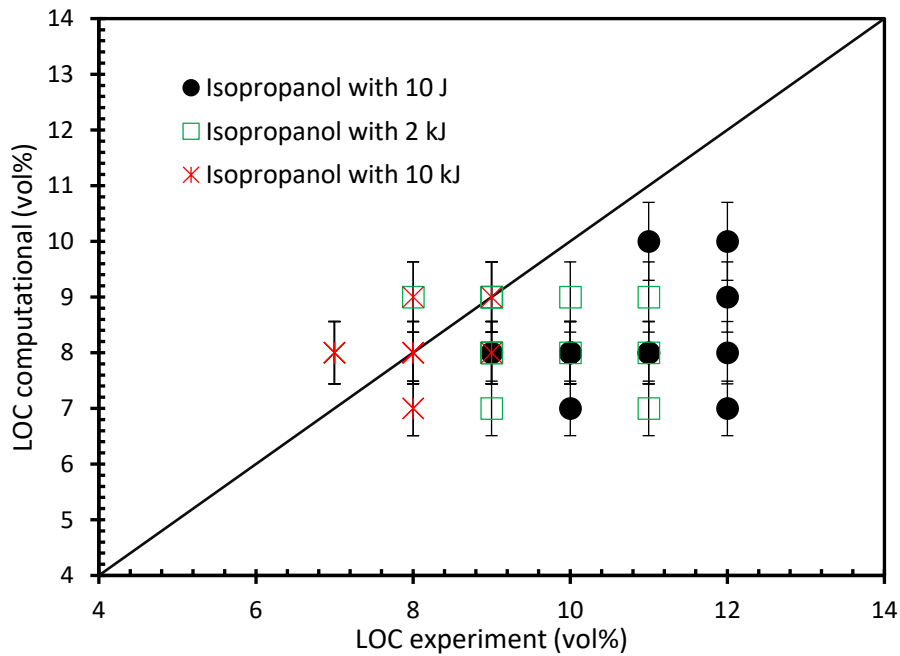


Figure 6.38: A comparison between computational and experimental results for the LOC of hybrid mixture of isopropanol and dusts with different ignition energies.

Using the calculation procedure as described in eq. (6.2.15), simple graphs could be plotted, from which the LOC of hybrid mixtures could be directly be obtained, if the LEL and the fuel number of hybrid mixtures are known, as shown in Figures 6.39 to Figure 6.41. The LEL of hybrid mixtures could be obtained by summing up the MEC of dusts obtained from Schönwald model and the

LEL of gas obtained from Zabetakis model, multiplied by the respective mass fraction of the individual component in the mixture as shown in eq. (6.19). This equation has been validated with experimental results which seems to fit very good with the experimental.

$$\varphi_{LEL_hybrid} = [(055 \frac{100}{1+1.193k} \cdot \beta_g \cdot \rho_{fuel}) + (\frac{a}{H_0} - b) \cdot \beta_d] \quad (6.2.19)$$

Moreover, the fuel number of hybrid mixtures could also be obtained by simply summing the fuel numbers of individual component multiplied by the respective mass fraction as shown in eq. (6.2.20).

$$\varphi_{LOC_hybrid} = [(\sum_{i=1}^N v_{O_2,i} \frac{\mu_i}{M_i} - \frac{\mu_{O_2}}{M_{O_2}})_g \cdot \beta_g + (\sum_{i=1}^N v_{O_2,i} \frac{\mu_i}{M_i} - \frac{\mu_{O_2}}{M_{O_2}})_d \cdot \beta_d] \quad (6.2.20)$$

Figures 6.39 to 6.41 provide diagrams for the estimation of the LOC of hybrid mixtures with respect to its dependence on LEL and the fuel number of hybrid mixtures with 2 kJ chemical igniters as ignition source. These diagrams are applicable to all kinds of carbonaceous dusts and gases mixtures. Dust specific properties are contained in the values of MEC and fuel number as well as for the gases. However, other dust-specific properties influencing the course of dust explosions like particle size distribution, moisture content, specific surface area etc. are included only as they influence the MEC. It could be seen that there was no difference between mixtures of dusts and methane, acetone and isopropanol. For example, considering the LEL mixture of 75g/m³, the LOC record was 5.6 vol% for the three gases and dusts mixtures. Moreover, Figures B.40 to B.47 at Appendix B provide diagrams for the estimation of the LOC of acetone, isopropanol and dusts hybrid mixtures with different ignition energies.

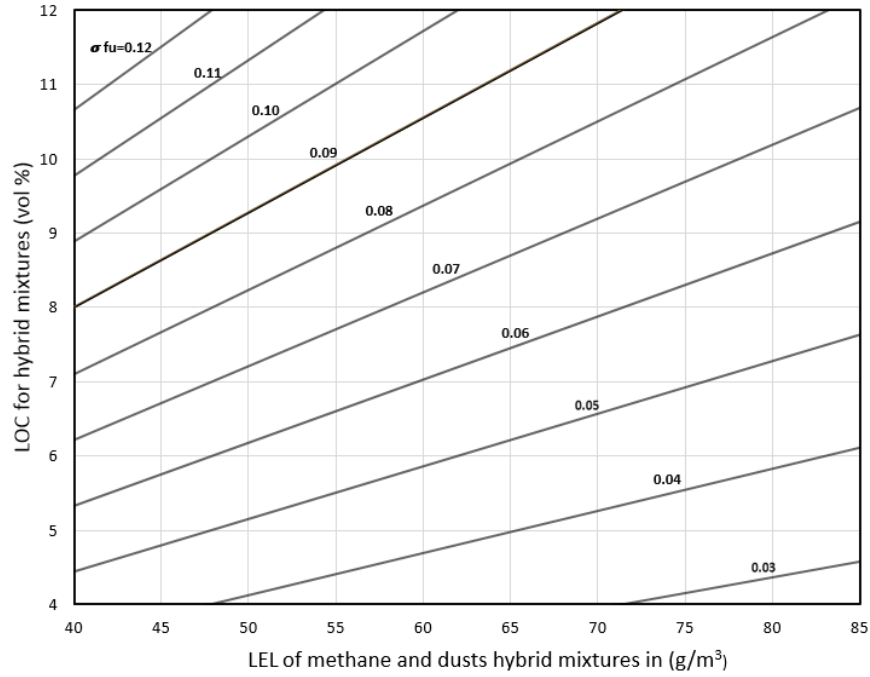


Figure 6.39: A diagram to estimate the LOC of hybrid mixture of methane and dusts in dependence on $LEL_{-hybrid}$ and the fuel number with 2 kJ chemical igniter.

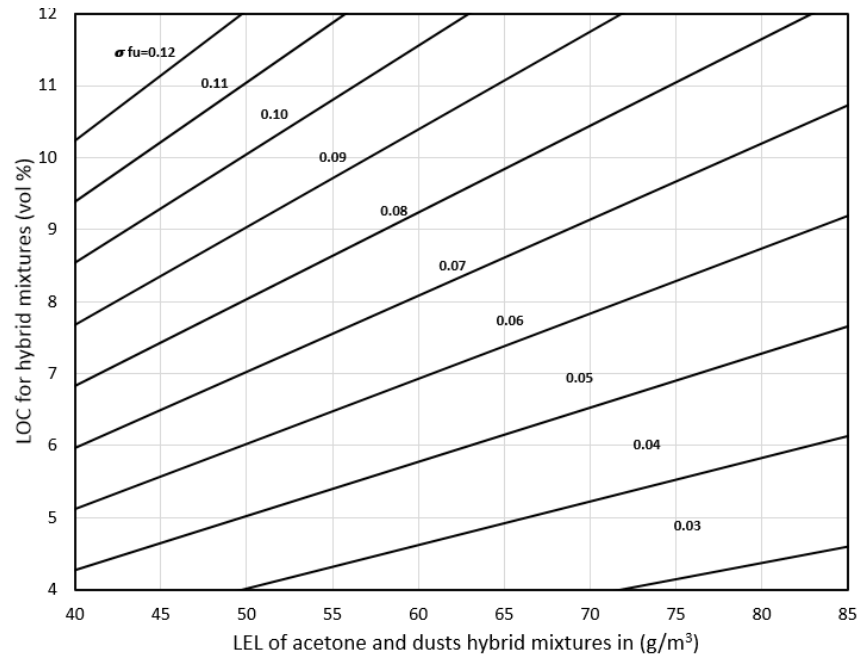


Figure 6.40: A diagram to estimate the LOC of hybrid mixture of acetone and dusts in dependence on $LEL_{-hybrid}$ and the fuel number with 2 kJ chemical igniter.

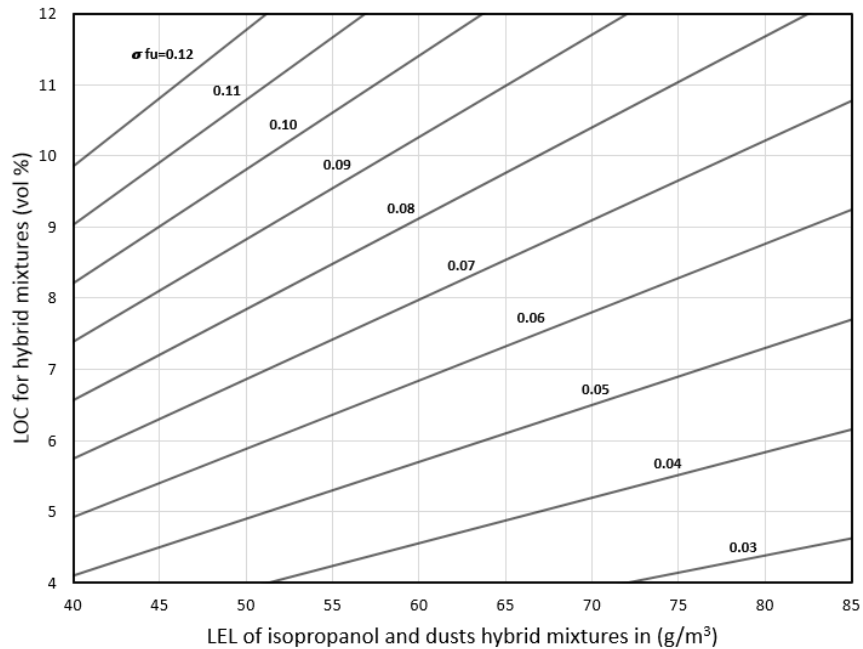


Figure 6.41: A diagram to estimate the LOC of hybrid mixture of isopropanol and dusts in dependence on $LEL_{-hybrid}$ and the fuel parameter fuel number with 2 kJ chemical igniter.

6.3 Minimum ignition energy

The minimum ignition energy (MIE) is determined as the minimum amount of electrical energy stored in a capacitor which, when released as a high voltage spark, is just sufficient to ignite fuel mixtures at its most easily ignitable concentration in air. It is very important to know the lowest energy that could ignite materials which are being handled or processed in the facility in order to prevent any hazard that might result from electrical discharge. For the last centuries, many studies have been carried out and have demonstrated the specific behavior of the MIE of single substance explosions [122, 174-178], However, only limited information exists in the literature for the MIE of hybrid mixtures. Such kind of mixtures are usually encountered in various processes and systems where substances of different states of aggregate are handled. There is no accurate mathematical model/standard to determine the ignition sensitivity of such mixtures. Hence, investigations on the MIE of hybrid mixtures of eight combustible dusts and two flammable gases have been carried out. This was achieved by performing series of experiments in the modified

Hartmann apparatus as described in section 5.4. A mathematical model was developed and a comparison of this model with the experimental results was also accomplished.

6.3.1 Minimum ignition energy of single substances

In order to investigate the MIE of hybrid mixtures, the results from single substances were initially obtained. Figure 6.42 presents the results obtained for the MIE of dusts. It could be seen that brown coal recorded the lowest value with MIE of 17 mJ while charcoal recorded the highest value of MIE of 500 mJ. The reason for this high MIE of charcoal could be attributed to its high particle size and low volatile content compared to other dusts as presented in Table 4.1.

Minimum ignition energy of a dust cloud is strongly dependent on the size of the dust particle. An increase in the dust particle size decreases the surface area available for the ignition to prevail and consequently, largely increases minimum ignition energy [119]. Thus, dust particles with smaller median value are more easily to ignite as compared to the ones with courser size. Moreover, decreasing particle size would greatly increase the number of particles under the same dust concentration, which would also increase the effective reaction surface of the dusts [22].

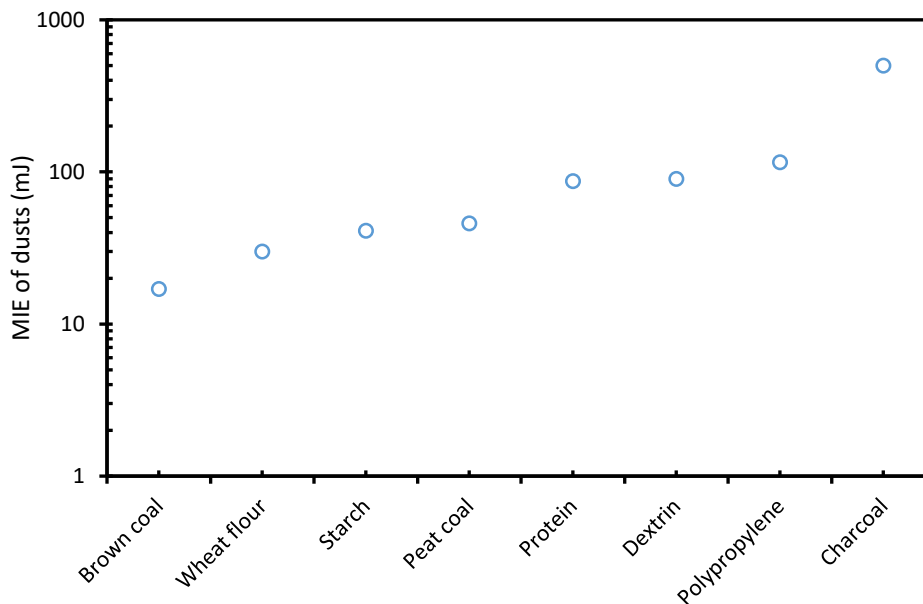


Figure 6.42: Experimental results for the minimum ignition energy of dusts.

On the other hand, the higher the volatility the more the dust is prone to ignition. This behavior could be explained by the consideration that the dusts with higher volatile content tend to produce more combustible gas at the same conditions, which contributes to the gas phase

combustion. The lowest achievable ignition energy by the device used in this research work was limited to a value of 4 mJ. Thus, the MIE of pure gases could not be tested directly, as their values lie well below 4 mJ. Hence, the MIE values for the gases used (methane = 0.28 mJ and propane = 0.25 mJ) were taken from literature [179].

6.3.2 Minimum ignition energy of hybrid mixtures

For the next step, the MIE of hybrid mixtures based on the results from the single dust and gas test was considered. The main focus of the hybrid mixture test was to verify if addition of a non-explosible concentration of gas could decrease the MIE of the dust. Detailed discussion on how the MIE of dusts and hybrid mixtures were obtained has already been presented in section 5.4. The lower explosion limits of the gases (methane = 5 vol% and propane = 2.0 vol%) were initially determined at the same test conditions used to estimate MIE of dusts. After obtaining the MIE of individual dust, concentrations of the gases (methane = 1.0 vol%, 2.0 vol%, 3.0 vol%, 4.0 vol% and propane = 0.6 vol%, 1.0 vol%, 1.4 vol% and 1.7 vol%) below the obtained LELs were added to the dust and the experiments were performed at an ignition energy below the MIE of the dust.

Figures 6.43 to 6.50 present the results for the MIE of various hybrid mixtures as well as the comparison with the empirical model. Details information of the empirical model could be seen in section 6.3.3. Each plot shows the MIE of hybrid mixtures on the Y-axis and the concentration of gases on X-axis. The hollow red square represents the experimental hybrid MIE of dust with propane, the hollow blue triangle represents experimental hybrid MIE of dust with methane, the dotted red line indicates the empirical model estimation of the hybrid MIE with propane and the solid blue line represents computational estimation of hybrid MIE with methane. An error bar based on the error and uncertainty analyses is plotted on the experimental result. The total quantifiable error obtained from the experimental work is 8.1%. See Appendix C.2 for more details on how the error and uncertainty analysis was carried out. Moreover, a statistical analysis based on the capacitance and ignition energy of hybrid mixture was performed (see Table C.5 in appendix C). It was noticed that, the higher the capacitance, the lower the ignition energy and the higher the probability for the material to ignition. This findings confirms the work done by **Beyer et al. [180, 181]** of which they determined the minimum ignition energy on the basis of a statistical approach using hydrogen, ethene and propane as a fuel. They noted that the ignition

probability is inversely proportional to the ignition energy, the lower the ignition energy the higher the probability for the material to ignite.

Figures 6.43 to 6.45 show the results obtained for the mixtures of food substances (starch, protein and wheat flour) and gases. A decrease in MIE value of dust materials by the addition of a non-explosible concentration of gas was recorded. With respect to starch, a series of tests were performed below the MIE by adding gas at a concentration below the LEL as shown in Figure 6.43. It could be noticed that the ignition energy decreases with increasing concentration of the added gas. For example, the MIE of the hybrid mixture decreased from 40 mJ to 22 mJ, 15 mJ and 4.3 mJ when methane at concentrations of 1 vol%, 2 vol% and 4 vol% was added. A similar trend as explained in the case of methane and starch was also observed in starch and propane mixtures.

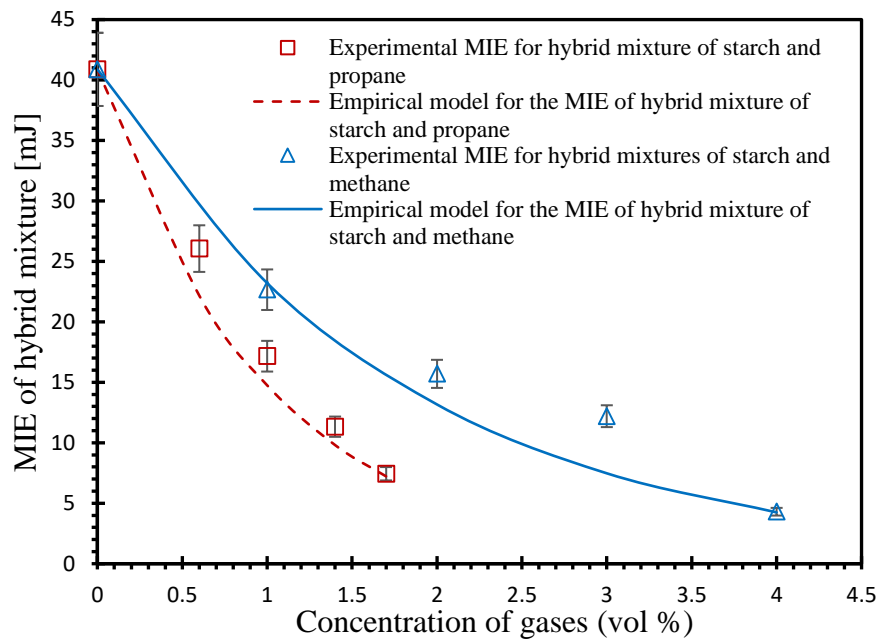


Figure 6.43: Ignition energy of hybrid mixture of starch with propane and methane in dependence on gases concentration and its comparison with empirical model.

In the case of wheat flour and protein, a similar explosion behavior was noticed as presented in Figures 6.44 and 6.45, respectively. It was also noticed that the MIE of the hybrid mixture compared to that of the dust decreased when a non-explosible concentration of the gas was added. The presented empirical model to estimate the MIE of hybrid mixture was in good agreement with the experimental results for both methane and propane with starch as well as wheat flour. However, in the case of protein and methane hybrid mixtures, the computational

estimation was a bit higher than the experimental results at methane concentrations of 1 vol% and 2 vol% with a maximum deviation of 11 mJ which falls outside the error margin.

Out of the three food substances tested, it was noticed that the effect of the gases on the MIE of starch was more significant, followed by protein and wheat flour with the least MIE values obtained with the addition of 4 vol% methane being: starch = 4.3 mJ, protein = 8.5 mJ and wheat flour = 11.7 mJ. A similar trend was observed for the other concentrations of methane as well as propane. This trend could be explained by considering two properties of the dust which include: particle size and volatile content. For the three food materials, the average particle sizes and volatile contents are: starch = 14 μm , 93.8 wt%, protein = 46 μm , 81.5 wt% and wheat flour = 52 μm , 79.6 wt%. The MIE of dust cloud strongly depends on the particle size. Thus decreasing particle size would greatly increase the number of particles under the same dust concentration, which would also increase the effective reaction surface of the dusts. Moreover, particle size of the dust particle could also affect the devolatilization rate. Therefore, by decreasing the particle size the devolatilization rate increases thereby increasing the combustion rate. Furthermore, volatile content of the dust could also play a crucial role in determination the MIE of dust and hybrid mixtures. The dusts with higher volatile content tend to produce more combustible gases at the same conditions which may contribute to the gas phase combustion.

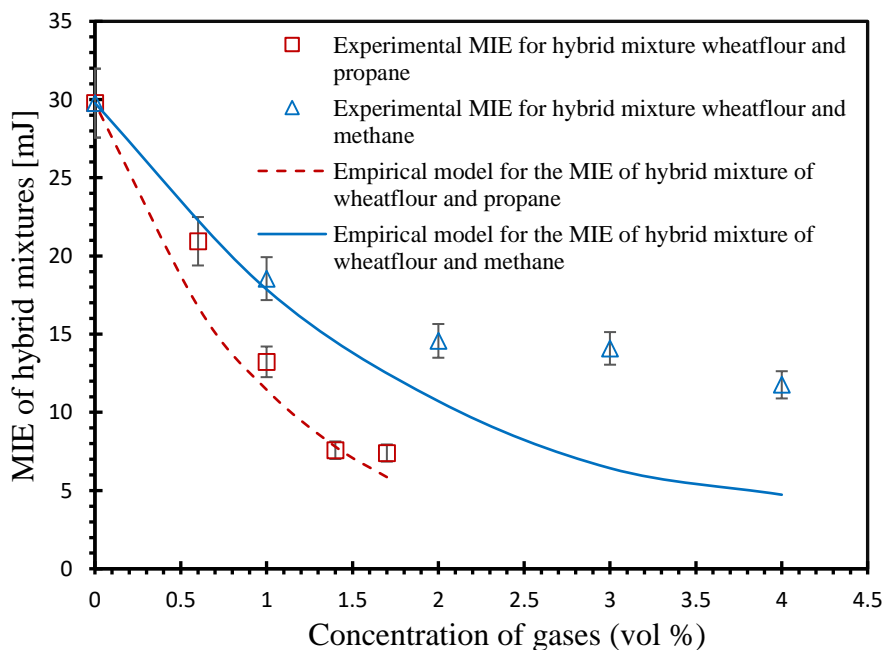


Figure 6.44: Ignition energy of hybrid mixture of wheat flour with propane and methane in dependence on gases concentration and its comparison with empirical model.

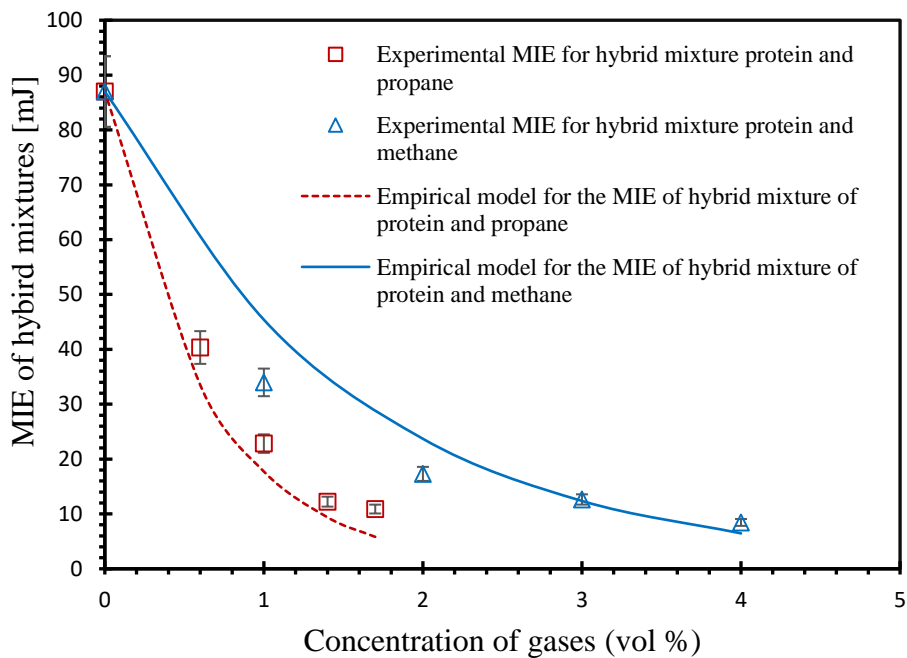


Figure 6.45: Ignition energy of hybrid mixture of protein with propane and methane in dependence on gases concentration and its comparison with empirical model.

With regard to the polymer materials, polypropylene (thermoplastic polymer) and dextrin (polymers of D-glucose) with methane and propane, a similar ignition trend as explained above was noticed. The MIE of the hybrid mixture drastically decreases by the addition of a non-explosible gas concentration as shown in Figure 6.46 and 6.47. This reflects the fact that the ignition sensitivity of a hybrid mixture is quite higher than that of the individual dust. The MIE of hybrid mixtures with polypropylene dust falls by 93 % for 1.7 vol% propane and 96 % for 4 vol% methane compared to the MIE of the dust alone. It was also noticeable that the experimental results were in agreement with the results obtained from the empirical model with the exception of 1 vol% propane, for which deviations are observed.

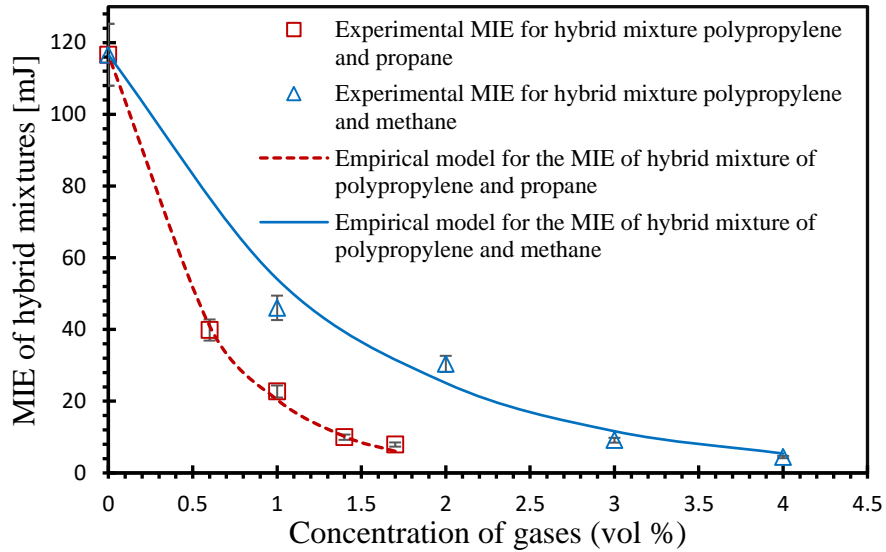


Figure 6.46: Ignition energy of hybrid mixture of polypropylene with propane and methane in dependence on gases concentration and its comparison with empirical model.

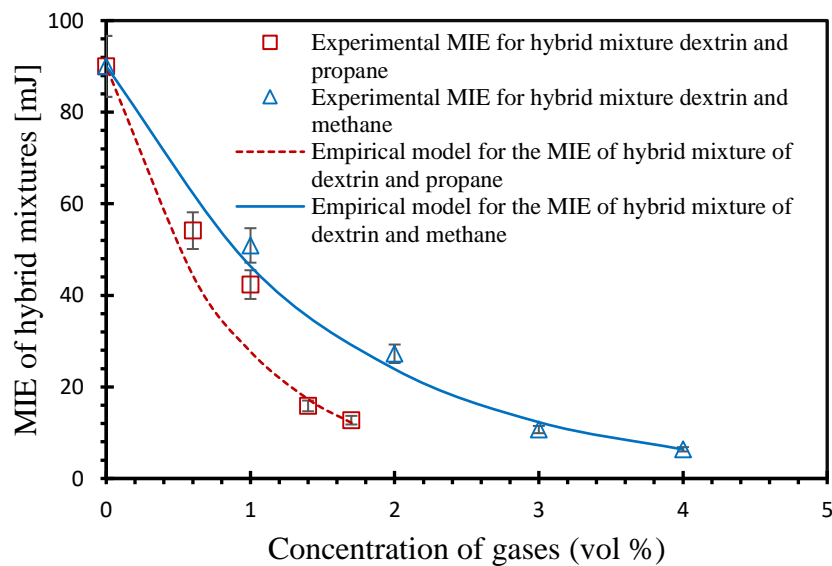


Figure 6.47: Ignition energy of hybrid mixture of dextrin with propane and methane in dependence on gases concentration and its comparison with empirical model.

The particle size and the volatile contents of the dusts could be a contributing factor to the various effects on the MIE of hybrid mixtures. Owing to its lower particle size and higher volatile content, the MIE of polypropylene is more affected as compared to dextrin, by addition of non-explosible concentration of methane and propane. The median particle size and the volatile content recorded for these two materials are: polypropylene = 34 μm , 99 wt% and dextrin = 56 μm , 98.17 %wt. The MIE recorded for 1.7 vol% of propane is 7.92 mJ and 12.74 mJ for polypropylene and

dextrin respectively. A similar trend is also noticed for the other concentration of propane and methane.

Again, three different coal materials (peat coal, charcoal and brown coal) were tested. The choice of these materials was based on their reaction mechanism as well as the range of the individual MIE. Among the three coal materials, charcoal exhibited the highest MIE of 500 mJ while peat and brown coal recorded values of 46 mJ and 17 mJ, respectively. This might be due to the reaction mechanisms of these materials. Both peat coal and brown coal undergoes homogeneous reaction in which the combustion rate is strongly linked with the generation rate of combustible volatiles. The coal dust initially devolatilized forming combustible volatile gas, which then mixed with air in the space between the particle. Oxidation of pyrolysis gases, where the gas phase combustion of premixed volatile-air then takes place or in other words, the oxidation of homogeneous gas takes place. Contrary to peat and brown coal, charcoal undergoes a heterogeneous reaction. The combustion rate of the surface-heterogeneous-oxidation-prone dust (charcoal) is mainly governed by two alternative processes of particle melting and the diffusion of oxygen to particle surface. Under low dust concentrations, the oxygen diffusion process is very fast due to the sufficient oxygen in explosion vessel and, therefore, the particle melting rate becomes a limiting one, attributing to the larger inter-particle space and less efficient heat transfers. Conversely, when particle melting rate is promoted to an enough high degree with the increase of dust concentration, the combustion rate of charcoal dust would then be controlled by the oxygen diffusion process.

Figures 6.48 to 6.50 present the results obtained for the MIE of hybrid mixtures of the various coal substances with methane and propane. A drastic reduction in the MIE of various coal dusts was noticed upon the addition of gases concentrations below the respective explosible limit.

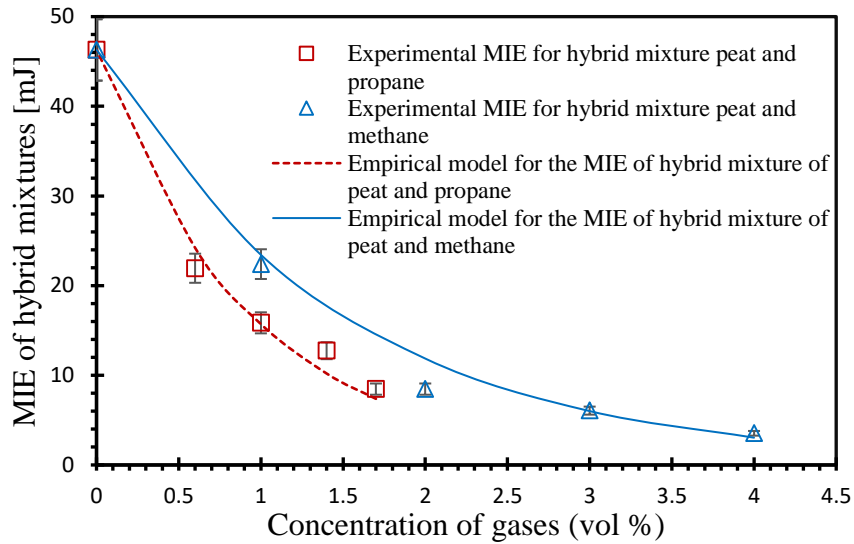


Figure 6.48: Ignition energy of hybrid mixture of peat with propane and methane in dependence on gases concentration and its comparison with empirical model.

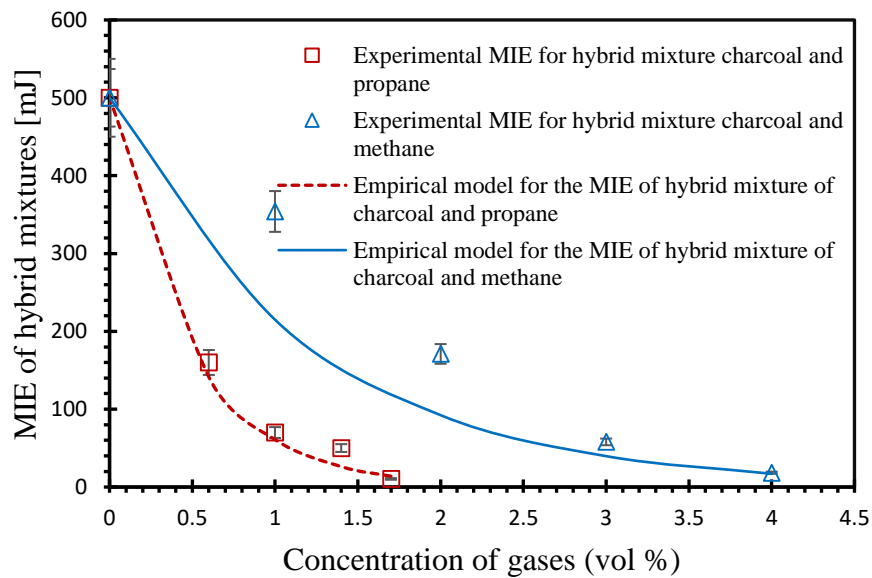


Figure 6.49: Ignition energy of hybrid mixture of charcoal with propane and methane in dependence on gases concentration and its comparison with empirical model.

Moreover, the empirical model to estimate the MIE of hybrid mixture was in agreement with the experimental results. It must be emphasized that this model does not give an exact prediction of the MIE of hybrid mixtures, rather a fair idea at where the MIE could lie. Particle size and volatile content also play a vital role in the ignition of coal dust with respect to MIE of hybrid mixtures. Brown coal with smallest particle size with median value of 37 μm records the lowest MIE on addition of non-explosible concentration of methane and propane as compared to peat coal and charcoal with median value 45 μm and 79 μm respectively. Table B1 in Appendix B provides a

summary of all the experimental results as well as the comparison with the empirical model with the deviations.

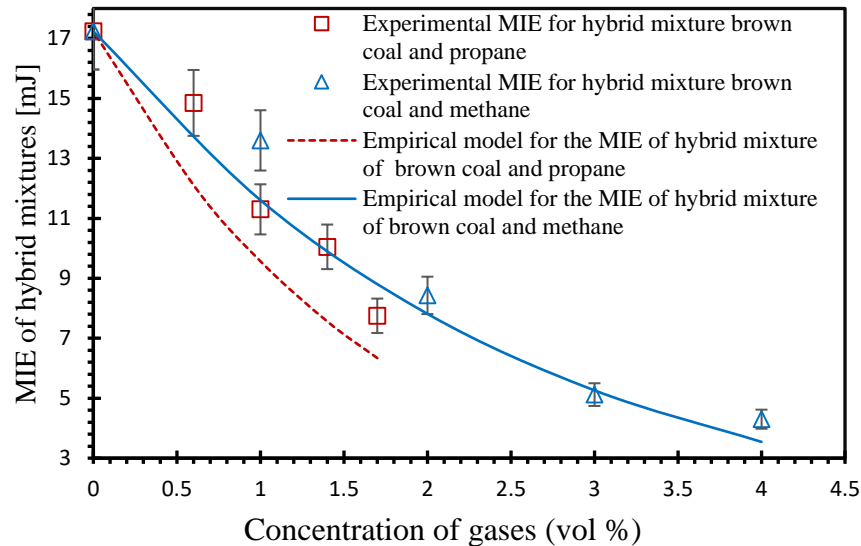


Figure 6.50: Ignition energy of hybrid mixture of brown coal with propane and methane in dependence on gases concentration and its comparison with empirical model.

The results obtained from this work conform to the work done by **Franke et al. [70]**. The authors observed that adding small fractions of methane to coal dusts, considerably reduce the MIE by factors of the order of 10s to 100s when the methane content was increased from 0 to 3 vol%. Furthermore, **Pellmont [69]** also mentioned that the ignition sensitivity of a combustible dust is boosted when fed with a small amount of flammable gas with a concentration below the lower explosion limit. Hence, the effects of the MIE on hybrid mixture explosions cannot be predicted by simply overlapping the effects of single substance explosion. Moreover, one cannot rely on the MIE of only one substance to be able to determine the safety of a system or a process when one or more combustible materials with different states of aggregate are used or present. The mathematical model presented is in good agreement with the experimental results from a safety point of view.

The decrease in the MIE of combustible dusts upon the addition of non-exposable concentrations of flammable gases could be attributed the following reasons: The hybrid mixture tests were performed by dispersing a combustible dust with a non-ignitable concentration of a flammable gas air mixture into the combustion chamber with an electric spark generated between two

electrodes as an ignition source. Usually, the spark generated is capable of igniting a flammable gas alone (provided the concentration is within the explosible range) but since the concentration of the gases used were below the lower explosion limits, the gases alone could not be ignited. According to the thermal theory of electric spark ignition by **Elbe et al. [182]**, the spark produces a small volume of hot gas immediately after the discharge, which rapidly increases the temperature within the flame kernel. As soon as the dust is dispersed into the chamber, the particles located in the ignition kernel are heated by this hot gas producing volatile matters or combustible gases. This volatile matter then mixes with air in the space between the particles as well as the added flammable gas, thereby boosting the total concentration of combustible gases which are capable to ignite. Adding a very low concentration of flammable gas to a combustible dust could also induce a change in the rate-limiting step of the combustion reaction, that is from devolatilization of the dusts to a homogeneous gas phase reaction, which implies a drastic decrease in MIE of hybrid mixtures. The modification of rate-limiting step of the combustion reaction depends on the size of the particle. Size reduction could alter a diffusion controlled regime for large size particles to a kinetically controlled for small size ones **[183, 184]**.

Moreover, adding a low concentration of flammable gas to a combustible dust could boost the heat transfer from one burning particle to the other. The spark produced by the electrostatic discharge in the combustion chamber generates an energy which burns the nearest particle. The heat produced from the burnt particle is then transferred to the next particle but in case the energy produced by the spark is not high enough, the heat produced by the first burnt particle will not be enough to burn the next one. So, the addition of easily ignitable substances such as flammable gas could boost the heat transfer process by bridging the heat transfer gap between the first burnt particle and the next one.

Furthermore, the effect of adding a low concentration of gas on the MIE of dust could be explained using the electrical theory proposed by **Elbe et al. [182]**. The authors explained that the electrical discharge from the electric spark could also activate a chemical reaction by producing free radicals/ions in the discharge zone, which diffuse into the surrounding fuel-air mixture to initiate a self-propagating combustion chain. The ignition conditions of the mixture are dependent on the concentration of the reactive particles. This means that, even if the free radicals

discharge could not initiate a self-propagating combustion for the dusts, the addition of easily ignitable combustible gas could enhance this reaction.

6.3.3 Empirical model to estimate the minimum ignition energy

The minimum ignition energy of decreases as the concentration of the added gas is increased. A general trend for this behavior is shown in Figure 6.51. The solid line indicates the results for the effect of adding a non-explosible gas (propane) concentration on the MIE of dust (polypropylene) while the dotted line represents a trend line with R^2 of 0.99.

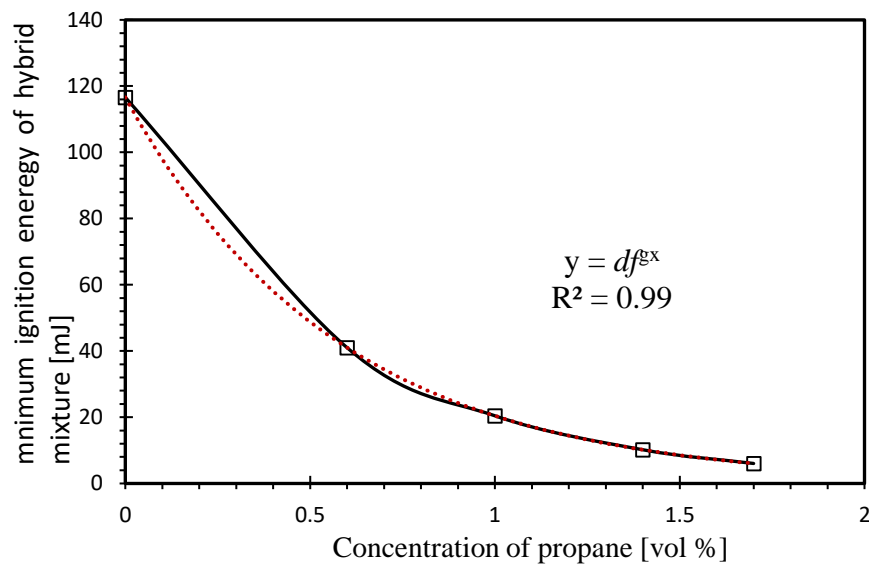


Figure 6.51: The trend of MIE of hybrid mixture of polypropylene and propane.

The general function gives a linear plot on the semi-logarithmic graph. This semi-logarithmic method to estimate the minimum ignition energy of hybrid mixtures was initially proposed by **Laurence Britton [185]**. A similar principle was adopted in this correlation.

$$y = df^{gx} \quad (6.3.1)$$

Here, d and f are positive constants and g is any constant.

eq. (6.3.1) can be derived to obtained eq. (6.3.2), (see Appendix 8.4:C for detail derivation)

$$MIE_{hybrid} = \frac{(MIE_{dust})}{(MIE_{dust}/MIE_{gas})^{\frac{c}{c_0}}} \quad (6.3.2)$$

Hence, the MIE of hybrid mixture MIE_{hybrid} could be estimated mathematically from eq. (6.3.2)

Where; C is the gas volume concentration (vol %), C_0 is the gas concentration (% vol) leading to the lowest MIE, MIE_{dust} and MIE_{gas} are minimum ignition energy of dust and gas respectively.

Note: this mathematical model is valid if, $C \leq C_0$. A summary for the validity of this model could be referred to Table B1 in Appendix B.

6.4 Minimum ignition temperature

Minimum ignition temperature (MIT) is a critical parameter when conducting hazard assessments for processes involving fuel mixtures, when hot surface is considered as an ignition source. It is the lowest temperature of a heated surface which can ignite a fuel oxidizer mixture within the explosible range. Hot surfaces capable of igniting fuel-air mixture exist in a number of situations in the industry such as furnaces, burners and dryers of various kinds. In addition, hot surfaces can be generated accidentally by overheated bearings and other mechanical parts. An explosible atmosphere generated in an uncontrolled way in the proximity of a hot surface with temperature above the actual minimum ignition temperature can result in an explosion [55, 186]. Consequently, in the prevention and mitigation of explosions, it is important to know the MIT of fuel mixtures in order to take adequate precautions to ensure that the hot surface temperature does not reach this value.

This section presents the results for the MIT of hybrid mixtures of dust, gas and solvent-vapor. Combinations of six combustible dusts (Lycopodium, starch, HDPE, toner, CN4 and wood), three flammable gases (methane, propane, hydrogen) and four vaporized solvents (ethanol, isopropanol, toluene and hexane) were employed. It should be noted that, part of the presented results in this section have been published in the following articles [187, 188]. All tests were performed in the modified Godbert-Greenwald furnace under the same initial and testing conditions.

Three main testing cases were considered:

1. Testing for the MIT of single substance
2. Testing for the MIT of hybrid mixtures (two-phase or two component mixtures)
3. Testing for MIT of three component hybrid mixture mixtures.

6.4.1 Minimum ignition temperature single substances

With respect to the first case, Figure 6.52 presents the results obtained for the MIT of dusts. It can be noticed that the plastic material (high density polyethylene) recorded the lowest ignition temperature while coal dust (CN4) recorded the highest with a difference of 300 K. The MIT of dust materials is influenced by various parameters such as particle size, moisture content, volatile contents and so on. The results illustrate that the dusts with higher volatile content ignite at lower temperature. This could be explained based on the phenomenon that the dusts with higher volatile content may produce more combustible gas at the same conditions, which contributes to the gas phase combustion (see section 6.3.1 for more information). The volatile content as well as other parameters for the dust samples are presented in Table 4.1. A comparison between the volatile contents of the dusts (HD-PE = 99.17 wt%, starch = 93.77 wt%, lycopodium = 91.06 wt %, toner = 90.18 wt%, wood = 84.38 wt% and CN4 = 17.08 wt%) and the MIT results reveal that materials with the lower volatile content have higher ignition temperatures as seen in case of CN4 and HDPE.

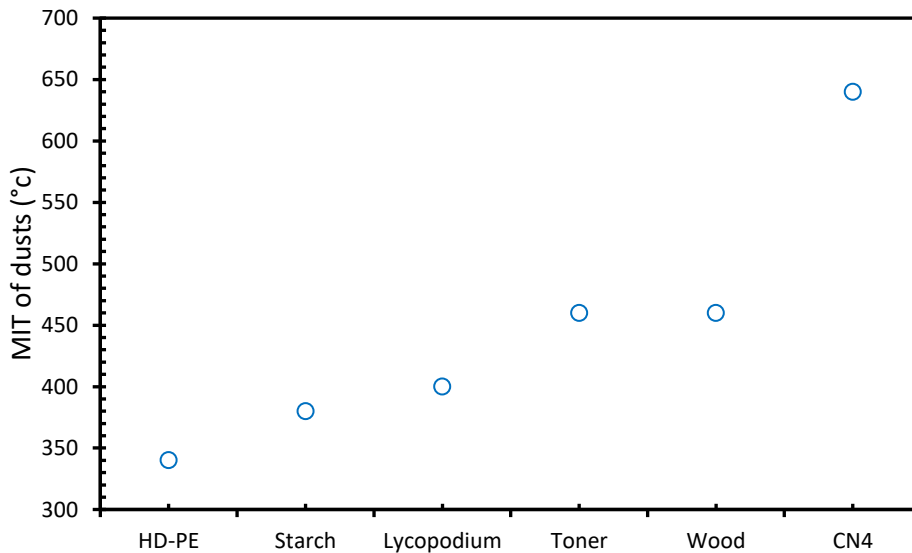


Figure 6.52: MIT of the dust materials.

Moreover, Figure 6.53 presents the results obtained for the MIT of gases and solvent vapor. With respect to the gases (methane, hydrogen and propane), it was noticed that methane had the highest MIT followed by hydrogen and propane. This trend could be attributed to their basic chemical and physical properties such as heat of combustion as presented in Table 4.2. For example, materials with higher heat of vaporization have higher ignition temperature as seen in

case of methane and propane having the heat of combustion of -286 kJ/mol and -890 kJ/mol and MIT of 600 °C and 500 °C respectively.

Furthermore, Figure 6.53 presents the results obtained for the MIT of the solvent vapor (hexane, ethanol, isopropanol and toluene). It is clear from the results that toluene with MIT of 520 °C has the highest value followed by isopropanol (440 °C), ethanol (410 °C) and hexane (240 °C). This trend could also be as a result of the chemical and physical properties pertaining to the solvents as shown in Table 4.3. It was noticed that the boiling point was at the same level as the MIT of the solvents. As the boiling point increases, the temperature at which the solvent turns to vapor also increases, which consequently increases the ignition temperature. This is confirmed by the results obtained for hexane, ethanol, isopropanol and toluene with their boiling points of 68.5 °C, 78 °C, 82 °C and 111 °C respectively as compared to their MIT results shown in Figure 6.53.

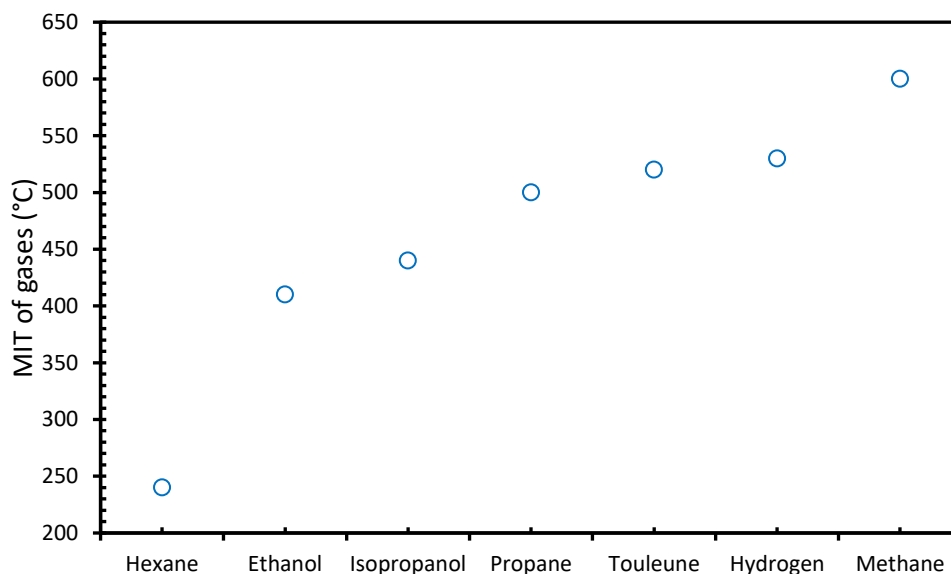


Figure 6.53: MIT for the gases and solvents used.

In order to validate the experimental procedure used for hybrid mixture testing, the MIT of pure gases were initially tested and the results were compared with literature values obtained from the standard procedure. From Figure 6.54 it could be seen that the experimental results according to the method described in section 5.3 are in agreement with the work done by **Brandes et al. [83]** with maximum deviations of 15 K. This deviation is within the error margin obtained from the measurement uncertainties (see Appendix C.3 for detail information on the error analysis).

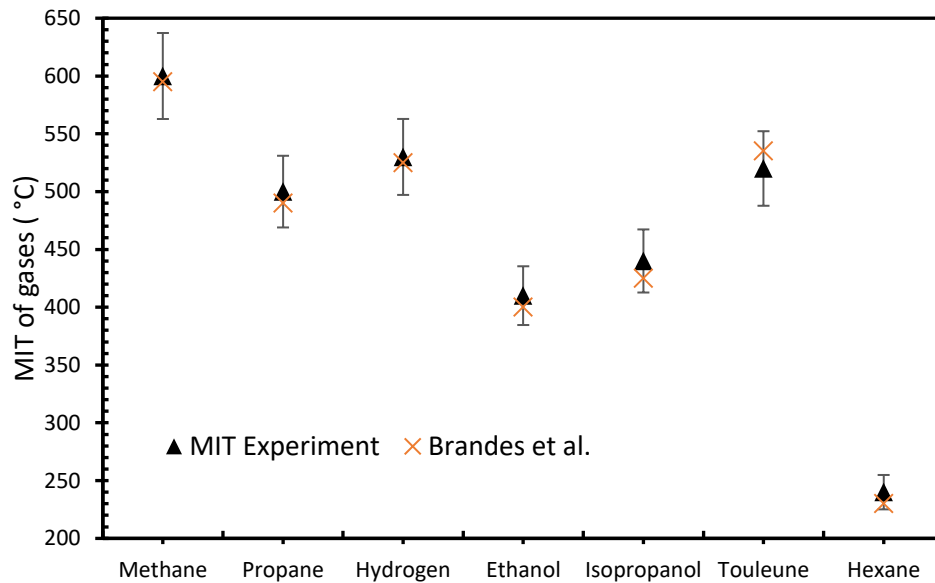


Figure 6.54: Comparison of experimental MIT values of gases and solvent-vapor obtained with the GG furnace and according to standard procedure by Brandes et al.

This has proven that even if the method used here differs from the standard procedure, it is justifiable to use this method for determining the MIT of hybrid mixtures. However, it is important to know that the method used does not seek to replace the standard procedure for gas-air mixtures, but can be used to determine the MIT of mixtures consisting of component in different states of aggregation.

Moreover, the results obtained for the MIT of gases are 5 to 15 °C higher than the ones reported from the standard test. This might be due to turbulence produced by the system, which intensifies the heat transfer inside the gas, so that local overheating of the gas is prevented [189].

6.4.2 Minimum ignition temperature of two-phase hybrid mixtures

In the next step, the MIT of hybrid mixtures of combustible dusts, gases and solvents were considered based on the results obtained from the single-fuel test. Two different test series were considered, which reflect the effect of adding non-explosible concentrations of dusts on the MIT of gases or vapor and the effect of adding non-explosible concentrations of gases on the MIT of dusts. With respect to the first test series, after obtaining the MIT of the single-fuel-air mixture, the temperature of the GG furnace was further decreased to check if an addition of a non-explosible concentration of combustible dust would decrease the MIT of gases. The concentrations of the dust were selected such that the dust itself if mixed with air would not have

formed an explosible mixture in the GG furnace. The detailed test procedure for determination of the MIT of hybrid mixture could be seen in section 5.3. Moreover, Table 6.15 presents both the tested minimum explosible concentration of dusts (MEC) and the lower explosion limits of gases (LEL) which were determined using the same MIT equipment and testing procedure. It must be mentioned that, the added concentrations of hybrid mixtures were all below the lower explosion limits.

Table 6.15: LEL and MEC of gases and dusts.

Dust	MEC (g/m ³)	Gases	LEL (vol %)
Starch	145	Methane	4.0
Lycopodium	108	Propane	2.0
Wood	217	Hydrogen	5.0
Toner	87	Toluene	1.1
CN4	304	Ethanol	3.0
HD-PE	174	Isopropanol	2.0
		Hexane	1.6

Figure 6.55 presents the results for the effect of adding non-explosible concentrations of dusts on the MIT of gases. The red square sign symbolizes the MIT of gases and the rest of the signs symbolize hybrid mixtures explosions. It could be seen that explosions were obtained below the MIT of the gases when a concentration of dust which itself is not ignitable at that particular temperature was added. For example, methane with the MIT of 600 °C, recorded an explosion at 530 °C when 30 g/m³ of toner was added, although toner is not ignitable at 600 °C in its pure form. A similar explosion behavior could be seen with the mixtures of propane, hydrogen, toluene, ethanol and isopropanol and the other dusts with an exception of hexane, for which no effect was noticed in all cases. This distinctive behavior of hexane could be explained by the consideration of its ignition temperature, which is much lower than the MIT of all other dusts. The decrease of the MIT of gases upon addition of non-explosible concentrations of dusts could be due to pyrolysis and devolatilization of dusts, resulting in volatile matter addition to the already introduced gas. As already discussed in section 2.4.1, introduction of combustible dust (organic dust) into the heated furnace heats the organic particles. This produces volatile matters or combustible gases. These volatile gases are then mixed with either combustible gas or vapor to increase the gaseous fuel content, which consequently increases the ignitability of the mixture.

In the case of hexane and the dust mixtures, this mechanism does not hold since the MIT of dust samples are all above the MIT of hexane. The effect of dusts on the MIT of hexane was tested at a temperature well below the MIT of hexane (240 °C), which could not devolatilize any content of dusts and hence no effect of dust was seen on the MIT of hexane.

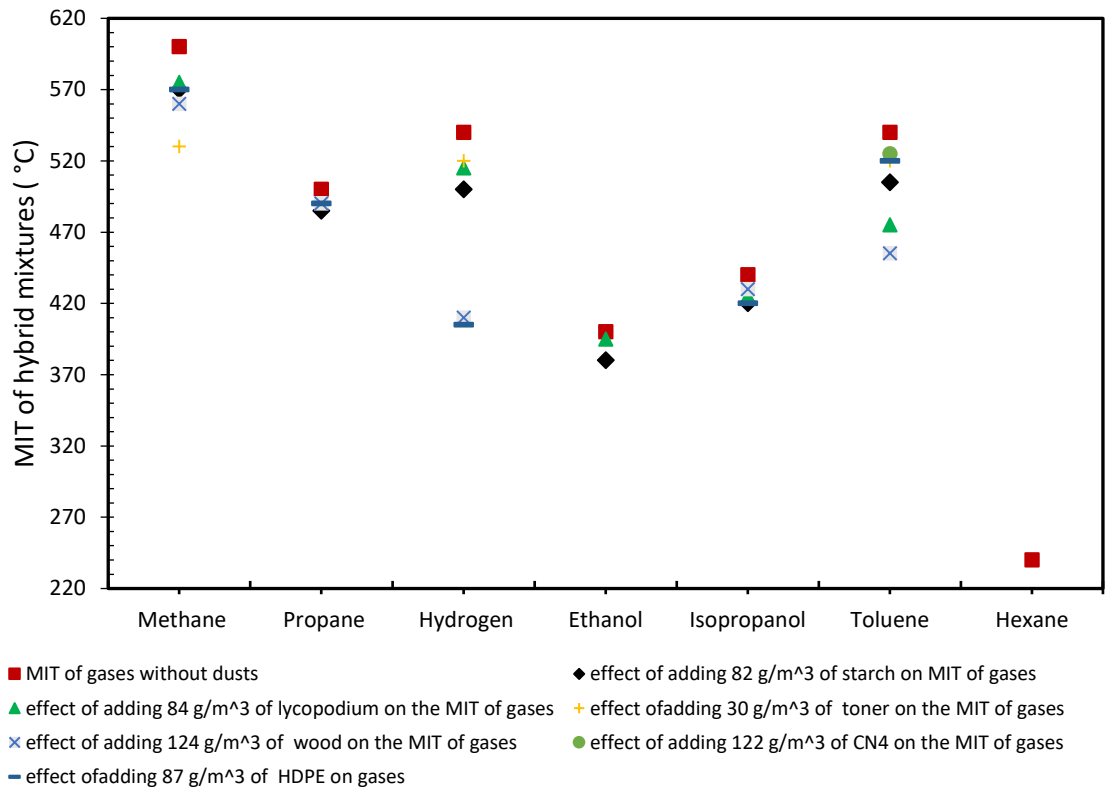


Figure 6.55: MIT of two-phase hybrid mixture of dust and gas: effect of admixture of dust on the MIT of gases.

Moreover, the effects of addition of non-explosible concentrations of flammable gases on the MIT of dusts were also studied, by adding a volume fraction of gas which was below the lower explosion limits to the dust. After obtaining the MIT of the single dusts, further tests were performed below the MIT by adding a non-explosible concentration of gas. Figure 6.56 presents the results obtained for the effect of gases on the MIT of dust. A similar explosion behavior as explained above was also noticed here, the MIT of dust decreased when a non-explosible concentration of gas was added. For example, the MIT of wood decreased from 460 °C to 420 °C and to 400 °C when 2 vol% of methane and 0.8 vol% of hexane were added, respectively. A similar behavior was also observed for the other dusts and gases mixtures. It was generally noticed that

hexane had a significant effect on all the dust samples compared to the other gases. This could be as a result of its lower ignition temperature in comparison to the dusts. When the temperature is lower than the MIT of the dust, the volatile matters with low ignition temperature initially devolatilizes, producing combustible gases which might not be able to ignite alone, however, when easily combustible gas is added to devolatilized gas, it could lead to ignition. This was seen in the case of hexane and since its MIT is far lower than that of the dusts, it becomes ignitable at the MIT of the dusts provided the added concentrations are within the explosible range. So adding a non-explosible concentration of hexane at the MIT of the dusts could add up to the already present devolatilized gases generating an explosible atmosphere.

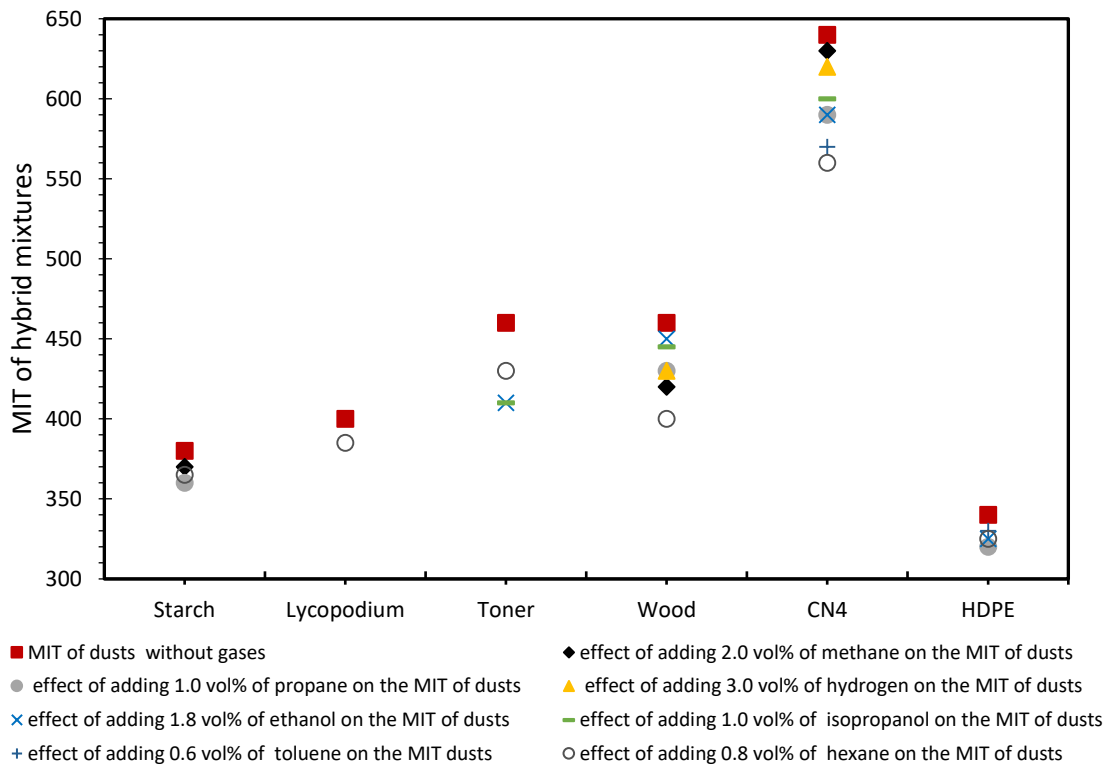


Figure 6.56: MIT of two-phase hybrid mixture of dust and gas: effect of admixture of gas on the MIT of dusts.

Furthermore, the MIT of two component mixtures were also tested (i.e. mixtures of solvent-vapor and gas). Figure 6.57 provides the results for the effect of solvents on the MIT of gases. It could be seen that the MIT of a gas decreases upon addition of a non-explosible concentration of solvent-vapor, which is either not explosible or below their respective lower explosion limit. For example, methane and propane with the MIT of 600 °C and 500 °C decreased to 510 °C and 445

°C respectively when 1.8 vol% of ethanol was added. However, no explosion was observed when non-explorable concentrations of gases were added to the solvents. With the exception of toluene, the MIT of the solvents were all below the MIT of the gases. Since the MIT of the gases are by far higher than that of the solvents, this means that irrespective of the added concentration, the gas will not ignite itself. So when a non-explorable gas concentration is added to the solvent, there exists a possibility that the added gas concentration might not influence the ignition of the solvent.

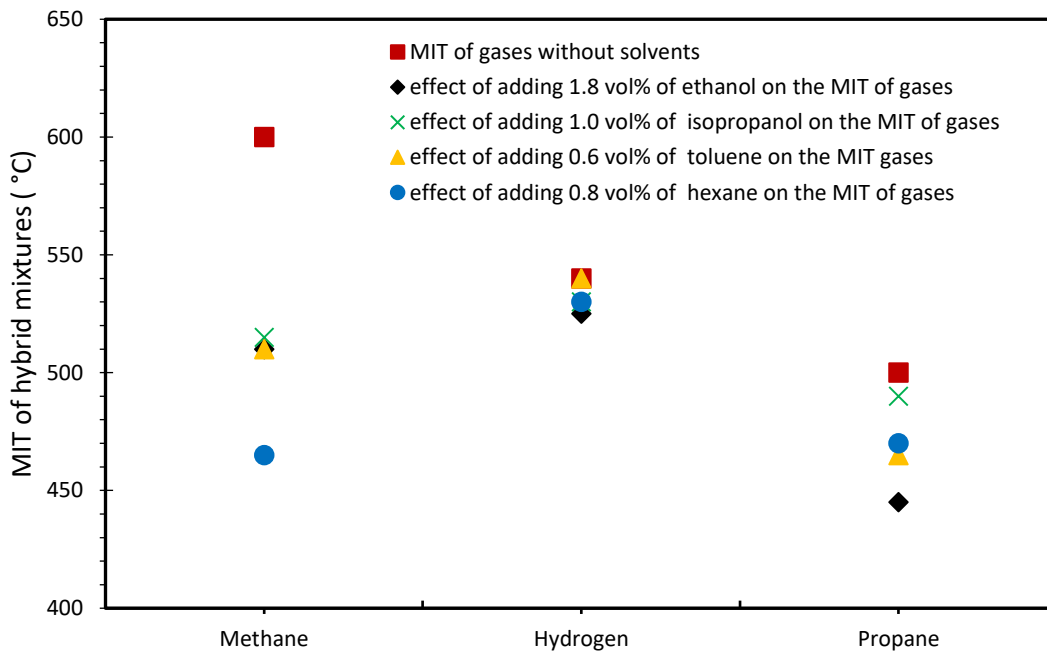


Figure 6.57: MIT of two component mixture of solvent-vapor and gas: effect of admixture of solvent on the MIT of gases

6.4.3 Minimum ignition temperature of three-components hybrid mixtures

Based on the results obtained from the single and double-phase or component mixtures, the MIT of three component hybrid mixtures were tested. This was achieved by adding non-explorable concentrations of a third substance below their respective lower explosion limit to the non-explosion temperature of the double-phase or component. In this case, three test variables were considered:

1. The effect of adding non-explorable concentrations of gases and solvents on the MIT of dusts
2. The effect of adding non-explorable concentrations of dusts and solvents on the MIT of gases
3. The effect of adding non-explorable concentrations of gases and dusts on the MIT of solvents

With regards to the first test variable, non-explosible concentrations of both gas and solvent were added to the dust at a temperature below its MIT. Table 6.16 shows the effect of adding non-explosible concentrations of gases and solvents on the MIT of dusts. It could be seen that an ignition was recorded at the temperature where no ignition was obtained for the two-phase mixture. For example, by adding 1.8 vol% of ethanol vapor, the MIT of toner was decreased from 460 °C to 450 °C. This temperature was further decreased to 400 °C on the addition of 1.0 vol% of propane.

Table 6.16: Effect of admixture of solvents and gases on the MIT of dusts, (all in °C).

Dust	MIT of only dusts	admixture of 0.8 vol% hexane on the MIT of dusts	admixture of 2.0 vol% methane on the MIT of dusts	admixture of 2.0 vol% methane and 0.8 vol% hexane on the MIT of dusts	admixture of 1.0 vol% propane on the MIT of dusts	admixture of 1.0 vol% propane and 0.8 vol% hexane on the MIT of dusts	admixture of 3.0 vol% hydrogen on the MIT of dusts	admixture of 3.0 vol% hydrogen and 0.8 vol% hexane on the MIT of dusts
HDPE	340	325	340	325	340	320	340	300
Lycopodium	410	385	410	385	410	385	410	390
Starch	370	365	370	360	370	355	370	370
Toner	460	430	460	430	460	420	460	440

Dust	MIT of only dusts	admixture of 1.0 vol% isopropanol on the MIT of dusts	admixture of 2.0 vol% methane on the MIT of dusts	admixture of 2.0 vol% methane and 1.0 vol% isopropanol on the MIT of dusts	admixture of 1.0 vol% propane on the MIT of dusts	admixture of 1.0 vol% propane and 1.0 vol% isopropanol on the MIT of dusts	admixture of 3.0 vol% hydrogen on the MIT of dusts	admixture of 3.0 vol% hydrogen and 1.0 vol% isopropanol on the MIT of dusts
HDPE	340	340	340	340	340	340	340	340
Lycopodium	410	410	410	410	410	410	410	410
Starch	370	370	370	370	370	370	370	370
Toner	460	445	460	445	460	435	460	440

Dust	MIT of only dusts	admixture of 1.8 vol% ethanol on the MIT of dusts	admixture of 2.0 vol% methane on the MIT of dusts	admixture of 2.0 vol% methane and 1.8 vol% ethanol on the MIT of dusts	admixture of 1.0 vol% propane on the MIT of dusts	admixture of 1.0 vol% propane and 1.8 vol% ethanol on the MIT of dusts	admixture of 3.0 vol% hydrogen on the MIT of dusts	admixture of 3.0 vol% hydrogen and 1.8 vol% ethanol on the MIT of dusts
HDPE	340	340	340	340	340	340	340	340
Lycopodium	410	385	410	385	410	375	410	410
Starch	370	370	370	370	370	370	370	380
Toner	460	450	460	440	460	430	460	435

Dusts	MIT of only dusts	admixture of 0.6 vol% toluene on the MIT of dusts	admixture of 2.0 vol% methane on the MIT of dusts	admixture of 2.0 vol% methane and 0.6 vol% toluene on the MIT of dusts	admixture of 1.0 vol% propane on the MIT of dusts	admixture of 1.0 vol% propane and 0.6 vol% toluene on the MIT of dusts	admixture of 3.0 vol% hydrogen on the MIT of dusts	admixture of 3.0 vol% hydrogen and 0.6 vol% toluene on the MIT of dusts
HDPE	340	340	340	340	340	340	340	340
Lycopodium	410	410	410	410	410	410	410	410
Starch	370	370	370	370	370	370	370	370
Toner	460	460	460	460	460	450	460	460

Furthermore, Table 6.17 provides the results of adding non-explosible concentrations of dusts and solvents on the MIT of gases. Here, a non-explosible concentration of dust and solvent mixtures was added to the gas to check if explosion could be obtained at the non-ignition

temperature of the gas. A similar explosion behavior as explained above was also noticed. Ignition could be obtained at the temperature where both dust and solvent mixtures did not ignite. For example, the MIT of methane decreased from 600 °C to 585 °C when a non-explosible concentration of starch (82 g/m³) was added. This temperature further decreased to 490 °C by adding 1.8 vol% ethanol.

Table 6.17: Effect of admixture of dusts and gases on the MIT of solvents, (all in °C).

Solvents	MIT of only gases	admixture of 2.0 vol% methane on the MIT of gases	admixture of 87 g/m ³ HDPE on the MIT of solvents	admixture of 87 g/m ³ HDPE and 2.0 vol% methane on the MIT solvents	admixture of 84 g/m ³ lycopodium on the MIT of solvents	admixture of 84 g/m ³ lycopodium and 2.0 vol% methane on the MIT of solvents	admixture of 82 g/m ³ starch on the MIT of solvents	admixture of 82 g/m ³ starch and 2.0 vol% methane on the MIT of solvents	admixture of 30 g/m ³ toner on the MIT of solvents	admixture of 30 g/m ³ toner and 2.0 vol% methane on the MIT of solvents
Hexane	240	240	240	240	240	240	240	240	240	240
Isopropanol	440	440	420	420	425	425	420	420	440	440
Ethanol	395	395	395	395	395	395	385	385	395	395
Toluene	520	520	495	520	475	475	505	505	520	520

Solvents	MIT of only gases	admixture of 1.0 vol% propane on the MIT of gases	admixture of 87 g/m ³ HDPE on the MIT of solvents	admixture of 87 g/m ³ HDPE and 1.0 vol% propane on the MIT solvents	admixture of 84 g/m ³ lycopodium on the MIT of solvents	admixture of 84 g/m ³ lycopodium and 1.0 vol% propane on the MIT of solvents	admixture of 82 g/m ³ starch on the MIT of solvents	admixture of 82 g/m ³ starch and 1.0 vol% propane on the MIT of solvents	admixture of 30 g/m ³ toner on the MIT of solvents	admixture of 30 g/m ³ toner and 1.0 vol% propane on the MIT of solvents
Hexane	240	240	240	240	240	240	240	240	240	240
Isopropanol	440	440	420	415	425	425	420	420	440	440
Ethanol	395	395	395	395	395	395	385	385	395	395
Toluene	520	520	495	495	475	465	505	505	520	520

Solvents	MIT of only gases	admixture of 3.0 vol% hydrogen on the MIT of gases	admixture of 87 g/m ³ HDPE on the MIT of solvents	admixture of 87 g/m ³ HDPE and 3.0 vol% hydrogen on the MIT solvents	admixture of 84 g/m ³ lycopodium on the MIT of solvents	admixture of 84 g/m ³ lycopodium and 3.0 vol% hydrogen on the MIT of solvents	admixture of 82 g/m ³ starch on the MIT of solvents	admixture of 82 g/m ³ starch and 3.0 vol% hydrogen on the MIT of solvents	admixture of 30 g/m ³ toner on the MIT of solvents	admixture of 30 g/m ³ toner and 3.0 vol% hydrogen on the MIT of solvents
Hexane	240	240	240	240	240	240	240	240	240	240
Isopropanol	440	440	425	400	425	430	420	415	440	430
Ethanol	395	395	395	410	395	410	385	390	395	410
Toluene	520	520	495	495	475	475	505	505	520	520

Finally, Table 6.18 displays explains the results of adding non-explosible concentrations of dusts and gases on the MIT of solvents. In this case, non-explosible concentrations of dust and gas mixtures were added to the solvent to check if explosion could be obtained at the range of temperature below the MIT of the solvent. The same explosion behavior was also observed here and ignitions were obtained at a temperature where both dusts and gas mixtures could not ignite.

For example, the MIT of isopropanol was decreased from 440 °C to 420 °C when a non-explosible concentration of starch (82 g/m³) was added. This temperature further decreased to 410 °C when 2 vol% of methane, which also does not itself ignites at this specific temperature, was added to the mixture.

Table 6.18: Effect of admixture of dusts and solvents on the MIT of gases, (all in °C).

Gases	MIT of only gases	admixture of 0.8 vol% hexane on the MIT of gases	admixture of 87 g/m ³ HDPE on the MIT of gases	admixture of 87 g/m ³ HDPE and 0.8 vol% hexane on the MIT of gases	admixture of 84 g/m ³ lycopodium on the MIT of gases	admixture of 84 g/m ³ lycopodium and 0.8 vol% hexane on the MIT of gases	admixture of 82 g/m ³ starch on the MIT of gases	admixture of 82 g/m ³ starch and 0.8 vol% hexane on the MIT of gases	admixture of 30 g/m ³ toner on the MIT of gases	admixture of 30 g/m ³ toner and 0.8 vol% hexane on the MIT of gases
Methane	600	465	570	470	575	480	585	470	530	480
Propane	500	470	490	470	500	480	485	470	490	480
Hydrogen	540	530	510	490	515	500	505	495	540	515
Gases	MIT of only gases	admixture of 1.0 vol% isopropanol on the MIT of gases	admixture of 87 g/m ³ HDPE on the MIT of gases	admixture of 87 g/m ³ HDPE and 1.0 vol% isopropanol on the MIT of gases	admixture of 84 g/m ³ lycopodium on the MIT of gases	admixture of 84 g/m ³ lycopodium and 1.0 vol% isopropanol on the MIT of gases	admixture of 82 g/m ³ starch on the MIT of gases	admixture of 82 g/m ³ starch and 1.0 vol% isopropanol on the MIT of gases	admixture of 30 g/m ³ toner on the MIT of gases	admixture of 30 g/m ³ toner and 1.0 vol% isopropanol on the MIT of gases
Methane	600	515	570	500	575	515	585	530	530	450
Propane	500	490	490	470	500	480	485	480	490	490
Hydrogen	540	530	510	500	515	515	505	495	540	520
Gases	MIT of only gases	admixture of 1.8 vol% ethanol on the MIT of gases	admixture of 87 g/m ³ HDPE on the MIT of gases	admixture of 87 g/m ³ HDPE and 1.8 vol% ethanol on the MIT of gases	admixture of 84 g/m ³ lycopodium on the MIT of gases	admixture of 84 g/m ³ lycopodium and 1.8 vol% ethanol on the MIT of gases	admixture of 82 g/m ³ starch on the MIT of gases	admixture of 82 g/m ³ starch and 1.8 vol% ethanol on the MIT of gases	admixture of 30 g/m ³ toner on the MIT of gases	admixture of 30 g/m ³ toner and 1.8 vol% ethanol on the MIT of gases
Methane	600	510	570	470	575	490	585	490	590	510
Propane	500	445	490	445	500	440	485	430	490	445
Hydrogen	540	525	510	495	515	505	505	495	540	515
Gases	MIT of only gases	admixture of 0.6 vol% toluene on the MIT of gases	admixture of 87 g/m ³ HDPE on the MIT of gases	admixture of 87 g/m ³ HDPE and 0.6 vol% toluene on the MIT of gases	admixture of 84 g/m ³ lycopodium on the MIT of gases	admixture of 84 g/m ³ lycopodium and 0.6 vol% toluene on the MIT of gases	admixture of 82 g/m ³ starch on the MIT of gases	admixture of 82 g/m ³ starch and 0.6 vol% toluene on the MIT of gases	admixture of 30 g/m ³ toner on the MIT of gases	admixture of 30 g/m ³ toner and 0.6 vol% toluene on the MIT of gases
Methane	600	510	570	480	575	520	585	540	590	550
Propane	500	465	490	465	500	465	485	445	490	455
Hydrogen	540	540	510	510	515	515	505	505	540	540

It can be generalized from the experimental results that the minimum ignition temperature of hybrid mixtures is much lower than that of individual substances. This could be explained based on the ignition mechanism of both dust and hybrid mixtures with respect to the test in the GG

oven (the general mechanism of dust explosion has already been discussed in section 2.4.1). With respect to organic dusts, as the dust is introduced in the furnace, some transitions occur before the actual ignition happens. These changes are explained in the form of three main stages. In the first stage, which is the pre-heating stage, the moisture content in the dust is vaporized. Usually, dust with higher moisture content requires a higher ignition temperature because evaporation and heating of water represents an inert heat sink [22, 60]. The next stage is the pyrolysis and devolatilization step. This step is considered as the first step in the combustion process. During this stage, the organic particle is heated, producing volatile matters or combustible gases. The combustible gases are then mixed with air in the space between the particles. The final stage is the oxidation stage of pyrolysis gases, where the gas phase combustion of premixed volatile-air takes place or in other words, the oxidation of a homogenous gas takes place.

In the case of hybrid mixture explosions, where flammable gas or vaporizing solvent is added to the dust, it can be envisaged that this addition could promote the combustion. **Dufaud et al. [13]** analysed the minimum explosible concentration of dust for combustible gas-dust hybrid mixtures and stressed the impact of the introduction of highly flammable substances on the explosivity of dust clouds. They observed that the dust explosivity is strongly promoted by the addition of combustible gas. The authors further highlighted that this effect is more significant below 50 % of dust to gas ratio. Therefore, it can be deduced that dust still plays a significant role in the combustion kinetics down to this limit; for greater amounts of gases, the specific behavior of the combustible gases is clearly predominant. Such addition, as low as 1 vol. % induces changes in the rate-limiting step of the combustion reaction from devolatilization to homogeneous gas phase reaction and implies a drastic decrease in the MIT for hybrid mixtures.

Furthermore, the particle size of the dust is also a crucial factor to be considered with regard to the MIT of both dust and hybrid mixtures. This is because, smaller particle size results in higher the devolatilization rate. Moreover, modification of the rate-limiting step of the combustion reaction is also dependant on the particle size of the dust materials. Size reduction could lead to a change from a diffusion controlled regime for large size particles to kinetically controlled for small sized ones.

6.4.4 Models to predict the minimum ignition temperature of dusts

Three mathematical models to estimate the MIT of dusts were computed and compared with the experimental results. The choice of the models was based on the availability of the input data, applicability and the assumption with which the models were developed with regards to this study. Detailed discussion of these models could be referred to section 3.5.1.

Table 6.19 lists the parameters used in the dust model calculations. The mean particle size (D) and the heat of combustion (H) were determined using a Particle Analyser Camsizer XT and a bomb calorimeter, respectively. T_s represents the ignition temperature of the particle, D is the mean particle size and C_d is the concentration of dusts in the mixture.

Table 6.19: Parameters used in model calculation.

Gases	Methane	Propane	Hydrogen	toluene	Ethanol	Isopropanol
C_g (g/m ³)	13.36	18.86	2.70	25.20	34.9	24.5
Dusts	Starch	Lycopodium	Wood	Toner	CN4	
E (J/mol)	3.4*10 ⁵	3.74*10 ⁴	1.15*10 ⁵	1.10*10 ⁵	9.10*10 ⁴	
H (J/g)	15302	28447	16446	35792	26630	
T_s (K)	643	813	730	793	1003	
D (m)	2.95*10 ⁻⁵	3.16*10 ⁻⁵	3.07*10 ⁻⁴	1.34*10 ⁻⁵	7.56*10 ⁻⁵	
C_d (g/m ³)	82.29	84.91	124.57	30.40	122.85	

The activation energy for the lumped reaction of the solid particles was calculated from the thermogravimetric signal. Basic principle behind this is the mass change per unit time for a first order reaction. According to eq. (6.4.5), the activation energy E/R can be calculated [190].

$$\ln \left(-\frac{dw}{dt} \cdot \frac{1}{w} \right) = \ln A_c - \frac{E}{RT} \quad (6.4.5)$$

Figure 6.58 shows the comparison between the three dust models and the experimental results while Table 6.20 lists the summarized results with their deviations. As shown in the Figure 6.4.7, the "X" sign indicates the experimental results while the triangles, squares and circles indicate the models according Krishna, Mitsui and Cassel respectively. An error bar based on the experimental uncertainties of 6.2% as discussed in Appendix C.3 is plotted on the experimental results.

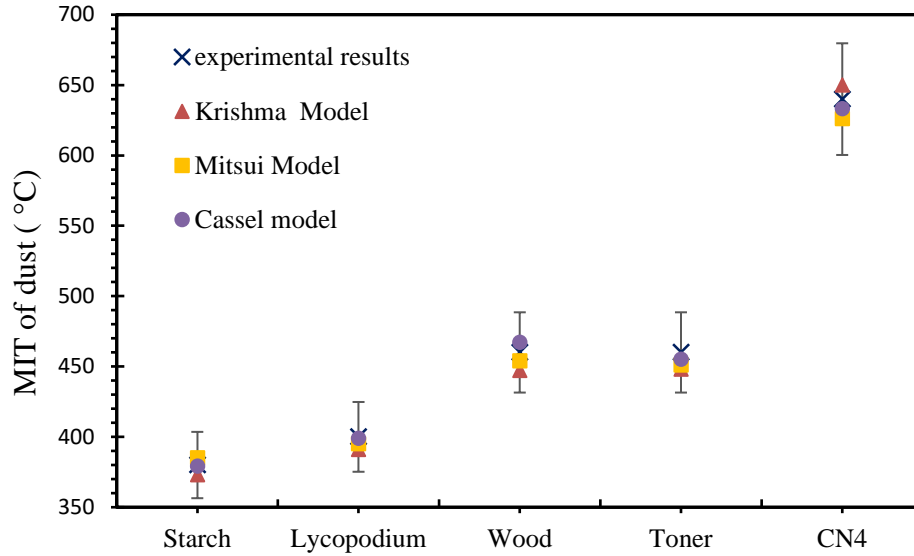


Figure 6.58: Comparing the MIT of the various dust models with the experimental results.

It can be seen from Figure 6.58 that both the Cassel and Mitsui model give a better prediction of the MIT of dust samples with deviations less than 10 K with the exception of CN4, for which the Mitsui model gives a deviation of 14 K as shown in Table 6.20. It could also be noticed that the Krishma model also shows good agreement with the experimental results with deviations between 10 K and 28 K. The deviations obtained from the comparison between these three models and the experimental results are within the experimental uncertainties.

Table 6.20: Comparison between the MIT of the various dust models and the experimental results.

Dust	Experimental results	Cassel (°C)	ΔT (K)	Krishma (°C)	ΔT (K)	Mitsui (°C)	ΔT (K)
Starch	380	379	-1	368	-12	378	-2
Lycopodium	400	399	-1	390	-10	396	-4
wood	460	457	-3	447	-13	454	-6
Toner	460	456	-4	440	-20	451	-9
CN4	640	634	-6	622	-28	626	-14

6.4.4.1 Proposed model to estimate the minimum ignition temperature of hybrid mixtures

This model is based on the **Jaeckel model [191]** to predict the minimum and maximum explosible concentrations for dust clouds. A one-dimensional heat transfer from a plane flame front to the adjacent unburned layer of the dust cloud was assumed. According to Jaeckel, the minimum explosible concentration (MEC) is the minimum amount of dust per unit volume of the dust cloud,

which by complete combustion liberates enough energy to heat the next unit volume of dust cloud to the ignition temperature. Jaeckel formulated the condition of self-sustained flame propagation through the dust cloud of concentration C_d , $C_{d, \min} < C_d < C_{d, \max}$ at constant volume as:

$$Q_G = C_d H_d \quad (6.4.6)$$

$$Q_L = L + (T_{i,d} - T_0)(C_d c_d + \rho_{air} c_{air}) \quad (6.4.7)$$

According to the Jaeckel Model:

$$C_d H_d \geq L + (T_{i,d} - T_0)(C_d c_d + \rho_{air} c_{air}) \quad (6.4.8)$$

When $C_d = MEC$, by neglecting the heat loss by radiation and equating the two sides, after rearranging, the minimum ignition temperature can be derived:

$$\rho_d H_d \cdot MEC = (T_{i,d} - T_0)(\rho_d c_d \cdot MEC + \rho_{air} c_{air}) \quad (6.4.9)$$

Rearranging eq. (6.4.9) one obtains:

$$T_{i,d} = T_0 + \frac{MEC \cdot H_d}{MEC \cdot c_d + \rho_{air} c_{air}} \quad (6.4.10)$$

With respect to gases, eq. (6.4.9) could be rewritten to eq. (6.4.11), $C_g = LEL$

$$\rho_g H_g \cdot LEL = (T_{i,g} - T_0)(\rho_g c_g \cdot LEL + \rho_{air} c_{air}) \quad (6.4.11)$$

Rearranging eq. (6.4.11) one obtains:

$$T_{i,g} = T_0 + \frac{\rho_g H_g \cdot LEL}{\rho_g c_g \cdot LEL + \rho_{air} c_{air}} \quad (6.4.12)$$

The minimum ignition temperature of hybrid mixture $T_{i, \text{hybrid}}$ presented in eq. (6.4.15) can be deduced according to eq. (6.4.9, 6.4.11 and 6.4.12). See section Appendix 8.4: D-2 for detail derivation.

$$T_{i, \text{hybrid}} = T_{i,g} \left(\frac{T_{i,d}}{T_{i,g}} \right)^{\frac{C_g}{C_d}} \quad (6.4.15)$$

The ignition temperature of a hybrid mixture can then be calculated from eq. (6.4.15):

Where T_{ig} is the MIT of gas [$^{\circ}C$], T_{id} is the MIT of dust [$^{\circ}C$], C_g is the gas concentration in the mixture [g/m^3], C_d is the dust concentration in the mixture [g/m^3], ρ_g is the density of gas [g/m^3], ρ_d is the density of dust [g/m^3], c_g is the heat capacity of gas [$kJ/kg.K$], c_d is the heat capacity of dust [$kJ/kg.K$], c_{air} is the heat capacity of air [$kJ/kg.K$], L is the heat loss by radiation [KJ], H_g is the heat of combustion of gas [kJ/mol], H_d is the heat of combustion of dust [kJ/mol], LEL is the lower explosion limit of gas [$vol\%$] and MEC is the minimum explosible concentration of dust [g/m^3].

$T_{i.g}$, $T_{i.d}$, C_d and C_g could be obtained from the experimental results of single dust and gas test as presented in Tables 6.20 and 6.21.

For thirty different combinations of hybrid mixtures of dust and gas both experimental results and the comparison with the model are presented.

Figures 6.59 to 6.64 show the MIT test results of dust and gas mixtures in comparison with the model. The 'X' symbolizes the MIT of hybrid mixtures, the 'square' symbolizes the MIT of pure dust, 'triangle' symbolizes the results from the model and the 'circle' symbolizes the MIT of pure gas. Moreover, Table 6.19 provides the various concentrations of dusts and gases used in the experiment as well as the model. In order to check accuracy of the model, an error bar based on the experimental uncertainties of 6.3% as discussed in Appendix C.3 for hybrid mixture test in the GG- furnace was plotted on the experimental results.

Figure 6.59 shows the comparison between the model and the experimental results for hybrid mixtures of methane and dust samples. The model gives a good prediction of the MIT of hybrid mixtures and the deviations obtained are within the error margin.

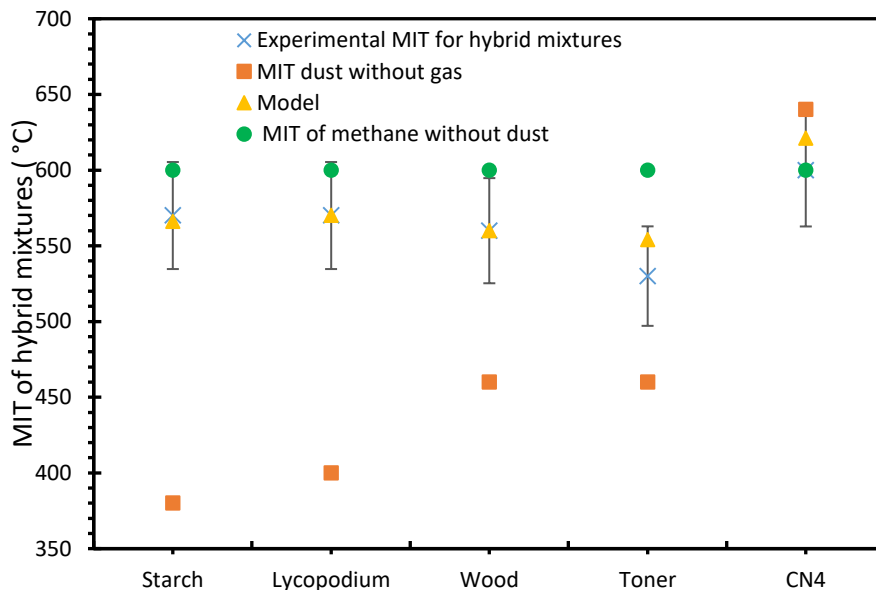


Figure 6.59: A comparison between the model and the experimental result for hybrid mixtures of various dusts and methane gas.

In the case of propane, Figure 6.60 shows the comparison between the model and the experimental results for hybrid mixtures with various dusts. It could also be seen that with the exception of CN4, all the other dust samples had an effect on the MIT of propane but with smaller

margins as compared to methane. Moreover, the model also reasonably predicts the MIT of hybrid mixtures of propane and the dusts with an exception of CN4, for which the experimental results deviated from the model with wide margin. This could be as a result of its high ignition temperature compared to the gases.

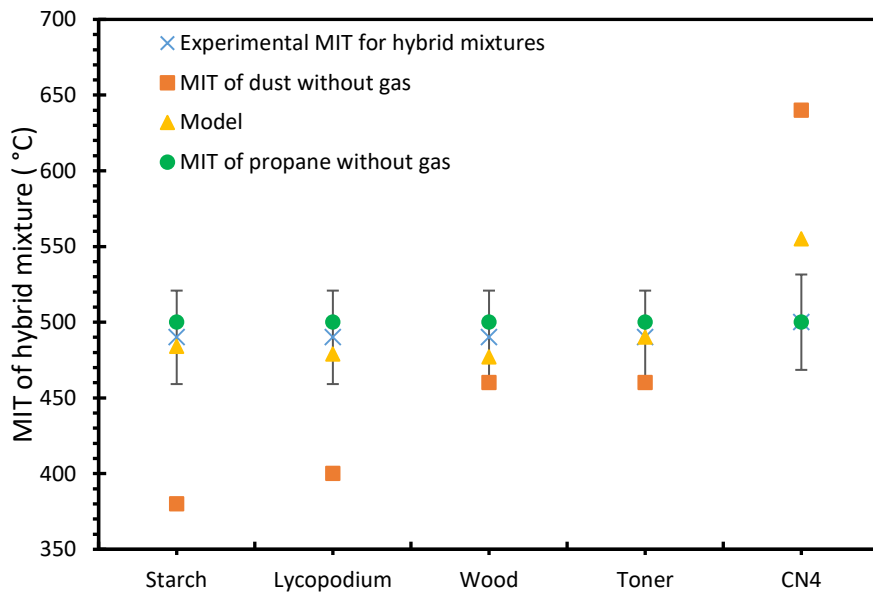


Figure 6.60: A comparison between the model and the experimental result for hybrid mixtures of propane gas and various dusts.

Figure 6.61 shows the results for hybrid mixtures of hydrogen gas and various dusts. It could be seen from the figure that with the exception of CN4 all the other dust materials had an effect on the MIT of hydrogen and the model gives a good prediction of the MIT of hybrid mixtures within the measurement uncertainties.

With regards to the effect of dusts on the MIT of solvent vapors, Figure 6.62 shows the comparison of the model with the experimental results for hybrid mixtures of toluene vapor and the various dust materials. It could be noticed that with the exception of toner, all the other dusts had an effect on the MIT of toluene. For example, the MIT of toluene decreased from 540 °C to 475 °C and 450 °C when a non-explosible concentration of starch and wood dust were respectively added. Again, the model was in agreement with the experimental results for the MIT of hybrid mixtures of toluene and the various dusts.

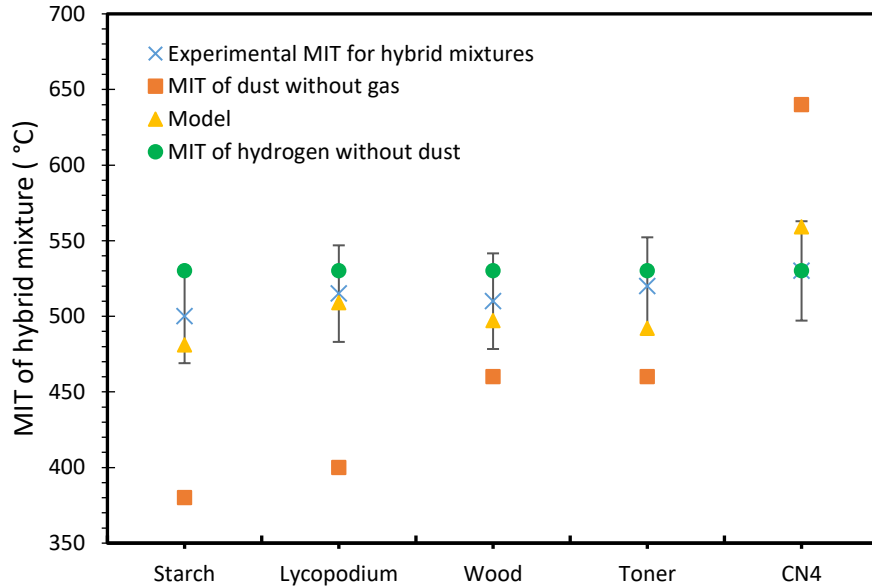


Figure 6.61: A comparison between the model and the experimental results for hybrid mixtures of hydrogen gas and various dusts.

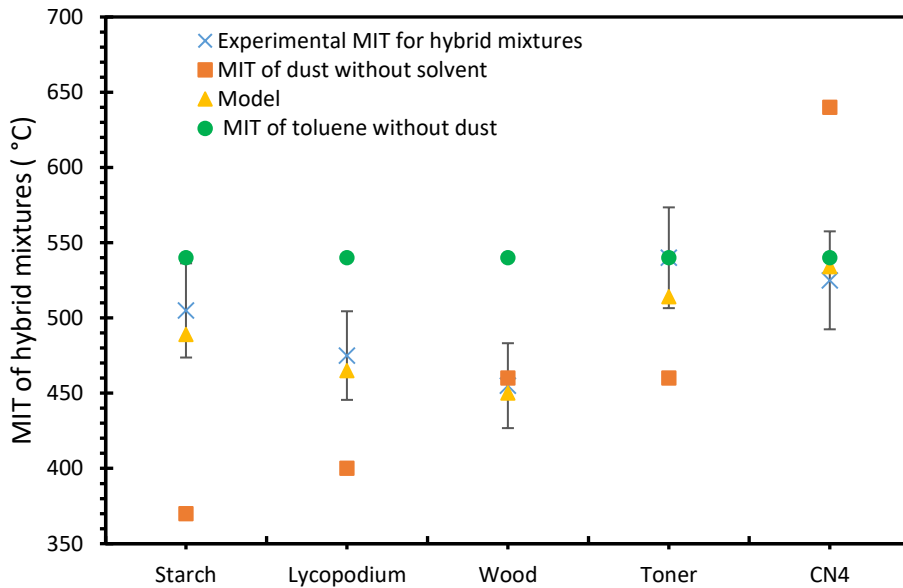


Figure 6.62: A comparison between the model and the experimental results for hybrid mixtures of toluene vapor and various dusts.

Furthermore, the comparison between the model and the experimental results for hybrid mixtures of ethanol vapor and various dusts were also undertaken as shown in Figure 6.63. It could be seen from the figure that out of the five dusts tested only starch and lycopodium had an effect on the MIT of ethanol. With respect to the comparison of the experimental results with the

model, a good agreement was noticed with the exception of CN4, for which a deviation of 24 K was observed. The same behavior was also noticed for isopropanol and the various dusts as shown in Figure 6.64.

Table 6.21 summarizes the values of the MIT according to the model and the experimental results for hybrid mixtures of gases and dusts. The table also displays deviations (ΔT) of all the test results from the model. It should be noted that the parameters used in the mathematical estimation of the model were taken from the results of a single material testing. So at the point where no effect was observed for hybrid mixture test, the model was computed and results were provided.

It was generally noticed that CN4 behaved differently from the other dust. The deviation from the experimental results and the calculate results from the model was very wide. This might due to the high ignition temperature of CN4. Moreover, CN4 reacts heterogeneously, while the other dusts react homogeneously (seen section 2.4.1 for a detail reaction mechanism for both homogeneous and heterogeneous reactions).

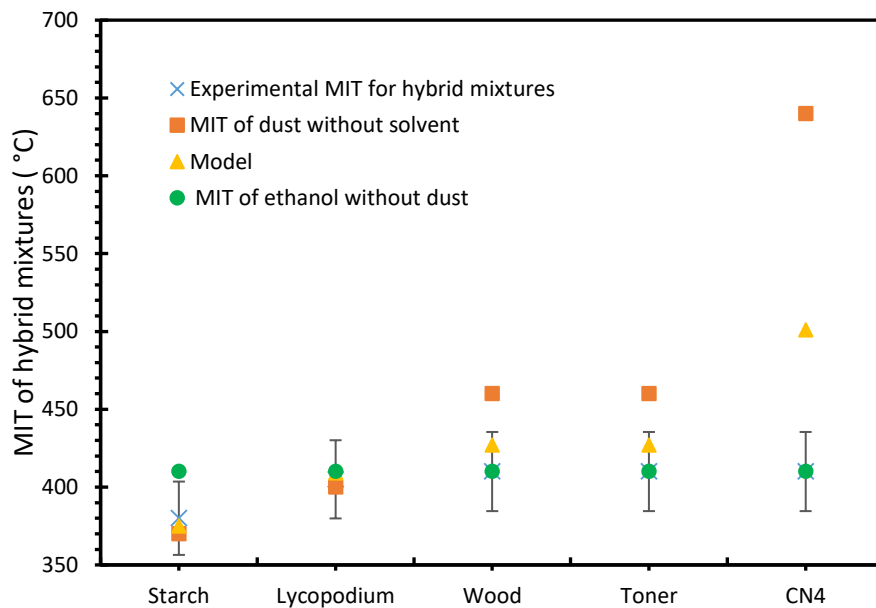


Figure 6.63: A comparison between the model and the experimental results for hybrid mixtures of ethanol vapor and various dusts.

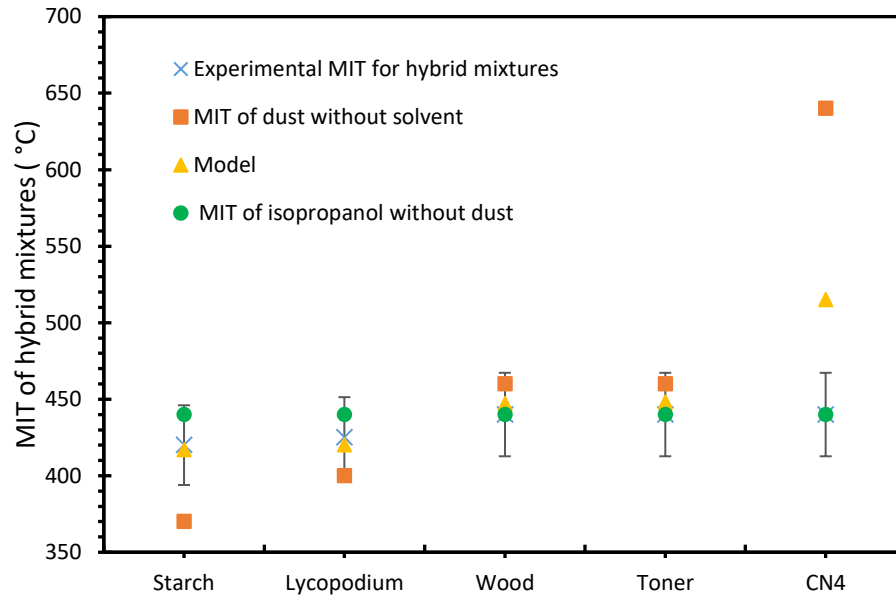


Figure 6.64: A comparison between the model and the experimental results for hybrid mixtures of isopropanol vapor and various dusts.

Table 6.21: Summary for comparison of the models with experimental results for hybrid mixtures of flammable gases and various dusts.

Hybrid mixtures		Experimental Gas MIT (K)	Experimental Hybrid MIT (K)	Model MIT (K)	ΔT (K)
Methane	Starch	873	843	834	-9
	Lycopodium		843	839	-5
	Wood		833	851	+16
	Toner		803	811	+8
	CN4		873	876	+3
Hydrogen	Starch	803	783	793	+14
	Lycopodium		788	798	+8
	Wood		803	801	-2
	Toner		803	796	-5
	CN4		803	805	+2
Propane	Starch	773	763	746	-17
	Lycopodium		773	753	20
	Wood		763	767	+4
	Toner		763	751	-13
	CN4		773	790	+17
Ethanol	Starch	683	653	670	+17
	Lycopodium		678	678	0
	Wood		683	696	+5
	Toner		683	714	+31
	CN4		683	703	+20
Toluene	Starch	813	778	758	-20
	Lycopodium		748	767	+19
	Wood		728	746	+18
	Toner		813	731	+18
	CN4		798	796	-2
Isopropanol	Starch	713	693	694	+1
	Lycopodium		698	701	+3
	Wood		713	716	+3
	Toner		713	729	+16
	CN4		713	737	+24

6.5 Explosion severity

Knowledge of the explosion severity, i.e. maximum overpressure (P_{\max}) and the maximum rate of pressure rise $(dP/dt)_{\max}$ of dusts, gases/vapor, spray and their mixtures is essential for the determination of safety limits of any type of equipment used for storing and processing combustible fuel mixtures. In particular, these values are used by manufacturers to validate the design of protection systems such as: explosion venting, explosion suppression and explosion containment. Numerous studies on the explosion severity of single substances have been done

in the past decades with the aim to prevent explosions as well as to protect equipments [22, 53, 91, 192, 193]. However, one cannot rely on the results from single substances to ensure full protection of equipment or processes, when dealing with mixtures of different states of aggregate (hybrid mixtures). Research on the explosion severity of hybrid mixtures is very limited and is mostly focused on mixtures of dusts and gases. Data on mixtures such as: sprays/vapors with either dusts or gases are not available. Hence, this section presents detailed results on the explosion severity of different combinations of mixtures: spray-gas, spray-dust, gas-dust as well as spray-gas-dust. For the experimental phase of this section, the 20-liter explosion sphere with a 10 J electric spark as an ignition source was employed. All tests were performed under turbulence condition (60 ms as ignition delay time). Mixtures of various combinations of six solvents (ethanol, isopropanol, acetone, toluene, heptane, and hexane), three gases (methane, propane and hydrogen) and two dusts (lycopodium and brown coal) were considered.

6.5.1 Explosion severity of single substances

Figure 6.65 presents the experimental results obtained for explosion over pressure and the rate of pressure rise of solvents as spray. Out of the six solvents, hexane recorded the highest value of both P_{\max} and $(dP/dt)_{\max}$ while ethanol recorded the lowest value. This behavior could be attributed to thermodynamic properties related to the combustion behavior of the solvents, such as: heat capacity, heat of combustion, heat of vaporization and burning velocity as presented in Table 4.3. For example, the heat of combustion relates to the total energy released as a result of complete combustion of the material under standard conditions. The higher the heat of combustion is, the higher the explosion severity will be. This was observed in the results obtained for the solvents. For example, hexane with the highest heat of combustion (-4863 kJ/mol) recorded the highest value of P_{\max} as shown in Figure 6.65 (see Table 4.3 for the heat of combustion values for solvents).

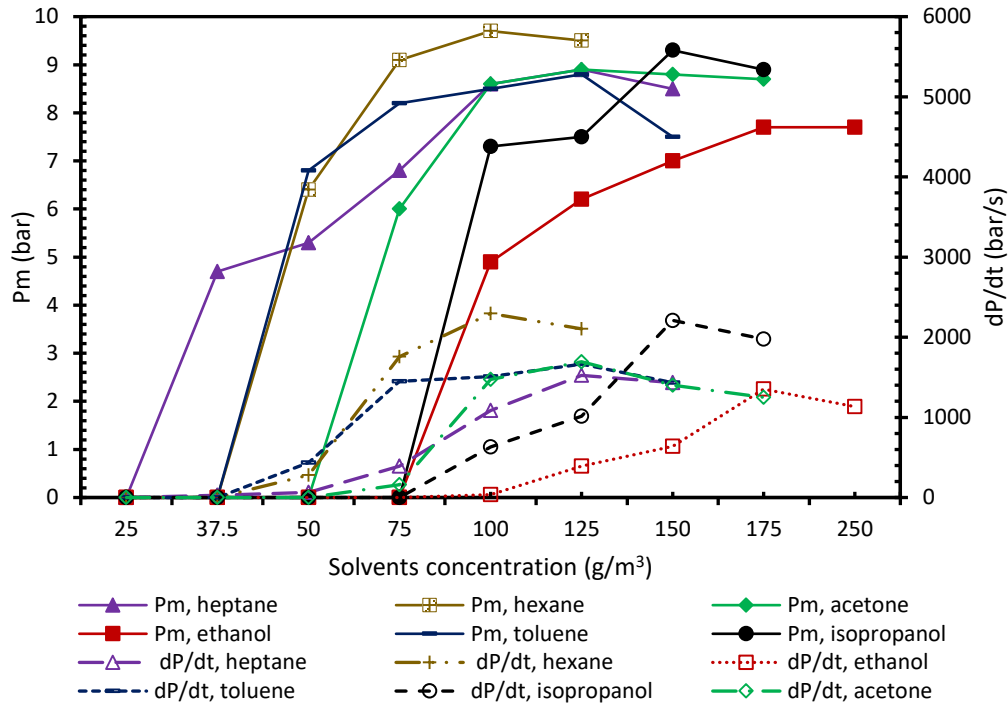


Figure 6.65: Maximum explosion pressure and rate of pressure rise of solvents.

Figure 6.66 presents the results obtained for the maximum explosion pressure and the rate of pressure rise for pure methane and hydrogen. Ignition of methane or hydrogen- air mixtures was performed at the same conditions as the dusts (turbulence condition with ignition delay time of 60 ms), in order to achieve comparable results. P_{max} and $(dP/dt)_{max}$ for methane and hydrogen were obtained at the optimum concentration of 10 vol% and 35 vol% respectively, which is equivalent to the stoichiometric concentrations of both gases. The recorded values of P_{max} and $(dP/dt)_{max}$ are 7.6 barg, 8.4 barg and 1282 bar/s, 4456 bars/s for methane and hydrogen respectively. The severity of hydrogen-air mixture explosion was much higher than methane (three times higher for $(dP/dt)_{max}$). This might be attributed to the reaction mechanism and thermodynamic properties of the gases such as: heat of vaporization, heat of combustion and burning velocity, as presented in Table 4.2. For instance, the burning velocity measures the rate at which reactants move into the flame from a reference point located on the moving frame i.e. how quickly the flame is traveling from a fixed reference point. The higher the burning velocity of the fuel mixture, the faster the flame can travel within a certain time frame and hence, the higher the explosion severity. This can be confirmed by the results obtained for the gases. Hydrogen with burning velocity of 3.06 m/s recorded $(dP/dt)_{max}$ which is almost eight times higher than that of

methane with burning velocity of 0.39 m/s. The deflagration index (KG) for methane was recorded to be 348 bar*m/s which is much higher compared to the recorded value by Bartknecht [194] who obtained 55 bar*m/s. An explanation to this huge difference could be the initial turbulence conditions used in this work while, Bartknecht performed his test in an initially quiescent environment.

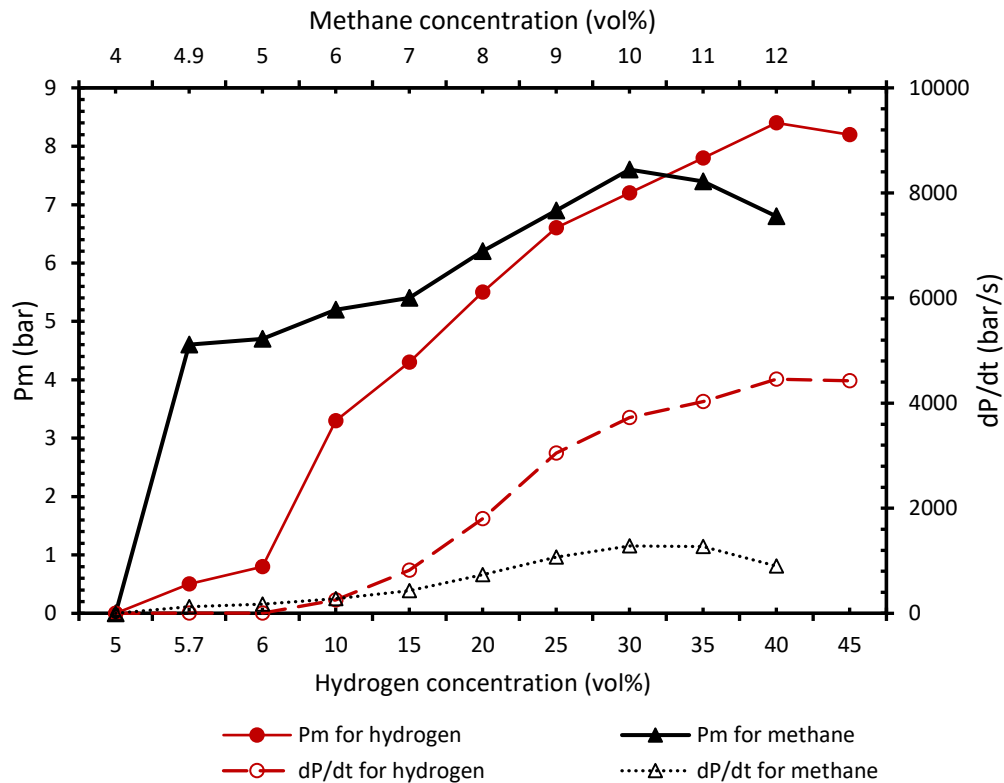


Figure 6.66: Maximum explosion pressure and rate of pressure rise of methane and hydrogen.

Figure 6.67 presents the results obtained for the maximum explosion pressure and rate of pressure rise of lycopodium and brown coal. A similar explosion behavior was observed with regards to the concentration at which the P_{max} and $(dP/dt)_{max}$ was obtained (750 g/m^3). The P_{max} and $(dP/dt)_{max}$ values obtained for lycopodium were 0.2 barg and 16 bar/s higher than those for brown coal. This could be attributed to the material and thermodynamic properties of the dusts such as: particle size distribution, heat of combustion, volatile content and moisture content as shown in Table 4.1. The amount of moisture present in the dust plays a major role for the violence of the explosion. Dusts with greater moisture content is more difficult to ignite and will burn more slowly due to the moisture within the dust, absorbing the heat during evaporation. For example, lycopodium with median particle size = $32 \mu\text{m}$, heat of combustion 28 MJ/Kg of, moisture content

= 0.35 wt% and volatile content = 91.06 wt% recorded higher P_{\max} and $(dP/dt)_{\max}$ than brown coal with median particle size = 37 μm , heat of combustion 21 MJ/Kg, moisture content = 1.56 wt% and volatile content = 55 wt%.

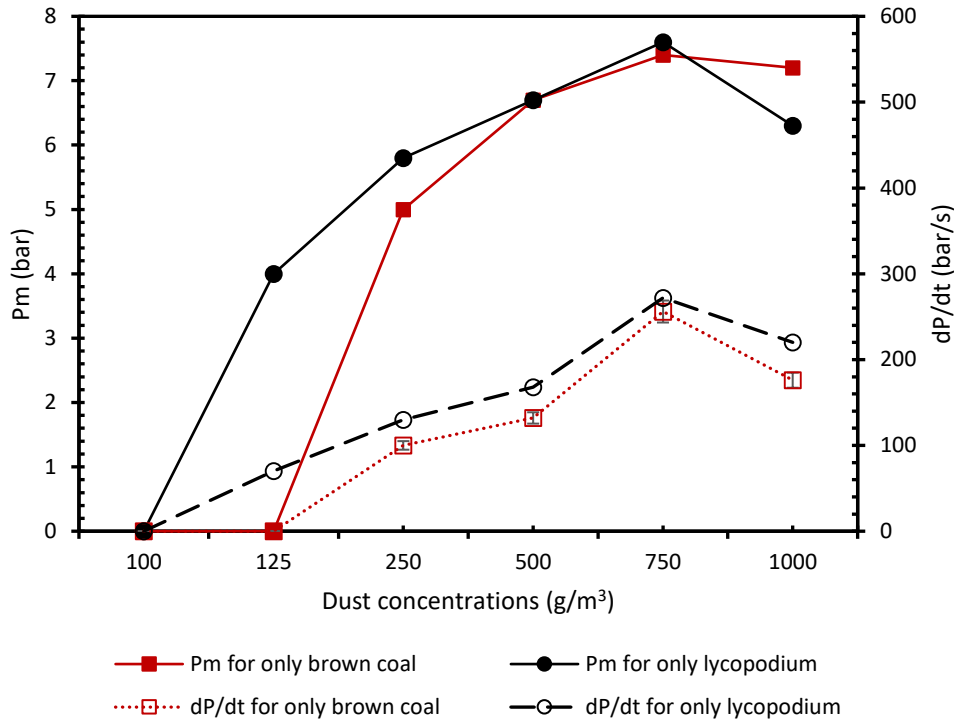


Figure 6.67: Maximum explosion pressure and rate of pressure rise of lycopodium and brown coal.

6.5.2 Explosion severity of two-phase hybrid mixtures

In the next step, both the maximum explosion pressure and the rate of pressure rise of hybrid mixtures were investigated. Three different combinations were considered which include: mixtures of combustible dust with combustible gas and air, mixtures of combustible dust with solvent (spray) and air as well as mixtures of combustible gas with combustible solvent (spray) and air.

With regards to mixtures of combustible dusts with flammable gases and air, different concentrations of gases (methane and hydrogen) below the respective lower explosion limits were added to the dusts (lycopodium and brown coal). This was done to determine the effects of adding non-explorable concentrations of gases on the maximum explosion pressure and the rate of pressure rise of the dusts. Figure 6.68 shows the results obtained for both P_{\max} and $(dP/dt)_{\max}$

for mixtures of lycopodium and methane. It could be seen from the figure that $(dP/dt)_{\max}$ increases as the concentration of methane increases. For example, in the case of lycopodium, $(dP/dt)_{\max}$ was increased from 272 bar/s to 322 bar/s, 369 bar/s, 410 bar/s and 504 bar/s when methane concentrations of 1 vol%, 2 vol%, 3 vol% and 4 vol% were respectively added. However, not much variation was seen for P_{\max} values. The P_{\max} value, generally depends on the heat of combustion of the fuel, however, this (heat of combustion value) does not differ significantly for gases and dusts. This implies that mixing fuel gas and dust (hybrid mixture) will not significantly change the P_{\max} values.

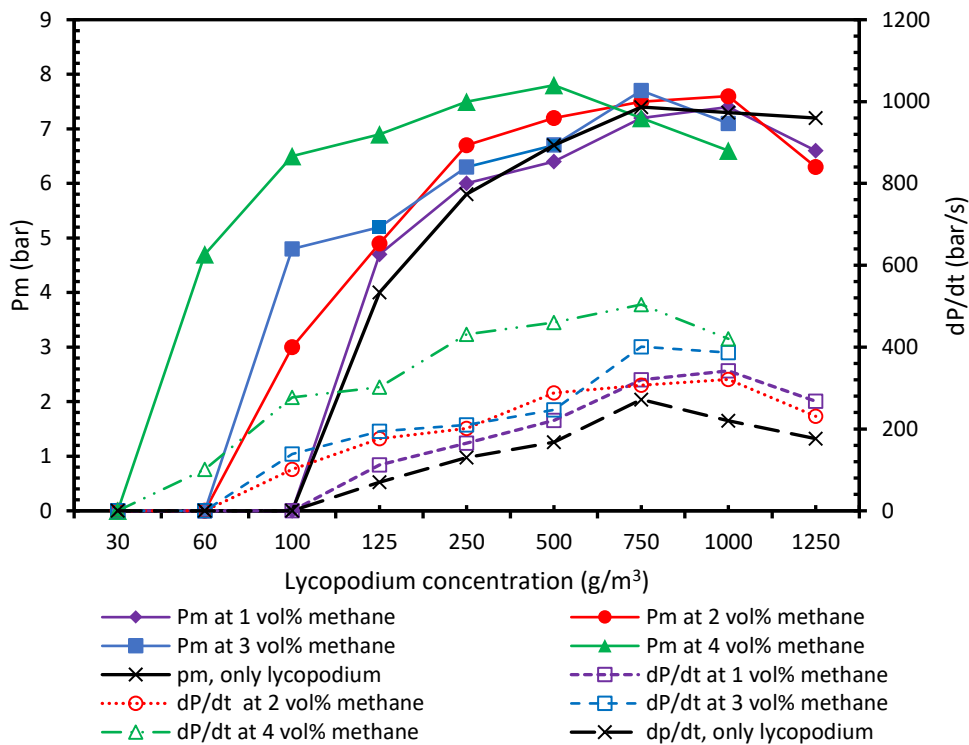


Figure 6.68: Maximum explosion pressure and rate of pressure rise of a mixtures of methane and lycopodium in dependence on the lycopodium concentration.

Using brown coal as dust did not significantly change the explosion behavior as presented in Figure 6.69. The $(dP/dt)_{\max}$ increased as the concentration of the gas increases. Moreover, there were no significant changes in the P_{\max} values. Similar explosion behavior was observed when hydrogen was added to both lycopodium and brown coal as presented in Table 6.22 and Figures B.1 and B.2 at Appendix B. It must also be mentioned that the peak value of P_{\max} and $(dP/dt)_{\max}$ generally shift to the lean dust concentrations with flammable gas admixture.

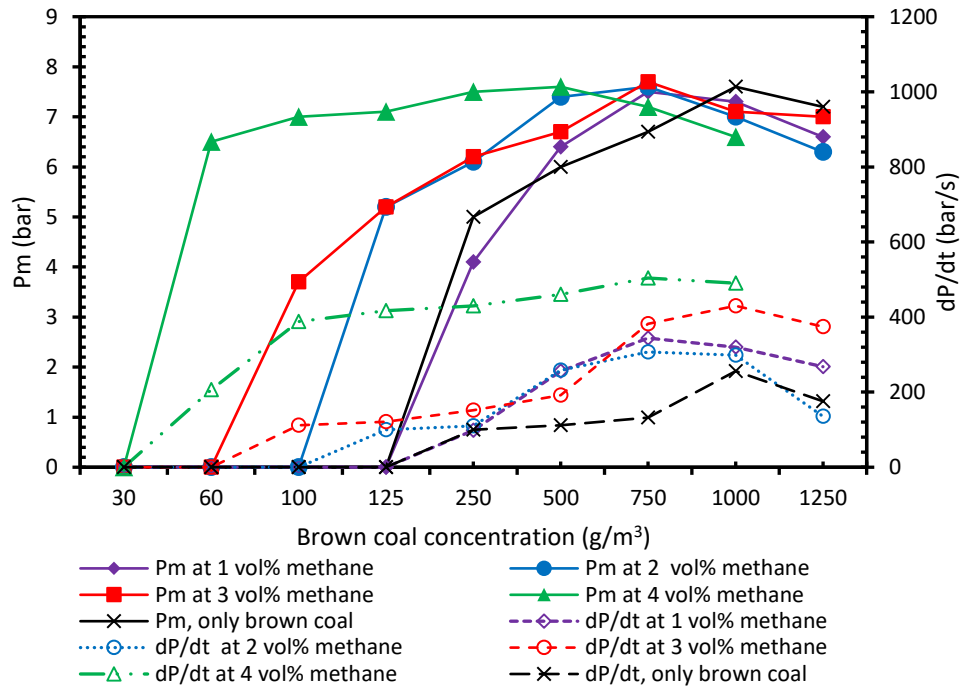


Figure 6.69: Maximum explosion pressure and rate of pressure rise of a mixtures of methane and brown coal in dependence on the brown coal concentration.

Moreover, hybrid mixtures of combustible dusts and flammable solvents (as spray) were also investigated. Different concentrations of solvents below their respective lower explosion limits were added to the dusts. This was done to determine the effect of adding a non-explosible concentration of solvent on the explosion severity of dusts. Figure 6.70 presents experimentally obtained maximum explosion pressure and rate of pressure rise of mixtures of isopropanol and lycopodium, in dependence on the lycopodium concentration. It could be seen from the figure that the values for $(dP/dt)_{max}$ increases as the concentration of the gas increases. For example, the $(dP/dt)_{max}$ value for lycopodium increased from 272 bar/s to 364 bar/s, 404 bar/s and 546 bar/s when isopropanol concentrations of 25 g/m³, 50 g/m³ and 75 g/m³ were respectively added. On the other hand, there was no significant difference in the P_{max} values.

Furthermore, Figure 6.71 presents experimentally determined maximum explosion pressure and rate of pressure rise of a mixture of isopropanol and brown coal and their dependence on the brown coal concentration. It was observed that both $(dP/dt)_{max}$ and P_{max} increased as the concentration of the isopropanol spray increased. A similar explosion behavior was observed when ethanol, acetone, hexane, toluene and heptane were added to both lycopodium and brown as presented in Table 6.22 and Figures B.3 to B.11 at Appendix B.

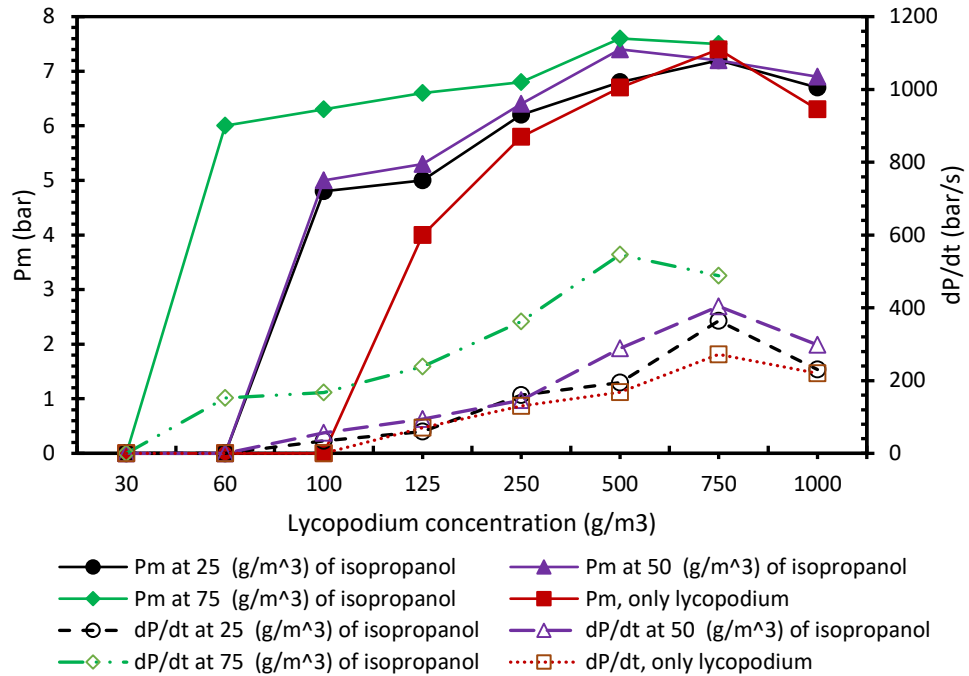


Figure 6.70: Maximum explosion pressure and rate of pressure rise of a mixtures of isopropanol and lycopodium in dependence on the lycopodium concentration.

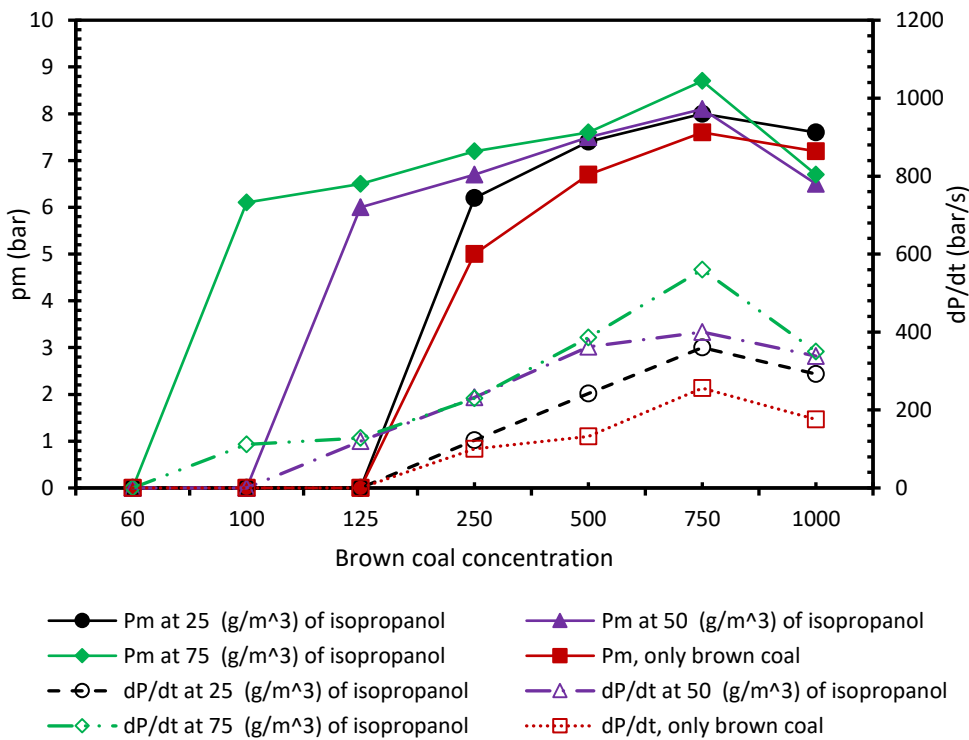


Figure 6.71: Maximum explosion pressure and rate of pressure rise of a mixtures of isopropanol and lycopodium in dependence on the lycopodium concentration.

Table 6.22: Summary of results for the explosion severity of dust- gas as well as dusts-spray mixtures

Only substance	symbols	P _{max} (bar)	(dP/dt) _{max}	Hybrid combinations	P _{max} (bar)	(dP/dt) _{max} (bar/s)	Hybrid combinations	P _{max} (bar)	(dP/dt) _{max} (bar/s)
Lycopodium	LY	7.6	272	LY + 25 g/m ³ ET	6.7	320	BC + 25 g/m ³ ET	8.1	408
Brown coal	BC	7.2	256	LY + 50 g/m ³ ET	7.1	400	BC+50 g/m ³ ET	8.3	438
				LY + 75 g/m ³ ET	7.2	410	BC+75 g/m ³ ET	8.5	608
Ethanol	ET	7.7	1352						
Isopropanol	IS	9.3	2210	LY + 25 g/m ³ IS	7.2	364	BC + 25 g/m ³ IS	8.0	360
Acetone	AC	8.9	1694	LY + 50 g/m ³ IS	7.4	404	BC + 50 g/m ³ IS	8.1	400
Toluene	TL	8.8	1664	LY + 75 g/m ³ IS	7.6	546	BC+ 75 g/m ³ IS	8.7	560
Hexane	HX	9.7	2296						
Heptane	HP	8.9	1524	LY + 12.5g/m ³ AC	6.8	238	BC + 12 g/m ³ AC	8.3	320
				LY + 25 g/m ³ AC	7.3	272	BC + 25 g/m ³ AC	8.1	346
Methane	ME	7.6	1282	LY + 37.5 g/m ³ AC	7.4	300	BC + 37.5 g/m ³ AC	8.1	388
Hydrogen	HY	8.4	4456						
				LY + 12.5 g/m ³ TL	6.9	296	BC + 12.5 g/m ³ TL	7.9	346
				LY + 25 g/m ³ TL	7.0	352	BC + 25 g/m ³ TL	8.2	468
				LY + 37.5 g/m ³ TL	7.3	461	BC + 37.5 g/m ³ TL	8.1	488
				LY + 12.5 g/m ³ HX	7.2	282	BC + 12.5 g/m ³ HX	8.1	400
				LY + 25 g/m ³ HX	7.7	483	BC + 25 g/m ³ HX	8.3	668
				LY + 37.5 g/m ³ HX	7.7	597	BC + 37.5 g/m ³ HX	8.4	696
				LY + 12 g/m ³ HP	7.0	298	BC + 12g/m ³ HP	8.0	366
				LY + 25 g/m ³ HP	7.3	372	BC + 25g/m ³ HP	8.1	504
				LY + 37.5 g/m ³ HP	7.7	400	BC + 37.5g/m ³ HP	8.2	670
				LY + 1 vol % ME	7.0	298	BC + 1 vol % ME	7.5	344
				LY + 2vol % ME	7.4	322	BC + 2 vol % ME	7.6	407
				LY + 3 vol % ME	7.7	369	BC + 3 vol % ME	7.7	430
				LY + 4 vol % ME	7.6	409	BC + 4 vol % ME	7.6	504
				LY + 1 vol % HY	7.1	315	BC + 1 vol % HY	6.8	224
				LY + 2 vol % HY	7.2	322	BC + 2 vol % HY	7.6	396
				LY + 3 vol % HY	7.7	362	BC + 3 vol % HY	7.5	430
				LY + 4 vol % HY	7.3	400	BC + 4 vol % HY	7.5	570

Again, in order to understand the explosion severity of hybrid mixtures, mixtures of gases and solvents (as spray) were tested. For this purpose, concentrations of gases below the respective lower explosion limits were added to the solvents. In all test series, a specific concentration of gas was kept constant and the concentration of the solvent was varied until a point where both the P_{max} and (dP/dt)_{max} were obtained. This was done to determine how the explosion severity might change when a non-explosible concentration of gas is added to the spray. Figure 6.72 presents the maximum explosion pressure and rate of pressure rise of a mixture of methane and isopropanol spray in dependence on the isopropanol concentration. It was observed that the values of P_{max} and (dP/dt)_{max} of isopropanol rather decreased when a non-explosible concentration of methane was added. For example, in the case of isopropanol, the (dP/dt)_{max} value decreased from 2210 bar/s to 1524 bar/s, 1778 bar/s, 1794 bar/s and 1840 bar/s when 1

vol%, 2 vol%, 3 vol% and 4 vol% of methane was added. It should be noted here that these values are higher than that of methane. This result is in accordance with the finding from [14, 18, 104] of which they concluded that the explosion severity of hybrid mixtures lies between the values of individual substances.

Using hydrogen as showed different explosion behavior. There were no significant changes in P_{max} values, with maximum deviation of 0.4 bars as shown in Figure 6.73. It was observed that $(dP/dt)_{max}$ values for hydrogen and isopropanol mixture were all above the recorded value of pure isopropanol (2210 bar/s) and lower than pure hydrogen (4456 bar/s). For example, the $(dP/dt)_{max}$ of isopropanol increased from 2210 bar/s to 2224 bar/s, 2350 bar/s and 2388 bar/s when 1 vol%, 3 vol% and 4 vol% of hydrogen was added. A similar explosion behavior was observed when hydrogen was added to ethanol, acetone, hexane toluene and heptane as presented in Table 6.23 and Figures B.12 to B.21 at Appendix B.

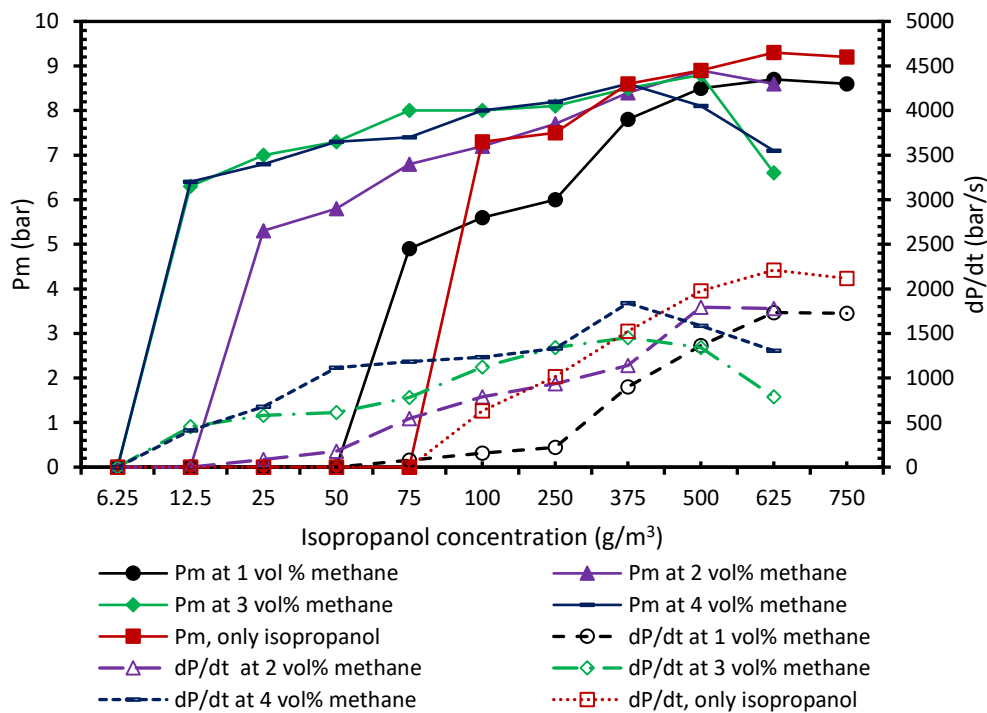


Figure 6.72: Maximum explosion pressure and rate of pressure rise of a mixtures of methane and isopropanol spray in dependence on the isopropanol concentration.

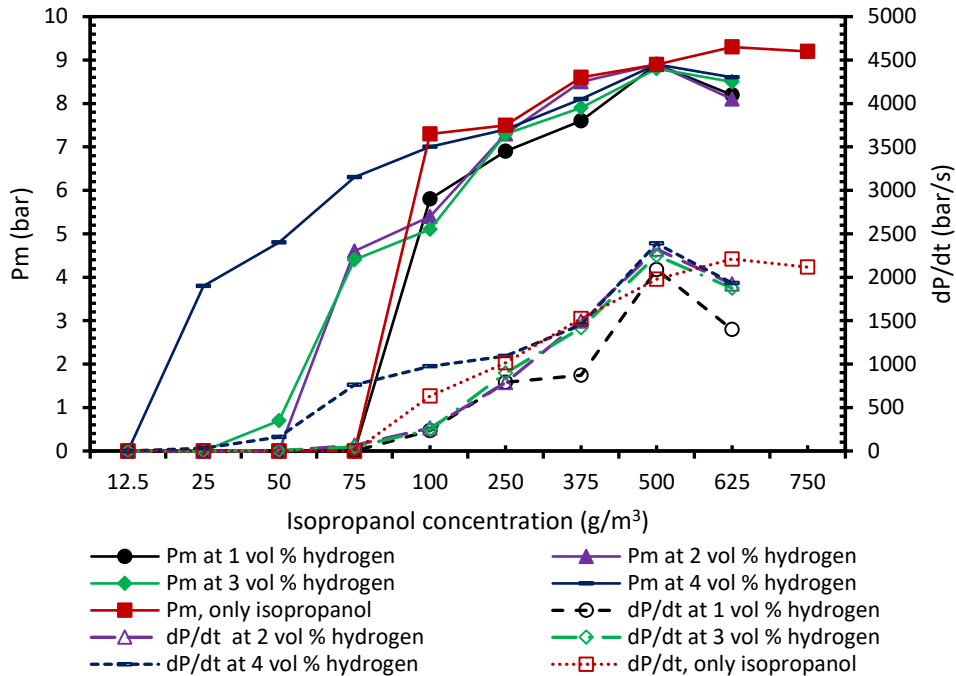


Figure 6.73: Maximum explosion pressure and rate of pressure rise of a mixtures of hydrogen and isopropanol spray in dependence on the isopropanol concentration.

Table 6.23: Summary of results for the explosion severity of gas-spray mixtures.

Only substance	symbols	P_{max} (bar)	$(dP/dt)_{max}$ (bar/s)	Hybrid combinations	P_{max} (bar)	$(dP/dt)_{max}$ (bar/s)	Hybrid combinations	P_{max} (bar)	$(dP/dt)_{max}$ (bar/s)				
Methane Hydrogen	ME	7.6	1282	ET + 1 vol% ME	7.3	1350	ET + 1 vol% HY	8.2	1576				
	HY	8.4	4456	ET + 2 vol% ME	7.6	1490	ET + 2 vol% HY	8.4	1600				
				ET + 3 vol% ME	7.9	1546	ET + 3 vol% HY	8.5	1884				
				ET + 4 vol% ME	8.5	1770	ET + 4 vol% HY	8.9	2178				
Ethanol	ET	7.7	1352										
Isopropanol	IS	9.3	2210	IS + 1 vol% ME	8.7	1734	IS + 1 vol% HY	8.9	2088				
Acetone	AC	8.9	1694	IS + 2 vol% ME	8.9	1794	IS + 2 vol% HY	8.9	2224				
Toluene	TL	8.8	1664	IS + 3 vol% ME	8.8	1840	IS + 3 vol% HY	8.8	2350				
				IS + 4 vol% ME	8.6	1453	IS + 4 vol% HY	8.9	2334				
				TL + 1 vol% ME	8.5	1568	TL + 1 vol% HY	7.4	1252				
				TL + 2 vol% ME	8.5	1426	TL + 2 vol% HY	7.9	1588				
				TL + 3 vol% ME	8.5	1456	TL + 3 vol% HY	8.4	1652				
				TL + 4 vol% ME	8.9	1892	TL + 4 vol% HY	8.4	1708				
Hexane	HX	9.7	2296										
Heptane	HP	8.9	1524	AC + 1 vol% ME	9.0	1760	AC + 1 vol% HY	10.2	1880				
				AC + 2 vol% ME	9.0	1633	AC + 2 vol% HY	9.8	1828				
				AC + 3 vol% ME	8.8	1570	AC + 3 vol% HY	9.2	1810				
				AC + 4 vol% ME	8.9	1868	AC + 4 vol% HY	9.3	1890				
								TL + 1 vol% ME	8.5	1568	TL + 1 vol% HY	7.4	1252
								TL + 2 vol% ME	8.5	1426	TL + 2 vol% HY	7.9	1588
								TL + 3 vol% ME	8.5	1456	TL + 3 vol% HY	8.4	1652
								TL + 4 vol% ME	8.9	1892	TL + 4 vol% HY	8.4	1708
								HX + 1 vol% ME	9.1	1570	HX + 1 vol% HY	9.2	1740
								HX + 2 vol% ME	9.1	1680	HX + 2 vol% HY	9.3	1818
								HX + 3 vol% ME	9.2	1865	HX + 3 vol% HY	9.5	2248
								HX + 4 vol% ME	8.7	1859	HX + 4 vol% HY	9.3	2181
				HX + 1 vol% ME	9.2	1848	HX + 1 vol% HY	9.0	2441				
				HX + 2 vol% ME	8.9	1826	HX + 2 vol% HY	8.9	2512				
				HX + 3 vol% ME	8.6	1622	HX + 3 vol% HY	8.9	2512				
				HX + 4 vol% ME	8.7	1576	HX + 4 vol% HY	9.3	2784				

6.5.3 Explosion severity for three-phase hybrid mixtures

Based on the results obtained from single and two-phase mixtures, both the maximum explosion pressure and the rate of pressure rise of three-phase hybrid mixtures were investigated. During the course of these experiments, the concentrations of gas and solvent were kept constant and the concentration of the dust was varied until a point, where both the P_{\max} and $(dP/dt)_{\max}$ were obtained.

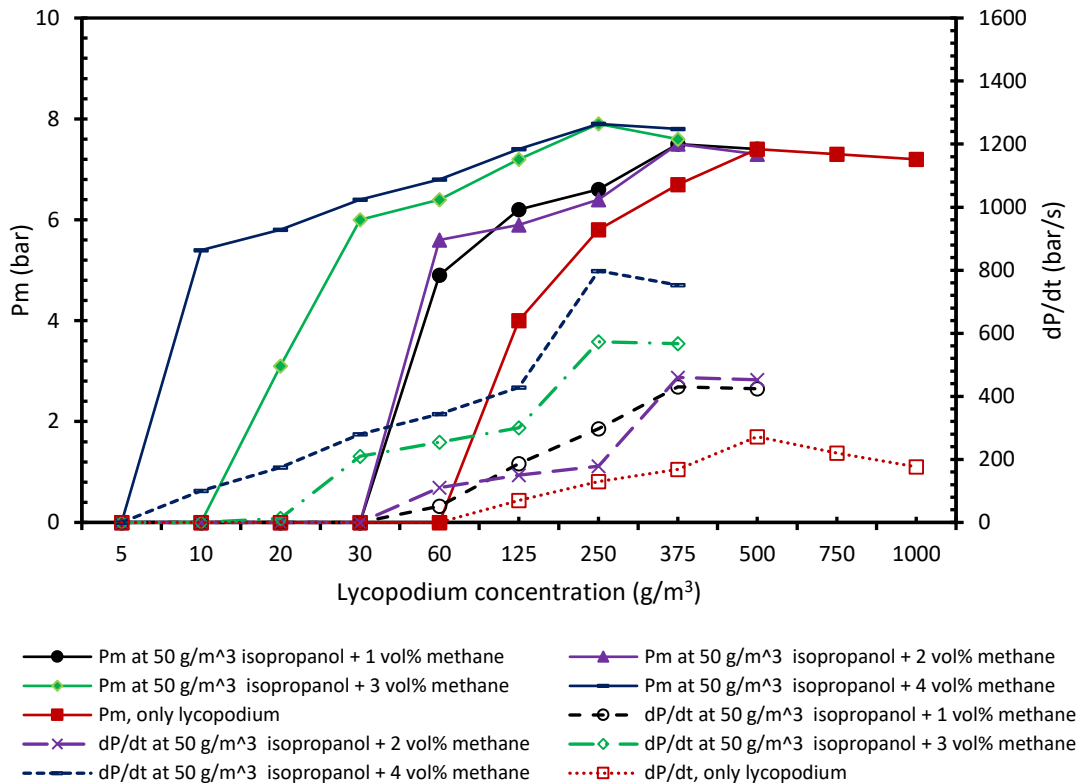


Figure 6.74: Maximum explosion pressure and rate of pressure rise of mixtures of lycopodium, methane and 50 g/m³ of isopropanol spray in dependence on lycopodium concentration.

Figure 6.74 presents experimentally obtained results for the maximum explosion pressure and rate of pressure rise for the mixtures of lycopodium, methane and 50 g/m³ of isopropanol spray and their dependence on lycopodium concentration. It was observed that both P_{\max} and $(dP/dt)_{\max}$ of lycopodium significantly increased when non-explosible concentrations of methane and isopropanol spray were added. For instance, the $(dP/dt)_{\max}$ of lycopodium with a value of 272 bar/s increased to 322 bar/s, 369 bar/s, 410 bar/s and 504 bar/s when methane concentrations of 1 vol%, 2 vol%, 3 vol% and 4 vol% were respectively added. These values of $(dP/dt)_{\max}$ were

further increased to 430 bar/, 460 bar/, 573 bar/ and 798 bar/s when a non-explosible concentration of a third phase, isopropanol (50 g/m³) was added.

Moreover, using brown coal as a dust did not significantly changed the explosion behavior. Figure 6.75 presents the results obtained for the maximum explosion pressure and rate of pressure rise of mixtures of brown coal, methane and 50 g/m³ of isopropanol spray and their dependence on brown coal concentration. Both P_{max} and $(dP/dt)_{max}$ of brown coal increased as the concentration of the gas increased. However, the difference in the P_{max} values was not significantly higher with maximum deviation of 0.7 bars. A similar explosion behavior was observed for other mixtures of dusts, gases and solvents as shown in Table 6.24 and Figures B.22 to B.35 at Appendix B.

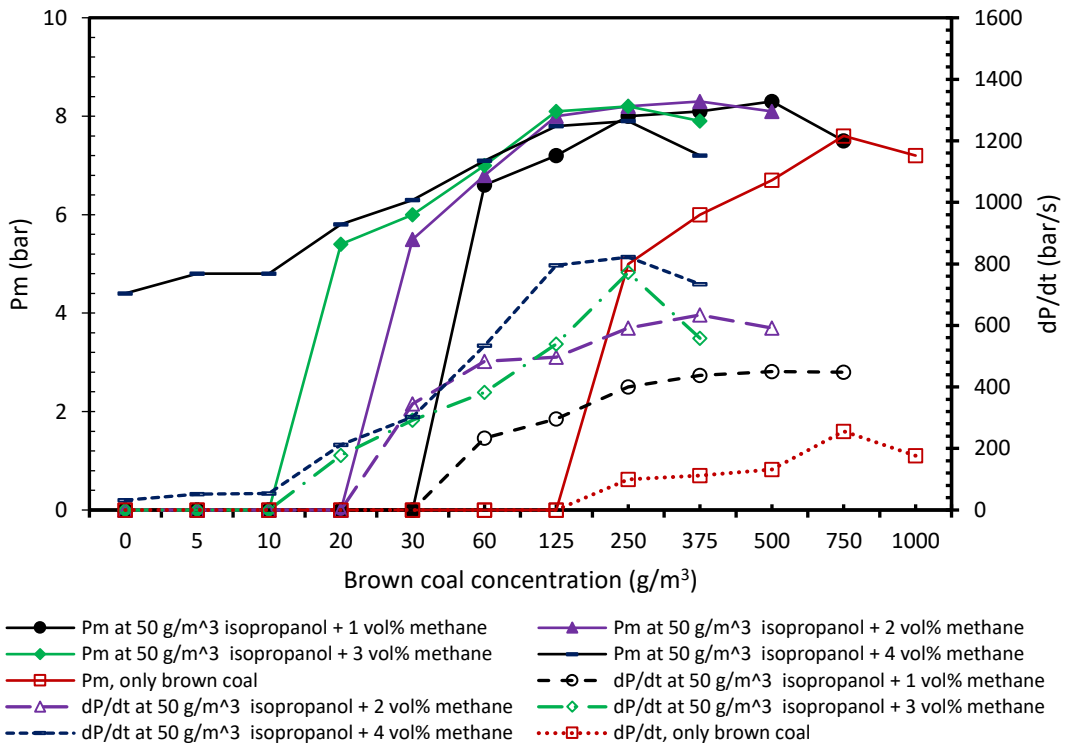


Figure 6.75: Maximum explosion pressure and rate of pressure rise of mixtures of brown coal, methane and 50 g/m³ of isopropanol spray in dependence on the dust concentration.

Table 6.24: Maximum explosion pressure and rate of pressure rise for three-phase hybrid mixtures

Hybrid combination	P _{max} (bar)	(dP/dt) _{max} (bar/s)	Hybrid combinations	P _{max} (bar)	(dP/dt) _{max} (bar/s)	Hybrid combination	P _{max} (bar)	(dP/dt) _{max} (bar/s)	Hybrid combination	P _{max} (bar)	(dP/dt) _{max} (bar/s)
LY + 25 g/m ³ IS + 1 vol% ME	7.6	436	BC + 25 g/m ³ IS +1 vol% ME	8.1	480	LY + 25 g/m ³ IS +1 vol% HY	7.8	476	BC + 25 g/m ³ IS+1 vol% HY	7.6	284
LY + 25 g/m ³ IS + 2 vol% ME	7.6	472	BC + 25 g/m ³ IS + 2 vol% ME	8.2	522	LY + 25 g/m ³ IS +2 vol% HY	7.6	484	BC + 25 g/m ³ IS +2 vol% HY	7.9	404
LY + 25 g/m ³ IS + 3 vol% ME	7.7	474	BC + 25 g/m ³ IS + 3 vol% ME	8.1	542	LY + 25 g/m ³ IS +3 vol% HY	7.7	481	BC + 25 g/m ³ IS +3 vol% HY	8.1	532
LY + 25 g/m ³ IS + 4 vol% ME	7.8	688	BC + 25 g/m ³ IS + 4 vol% ME	8.1	730	LY + 25 g/m ³ IS +4 vol% HY	7.7	578	BC + 25 g/m ³ IS +4 vol% HY	7.9	468
LY + 50 g/m ³ IS + 1 vol% ME	7.4	424	BC + 50 g/m ³ IS + 1 vol% ME	8.3	450	LY + 50 g/m ³ IS +1 vol% HY	7.9	468	BC + 50 g/m ³ IS +1 vol% HY	7.4	452
LY + 50 g/m ³ IS + 2 vol% ME	7.5	460	BC + 50 g/m ³ IS + 2 vol% ME	8.3	634	LY + 50 g/m ³ IS +2 vol% HY	7.8	488	BC + 50 g/m ³ IS +2 vol% HY	7.0	520
LY + 50 g/m ³ IS + 3 vol% ME	7.9	573	BC + 50 g/m ³ IS + 3 vol% ME	8.2	772	LY + 50 g/m ³ IS +3 vol% HY	7.7	598	BC + 50 g/m ³ IS +3 vol% HY	8.1	526
LY + 50 g/m ³ IS + 4 vol% ME	7.9	753	BC + 50 g/m ³ IS + 4 vol% ME	7.9	822	LY + 50 g/m ³ IS +4 vol% HY	7.9	558	BC + 50 g/m ³ IS +4 vol% HY	8.3	622
LY + 75 g/m ³ IS + 1 vol% ME	6.0	492	BC + 75 g/m ³ IS +1 vol% ME	8.2	578	LY + 75 g/m ³ IS +1 vol% HY	7.9	588	BC + 75 g/m ³ IS +1 vol% HY	8.2	570
LY + 75 g/m ³ IS + 2 vol% ME	7.0	500	BC + 75 g/m ³ IS + 2 vol% ME	8.2	647	LY + 75 g/m ³ IS +2 vol% HY	7.7	562	BC + 75 g/m ³ IS +2 vol% HY	8.1	682
LY + 75 g/m ³ IS + 3 vol% ME	7.6	628	BC + 75 g/m ³ IS + 3 vol% ME	8.4	797	LY + 75 g/m ³ IS +3 vol% HY	7.7	623	BC + 75 g/m ³ IS +3 vol% HY	8.0	782
LY + 75 g/m ³ IS+4 vol% ME	8.4	1444	BC + 75 g/m ³ IS + 4 vol% ME	8.5	852	LY + 75 g/m ³ IS +4 vol% HY	7.7	602	BC + 75 g/m ³ IS +4 vol% HY	8.2	838
LY + 25 g/m ³ HX +1 vol% ME	7.9	480	BC + 25 g/m ³ HX+ 1 vol% ME	8.4	658	LY + 25 g/m ³ HX +1 vol% HY	8.0	390	BC + 25 g/m ³ HX +1 vol% HY	8.6	596
LY + 25 g/m ³ HX +2 vol% ME	8.1	542	BC + 25 g/m ³ HX +2 vol% ME	8.3	712	LY + 25 g/m ³ HX +2 vol% HY	7.9	522	BC + 25 g/m ³ HX +2 vol% HY	8.5	686
LY + 25 g/m ³ HX+ 3 vol% ME	8.3	846	BC + 25 g/m ³ HX +3 vol% ME	8.4	933	LY + 25 g/m ³ HX +3 vol% HY	8.0	622	BC + 25 g/m ³ HX +3 vol% HY	8.5	822
LY + 25 g/m ³ HX +4 vol% ME	8.0	810	BC + 25 g/m ³ HX +4 vol% ME	8.3	832	LY + 25 g/m ³ HX +4 vol% HY	7.9	1192	BC + 25 g/m ³ HX +4 vol% HY	8.6	900

From the above discussion, it was generally noticed that hybrid mixture explosions are more severe, compared to individual materials. The addition of non-explosible concentrations of either gas or solvent increases both P_{\max} and $(dP/dt)_{\max}$ of the dusts. These results confirm the findings of **Bartknecht [194]** of which he mentioned that the maximum explosion pressure increases as the concentration of the gases increases, whereas a more dramatic effect was observed on the hybrid deflagration index. Moreover, **Dufaud et al. [13]** also observed that deflagration index of hybrid mixtures were higher than that of the pure fuels, thus concluding that there are more than simple additive effects on explosion severity. Furthermore, **Amyotte et al. [18]** observed a significant increase of the deflagration index when non-explosible concentration of gases were added to the dust. With respect to mixtures of three phases as presented above, the explosion

becomes more severe compared to single substance or two phases. Hence, based on the present research as well as the finding from the literature, it can be concluded that the effect of the explosion severity of hybrid mixture cannot be predicted by simply overlapping the explosion behavior of individual materials.

Chapter Seven

7 Conclusion and Recommendations

7.1 Conclusion

Hybrid mixture explosions involving materials of different state of aggregation continue to occur in industries that either handle or process combustible dusts, gases and solvents. In order to prevent or to mitigate the hazards associated with these mixtures, various explosion parameters of these mixtures need to be known. As a result of this, a comprehensive study on the explosion characteristics of these mixtures has been carried out. This was done by performing an experimental and theoretical investigation on different explosion properties such as: minimum ignition temperature, minimum ignition energy, limiting oxygen concentration, lower explosion limit, minimum explosible concentration and maximum explosion pressure as well as maximum rate of pressure rise. Different combinations of twenty combustible dusts, three gases and six solvent mixtures were investigated. Based on the findings from this research study, the following conclusion could be made:

Lower explosion limits

The lower explosion limits of single dusts, gases, as well as two-phase and three-phase hybrid mixtures were investigated. Experiments were performed in two different laboratory equipments i.e. the standard 20-liter sphere and the Godbert-Greenwald (GG)

furnace with six different solvents, three gases and six dusts. The experimental results demonstrated a significant enhancement in the possibility of an explosion by solvent, gas or spray admixture with dust and vice versa. These also confirmed that a hybrid mixture explosion is possible even when the concentrations of both components are lower than their minimum explosion concentration or lower explosion limit. Furthermore, three different mathematical models to predict the lower explosion limits of dusts, gases and hybrid mixtures were presented. Comparisons between these models and the experimental results were done. With respect to dusts, it was noticed that all the models results were far below the experimental results which seems to be good, from a safety point of view. Moreover, the calculated results from the gas models were in good agreement with experimental results with a maximum deviation of 0.4 vol%. With respect to hybrid mixtures, the calculated results from Le Chatelier's, Mannan et al. and the Bartknecht models were below compared with the experimental values. The results of these comparisons showed that the suggested relations to predict the lower explosion limit are not reliable for some mixtures. The dependency on the specific material is obvious and leads to the conclusion that a simplified formula based on the lower explosion limits of pure substances might not be sufficiently safe. In this case more knowledge on the reaction mechanism is necessary to better understand and predict the behavior. Moreover, a ternary phase diagram proposed in this thesis could help to distinguish between ignition and non-ignition regions when dealing with three-phase mixtures.

Limiting oxygen concentration

An investigation into the limiting oxygen concentration of fifteen combustible dusts, one gas, two solvents and their mixtures in the standard 20-liter explosion chamber has been undertaken. Three different ignition energies (10 J, 2 kJ and 10 kJ) were used as ignition sources. The results show that an electrical igniter providing approximately 10 J of energy led to significantly higher limiting oxygen concentration values than pyrotechnical igniters of either 2 kJ or 10 kJ. This could be due to the fact that the chemical igniters possibly “overdrive” the explosion by producing a hot flame which covers the entire explosion chamber during combustion. Ignition energy of 2 kJ being used for the 20-liter sphere,

according to European standard EN 14034-4 would be in good agreement with the ASTM standard E2931-13, which recommends chemical igniters of 2.5 kJ energy. Moreover, with respect to hybrid mixtures investigation, the 20-liter sphere was modified to allow an input of gases, vapors and sprays. The limiting oxygen concentration of the hybrid mixtures were significantly lower than that of dust-air mixtures, when the “weak” electrical igniter was used. However, by using chemical igniters, no significant change in the limiting oxygen concentration could be observed. Furthermore, mathematical models to estimate the limiting oxygen concentration of dusts, gases and hybrid mixtures were presented. A comparison between these models and the experimental results were also achieved. Based on the calculations from this model for the limiting oxygen concentration of dusts and hybrid mixtures, a simple diagram was presented which allows to directly estimate the limiting oxygen concentration from properties which are comparatively easy to determine, namely the elemental analysis of the dust and the heat of combustion. A good agreement between the models and the experimental results were observed for all combinations, with the exception of 10 kJ chemical igniter where some deviations were recorded, but these deviations were all within the safety margins.

Minimum ignition energy

Investigation of the minimum ignition energy of a hybrid mixture of two flammable gases (methane and propane) and eight combustible dusts (wheat flour, starch, protein, polyethylene, peat, dextrin, wood coal and brown coal) were carried out in the modified Hartmann apparatus. The device used was limited to a lowest ignition energy of 4 mJ. Thus, the minimum ignition energy of pure gases could not be tested directly, as their values are all below 4 mJ. Hence these values (minimum ignition energy of gases) were taken from the literature. The effect of adding non-explosible concentration of gas on the minimum ignition energy of dust was the prime focus of this study. The experimental results demonstrated a significant decrease of the minimum ignition energy of the dusts and increase in the likelihood of explosion when a small amount of gas that was below its lower explosion limit was mixed with the dust, thereby boosting the ignition sensitivity of the dust. For example, the minimum ignition energy of polypropylene was observed to

decrease from 116 mJ to 5 mJ when only 1 vol % of propane (below its lower explosion limit) was added. Moreover, an empirical model to predict the minimum ignition energy of hybrid mixtures was presented and further comparison with the experimental results was done. A good agreement between the model and the experimental results were observed. Finally, it could be mentioned that the ignition sensitivity of hybrid mixtures cannot be predicted by simply overlapping the effects of the single substance.

Minimum ignition temperature

Investigation of the minimum ignition temperature of dust, vapor or gas and their hybrid mixtures was studied using the Godbert-Greenwald furnace. Six combustible dusts, three gases and four solvent-vapors were used. These experimental results affirmed that addition of gas or vapor and dust have an influence on minimum ignition temperature of hybrid mixtures, even though the added concentrations are below their respective lower explosion limits. The addition of combustible gases can be seen as a replacement for volatiles released from the dust during pyrolysis and hence significantly affects the minimum ignition temperature of hybrid mixtures. Based on these findings, it could be deduced that the minimum ignition temperature of hybrid mixture explosions cannot be predicted by simply overlapping the effects of the single substance explosion. Moreover, three existing mathematical models to predict the minimum ignition temperature of dusts were discussed. A comparison between these models and the experimental results was done, which showed a good agreement with each other within the experimental uncertainties. Finally, a mathematical model to estimate the minimum ignition temperature of hybrid mixtures was proposed and compared with the experimental results. It was also noticed that the newly proposed model was in good agreement with the experimental results from a safety point of view as well as within the experimental uncertainties, with an exception of CN₄, for which some deviations were noticed. These deviations for CN₄ were attributed to the high ignition temperature in comparison to the gases.

Explosion severity

The maximum explosion pressure (P_{\max}) and rate of pressure rise $(dP/dt)_{\max}$ of dusts (lycopodium and brown coal), solvents (ethanol, isopropanol, toluene, acetone, hexane and heptane), gases (methane and hydrogen) as well as two and three-phase hybrid mixtures were investigated. Experiments were performed in the standard 20-liter sphere with 10 J electrical igniter as ignition source as well as 60 ms as ignition delay time. It was generally noticed that the explosion severity of a hybrid mixture of dust and gas/spray was higher than that of dust but lower than either gas or solvent. The addition of a flammable gas/vapor to a dust-air mixture increases the maximum explosion pressure to some extent and significantly increases the maximum rate of pressure rise of the dust mixture, even though the concentration of the flammable gas/vapor is below its lower explosion limit. For instance, lycopodium with a maximum rate of pressure rise value of 272 bar/s increased to 322 bar/s, 369 bar/s, 410 bar/s and 504 bar/s when methane concentration of 1 vol%, 2 vol%, 3 vol% and 4 vol% was respectively added. These values of maximum rate of pressure rise further increased to 430 bar/s, 460 bar/s, 573 bar/s and 798 bar/s when a non-explosible concentration of a third phase, isopropanol (50 % lower than the lower explosion limit) was added. The explosion severity of hydrogen was found to be more pronounced than methane. This was attributed to the higher burning velocity and higher heat of combustion of hydrogen compared to methane.

In summary, the findings from this study have demonstrated a significant decrease in the minimum ignition temperature, minimum ignition energy and limiting oxygen concentration of gas, solvent or dust and increase in the possibility of explosion when a small amount of dust, which was either below the minimum explosion concentration or not ignitable by itself, was mixed with gas and vice versa. Moreover, it was generally observed that the addition of a non-explosible concentration of flammable gas or spray to a dust-air mixture increases the maximum explosion pressure to some extent and significantly increases the maximum rate of pressure rise of the dust mixture, even though the added concentrations of gases or vapor are below its lower explosion limit. It could finally be concluded that, one cannot rely on the explosion properties of

a single substance to ensure the safety of a process or system when substances with different states of aggregate are present.

7.2 Recommendations

In view of the above conclusions, some future studies are suggested to examine the implications of the findings presented in this thesis and improve the understanding of hybrid mixtures explosion.

1. Development of a standard method for the determination of the explosion properties of hybrid mixtures. A general acceptable procedure will help the comparison of results from another laboratory.
2. Development of a standard method to measure the minimum ignition energy of hybrid mixtures. This new method should allow for the generation of lower ignition energies. The equipment used for the present thesis was limited to 4 mJ, as a result of this, mixtures with lower ignition energies were not studied
3. Injection of spray into the combustion chamber should be improved. For example, the activation of the nozzle could be done automatically instead of manual method, to avoid human error
4. Mathematical models based on physiochemical and thermodynamic properties of hybrid mixture should be developed to predict the explosion behavior of hybrid mixtures
5. Undertake an extensive study on the mechanism of hybrid mixture explosion
6. Based on the developed models, the explosion properties of hybrid mixtures could be simulated and compared with the experimental results.
7. More studies should be done on the influence of properties such as particle size, initial temperature, initial turbulence and moisture contents on the ignition sensitivity and severity of hybrid mixtures.
8. Influence of flammable solvent on the explosion behavior of dust (pre-wetted).

References

1. Mannan, S., *Lees' Process Safety Essentials: Hazard Identification, Assessment and Control*. 2013: Butterworth-Heinemann.
2. Khan, F.I. and S. Abbasi, *Major accidents in process industries and an analysis of causes and consequences*. *Journal of Loss Prevention in the process Industries*, 1999. **12**(5): p. 361-378.
3. CSB, *Investigation Report: Combustible Dust Hazard Study. Report No. 2006H1, U.S. Chemical Safety and Hazard Investigation Board, Washington, USA*. 2006.
4. Goff, C., *The Westray Mine disaster: Media coverage of a corporate crime in Canada*. *Contemporary issues in crime and criminal justice: Essays in honor of Gilbert Geis*, 2001: p. 191-212.
5. OSHA, E., *EPA/OSHA Joint Chemical Accident Investigation Report, BPS, Inc., West Helena, Arkansas. EPA 550-R-99-003*. 1999.
6. Masson, F. *Explosion d'un silo de céréales à Blaye (33): Rapport de synthèse*. in *Risque et génie civil. Colloque*. 2000.
7. Mann, J.A., *Upper Big Branch Mine--South Mine ID: Public Briefing, June 29, 2011*. 2012: DIANE Publishing.
8. CSB, *Case study, Final Report on AL Solutions Metal Dust Explosion and Fire that Killed Three in West Virginia Leads CSB to Reemphasize Call for OSHA Combustible Dust Standard, DC: U.S. Chemical Safety and Hazard Investigation Board*. 2014.

9. Aksoğan, P., D. Bayram, and I. Çiftçi, *Soma Coal Mine Disaster Information Report*. 2014, Amsterdam: Greenpeace.(<http://priceofoil.org/content/uploads/2014/06/Soma-Coal-Mine-Disaster-Report-GPMED.pdf>).
10. Pilão, R., E. Ramalho, and C. Pinho, *Explosibility of cork dust in methane/air mixtures*. *Journal of loss prevention in the process industries*, 2006. **19**(1): p. 17-23.
11. Denkevits, A., *Explosibility of hydrogen–graphite dust hybrid mixtures*. *Journal of Loss Prevention in the Process Industries*, 2007. **20**(4): p. 698-707.
12. Denkevits, A. and B. Hoess, *Hybrid H₂/Al dust explosions in Siwek sphere*. *Journal of Loss Prevention in the Process Industries*, 2015. **36**: p. 509-521.
13. Dufaud, O., L. Perrin, and M. Traore, *Dust/vapour explosions: Hybrid behaviours?* *Journal of Loss Prevention in the Process Industries*, 2008. **21**(4): p. 481-484.
14. Dufaud, O., et al., *Explosions of vapour/dust hybrid mixtures: a particular class*. *Powder Technology*, 2009. **190**(1): p. 269-273.
15. Considine, M. and G. Suter, *The 12th international symposium on loss prevention and safety promotion in the process industries translating knowledge into practice*. *Process Safety and Environmental Protection*, 2009. **87**(1): p. 1.
16. Chatrathi, K., *Dust and hybrid explosibility in a 1 m³ spherical chamber*. *Process Safety Progress*, 1994. **13**(4): p. 183-189.
17. Sanchirico, R., et al., *Study of the severity of hybrid mixture explosions and comparison to pure dust–air and vapour–air explosions*. *Journal of Loss Prevention in the Process Industries*, 2011. **24**(5): p. 648-655.
18. Amyotte, P., et al. *Determination of hybrid mixture explosion severity*. in *13th International Symposium on Loss Prevention and Safety Promotion in the Process Industries, Brugge, Belgium*. 2010.
19. Amyotte, P., et al., *Prevention and mitigation of dust and hybrid mixture explosions*. *Process Safety Progress*, 2010. **29**(1): p. 17-21.
20. Garcia-Agreda, A., et al., *Dust/gas mixtures explosion regimes*. *Powder Technology*, 2011. **205**(1): p. 81-86.
21. Khalili, I., et al., *Ignition sensitivity of gas–vapor/dust hybrid mixtures*. *Powder technology*, 2012. **217**: p. 199-206.

22. Eckhoff, R., *Dust explosions in the process industries: identification, assessment and control of dust hazards*. 2003: Gulf professional publishing.
23. Crowl, D.A., *Understanding explosions*. Vol. 16. 2010: John Wiley & Sons.
24. Bjerketvedt, D., J.R. Bakke, and K. Van Wingerden, *Gas explosion handbook*. Journal of hazardous materials, 1997. **52**(1): p. 1-150.
25. Oran, E.S. and F.A. Williams, *The physics, chemistry and dynamics of explosions*. Philosophical Transactions of the Royal Society of London A: Mathematical, Physical and Engineering Sciences, 2012. **370**(1960): p. 534-543.
26. Zabetakis, M.G., *Flammability characteristics of combustible gases and vapors*. 1965, DTIC Document.
27. Harris, R.J., *The investigation and control of gas explosions in buildings and heating plant*. 1983: E. & FN Spon in association with the British Gas Corp.
28. Harris, R., M. Marshall, and D. Moppett. *The response of glass windows to explosion pressures*. in *British Gas Corporation. I. Chem. E. Symposium Serious*. 1977.
29. Di Sarli, V., A. Di Benedettob, and G. Russob, *The Role of the Combustion Submodel for Large Eddy Simulation of Transient Premixed Flame-Vortex Interactions in Gas Explosions*. CHEMICAL ENGINEERING, 2012. **26**.
30. Maremonti, M., et al., *Post-accident analysis of vapour cloud explosions in fuel storage areas*. Process safety and environmental protection, 1999. **77**(6): p. 360-365.
31. Arizal, *Development of Methodology for Treating Pressure Waves from Explosions Accounting for Modeling and Data Uncertainties*. 2012, Universitätsbibliothek.
32. Kumar, A., *Guidelines for evaluating the characteristics of vapor cloud explosions, flash fires, and bleves*. Center for Chemical Process Safety (CCPS) of the AIChE, Published by the American Institute of Chemical Engineers, New York, NY (1994), 387 pages, [ISBN: 0-8169-0474-X]. Environmental Progress, 1996. **15**(1).
33. Shao, H., et al., *Analysis of vacuum chamber suppressing gas explosion*. International Journal of Mining Science and Technology, 2013. **23**(5): p. 653-657.
34. Crowl, D.A. and J.F. Louvar, *Chemical process safety: fundamentals with applications*. 2001: Pearson Education.

35. Johnson, D. and M. Vasey. *The prevention and mitigation of gas explosions*. in *SPE Health, Safety and Environment in Oil and Gas Exploration and Production Conference*. 1996. Society of Petroleum Engineers.
36. ASTM, *Standard E 1620: standard terminology relating to liquid particles and atomization*. Annual book of ASTM standards, 2004.
37. Schick, R., *Spray technology reference guide: understanding drop size*. *Spraying Systems Co. Bulletin*, 2008(459C).
38. Zehr, J., *Eigenschaften brennbarer Staube und Nebel in Luft*. Chapter in "*Handbuch der Raumexplosionen*" edited by H.H. Freytag, Verlag Chenfie GmbH, Weinheim 1965: p. 164-186.
39. Williams, A., *Combustion of liquid fuel sprays*. 2013: Butterworth-Heinemann.
40. Förster, H., *Eigenschaften brennbarer Nebel und Schäume*. Chapter in Steen 2000.
41. Gant, S., et al., *Generation of flammable mists from high flashpoint fluids: literature review*. Health and Safety Executive, Research Report RR980, 2013.
42. Burgoyne, J. and L. Cohen. *The effect of drop size on flame propagation in liquid aerosols*. in *Proceedings of the Royal Society of London A: Mathematical, Physical and Engineering Sciences*. 1954. The Royal Society.
43. Faeth, G.M. and D.R. Olson, *The ignition of hydrocarbon fuel droplets in air*. 1968, SAE Technical Paper.
44. Ballal, D. and A. Lefebvre. *Ignition and flame quenching of quiescent fuel mists*. in *Proceedings of the Royal Society of London A: Mathematical, Physical and Engineering Sciences*. 1978. The Royal Society.
45. Ballal, D. and A. Lefebvre, *Ignition and flame quenching of flowing heterogeneous fuel-air mixtures*. *Combustion and Flame*, 1979. **35**: p. 155-168.
46. Ballal, D.R. and A. Lefebvre. *A general model of spark ignition for gaseous and liquid fuel-air mixtures*. in *Symposium (international) on combustion*. 1981. Elsevier.
47. Peters, J. and A. Mellor, *An ignition model for quiescent fuel sprays*. *Combustion and Flame*, 1980. **38**: p. 65-74.
48. Bennet, J. and C. Ballal, *Ignition of combustible fluids by heated surface*. *Process Safety Progress*, 2001. **20**(1): p. 29-36.

49. Babrauskas, V., *Ignition handbook*. 2003.
50. Freeston, H., J. Roberts, and A. Thomas, *Crankcase explosions: an investigation into some factors governing the selection of protective devices*. Proceedings of the Institution of Mechanical Engineers, 1956. **170**(1): p. 811-824.
51. Jagger, S., A. Nicol, and A. Thyer, *A comprehensive approach to the assessment of fire-resistant hydraulic fluid safety*. 2003, HSL Report FR/02/05, Available from the Health and Safety Laboratory, Buxton, UK.
52. Association, N.F.P., *NFPA 654: Standard for the Prevention of Fire and Dust Explosions from the Manufacturing, Processing, and Handling of Combustible Particulate Solids*. 2005: National Fire Protection Association.
53. Abbasi, T. and S. Abbasi, *Dust explosions—Cases, causes, consequences, and control*. Journal of Hazardous Materials, 2007. **140**(1): p. 7-44.
54. M. Worsfold, P.A., *"Fires, explosions and combustible dusts hazards"*, Dalhousie University, Halifax, NS, Canada,. 3 June 2010.
55. Amyotte, P.D., *An introduction to dust explosions: understanding the myths and realities of dust explosions for a safer workplace*. 2013: Butterworth-Heinemann.
56. Medard, L.A., *Accidental Explosions: Physical and chemical properties*. Vol. 1. 1989: Halsted Press.
57. Gomez, C.O. and F.J. Vastola, *Ignition and combustion of single coal and char particles: A quantitative differential approach*. Fuel, 1985. **64**(4): p. 558-563.
58. Di Benedetto, A. and P. Russo, *Thermo-kinetic modelling of dust explosions*. Journal of Loss Prevention in the process industries, 2007. **20**(4): p. 303-309.
59. Du, B., et al., *Comparative study of explosion processes controlled by homogeneous and heterogeneous combustion mechanisms*. Journal of Loss Prevention in the Process Industries, 2014. **30**: p. 155-163.
60. Hertzberg, M., et al., *Thermokinetic transport control and structural microscopic realities in coal and polymer pyrolysis and devolatilization: their dominant role in dust explosions*. Prepr. Pap., Am. Chem. Soc., Div. Fuel Chem.:(United States), 1988. **32**(CONF-870802-).

61. Dufaud, O., et al., *Comparing Pyrolysis Gases and Dusts Explosivities: A Clue to Understanding Hybrid Mixtures Explosions?* Industrial & Engineering Chemistry Research, 2011. **51**(22): p. 7656-7662.
62. Russoa, P. and A. Di Benedettob, *Review of a Dust Explosion Modeling*. CHEMICAL ENGINEERING, 2013. **31**.
63. Dufaud, O., et al., *Highlighting the importance of the pyrolysis step on dusts explosion*. Chemical Engineering Transactions, 2012. **26**: p. 369-374.
64. Kletz, T.A. and P. Amyotte, *Process plants: A handbook for inherently safer design*. 2010: CRC Press.
65. Amyotte, P.R., M.J. Pegg, and F.I. Khan, *Application of inherent safety principles to dust explosion prevention and mitigation*. Process Safety and Environmental Protection, 2009. **87**(1): p. 35-39.
66. Abuswer, M., P. Amyotte, and F. Khan, *A quantitative risk management framework for dust and hybrid mixture explosions*. Journal of Loss Prevention in the Process Industries, 2013. **26**(2): p. 283-289.
67. Engler, K.O.V., *Beiträge zur Kenntniss der Staubexplosionen*. 1885: J. Springer.
68. Cardillo, P. and E. Anthony, *The flammability limits of hybrid gas and dust systems*. La Rivista dei Combustibili, 1978. **32**: p. 390-395.
69. Pellmont, G., *Explosions-und Zündverhalten von hybriden Gemischen aus brennbaren Stäuben und Brenngasen*. 1979, Diss. Techn. Wiss. ETH Zürich, Nr. 6498, 0000. Ref.: Richarz, W.; Korref.: Gut, G.
70. Franke, H., *Bestimmung der Minderstzudenergie von Kohlenstaub/Methan/Luft Gemisches (hybride Gemische)*. VDI-Berichte, 1978. **304**: p. 69-72.
71. Bartknecht, W., *Gas, vapor and dust explosions, fundamentals, prevention, control*. Int. Symp. Grain Elev. Explos. 1. 1981.
72. Cashdollar, K.L., *Coal dust explosibility*. Journal of loss prevention in the process industries, 1996. **9**(1): p. 65-76.
73. Siwek, R., *Determination of technical safety indices and factors influencing hazard evaluation of dusts*. Journal of Loss Prevention in the Process Industries, 1996. **9**(1): p. 21-31.

74. Jiang, J., Y. Liu, and M.S. Mannan, *A correlation of the lower flammability limit for hybrid mixtures*. Journal of Loss Prevention in the Process Industries, 2014. **32**: p. 120-126.
75. Jiang, J., et al., *Validation of a new formula for predicting the lower flammability limit of hybrid mixtures*. Journal of Loss Prevention in the Process Industries, 2015. **35**: p. 52-58.
76. Kosinski, P., et al., *Explosions of carbon black and propane hybrid mixtures*. Journal of Loss Prevention in the Process Industries, 2013. **26**(1): p. 45-51.
77. Sanchirico, R., et al., *Explosion of lycopodium-nicotinic acid-methane complex hybrid mixtures*. Journal of Loss Prevention in the Process Industries, 2015. **36**: p. 505-508.
78. Li, Q., et al., *Explosion characteristics of H₂/CH₄/air and CH₄/coal dust/air mixtures*. Powder Technology, 2012. **229**: p. 222-228.
79. Amyotte, P.R. and R.K. Eckhoff, *Dust explosion causation, prevention and mitigation: An overview*. Journal of Chemical Health and Safety, 2010. **17**(1): p. 15-28.
80. Coronado, C.J., et al., *Flammability limits: A review with emphasis on ethanol for aeronautical applications and description of the experimental procedure*. Journal of hazardous materials, 2012. **241**: p. 32-54.
81. ASTM, *Standard Test Method for Concentration Limits of Flammability of Chemicals*, in *ASTM E681-85* 1985.
82. Bond, J., *Sources of ignition: flammability characteristics of chemicals and products*. 1991: Butterworth-Heinemann.
83. Brandes, E., et al., *Sicherheitstechnische Kenngrößen*. 2003: Wirtschaftsverlag NW, Verlag für neue Wissenschaft.
84. Lian, P., et al., *Flammability of heat transfer fluid aerosols produced by electrospray measured by laser diffraction analysis*. Journal of Loss Prevention in the Process Industries, 2010. **23**(2): p. 337-345.
85. Lian, P., X. Gao, and M.S. Mannan, *Prediction of minimum ignition energy of aerosols using flame kernel modeling combined with flame front propagation theory*. Journal of Loss Prevention in the Process Industries, 2012. **25**(1): p. 103-113.
86. Cashdollar, K.L., et al., *Flammability of methane, propane, and hydrogen gases*. Journal of Loss Prevention in the Process Industries, 2000. **13**(3): p. 327-340.

87. Molnarne, M., T. Schendler, and V. Schröder, *Sicherheitstechnische Kenngrößen, Band 2: Explosionsbereiche von Gasgemischen*. 2003.
88. Vidal, M., et al., *A review of estimation methods for flash points and flammability limits*. Process safety progress, 2004. **23**(1): p. 47-55.
89. Coward, H.F. and G.W. Jones, *Limits of flammability of gases and vapors*. 1952, DTIC Document.
90. Brötz, W., *W. Bartknecht: Explosionen, Ablauf und Schutzmaßnahmen*. Springer-Verlag, Berlin, Heidelberg, New York 1978. 264 Seiten, Preis: DM 148,—. Berichte der Bunsengesellschaft für physikalische Chemie, 1980. **84**(6): p. 605-605.
91. Cashdollar, K.L., *Overview of dust explosibility characteristics*. Journal of Loss Prevention in the Process Industries, 2000. **13**(3): p. 183-199.
92. Amyotte, P.R., et al., *Laboratory investigation of the dust explosibility characteristics of three Nova Scotia coals*. Journal of Loss Prevention in the Process Industries, 1991. **4**(2): p. 102-109.
93. Castellanos, D., et al., *The effect of particle size polydispersity on the explosibility characteristics of aluminum dust*. Powder Technology, 2014. **254**: p. 331-337.
94. Encinar, J.M., et al., *Pyrolysis of maize, sunflower, grape and tobacco residues*. Journal of chemical technology and biotechnology, 1997. **70**(4): p. 400-410.
95. Yuan, J., et al., *An extensive discussion on experimental test of dust minimum explosible concentration*. Procedia Engineering, 2012. **43**: p. 343-347.
96. 1839., E., *Determination of explosion limits of gases and vapours*. Brussels: European Committee for Standardisation. 2003.
97. *EN 14034-3; Determination of determination of minimum explosion concentration of dusts*. Brussels: European Committee for Standardisation, 2007
98. Schonewald, I., *Staub explosion*. 31, pp .376 -378. 1971.
99. Shevchuk, V., et al., *Effect of the Structure of a Gas Suspension on the Process of Flame Propagation*. Combustion, Explosion, and Shock Waves, 1979. **15**(6): p. 723-727.
100. Buksowicz W., W.P., *Prog. of Astronautics and Aeronautics* 87 pp. 414-425. 1983.
101. Shebeko, Y.N., et al., *An analytical evaluation of flammability limits of gaseous mixtures of combustible–oxidizer–diluent*. Fire Safety Journal, 2002. **37**(6): p. 549-568.

102. Spakowski, A. and F.E. Belles, *Variation of pressure limits of flame propagation with tube diameter for various isooctane-oxygen-nitrogen mixtures*. 1952.
103. Glassman, I., R.A. Yetter, and N.G. Glumac, *Combustion*. 2014: Academic press.
104. Bartknecht, W., *Explosions, Springer-Verlag, Berlin Heidelberg New York*. 1981: Springer Science & Business Media.
105. Zlochower, I.A. and G.M. Green, *The limiting oxygen concentration and flammability limits of gases and gas mixtures*. *Journal of loss prevention in the process industries*, 2009. **22**(4): p. 499-505.
106. Standardization, E.C., *EN 50281-2-1, Potentially Explosible Atmospheres, Explosion Prevention and Protection, Determination of limiting oxygen concentration for Dust/air Mixtures*. ECS, Brussels, Belgium. 2007.
107. ASTM, *Standard test methods for limiting oxygen (oxidant) concentration in gases and vapors. E2079-07*. In: *ASTM International annual book of standards, Vol. 14.02*. West Conshohocken, PA: American Society for Testing and Materials. 2008b.
108. CEN and TR15281, *Guidance on Inerting for the Prevention of Explosions*. 2006.
109. 2263, V., *Staubbrände und Staubexplosionen – Gefahren, Beurteilung, Schutzmaßnahmen; Inertisierung (Dust Fires and Explosions – Hazards, Assessment, Protective Measures)*. 1992.
110. Wiemann, W., *Einfluß der Temperatur auf Explosionskenngrößen und Sauerstoffgrenzkonzentration*. VDI-Berichte, 1984(494): p. 89-98.
111. Sweis, F. and C. Sinclair, *The effect of particle size on the maximum permissible oxygen concentration to prevent dust explosions*. *Journal of hazardous materials*, 1985. **10**(1): p. 59-71.
112. White, P. and S. Smith, *Inert Atmospheres*. 1962, Butterworth, London.
113. Ono, R., et al., *Minimum ignition energy of hydrogen–air mixture: Effects of humidity and spark duration*. *Journal of Electrostatics*, 2007. **65**(2): p. 87-93.
114. Maly, R., *Spark ignition: its physics and effect on the internal combustion engine*, in *Fuel economy*. 1984, Springer. p. 91-148.
115. Strid, K.-G., *Experimental techniques for the determination of ignition energy*. *Oxidation and Combustion Reviews*, 1973: p. 1-46.

116. Maly, R. and M. Vogel. *Initiation and propagation of flame fronts in lean CH₄-air mixtures by the three modes of the ignition spark.* in *Symposium (International) on Combustion.* 1979. Elsevier.
117. CEN, *Determination of minimum ignition energy of dust/air mixtures, European Standard EN13821, European Committee for Standardization, Brussels.* 2002.
118. ASTM, *E582, Standard Test Method for Minimum Ignition Energy and Quenching Distance in Gaseous Mixtures.* American Society for Testing and Materials. 1988.
119. Cesana, C. and R. Siwek, *MIKE 3 Minimum Ignition Energy 3.3.* Kühner AG, Birsfelden, Switzerland, 2003.
120. Kalkert, N., *Theoretische und experimentelle Untersuchungen der Explosionskenndaten von Mischungen aus mehreren gas-und staubförmigen Brennstoffkomponenten und Luft.* 1980: na.
121. Nagy, J., *Development and control of dust explosions.* Vol. 8. 1983: CRC Press.
122. Eckhoff, R., *Minimum ignition energy (MIE)—a basic ignition sensitivity parameter in design of intrinsically safe electrical apparatus for explosive dust clouds.* Journal of Loss Prevention in the process industries, 2002. **15**(4): p. 305-310.
123. Wiecek, C., and R. Zalosh., *Effects of Spark Duration and Dust Cloud Velocity on the Minimum Ignition Energy Requirements.” Proceedings of the Eighth International Colloquium on Dust Explosions, Schaumburg, IL. Schaumburg: Safety Consulting Engineers, pp. 195-203.* 1998.
124. Pellmont, G., *“Einfluss der Temperatur auf das Zünd- und Explosionsverhalten von Nikotinsäure.” Report from Dr. Pellmont Explosionsschutz, Binningen, Switzerland.* 1997.
125. Borghese, A., et al. *Development of hot nitrogen kernel, produced by a very fast spark discharge.* in *Symposium (International) on Combustion.* 1989. Elsevier.
126. Glor, M. and K. Schwenzfeuer, *Einfluss der Sauerstoffkonzentration auf die Mindestzündenergie von Staüben.* Dechema Jahrestagung, 1999.
127. Wiecek, C., and Zalosh, R., *“Effects of Spark Duration and Dust Cloud Velocity on the Minimum Ignition Energy Requirements.” Proceedings of the Eighth International Colloquium on Dust Explosions, Schaumburg, IL. Schaumburg: Safety Consulting Engineers, pp. 195-203.* 1998.

128. ASTM, *Standard Test Method for Minimum Ignition Temperature of Dust Clouds*. ASTM International, pp. 1–10. 2006.
129. CEN, *EN 14522 Determination of the minimum ignition temperature of gases and vapours* 2005.
130. CEN, *EN 50281-2-1, European standard test method for the minimum ignition temperature for dust cloud*. 2007.
131. Zeeuwen, J.P., and . van Laar. G. F. M, “*Ignition Sensitivity of Flammable Dust/Air Mixtures.*” *Proceedings of the International Symposium on the Control of Risks in Handling and Storage of Granular Foods*, Paris: APRIA. 1985.
132. Janès, A., et al., *Experimental investigation of the influence of inert solids on ignition sensitivity of organic powders*. *Process Safety and Environmental Protection*, 2014. **92**(4): p. 311-323.
133. Pilão, R., E. Ramalho, and C. Pinho, *Overall characterization of cork dust explosion*. *Journal of hazardous materials*, 2006. **133**(1): p. 183-195.
134. Cassel, H. and I. Liebman, *The cooperative mechanism in the ignition of dust dispersions*. *Combustion and Flame*, 1959. **3**: p. 467-475.
135. Nagy, J. and D.J. Surincik, *Thermal phenomena during ignition of a heated dust dispersion*. Vol. 6811. 1966: US Dept. of the Interior, Bureau of Mines.
136. Mitsui, R. and T. Tanaka, *Simple Models of Dust Explosion. Predicting Ignition Temperature and Minimum Explosive Limit in Terms of Particle Size*. *Industrial & Engineering Chemistry Process Design and Development*, 1973. **12**(3): p. 384-389.
137. Mittal, M. and B. Guha, *Minimum ignition temperature of polyethylene dust: a theoretical model*. *Fire and materials*, 1997. **21**(4): p. 169-177.
138. Krishna, C. and A. Berlad, *A model for dust cloud autoignition*. *Combustion and Flame*, 1980. **37**: p. 207-210.
139. Zhang, D.-k. and T.F. Wall, *Ignition of coal particles: the influence of experimental technique*. *Fuel*, 1994. **73**(7): p. 1114-1119.
140. CEN, *EN 14034-1,2, Determination of explosion characteristics of dust clouds Part 1: Determination of the maximum explosion pressure and maximum rate of pressure rise*. 2004.

141. CEN, *EN 13673, 1-2 determination of the maximum explosion pressure and maximum rate of pressure rise with time for gases and vapor*. 2004.
142. Wiemann, W., *Influence of temperature and pressure on the explosion characteristics of dust/air and dust/air/inert gas mixtures*, in *Industrial dust explosions*. 1987, ASTM International.
143. Tamanini, F., *"Turbulence Effects on Dust Explosion Venting."* *Proceedings of the AIChF Loss Prevention Symposium, Session 8, Plant Layout, Houston*. 1989.
144. Carini, R.C. and K. Hules, *Coal pulverizer explosions*, in *Industrial Dust Explosions*. 1987, ASTM International.
145. ISO-5071, *Determination of the volatile and moisture contents combustible matter by gravimetric method*. 1996.
146. Li, Q., et al., *Experimental research of particle size and size dispersity on the explosibility characteristics of coal dust*. *Powder Technology*, 2016. **292**: p. 290-297.
147. ISO-17974, *Determination of the content of carbon, hydrogen, nitrogen and sulphur by infrared detection and nitrogen by thermal conductivity detection on analyser* 2002.
148. STANDARD, B. and B. ISO, *Determination of particle size distributions—Electrical sensing zone method*. 2007.
149. ISO-1928, *Determination of gross heat of combustion by the bomb calorimetric method and calculation of net heat of combustion*. 2009.
150. Rossini, F.D., et al., *Selected values of chemical thermodynamic properties*. Vol. 500. 1952: US Government Printing Office Washington, DC.
151. Reichardt, C. and T. Welton, *Solvents and solvent effects in organic chemistry*. 2011: John Wiley & Sons.
152. Standardization, E.C.f., EN 14034 1-4, *Potentially Explosible Atmospheres, Explosion Prevention and Protection. Determination of explosibility and severity of dust clouds Dust/air Mixtures in the 20-liters sphere*. ECS, Brussels, Belgium 2004.
153. Kuehner, A.G., *20 Liters Apparatus and KESP 7.0 Manual*. 2009.
154. Amyotte, P.R., et al., *The ignitability of coal dust-air and methane-coal dust-air mixtures*. *Fuel*, 1993. **72**(5): p. 671-679.

155. Garcia-Agreda, A., et al., *Dust/gas mixtures explosion regimes*. Powder Technology, 2011. **205**(1-3): p. 81-86.
156. Liu, X., Q. Zhang, and Y. Wang, *Influence of particle size on the explosion parameters in two-phase vapor–liquid n-hexane/air mixtures*. Process Safety and Environmental Protection, 2015. **95**: p. 184-194.
157. Lim, J. and Y.R. Sivathanu, *Optical patterning of a multi-orifice spray nozzle*. Atomization and Sprays, 2005. **15**(6).
158. Landman, G., *Ignition behaviour of hybrid mixtures of coal dust, methane, and air*. Journal of the South African Institute of Mining and Metallurgy, 1995. **95**(1): p. 45.
159. Addai, E.K., D. Gabel, and U. Krause, *Lower explosion limit of hybrid mixtures of burnable gas and dust*. Journal of Loss Prevention in the Process Industries, 2015. **36**: p. 497-504.
160. Addai, E.K., D. Gabel, and U. Krause, *Explosion characteristics of three component hybrid mixtures*. Process Safety and Environmental Protection, 2015. **98**: p. 72-81.
161. Le Chatelier, H., *Recherches expérimentales et théoriques sur la combustion des mélanges gazeux explosifs*. 1883: Dunod.
162. report, S., *Experimental investigation of explosion limits, explosion pressure and rate of explosion pressure rise, Bundesanstalt für Materialforschung und –prüfung, Germany, part 1*. 2002.
163. Addai, E.K., D. Gabel, and U. Krause, *Lower explosion limit/minimum explosible concentration testing for hybrid mixtures in the Godbert-Greenwald furnace*. Process Safety Progress, 2016.
164. Cashdollar, K.L., et al., *Laboratory and mine dust explosion research at the Bureau of Mines*, in *Industrial Dust Explosions*. 1987, ASTM International.
165. Proust, C. and B. Veyssiere, *Fundamental properties of flames propagating in starch dust-air mixtures*. Combustion Science and Technology, 1988. **62**(4-6): p. 149-172.
166. Continillo, G., et al., *Coal dust explosions in a spherical bomb*. Journal of Loss Prevention in the process industries, 1991. **4**(4): p. 223-229.
167. Wilén, C., et al., *Safe handling of renewable fuels and fuel mixtures*. 1999: Technical Research Centre of Finland.

168. Woskoboenko, F., *Explosibility of Victorian brown coal dust*. Fuel, 1988. **67**(8): p. 1062-1068.
169. Going, J.E., K. Chatrathi, and K.L. Cashdollar, *Flammability limit measurements for dusts in 20-L and 1-m³ vessels*. Journal of Loss Prevention in the Process Industries, 2000. **13**(3): p. 209-219.
170. Dastidar, A.G., *ASTM E2931: A new standard for the limiting oxygen concentration of combustible dusts*. Process Safety Progress, 2015.
171. Mittal, M., *Limiting oxygen concentration for coal dusts for explosion hazard analysis and safety*. Journal of loss prevention in the process industries, 2013. **26**(6): p. 1106-1112.
172. Krause, U., D. Weinert, and P. Wöhrn, *Rechnerische und graphische Bestimmung der Sauerstoffgrenzkonzentration explosionfähiger Staub/Luft-Gemische*. Staub. Reinhaltung der Luft, 1992. **52**(10): p. 361-368.
173. Monachov, V.T. and W. Hoffmann, *Brandgefährlichkeit von Stoffen: Untersuchungsmethoden*. 1984: Staatsverl. d. DDR.
174. Au, S., R. Haley, and P. Smy, *The influence of the igniter-induced blast wave upon the initial volume and expansion of the flame kernel*. Combustion and flame, 1992. **88**(1): p. 50-60.
175. Cesana, C., A. Kühner, and R. Siwek, *Handbuch 3.4*.
176. Explosionsschutz, W.B., *Grundlagen und Anwendung* Springer Verlag. Berlin, Heidelberg, New York, 1993.
177. Eckhoff, R.K. and G. Enstad, *Why are "long" electric sparks more effective dust explosion initiators than "short" ones?* Combustion and Flame, 1976. **27**: p. 129-131.
178. Eckhoff, R.K., *Towards absolute minimum ignition energies for dust clouds?* Combustion and Flame, 1975. **24**: p. 53-64.
179. Haase, H., *Electrostatic hazards: their evaluation and control*. 1977: Wiley-VCH.
180. Wähner, A., et al., *Determination of the minimum ignition energy on the basis of a statistical approach*. Journal of Loss Prevention in the Process Industries, 2013. **26**(6): p. 1655-1660.
181. Langer, T., et al., *MIE experiments and simultaneous measurement of the transferred charge—A verification of the ignition threshold limits*. Journal of Electrostatics, 2012. **70**(1): p. 97-104.

182. Lewis, B., *Combustion flames and explosions of gases 2nd ed.*[DEWEY]. 1961.
183. Di Benedetto, A., et al., *Modelling the effect of particle size on dust explosions*. Chemical Engineering Science, 2010. **65**(2): p. 772-779.
184. Bouillard, J., et al., *Ignition and explosion risks of nanopowders*. Journal of hazardous materials, 2010. **181**(1): p. 873-880.
185. Britton, L.G., *Short communication: estimating the minimum ignition energy of hybrid mixtures*. Process Safety Progress, 1998. **17**(2): p. 124-126.
186. Di Benedetto, A., V. Di Sarli, and P. Russo, *On the determination of the minimum ignition temperature for dust/air mixtures*. Chemical Engineering Transactions, 2010. **19**.
187. Addai, E.K., D. Gabel, and U. Krause, *Experimental investigation on the minimum ignition temperature of hybrid mixtures of dusts and gases or solvents*. Journal of Hazardous Materials, 2016. **301**: p. 314-326.
188. Addai, E.K., D. Gabel, and U. Krause, *Models to estimate the minimum ignition temperature of dusts and hybrid mixtures*. Journal of Hazardous Materials, 2016. **304**: p. 73-83.
189. Hattwig, M. and H. Steen, *Handbook of explosion prevention and protection*. 2008: John Wiley & Sons.
190. Krause, U., (ed. 1) *Fires in silos: hazards, prevention, and fire fighting*. 2009: John Wiley & Sons.
191. Liao, S., et al., *Determination of the laminar burning velocities for mixtures of ethanol and air at elevated temperatures*. Applied Thermal Engineering, 2007. **27**(2): p. 374-380.
192. Amyotte, P.R., et al., *Moderation of dust explosions*. Journal of Loss Prevention in the Process Industries, 2007. **20**(4): p. 675-687.
193. Zheng, Y.-P., et al., *A statistical analysis of coal mine accidents caused by coal dust explosions in China*. Journal of Loss Prevention in the Process Industries, 2009. **22**(4): p. 528-532.
194. Bartknecht, W., *Explosions: course, prevention, protection*. Springer Science & Business Media, 2012.

Appendixes

8 Appendixes

8.1 A. Detail process diagram for test in the GG furnace.

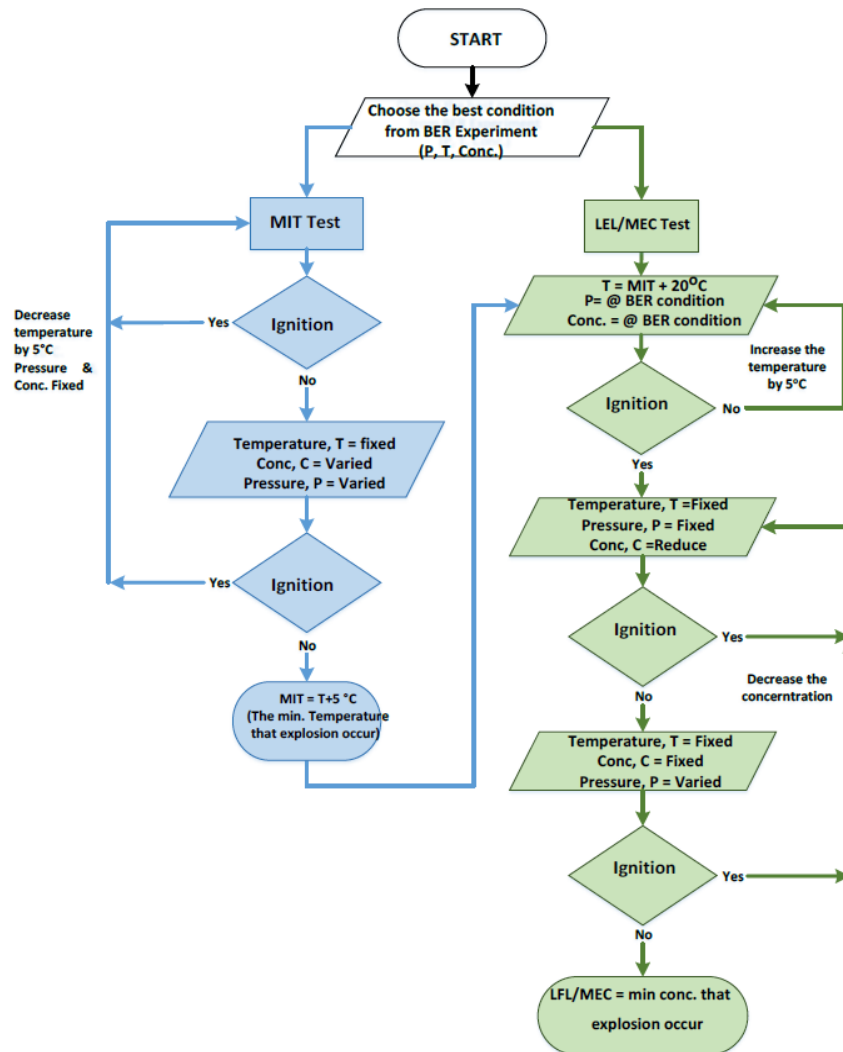


Figure A.1: MIT & MEC/LEL Test of single component flow chart

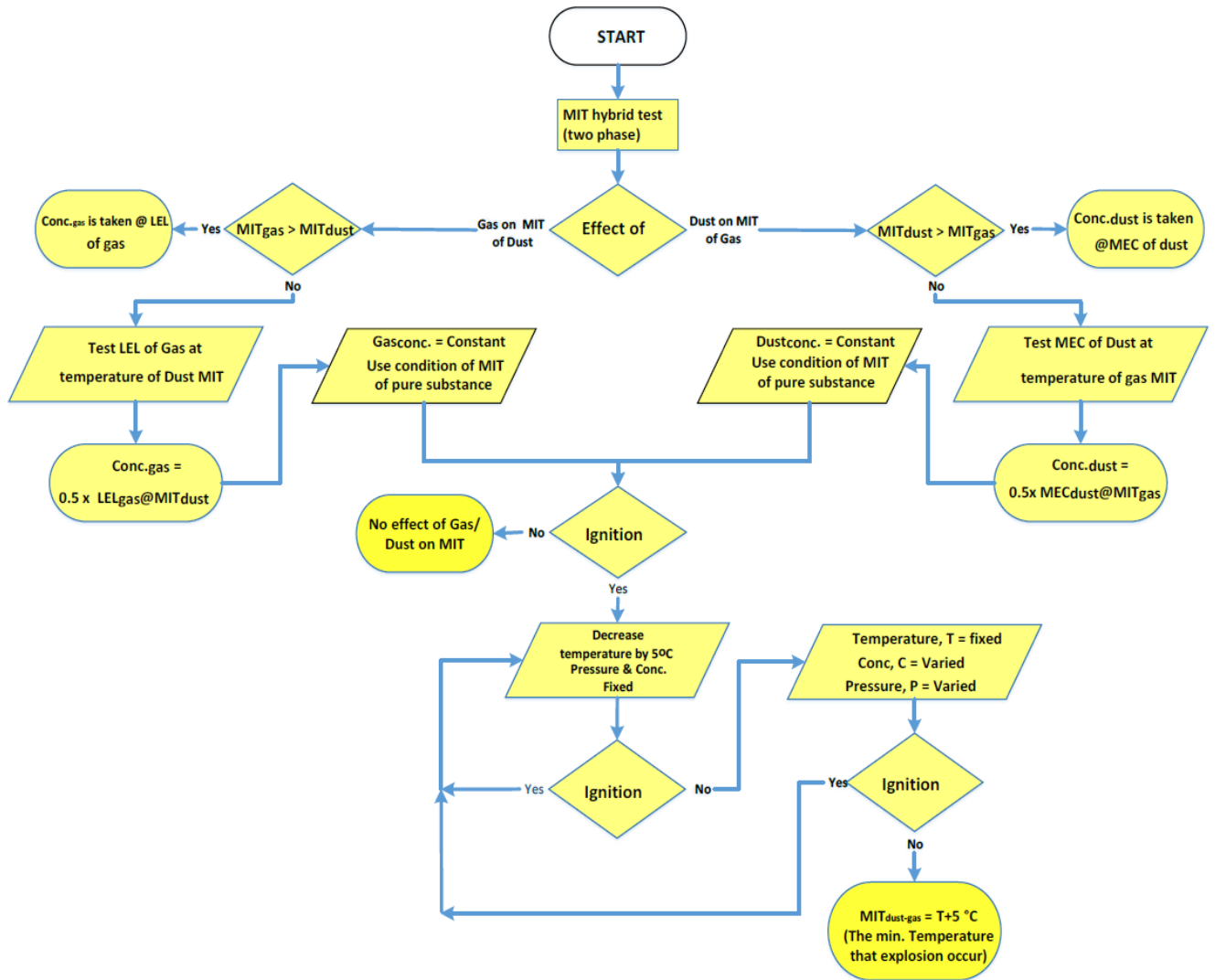


Figure A.2: Flow chart for MIT test of two-phase hybrid mixture

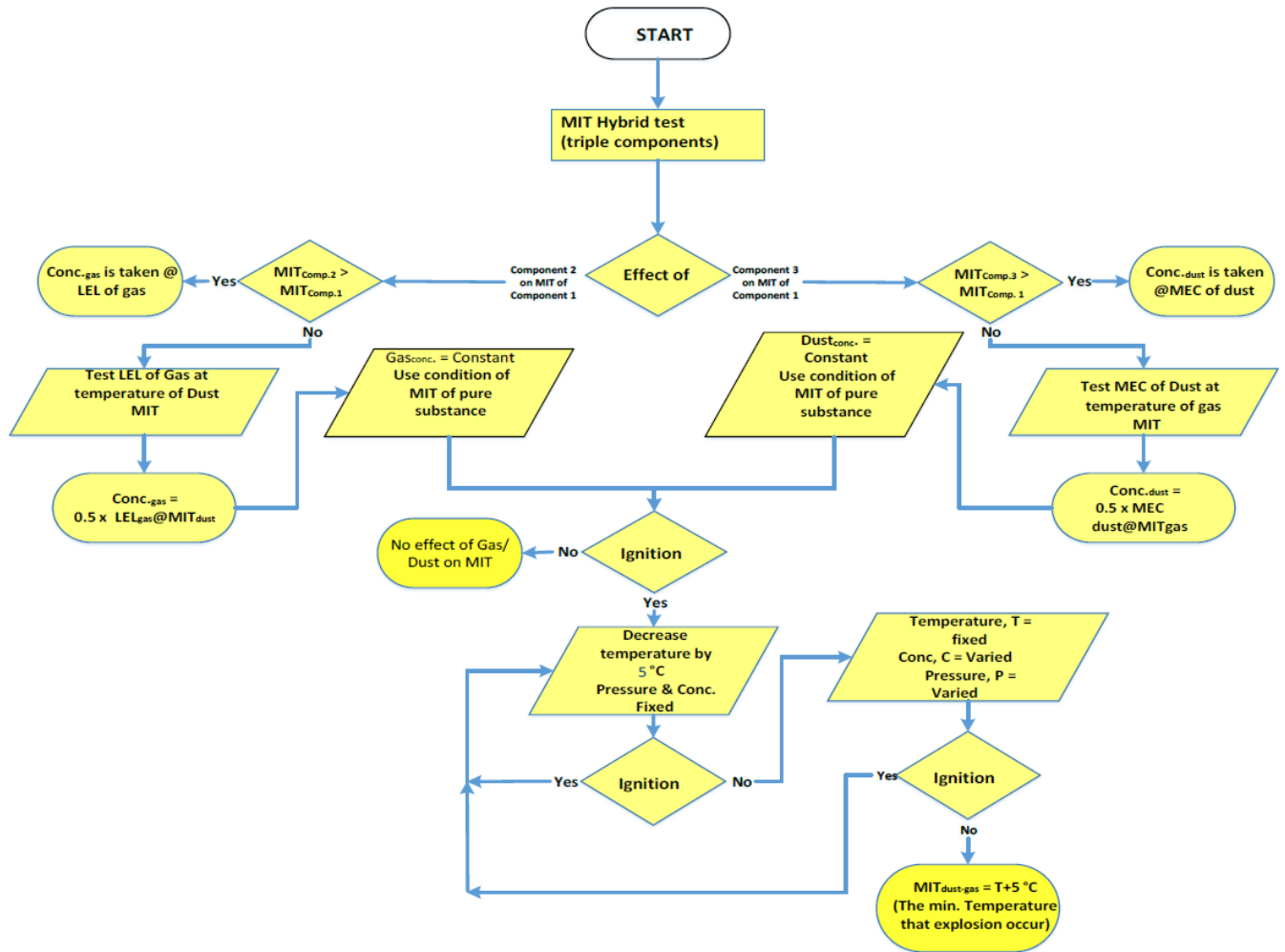


Figure A.3: Flow chart for MIT test of three-components hybrid mixture

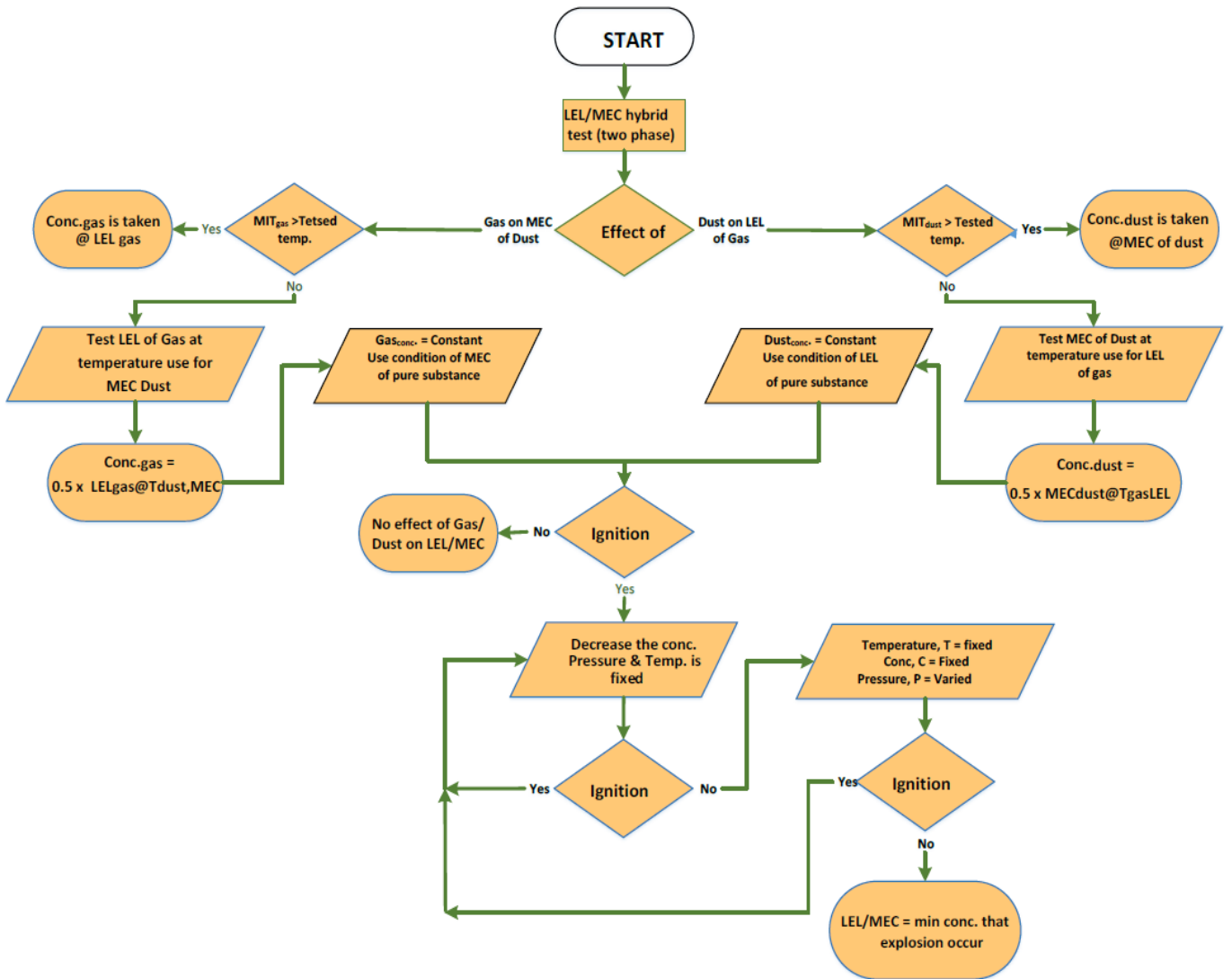


Figure A.4: Flow chart for MEC/LEL test of two-phase hybrid mixtures

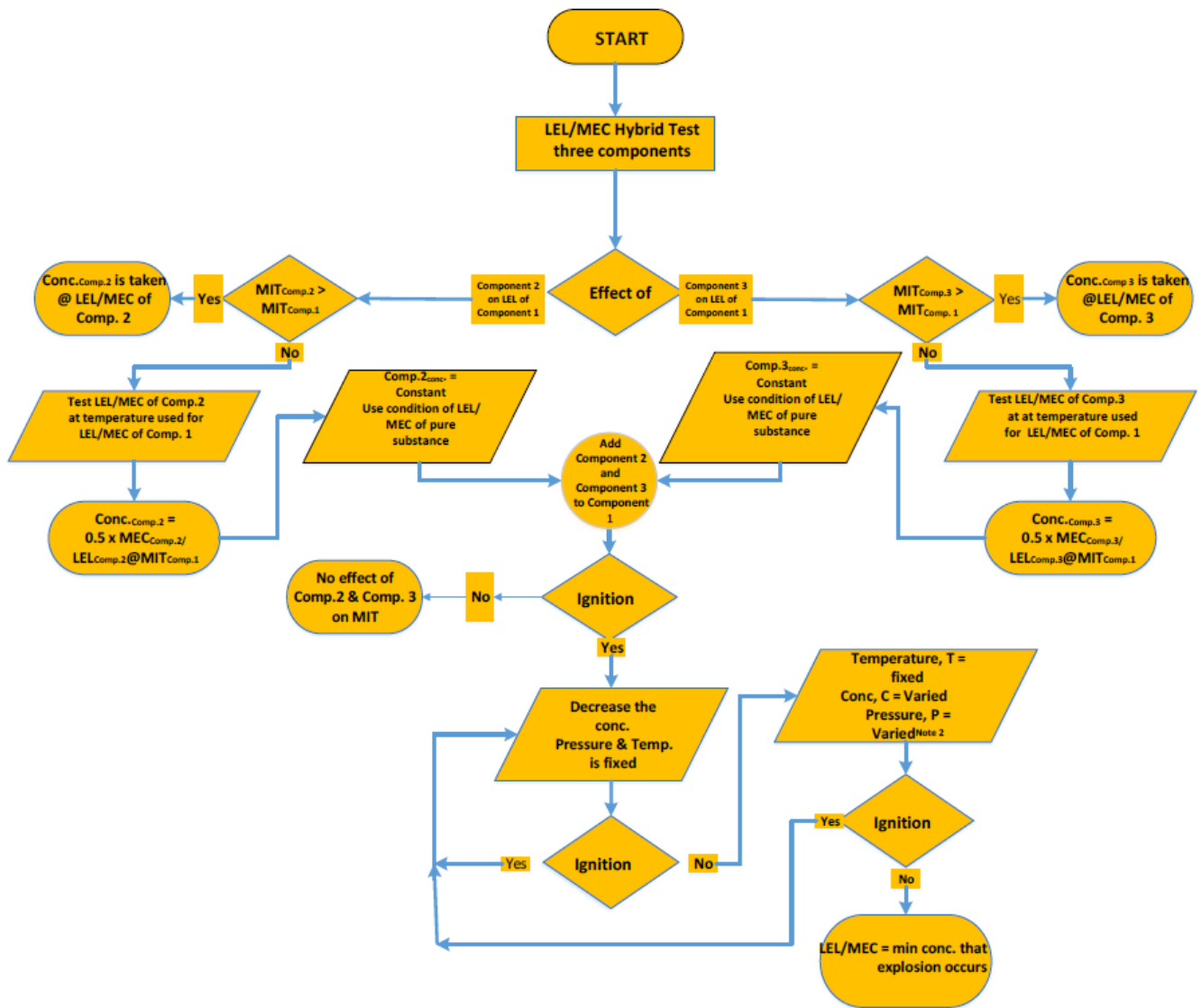


Figure A.5: Flow chart for MEC/LEL test of three-components hybrid mixture

8.2 Appendix B: Test results

B Experimental results for dust and gas hybrid mixtures

Table B.1: Summary of experimental results in comparison with model as well as the deviations (all in mJ).

Propane conc. vol%	Exp. Hybrid MIE for dust and propane	Model= Hybrid MIE for dust and propane	ΔE_{Hm}	Methane conc. Vol%	Exp. Hybrid MIE for dust and methane	Model= Hybrid MIE for dust and methane	ΔE_{Hm}
Starch							
1.7	7.44	7.22	0.21	4	4.30	4.24	0.05
1.4	11.33	9.81	1.51	3	12.20	7.47	4.72
1.0	17.16	14.71	2.40	2	15.70	13.17	2.52
0.6	26.06	22.13	3.88	1	22.66	23.20	-0.54
0.0	40.88	40.88	0.00	0	40.88	40.88	0.00
Wheat flour							
1.7	7.40	5.86	1.53	4	11.76	4.73	7.02
1.4	7.58	7.80	-0.22	3	14.09	6.43	7.65
1.0	13.23	11.44	1.78	2	14.57	10.71	3.85
0.6	20.94	16.77	4.16	1	18.55	17.86	0.68
0.0	29.77	29.77	0.00	0	29.77	29.77	0.00
Protein							
1.7	10.89	5.82	5.06	4	8.45	6.45	1.99
1.4	12.24	9.38	2.85	3	12.64	12.36	0.27
1.0	22.82	17.72	5.09	2	17.3	23.69	-6.39
0.6	40.34	33.49	6.84	1	33.98	45.40	-11.42
0.0	87.00	87.00	0.00	0	87.00	87.00	0.00
Polypropylene							
1.7	7.92	6.03	1.88	4	4.44	5.39	-0.95
1.4	9.97	10.18	-0.21	3	9.12	11.63	-2.51
1.0	22.71	20.43	2.27	2	30.41	25.09	5.31
0.6	39.85	41.01	-1.16	1	46.04	54.08	-8.04
0.0	116.6	116.6	0.00	0	116.6	116.60	0.00
Dextrin							
1.7	12.74	12.16	0.57	4	6.38	6.33	0.04
1.4	15.85	17.31	-1.46	3	10.69	12.30	-1.61
1.0	42.35	27.73	14.60	2	27.24	23.88	3.35
0.6	54.13	44.41	9.71	1	50.9	46.36	4.53
0.0	90.00	90.00	0.00	0	90.00	90.00	0.00
Peat coal							
1.7	8.46	7.37	1.08	4	3.53	3.04	0.48
1.4	12.74	10.19	2.54	3	6.06	6.00	0.05
1.0	15.85	15.71	0.13	2	8.46	11.86	3.40
0.6	21.94	24.20	-2.26	1	22.4	23.43	-1.03
0.0	46.29	46.29	0.00	0	46.29	46.29	0.00
Char coal							
1.7	10.40	13.94	-3.53	4	18.40	17.05	1.34
1.4	50.10	26.23	23.86	3	58.00	39.68	18.31
1.0	70.00	60.89	9.10	2	171.00	92.34	78.65
0.6	160.00	141.36	18.63	1	354.00	214.87	139.1
0.0	500.00	500.00	0.00	0	500.00	500.00	0.00
Brown coal							
1.7	7.75	6.33	1.41	4	4.30	3.54	0.75
1.4	10.05	7.56	2.48	3	5.12	5.26	-0.14
1.0	11.30	9.56	1.73	2	8.43	7.81	0.61
0.6	14.85	12.11	2.73	1	13.60	11.60	1.99
0.0	17.24	17.24	0.00	0	17.20	17.24	0.00

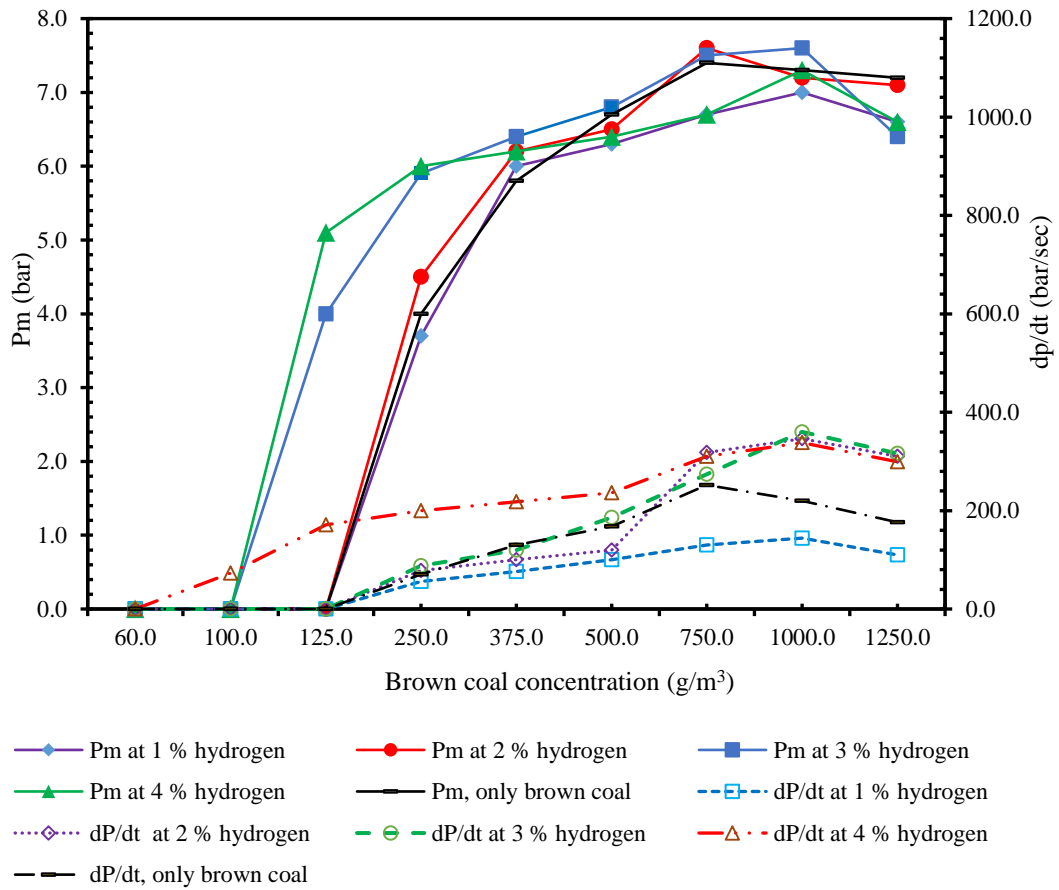


Figure B.1 Explosion overpressure and pressure rise with time for hybrid mixtures of hydrogen and brown coal.

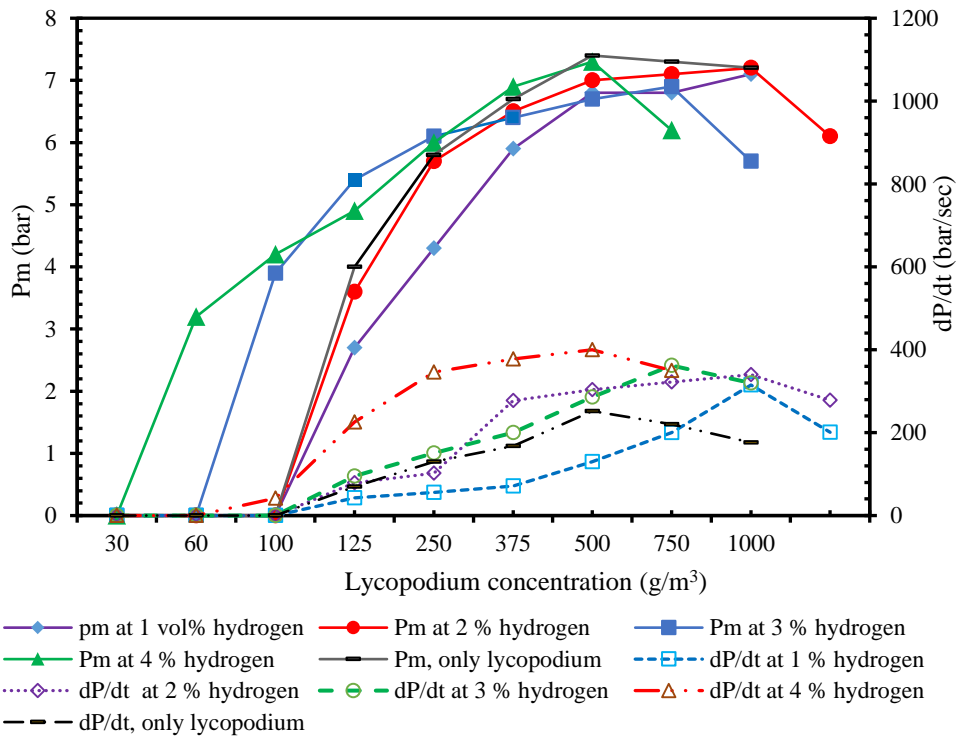


Figure B.2: Explosion overpressure and pressure rise with time for hybrid mixtures of hydrogen and lycopodium.

B: Experimental results for dust and spray hybrid mixture.

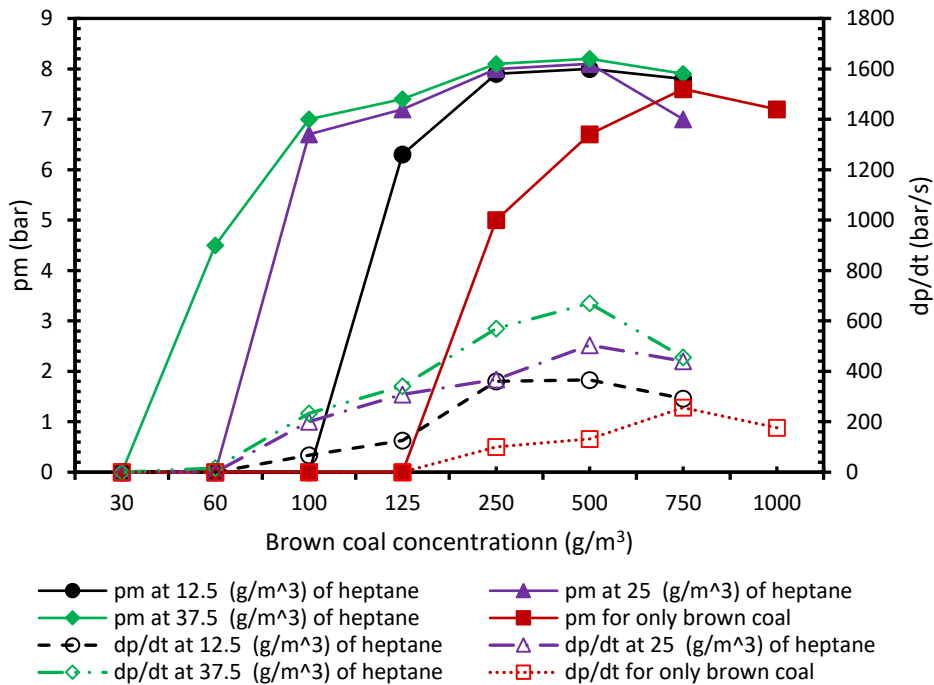


Figure B.3: Explosion overpressure and pressure rise with time for hybrid mixtures of heptane and brown coal.

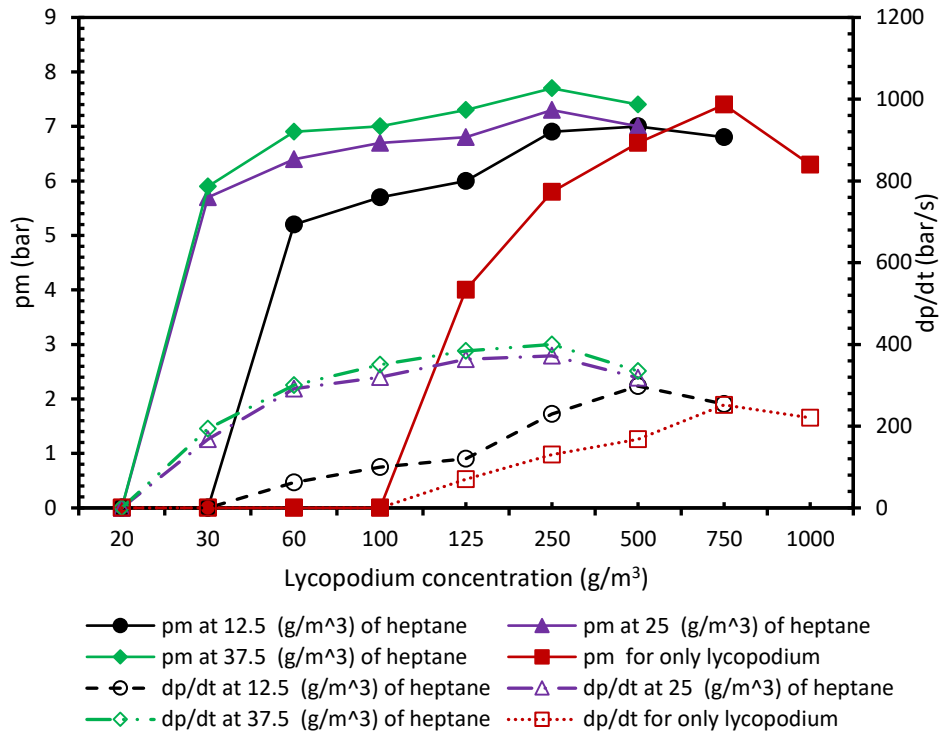


Figure B.4: Explosion overpressure and pressure rise with time for hybrid mixtures of heptane and lycopodium.

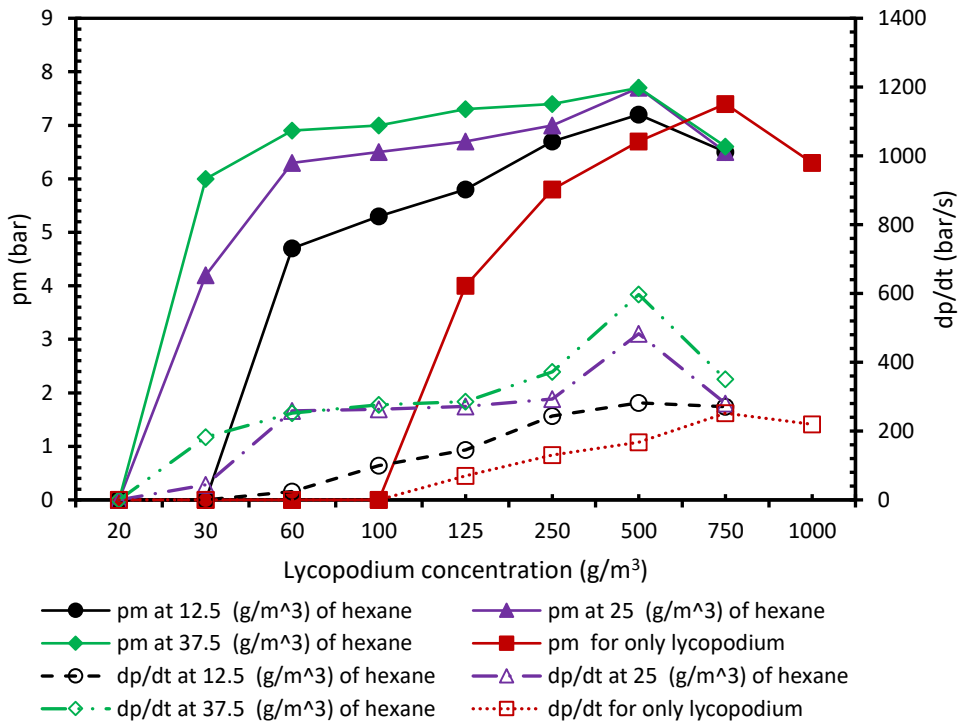


Figure B.5: Explosion overpressure and pressure rise with time for hybrid mixtures of hexane and lycopodium.

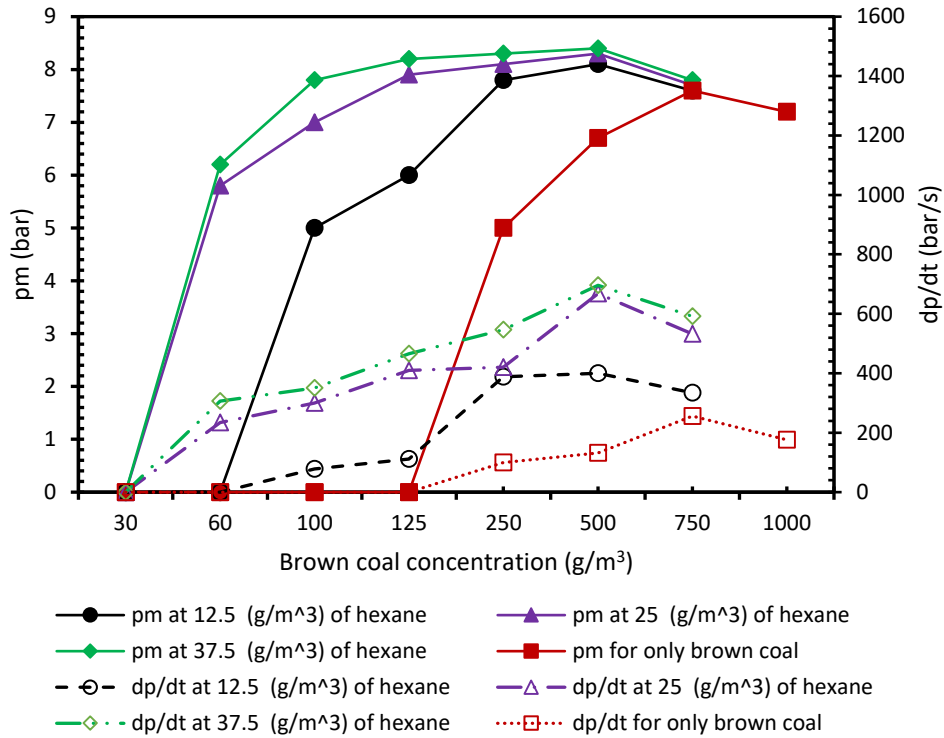


Figure B.6: Explosion overpressure and pressure rise with time for hybrid mixtures of hexane and brown coal.

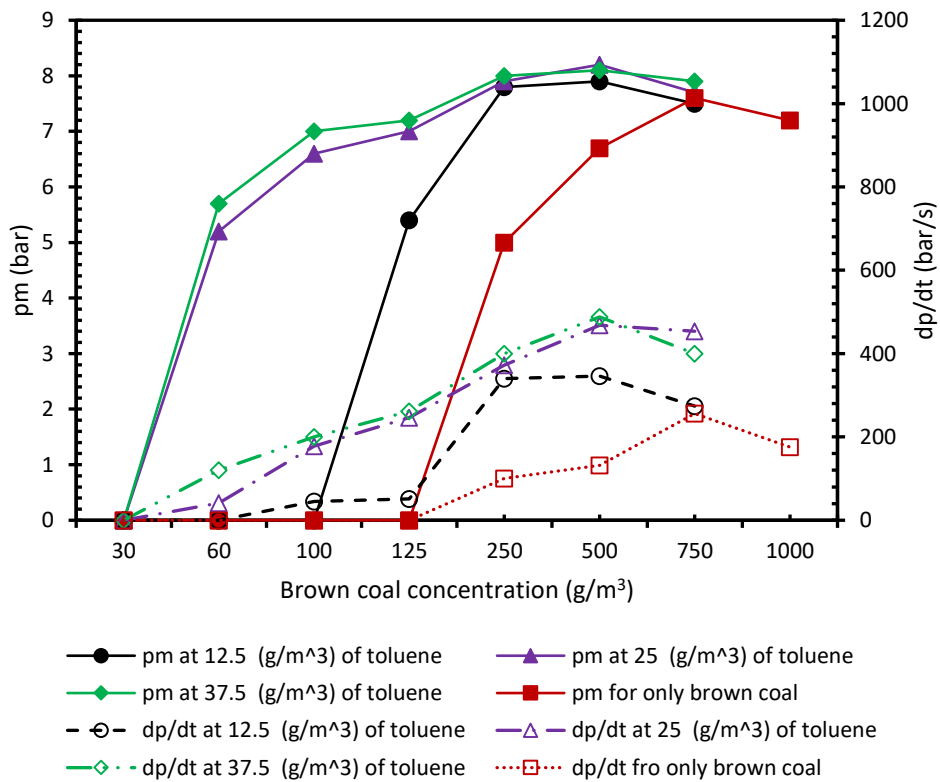


Figure B.7: Explosion overpressure and pressure rise with time for hybrid mixtures of toluene and brown coal.

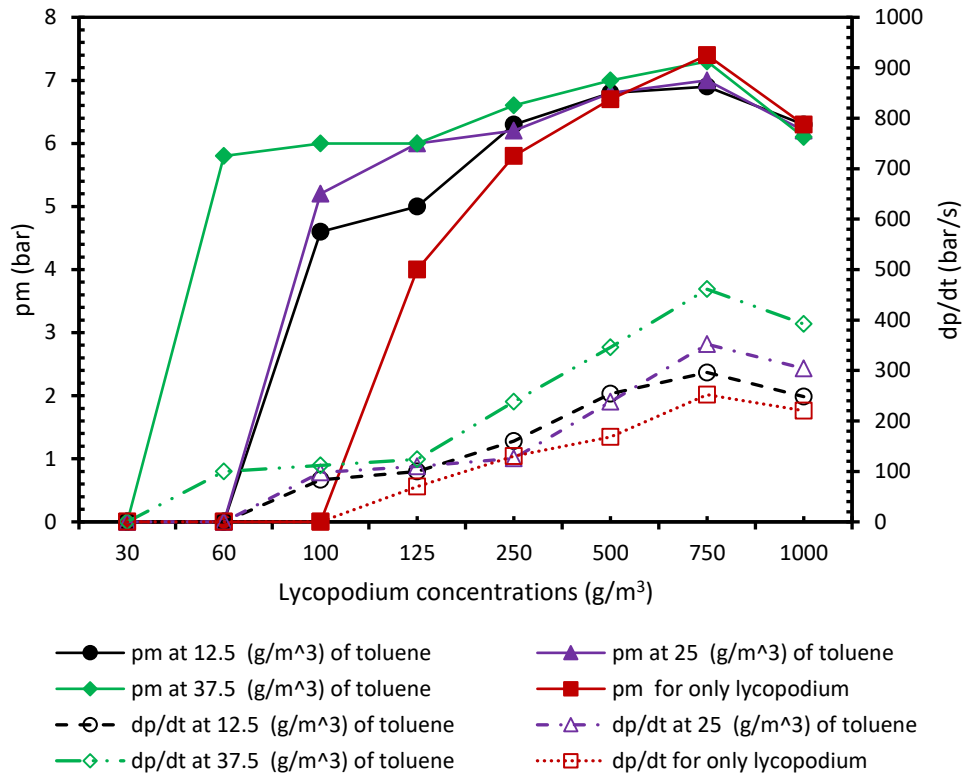


Figure B.8: Explosion overpressure and pressure rise with time for hybrid mixtures of toluene and lycopodium.

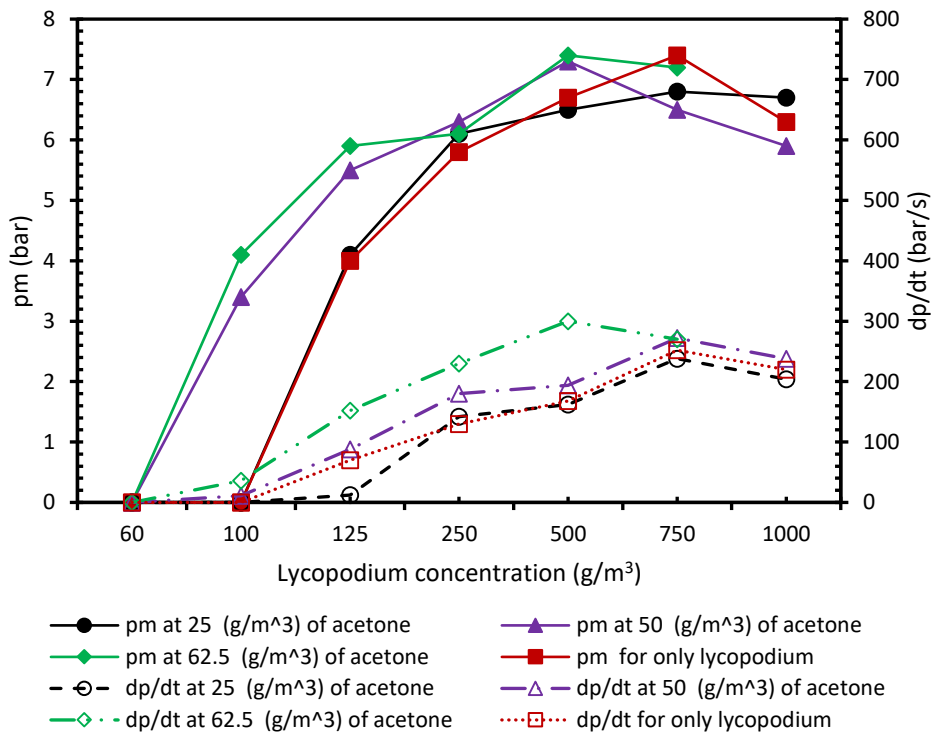


Figure B.9: Explosion overpressure and pressure rise with time for hybrid mixtures of acetone and lycopodium.

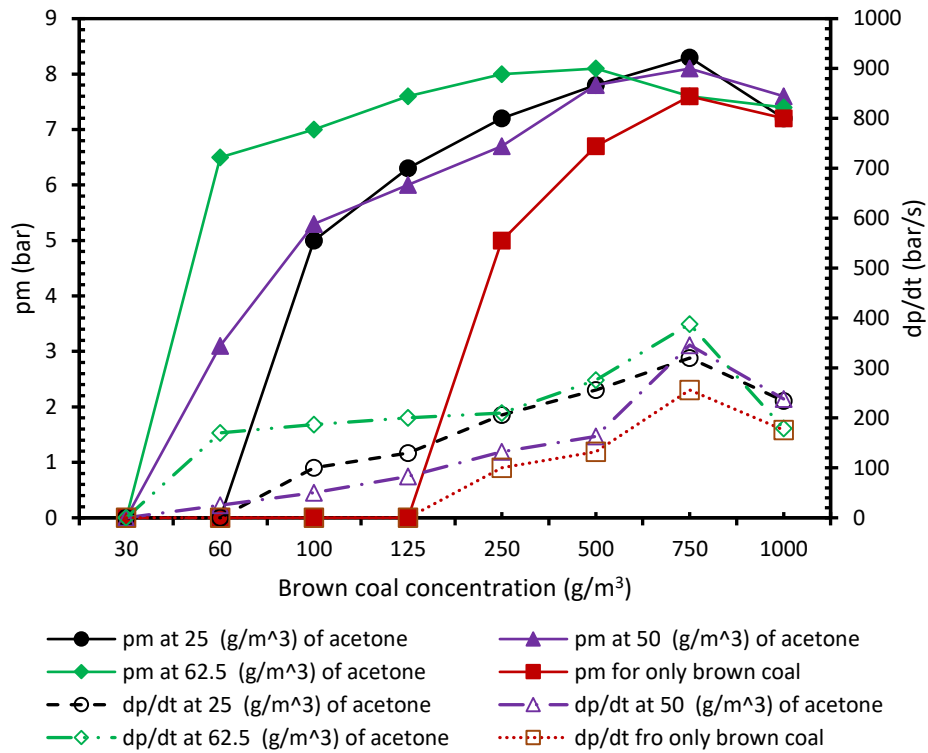


Figure B.10: Explosion overpressure and pressure rise with time for hybrid mixtures of acetone and brown coal.

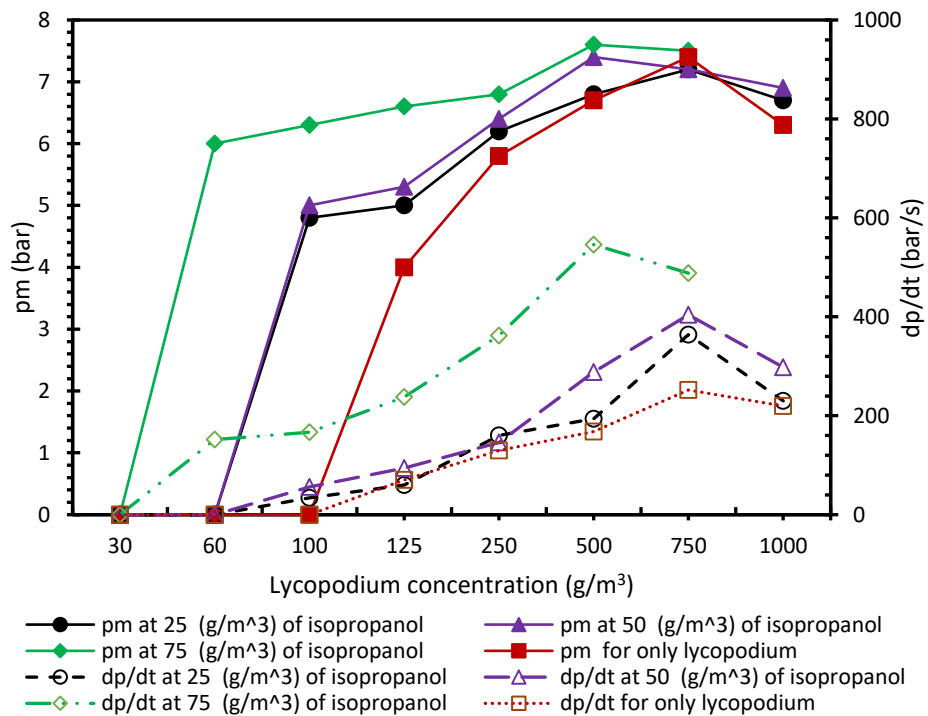


Figure B.11: Explosion overpressure and pressure rise with time for hybrid mixtures of isopropanol and lycopodium.

B.3 Experimental results for gas and spray hybrid mixture.

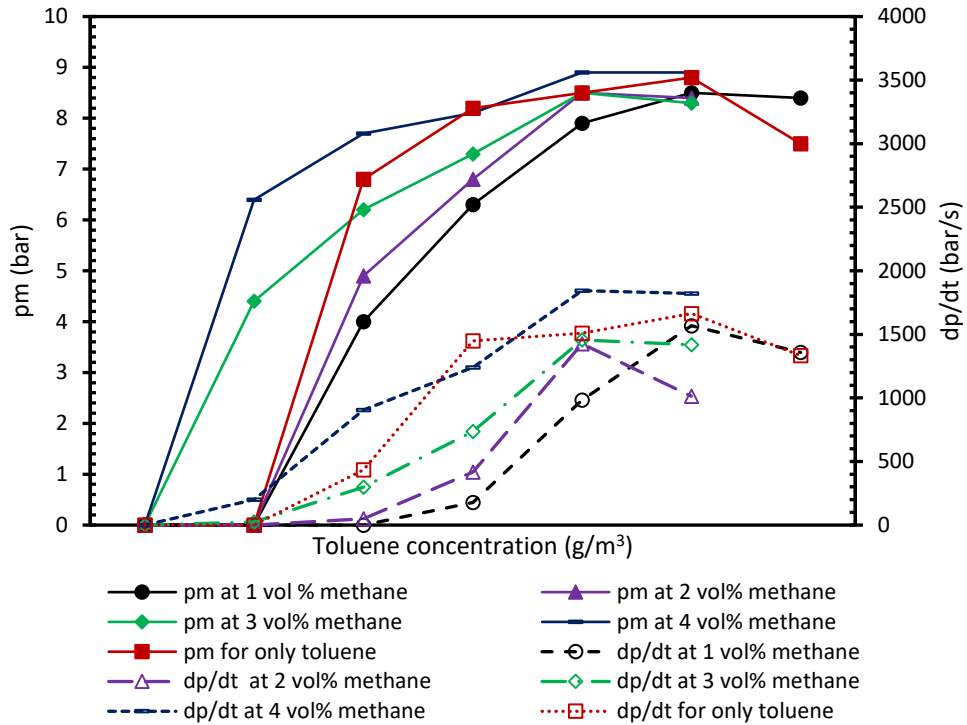


Figure B.12: Explosion overpressure and pressure rise with time for hybrid mixtures of methane and toluene.

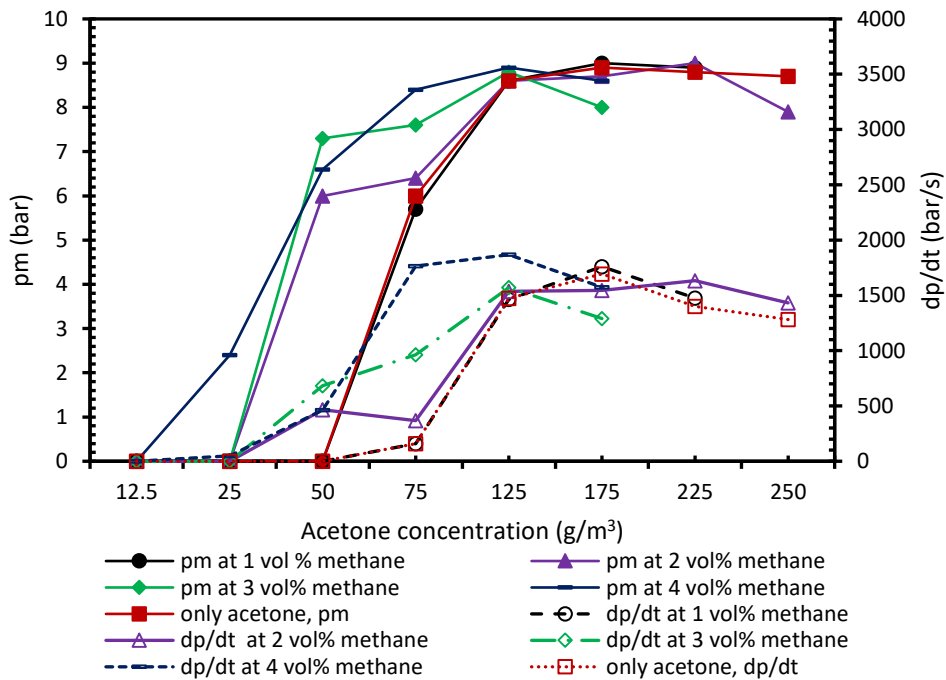


Figure B.13: Explosion overpressure and pressure rise with time for hybrid mixtures of methane and acetone.

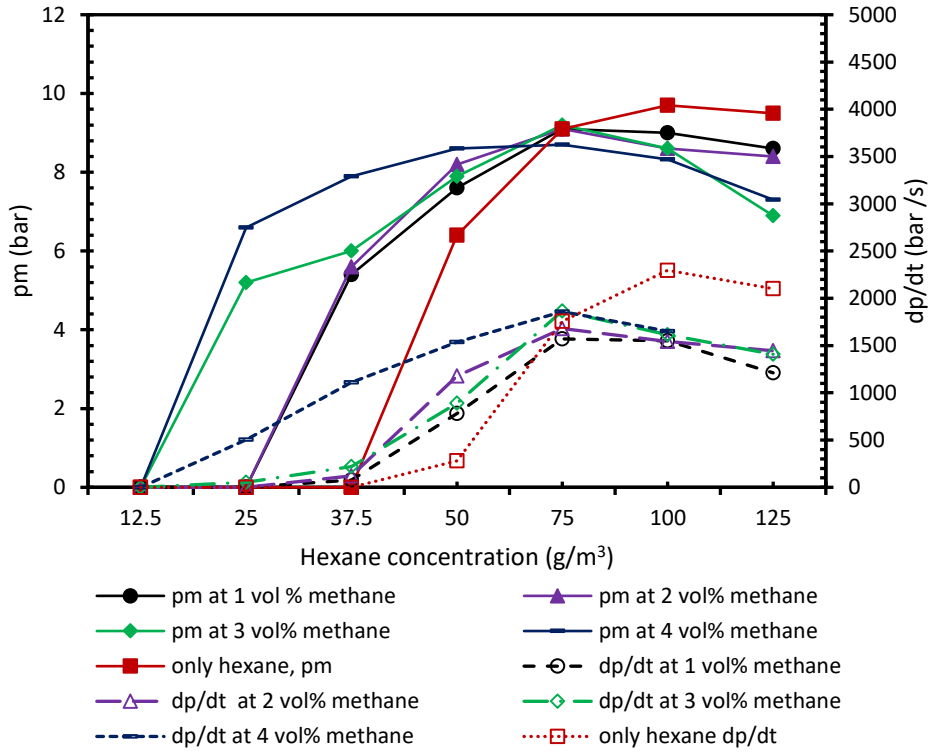


Figure B.14: Explosion overpressure and pressure rise with time for hybrid mixtures of methane and hexane.

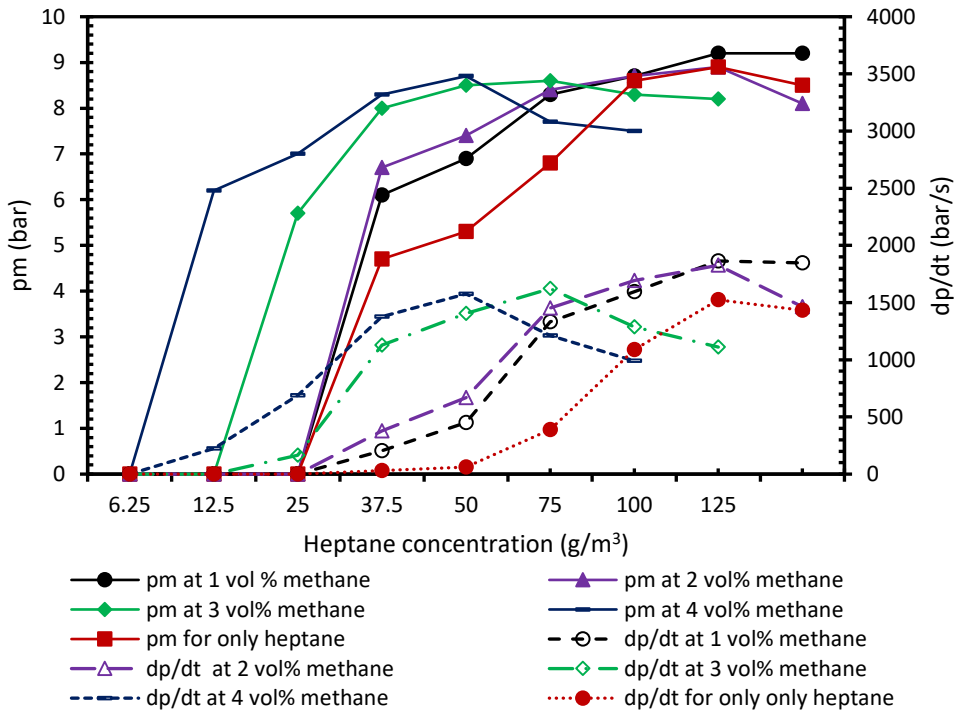


Figure B.15: Explosion overpressure and pressure rise with time for hybrid mixtures of methane and heptane.

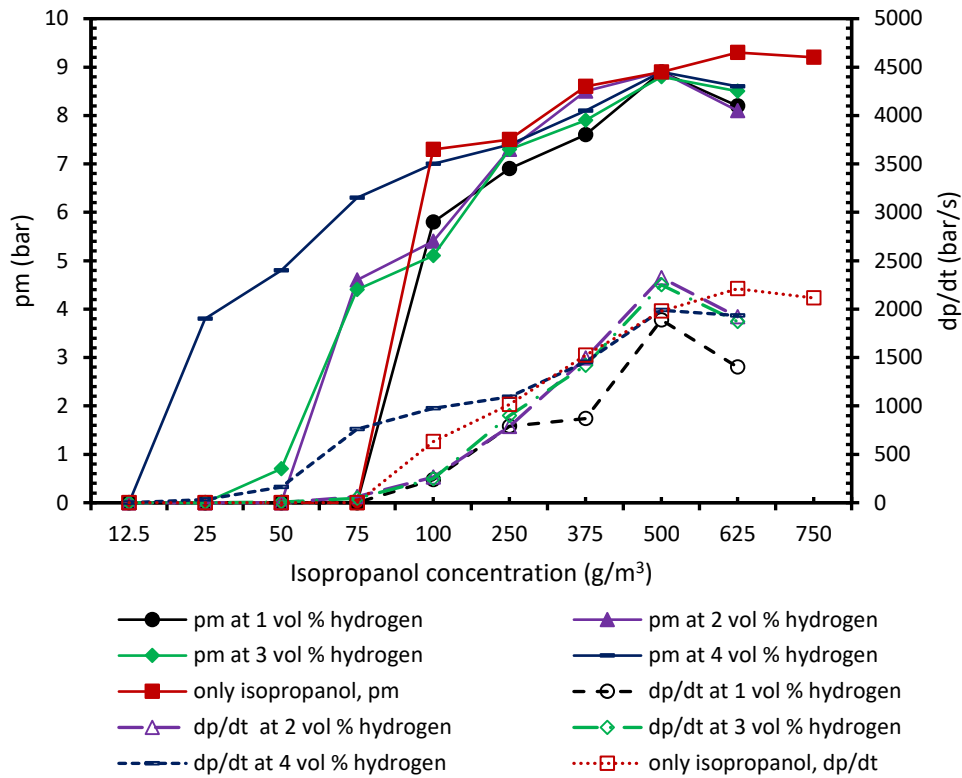


Figure B.16: Explosion overpressure and pressure rise with time for hybrid mixtures of hydrogen and isopropanol.

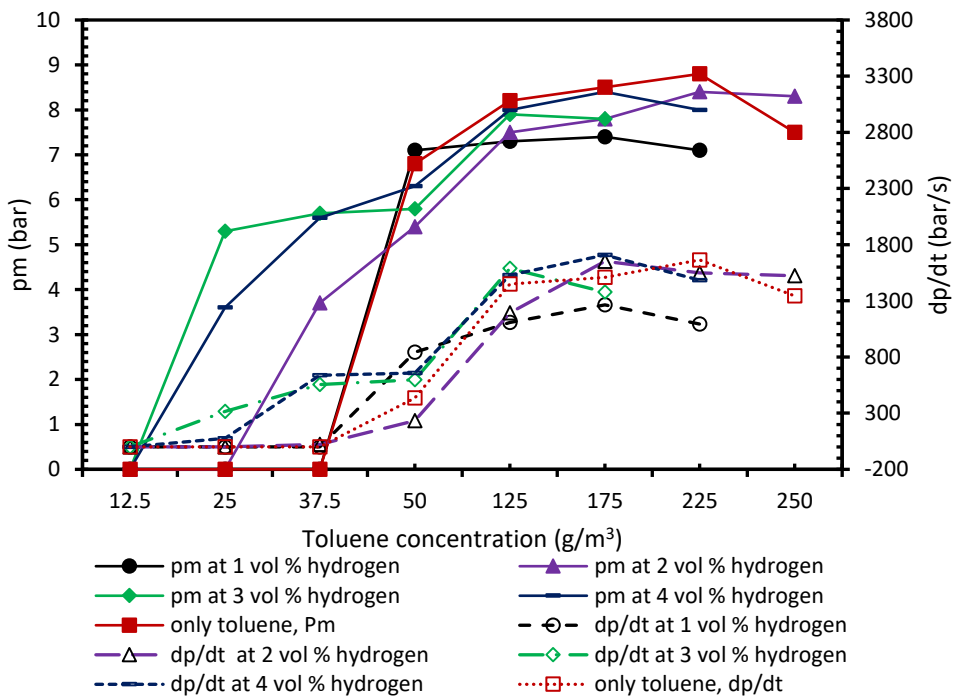


Figure B.17: Explosion overpressure and pressure rise with time for hybrid mixtures of hydrogen and toluene.

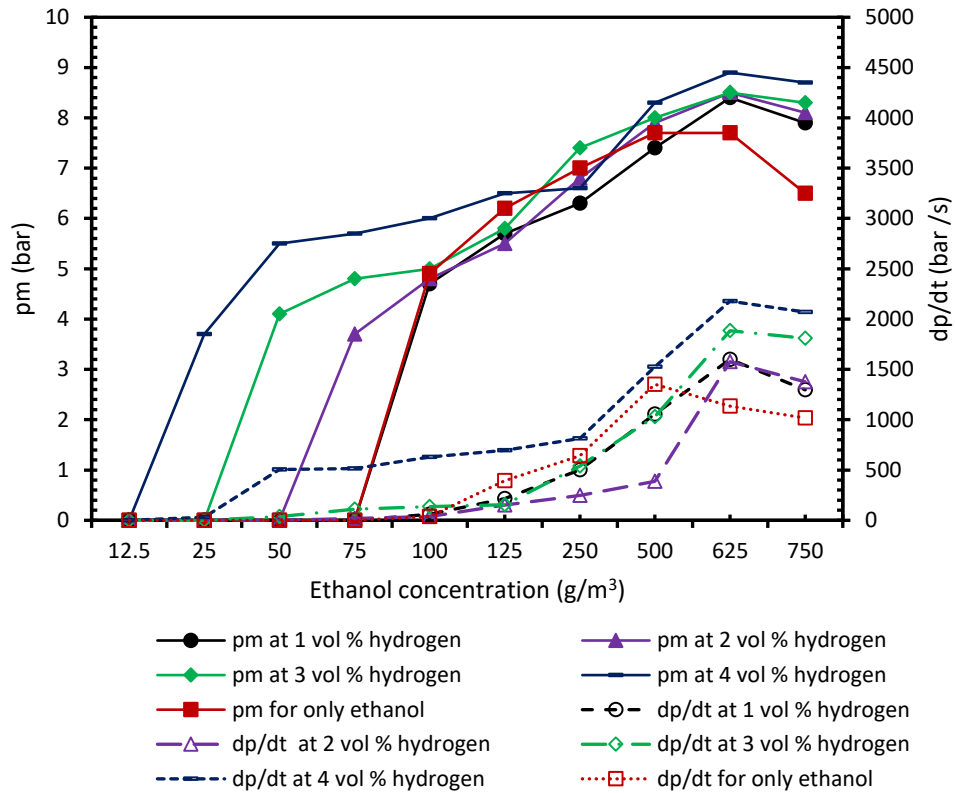


Figure B.18: Explosion overpressure and pressure rise with time for hybrid mixtures of hydrogen and ethanol.

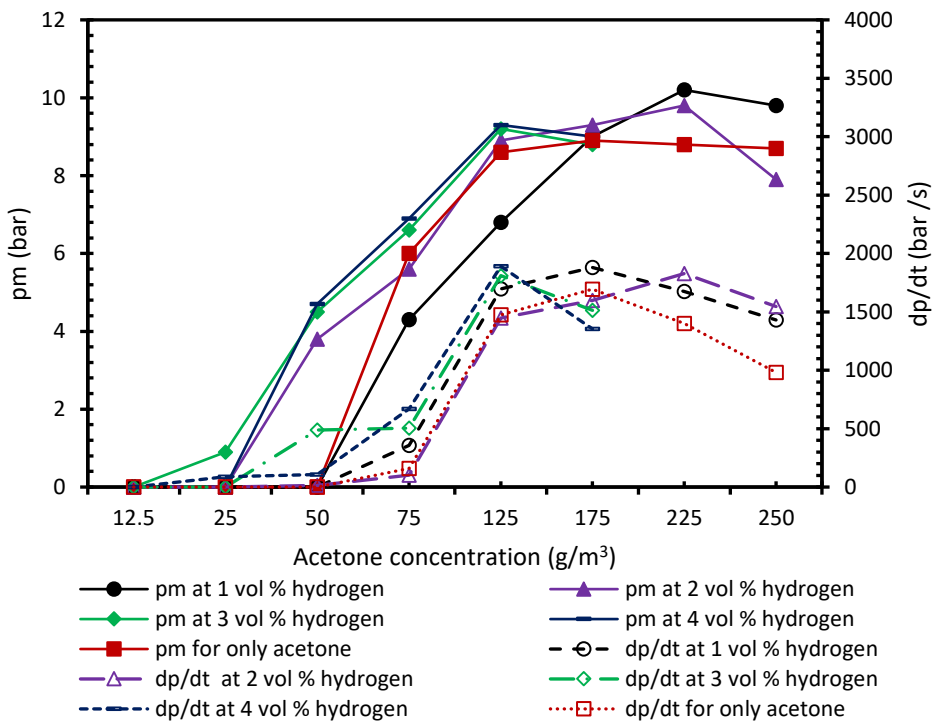


Figure B.19: Explosion overpressure and pressure rise with time for hybrid mixtures of hydrogen and acetone.

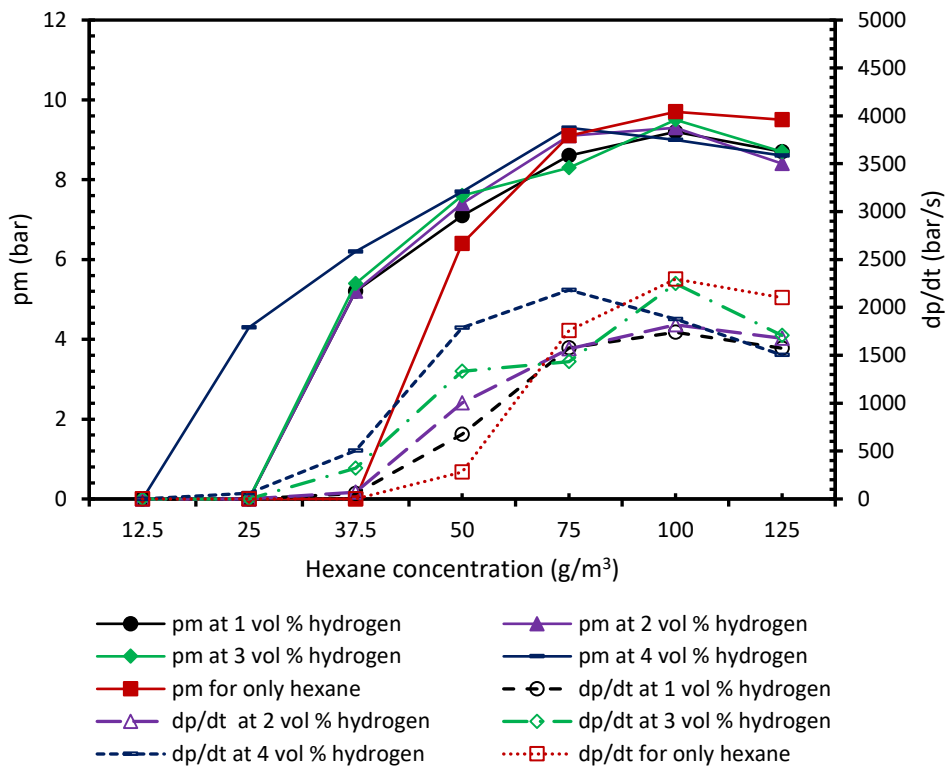


Figure B.20: Explosion overpressure and pressure rise with time for hybrid mixtures of hydrogen and hexane.

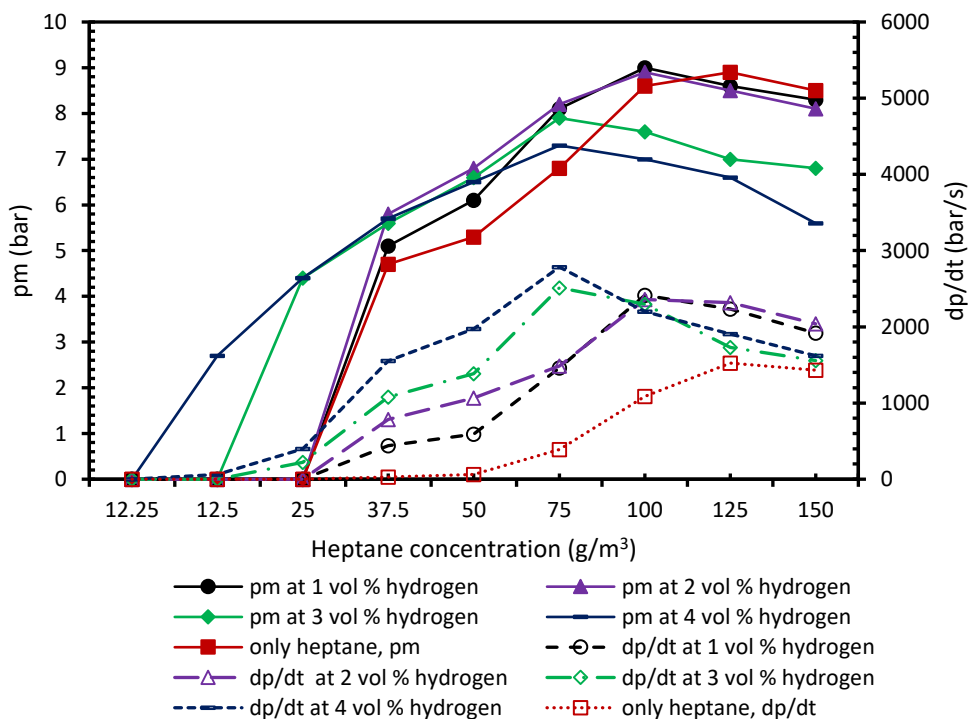


Figure B.21: Explosion overpressure and pressure rise with time for hybrid mixtures of hydrogen and heptane.

B.4 Three-phase hybrid mixtures test results

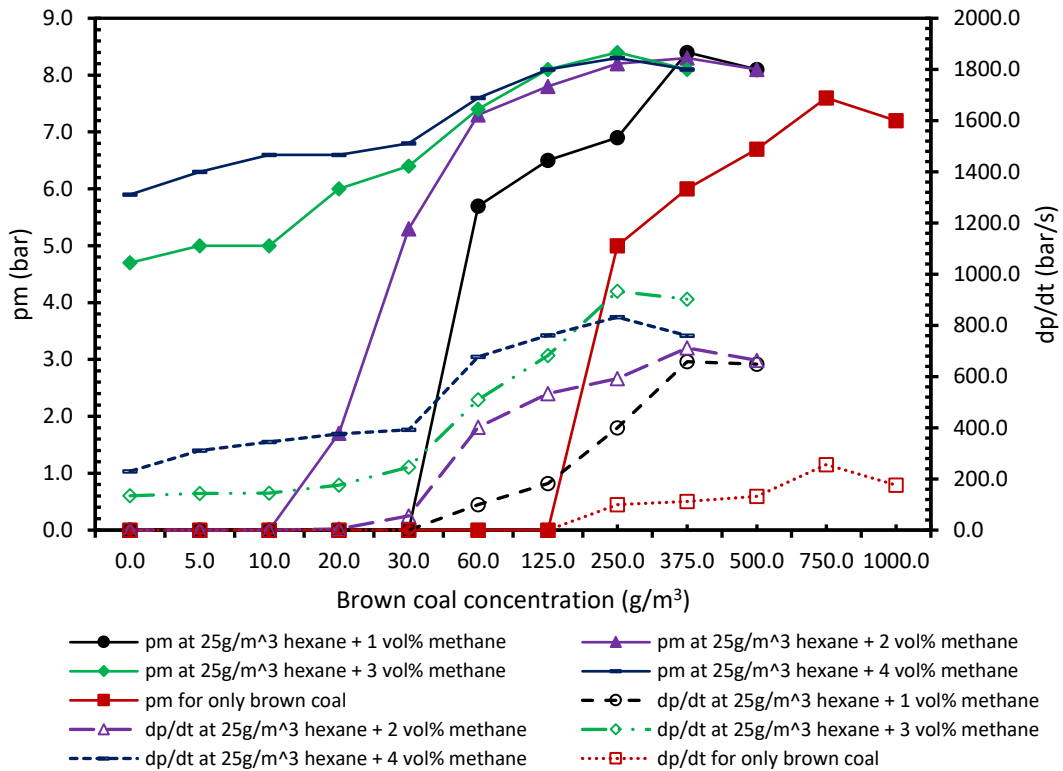


Figure B.22: Maximum explosion pressure and rate of pressure rise of mixtures of brown coal, methane and 25 g/m³ of hexane spray.

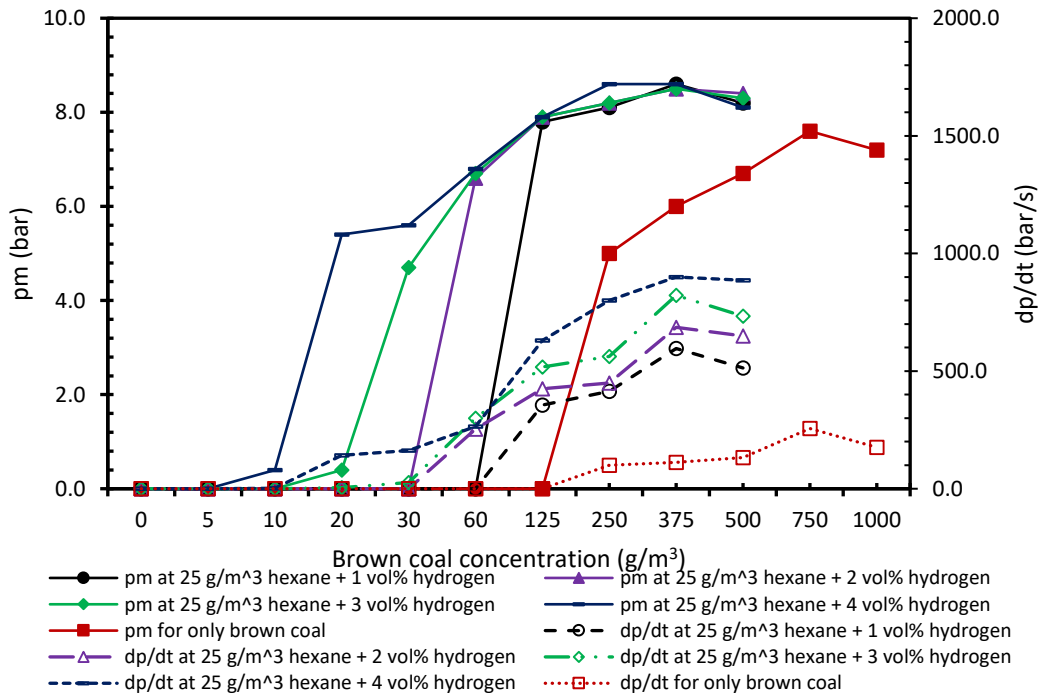


Figure B.23: Maximum explosion pressure and rate of pressure rise of mixtures of brown coal, hydrogen and 25 g/m³ of hexane spray.

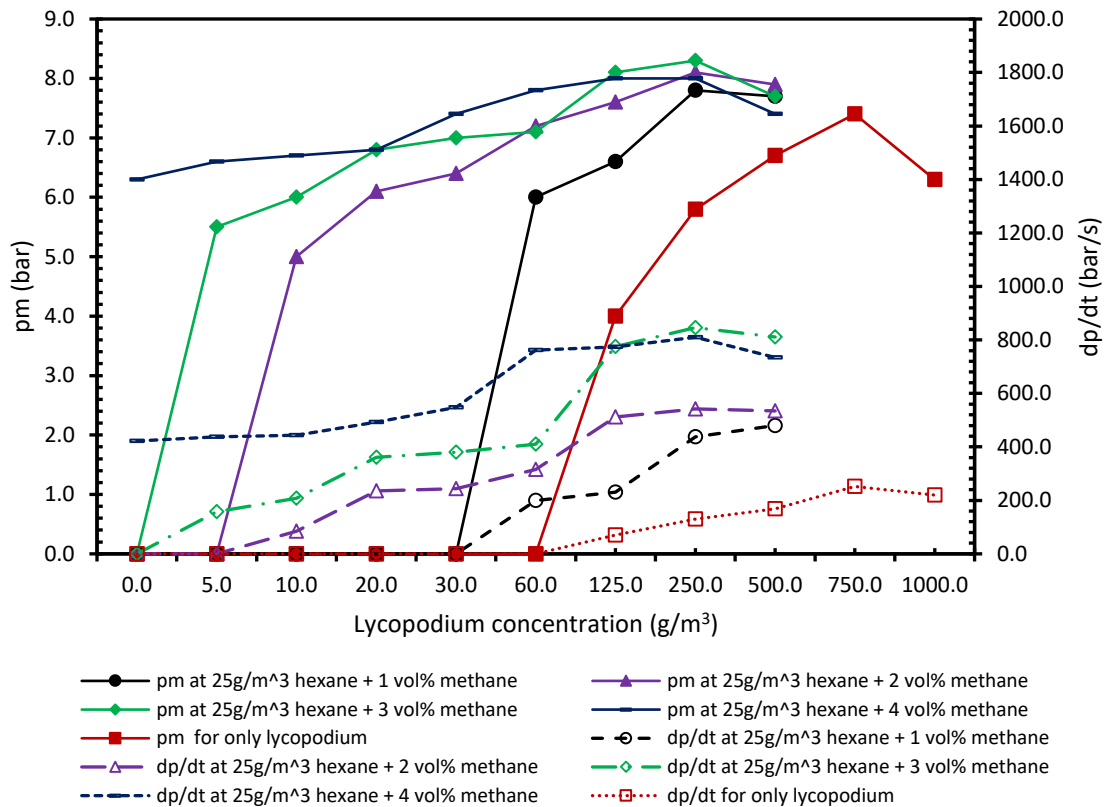


Figure B.24: Maximum explosion pressure and rate of pressure rise of mixtures of lycopodium, methane and 25 g/m³ of methane spray.

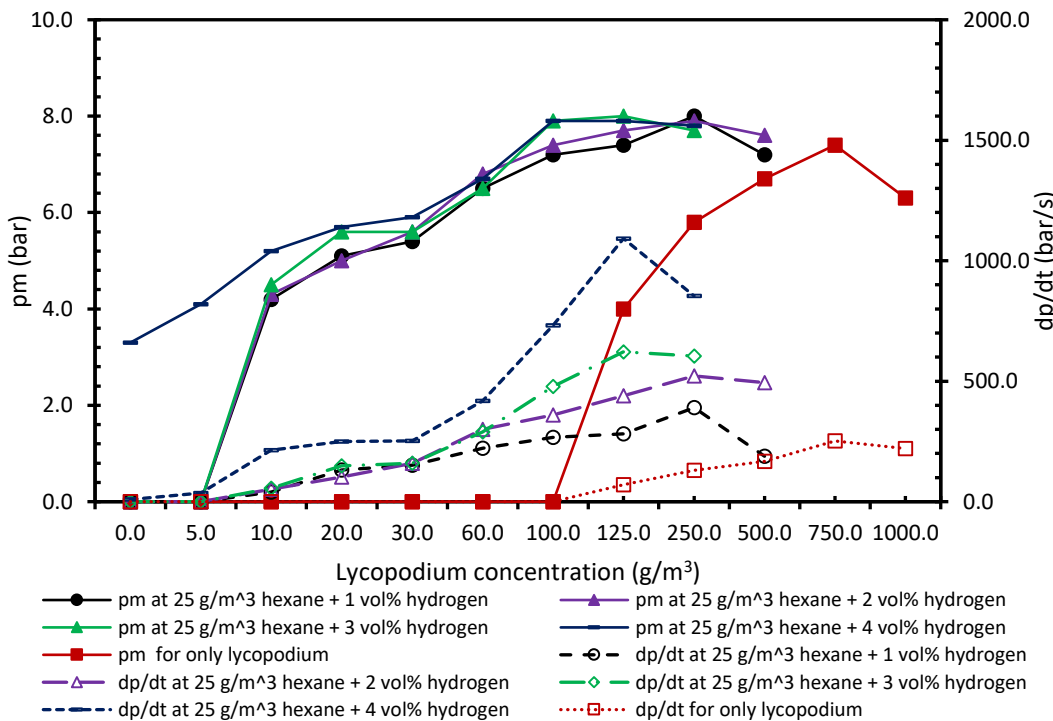


Figure B.25: Maximum explosion pressure and rate of pressure rise of mixtures of lycopodium, hydrogen and 25 g/m³ of hexane spray.

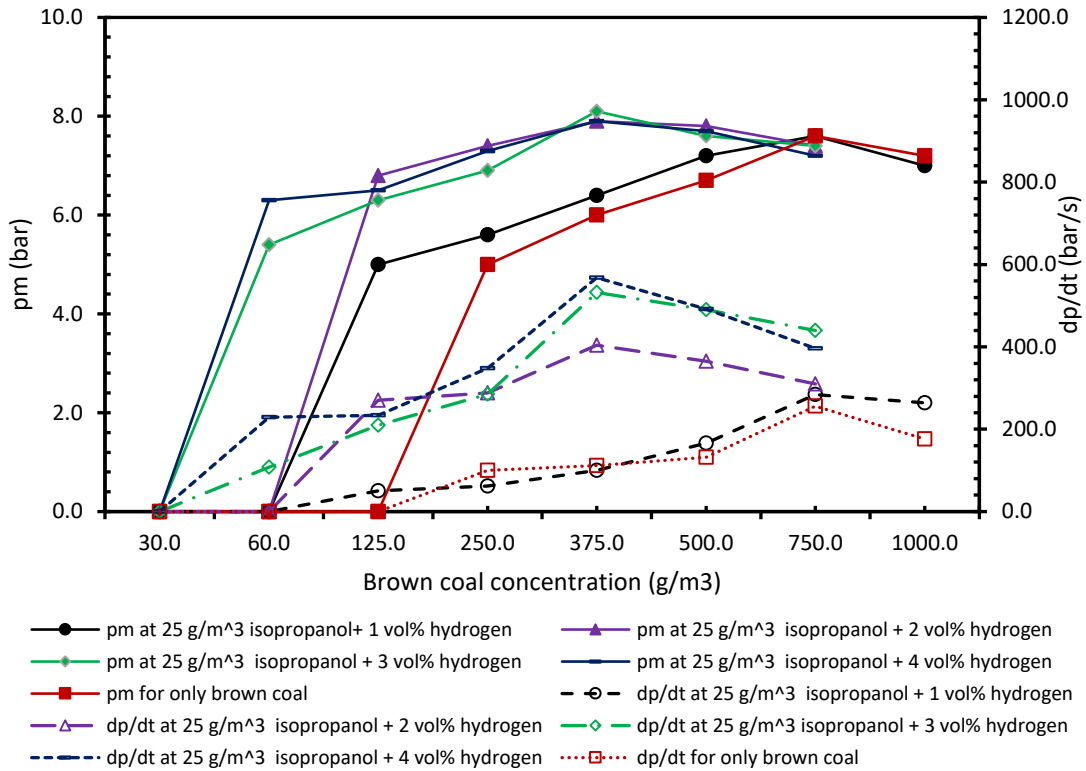


Figure B.26: Maximum explosion pressure and rate of pressure rise of mixtures of brown coal, hydrogen and 25 g/m³ of isopropanol spray.

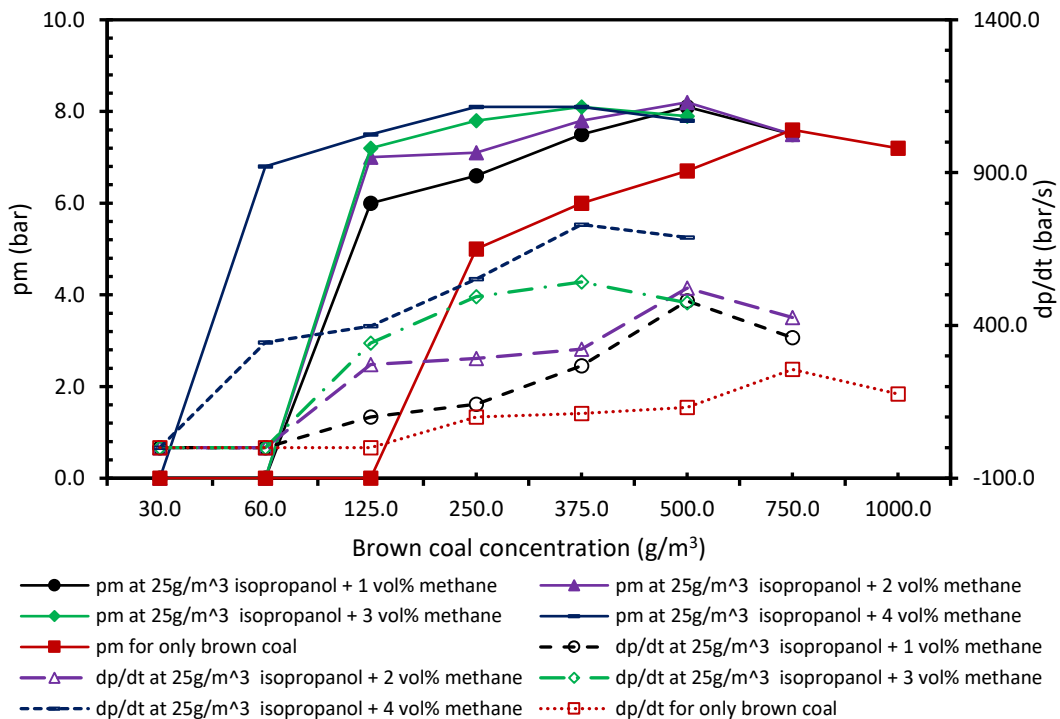


Figure B.27: Maximum explosion pressure and rate of pressure rise of mixtures of brown coal, methane and 25 g/m³ of isopropanol spray.

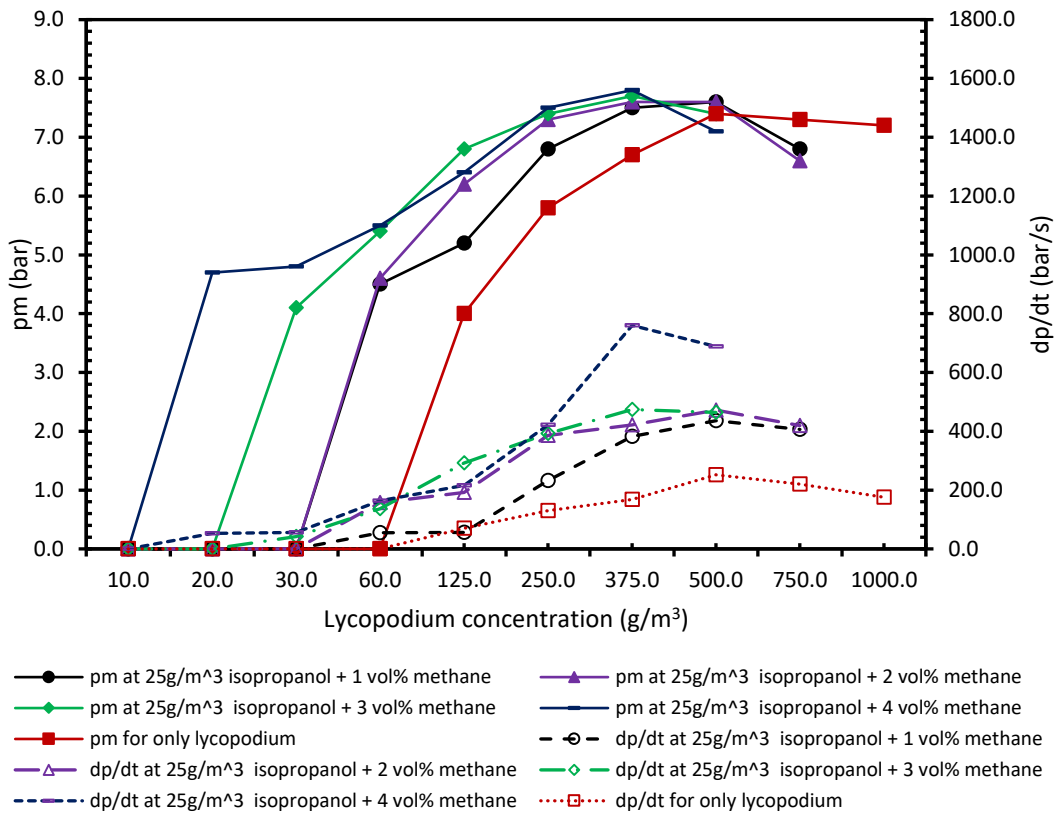


Figure B.28: Maximum explosion pressure and rate of pressure rise of mixtures of lycopodium, methane and 25 g/m³ of isopropanol spray.

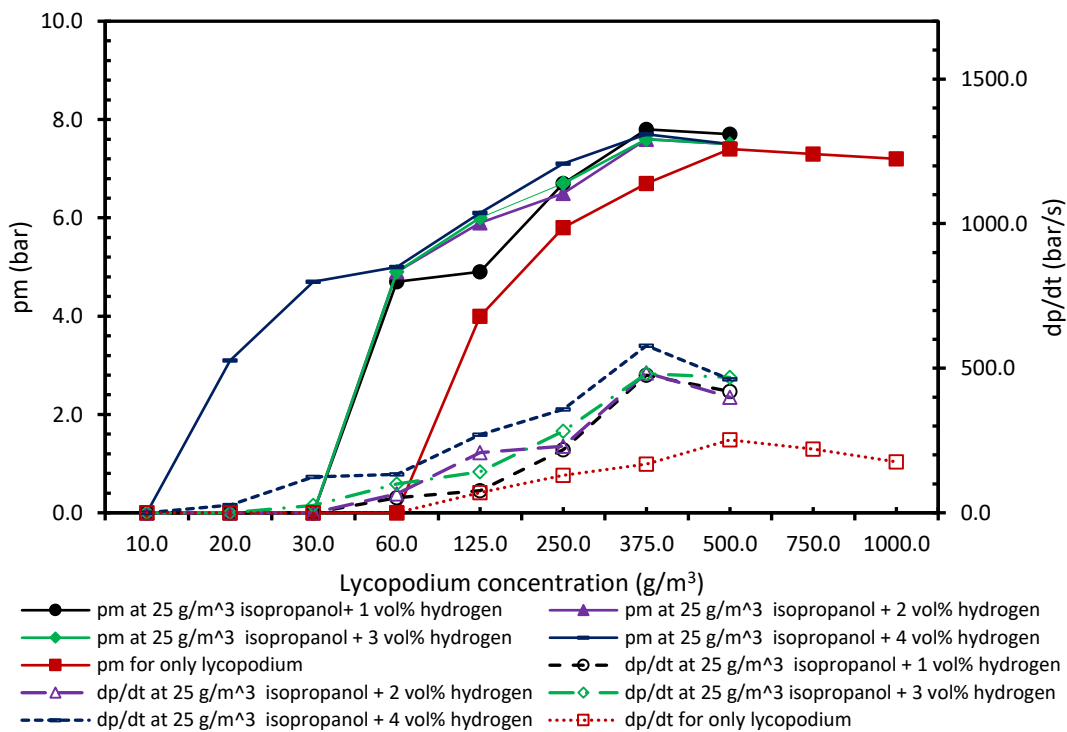


Figure B.29: Maximum explosion pressure and rate of pressure rise of mixtures of lycopodium, hydrogen and 25 g/m³ of isopropanol spray.

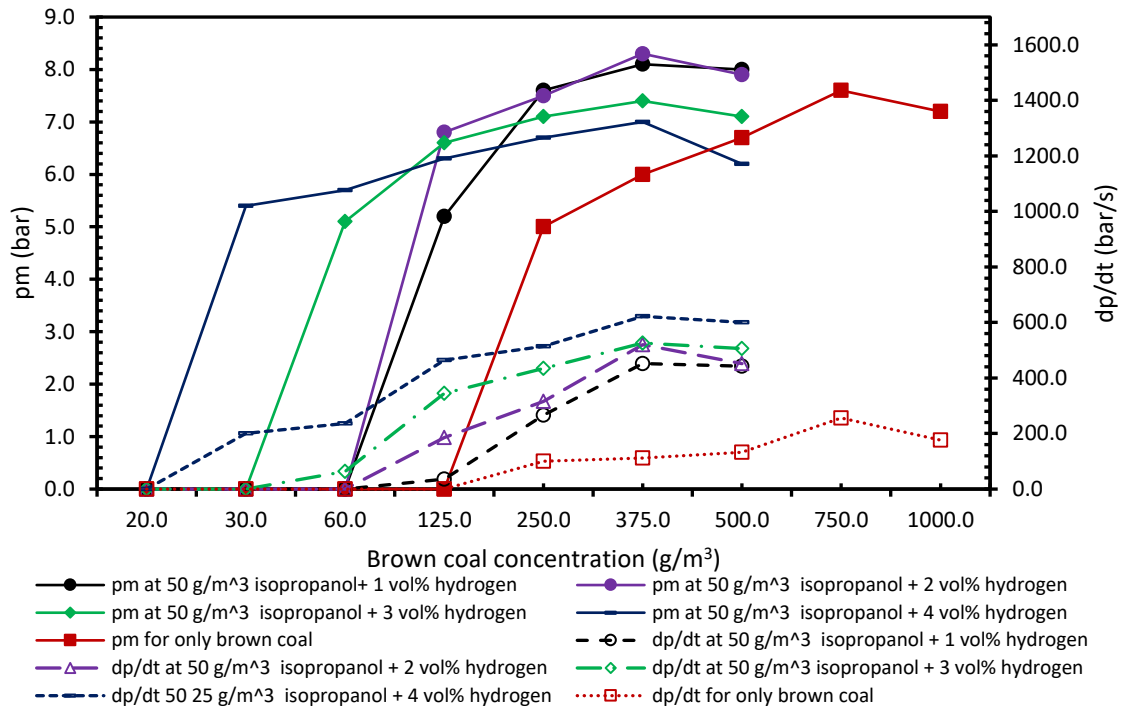


Figure B.30: Maximum explosion pressure and rate of pressure rise of mixtures of brown coal, hydrogen and 50 g/m³ of isopropanol spray.

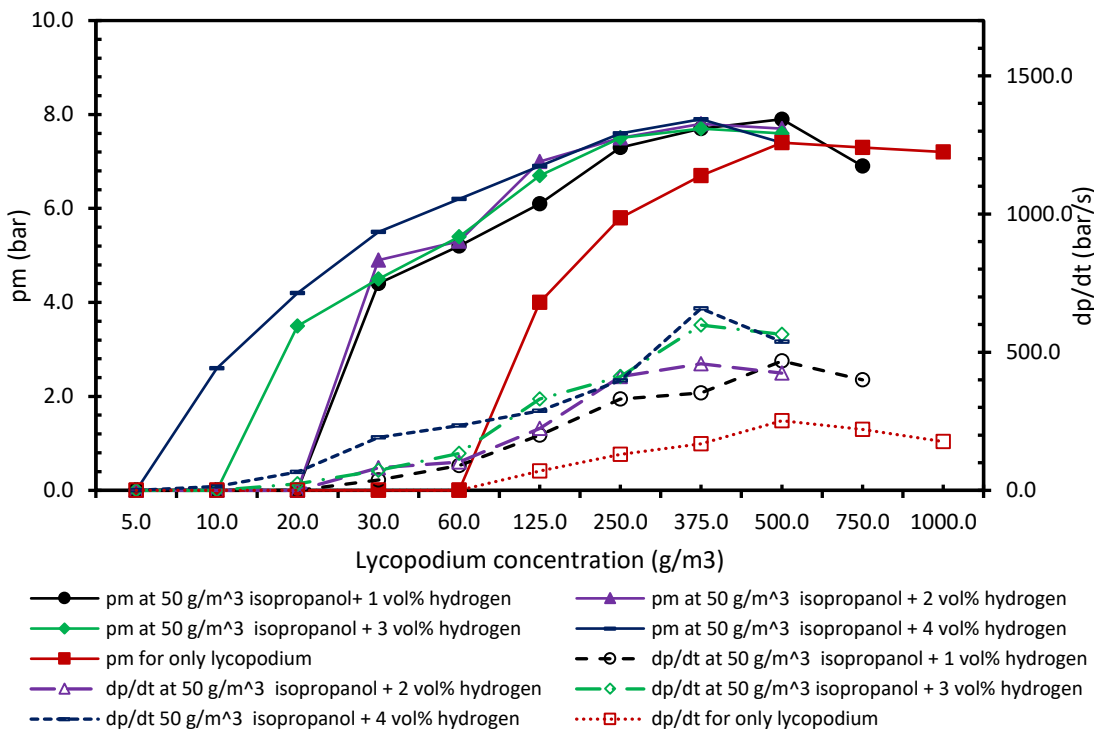


Figure B.31: Maximum explosion pressure and rate of pressure rise of mixtures of lycopodium, hydrogen and 50 g/m³ of isopropanol spray.

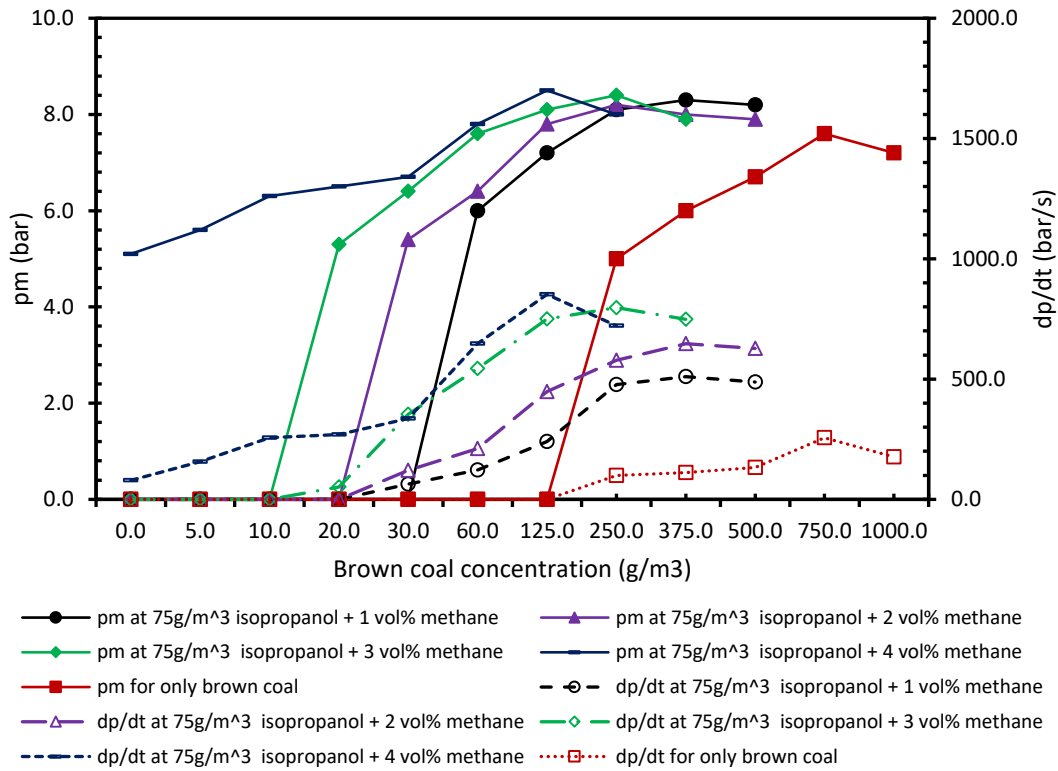


Figure B.32: Maximum explosion pressure and rate of pressure rise of mixtures of brown coal, hydrogen and 75 g/m³ of isopropanol spray.

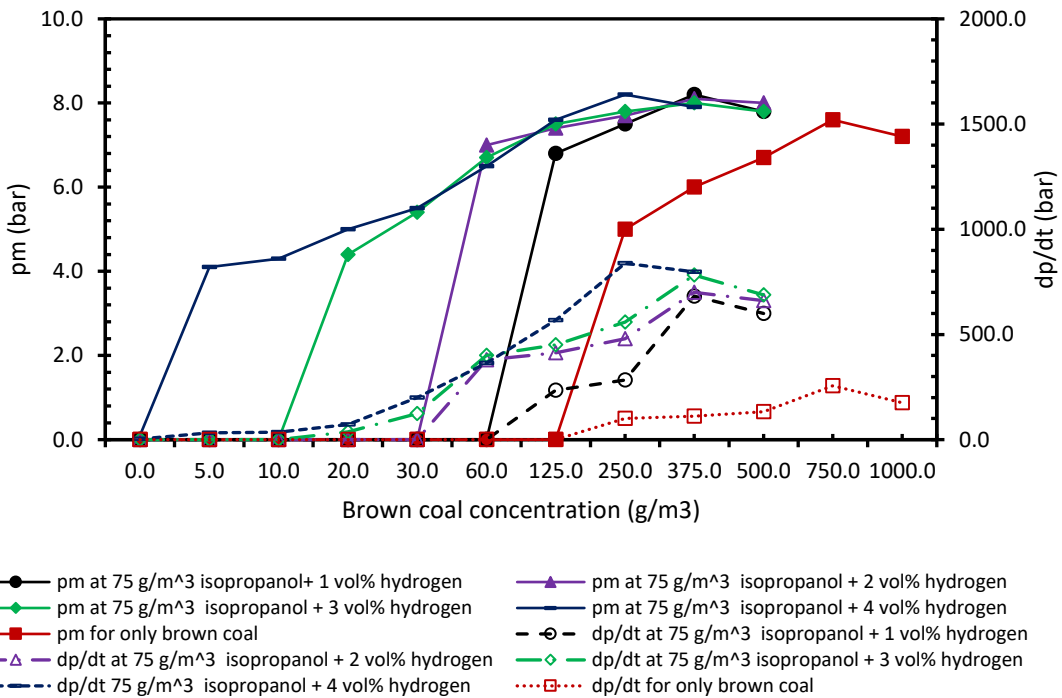


Figure B.33: Maximum explosion pressure and rate of pressure rise of mixtures of brown coal, hydrogen and 75 g/m³ of isopropanol spray.

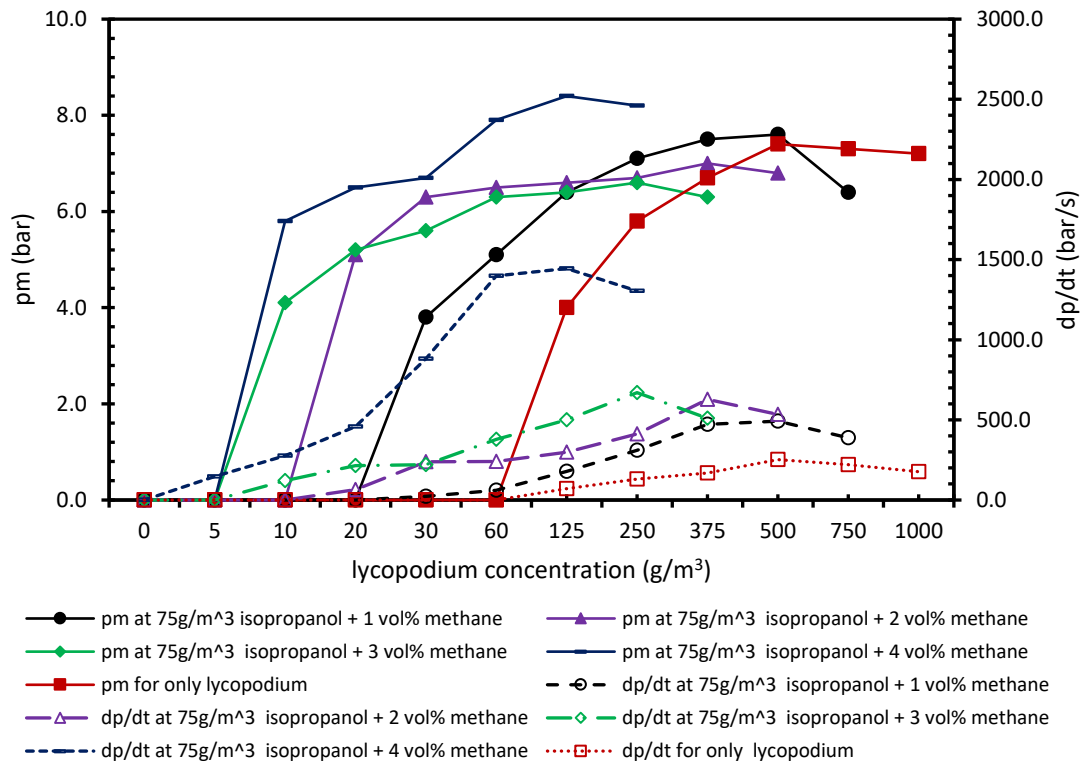


Figure B.34: Maximum explosion pressure and rate of pressure rise of mixtures of lycopodium, hydrogen and 75 g/m³ of isopropanol spray.

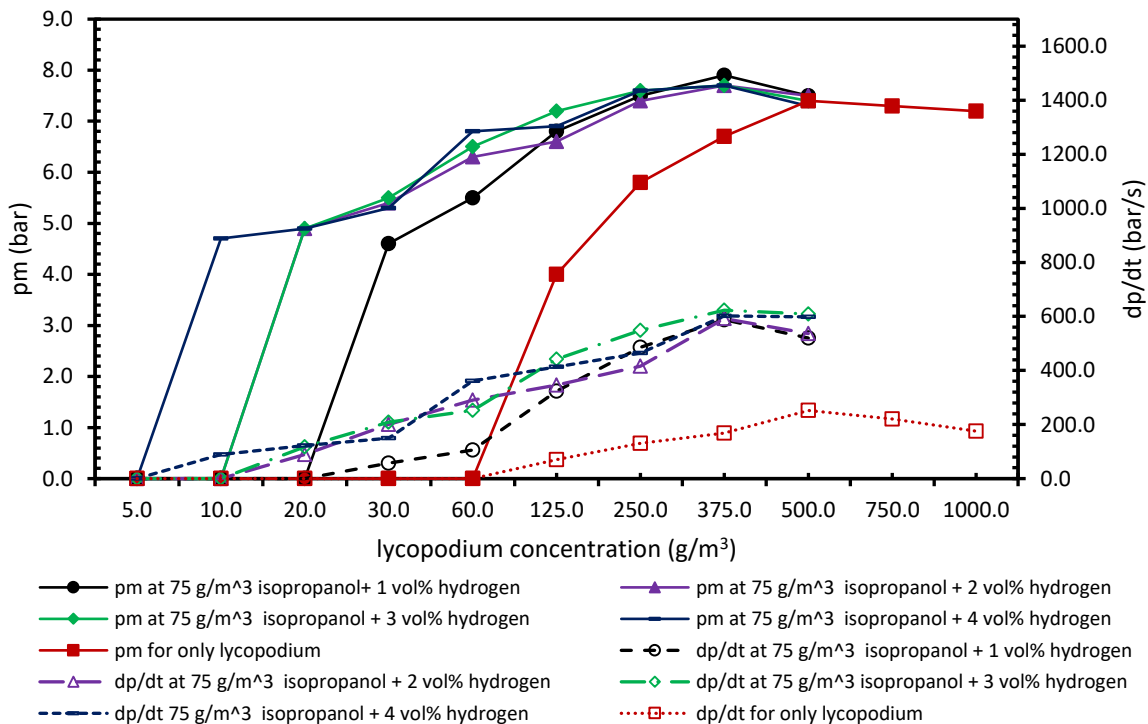


Figure B.35: Maximum explosion pressure and rate of pressure rise of mixtures of lycopodium, hydrogen and 75 g/m³ of isopropanol spray.

B.5 Comparisons between hybrid mixture models and the experimental results.

Figures B. 26 to B.27 present comparisons between the experimental results on the lower explosion limits of hybrid mixtures and mathematical models of Le Chatelier's, Bartknecht, Sam Mannan et al. (see section 3.2.1.3 for detail discussion of these models). The diagrams have the relative concentration of gas and dust on both axes. The X-axis represents the gas concentration used in the experiment divided by the LEL of gas (y/LEL) and the Y-axis shows the dust concentration used in the experiment divided by the MEC of dust (c/MEC). For these explosible limits, the measured values of the pure substances in the experimental setup were used instead of the literature values. The solid dots represent ignition, while the empty circle symbolizes no ignition. The Le Chatelier's equation is indicated by a green straight line, Bartknecht's equation is indicated by a red dashed curve below Le Chatelier's while, the Sam Mannan et al. equation is indicated by a violet dashed curve above Le Chatelier's line. These curves delimit the explosion region versus the non-explosible region.

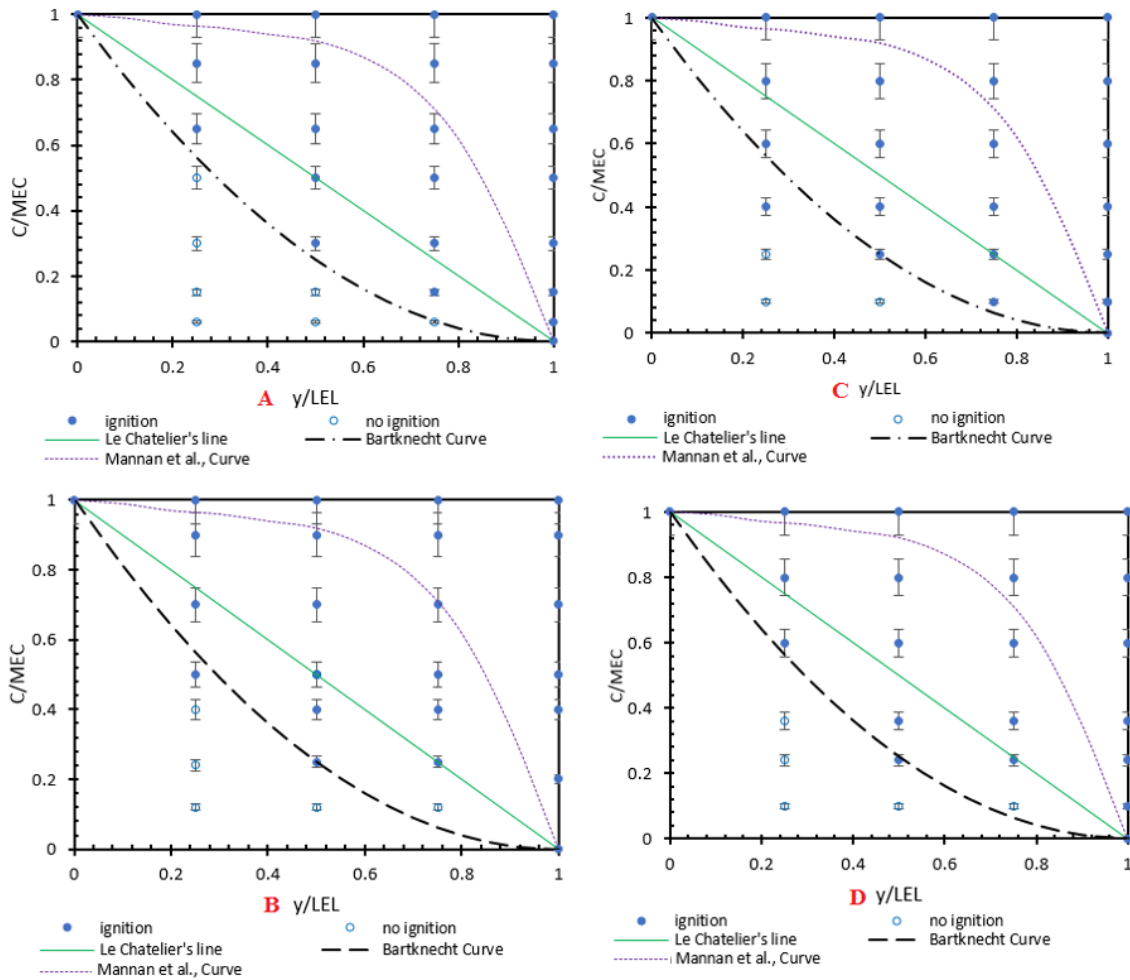


Figure B.36: Diagram showing a comparison between experimental results and three models: (A) brown coal-toluene, (B) lycopodium-toluene, (C) brown coal-acetone, (D) lycopodium-acetone

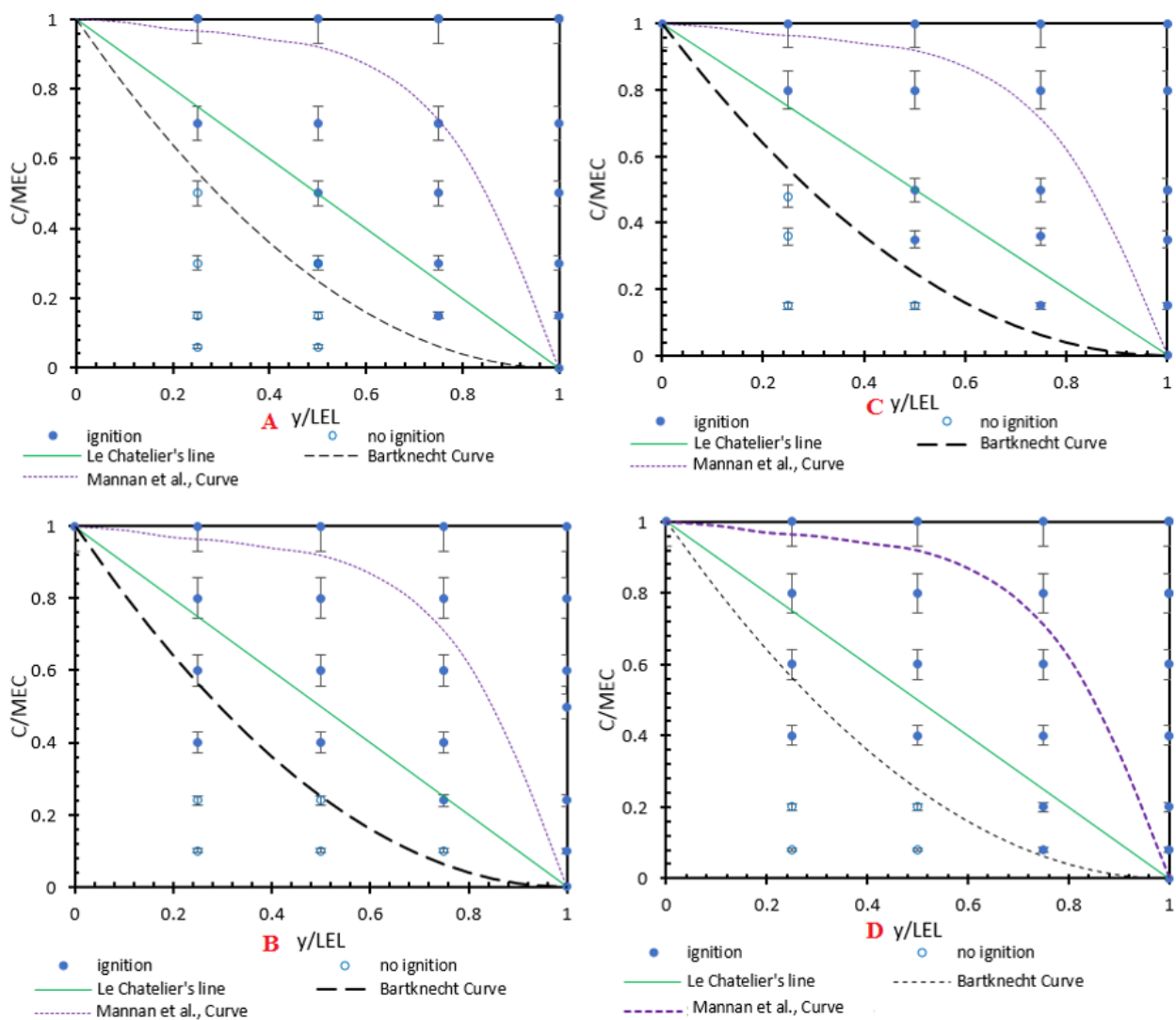


Figure B.37: Diagram showing a comparison between experimental results and three models: (A) brown coal-hexane, (B) lycopodium-hexane, (C) brown coal-heptane, (D) lycopodium-heptane

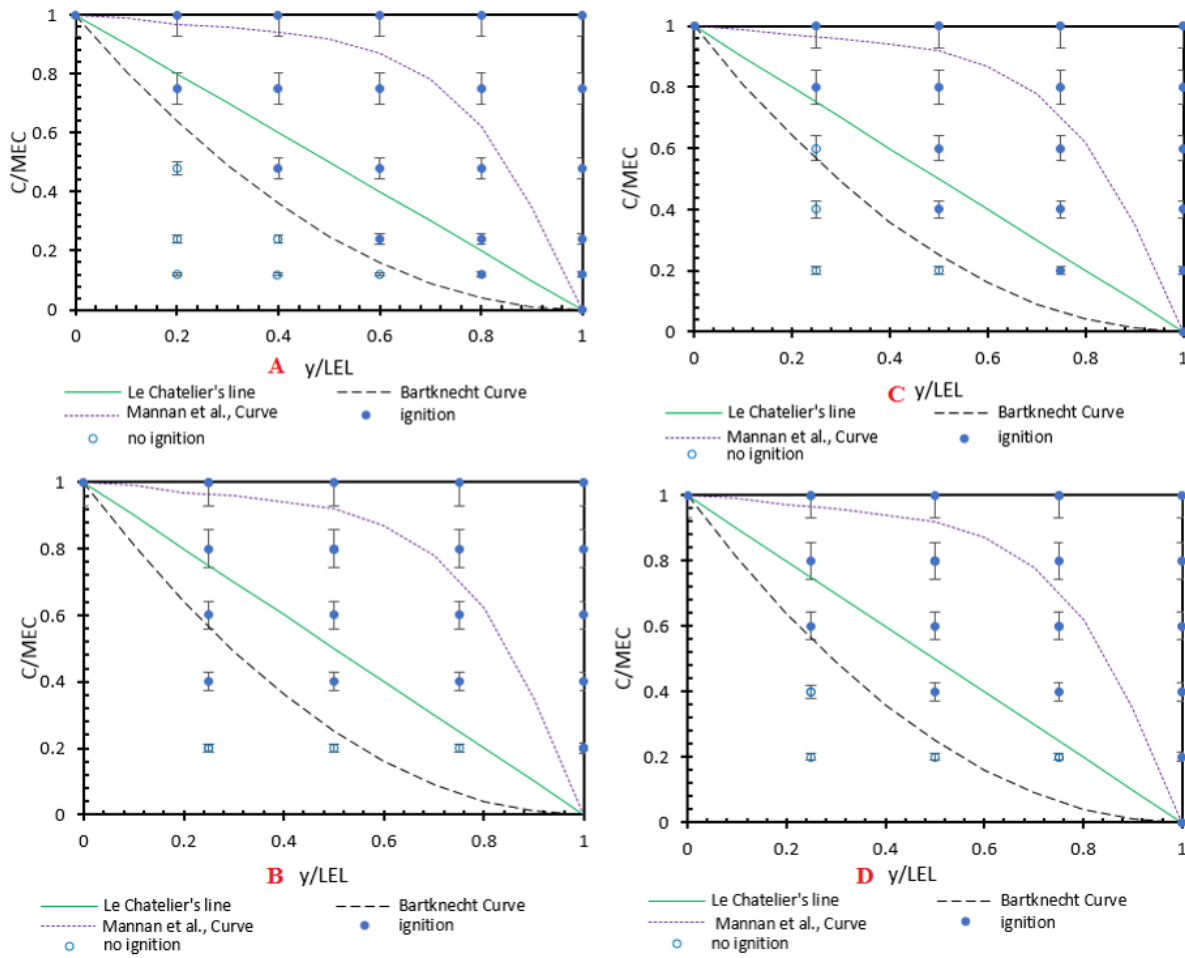


Figure B.38: Diagram showing a comparison between experimental results and three models: (A) methane-toluene, (B) hydrogen-toluene, (C) methane-acetone, (D) hydrogen-acetone.

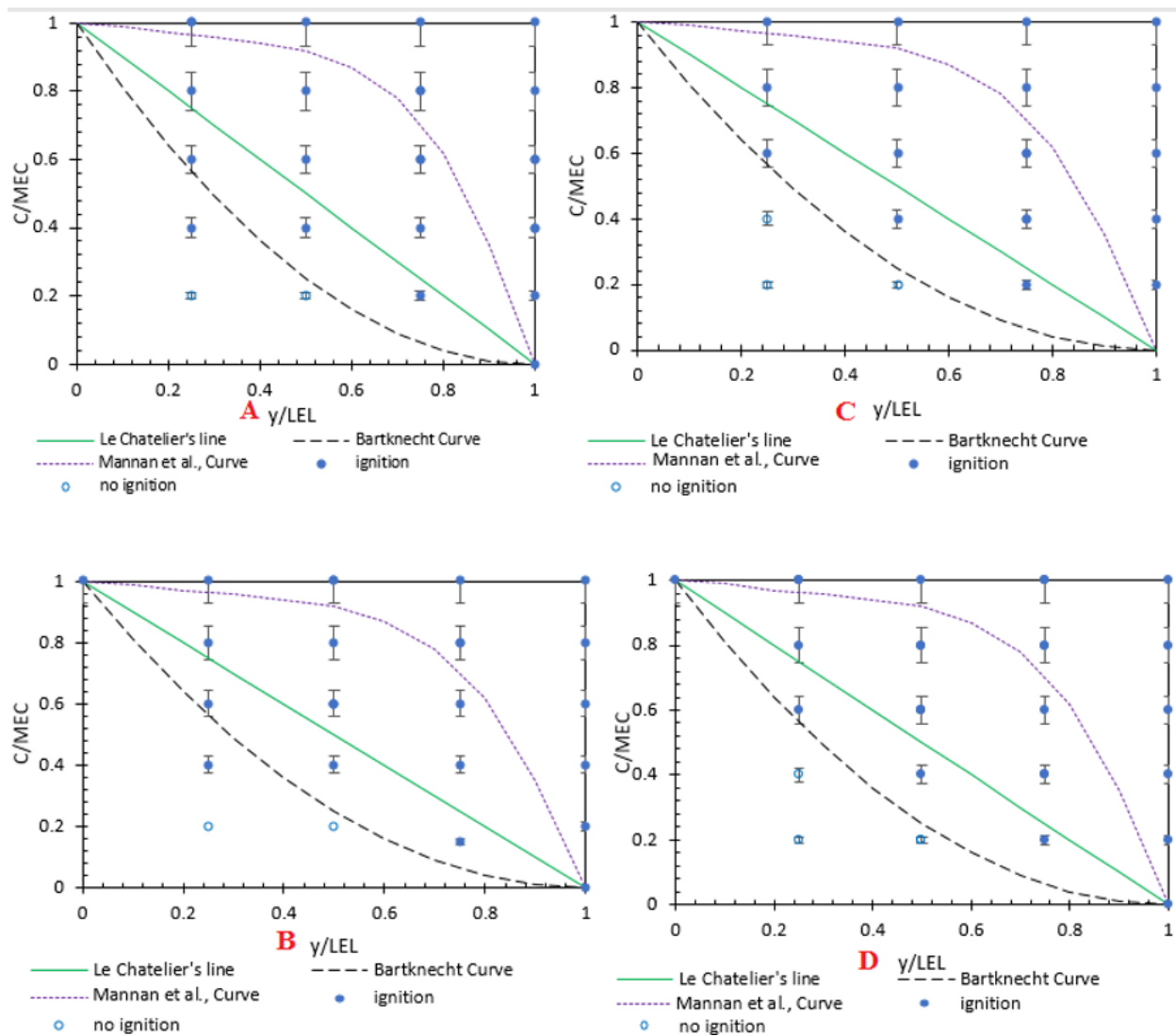


Figure B.39: Diagram showing a comparison between experimental results and three models: (A) methane-hexane, (B) hydrogen-hexane, (C) methane-heptane, (D) hydrogen-heptane

B.6 Diagrams to estimate Limiting oxygen concentration of dusts and hybrid mixtures

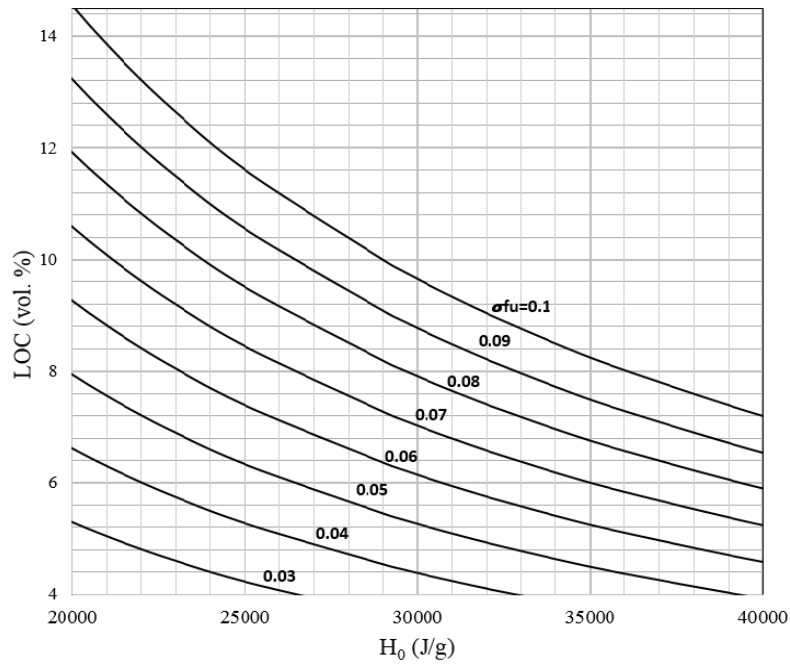


Figure B.40: A diagram to estimate the LOC of dust-air mixtures in dependence on heat of combustion and the fuel number

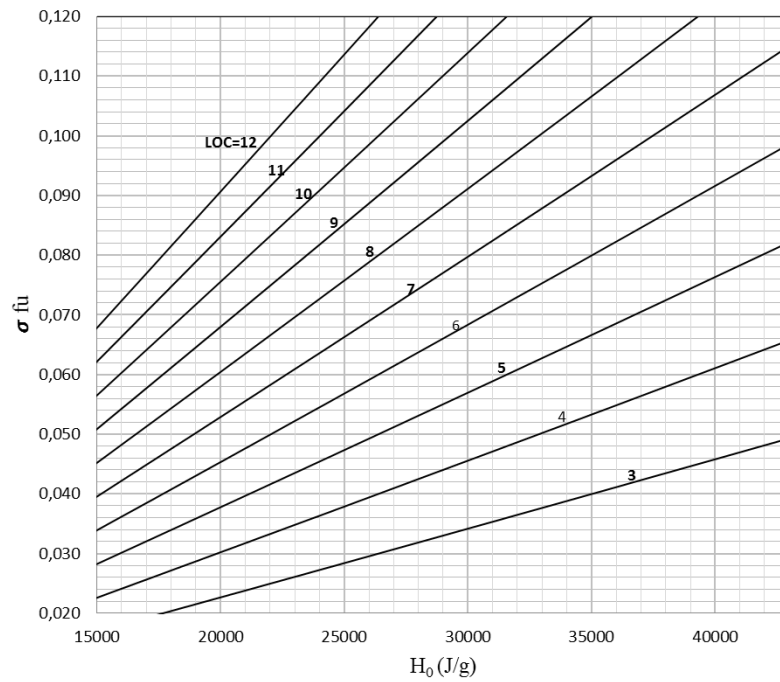


Figure B.34: A diagram to estimate the LOC of dust-air mixtures in dependence on heat of combustion and the fuel number

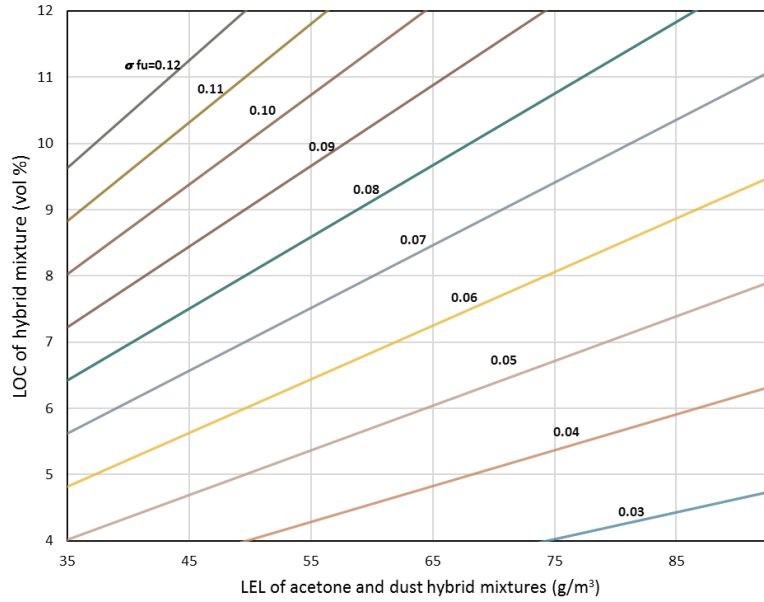


Figure B.42: A diagram to estimate the LOC of hybrid mixture of acetone and dusts in dependence on LEL-hybrid and the fuel number with 10 J electrical igniter

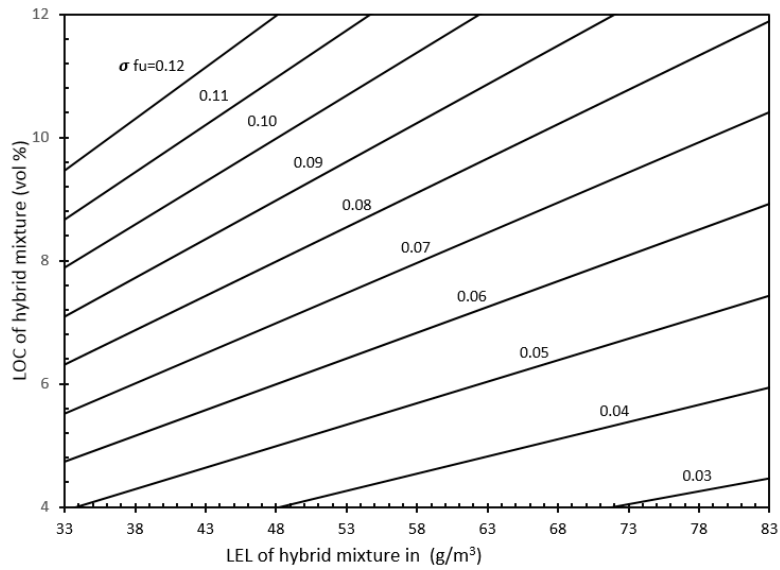


Figure B.43: A diagram to estimate the LOC of hybrid mixture of methane and dusts in dependence on LEL-hybrid and the fuel number with 10 J electrical igniter.

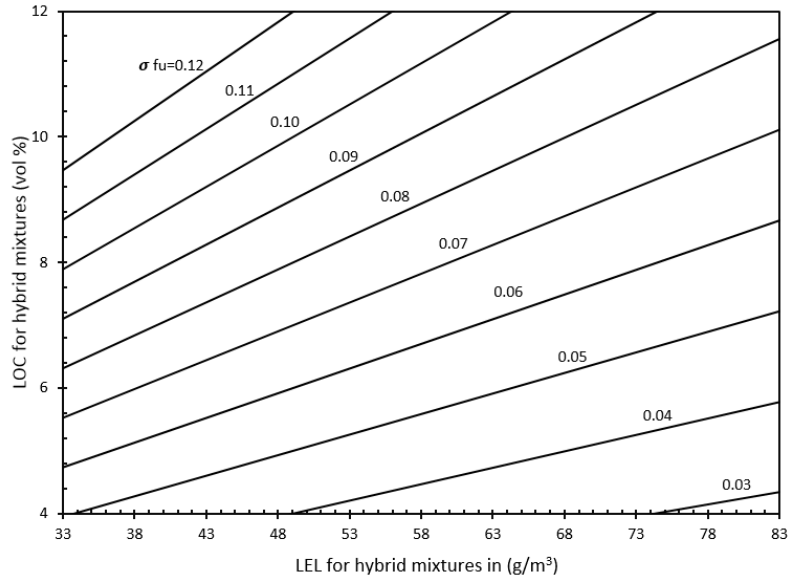


Figure B.44: A diagram to estimate the LOC of hybrid mixture of methane and dusts in dependence on LEL_{hybrid} and the fuel parameter fuel number with 10 kJ chemical igniter.

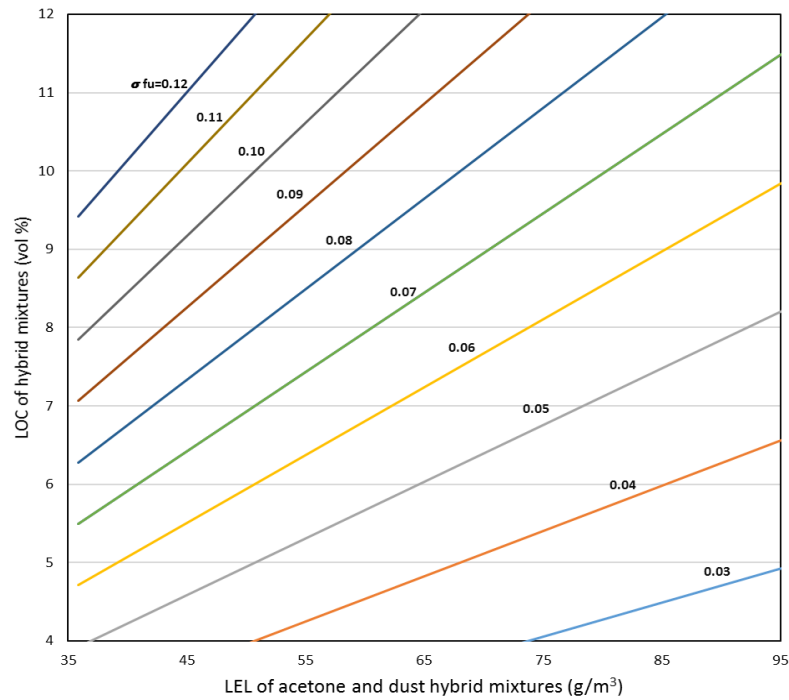


Figure B.45: A diagram to estimate the LOC of hybrid mixture of acetone and dusts in dependence on LEL_{hybrid} and the fuel number with 10 kJ chemical igniter

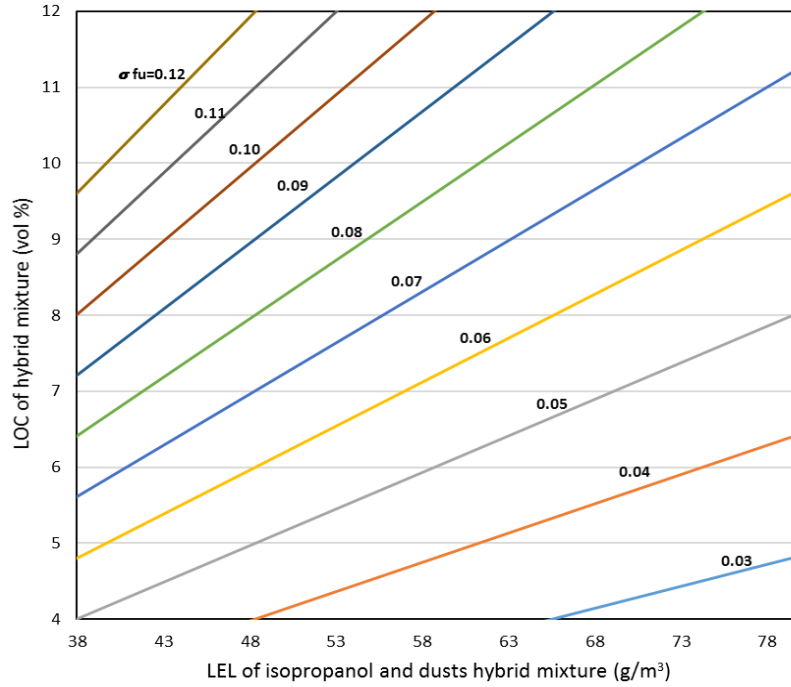


Figure B.46: A diagram to estimate the LOC of hybrid mixture of isopropanol and dusts in dependence on LEL-hybrid and the fuel number with 10 J electrical igniter.

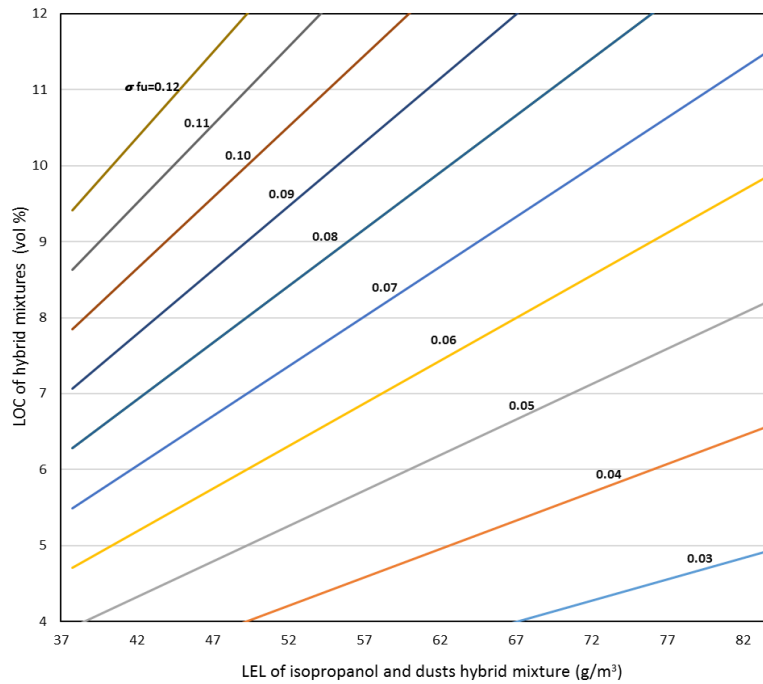


Figure B.47: A diagram to estimate the LOC of hybrid mixture of isopropanol and dusts in dependence on LEL-hybrid and the fuel number with 10 kJ chemical igniter.

8.3 Appendixes C Error and uncertainty analyses

C.1 Error and uncertainty analyses in the 20-liters sphere

The estimated uncertainties are based on all quantifiable errors, according to measured quantities and process control parameters. Table C.1 illustrates the error generation parameters, their uncertainties and measured values with regard to the determination of lower explosion limits, maximum explosion pressure, the rate of pressure rise and limiting oxygen concentration in the 20-liters sphere.

Table C.1: Parameters, their uncertainties and measurement ranges

Parameters	Uncertainties		Measured values	
	Symbol	Maximum error	Symbols	Value of measurement
Mass measurement	Δm	0.01 g	m	5 g
Gas concentration	ΔC_g	0.01 vol %	C_g	2.5 vol %
Spray concentration	ΔC_s	0.01 vol %	C_s	1 vol %
Dust dispersion pressure	ΔP_d	0.01 bar	P_d	20 bar
Spray dispersion pressure	ΔP_s	0.01 bar	P_s	10 bar
Pressure sensor reading	ΔP_r	0.01 bar	P_r	5 bar
Electrode gap	ΔL_e	0.1 mm	L_e	5 mm
Ignition source	ΔE_i	0.1 mm	E_i	10 J
Marginal error dust concentration	ΔV	5 g/m ³	V	250 g/m ³
Marginal error for oxygen concentration	ΔO_2	0.1 vol%	O_2	10 vol%

Knowing uncertainties of the individual source of error and the measured values, the relative error could be estimated. Table C.2 provides the calculated results for the individual relative errors.

$$\text{Individual relative error, (IRE)} = \frac{\text{Maximum error (uncertainties)}}{\text{measured value}}$$

Table C.2: Estimation of individual relative errors

Parameters	Symbol	Calculated value
Mass measurement	$\Delta m/m$	0.002
Gas concentration	$\Delta C_g/C_g$	0.004
Spray concentration	$\Delta C_s/C_s$	0.01
Dust dispersion pressure	$\Delta P_d/P_d$	0.0005
Spray dispersion pressure	$\Delta P_s/P_s$	0.001
Pressure sensor reading	$\Delta P_r/P_r$	0.002
Electrode gap	$\Delta L_e/Pr$	0.02
Ignition source	$\Delta E_i/E_i$	0.01
Marginal error	$\Delta V/V$	0.02

For the lower explosion limits of hybrid mixture, the total error could be obtained by combining the individual relative error as shown below;

$$\frac{\Delta C}{C} = \frac{\Delta m}{m} + \frac{\Delta C_g}{C_g} + \frac{\Delta C_s}{C_s} + \frac{\Delta P_d}{P_d} + \frac{\Delta P_s}{P_s} + \frac{\Delta P_r}{P_r} + \frac{\Delta L_e}{L_e} + \frac{\Delta E_i}{E_i} + \frac{\Delta V}{V}$$

$$\frac{\Delta C}{C} = 0.002 + 0.004 + 0.01 + 0.0005 + 0.001 + 0.002 + 0.02 + 0.01 + 0.02$$

$$\frac{\Delta C}{C} = 0.0695 = 6.95 \%$$

1.1.1. With respect to the limiting oxygen concentration, the total error could be obtained by combining the individual relative error as shown below;

$$\frac{\Delta C}{C} = \frac{\Delta m}{m} + \frac{\Delta C_g}{C_g} + \frac{\Delta C_s}{C_s} + \frac{\Delta P_d}{P_d} + \frac{\Delta P_s}{P_s} + \frac{\Delta P_r}{P_r} + \frac{\Delta L_e}{L_e} + \frac{\Delta E_i}{E_i} + \frac{\Delta V}{V} + \frac{\Delta O_2}{O_2}$$

$$\frac{\Delta C}{C} = 0.002 + 0.004 + 0.01 + 0.0005 + 0.001 + 0.002 + 0.02 + 0.01 + 0.02 + 0.01$$

$$\frac{\Delta C}{C} = 0.0695 = 7.95 \%$$

C.2 Uncertainty and error analysis for the minimum ignition energy test for hybrid mixtures in the Hartmann apparatus.

The estimated uncertainties are based on all quantifiable errors, according to measured quantities and process control parameters. Table C.3 illustrates the error generation parameters, their uncertainties and measured values with regard to the determination of the minimum ignition energy of hybrid mixtures using Hartmann apparatus.

Table C.3: Parameters, their uncertainties and measurement ranges

Parameters (error generation)	Symbol	Uncertainty	Symbols	Value of measurements
Mass measurement	Δm	0.01 g	m	1 g
Pressure measurement	ΔP	0.1 bar	p	7 bar
Input gas concentration	ΔC_g	0.01vol%	Cg	2 vol%
Voltage reading	ΔV_r	0.2 kV	Vr	8 kV
Electrode distance	ΔE_d	0.01 mm	Ed	5 mm
Marginally measured energy (hybrid mixtures)	ΔE_{Hm}	5 mJ	V_{Hm}	200 mJ

Knowing uncertainties of the individual source of error and the measured values, the relative error could be estimated. Table C.4 provides the calculated results for the individual relative errors.

$$\text{Individual relative error, (IRE)} = \frac{\text{Maximum error (uncertainties)}}{\text{measured value}}$$

Table C.4: Estimation of individual relative errors

Parameters (error generations)	Symbols	Calculated value
Mass measurement	$\Delta m / m$	0.01
Pressure measurement	$\Delta p / p$	0.014
Input gas concentration	$\Delta C_g / C_g$	0.005
Voltage reading	$\Delta V_r / V_r$	0.025
Electrode distance	$\Delta E_d / E_d$	0.002
Marginally measured energy (hybrid mixtures)	$\Delta E_{Hm} / E_{Hm}$	0.025

Hence, the total error could be obtained by combining the individual relative error.

Total Relative Error, $\frac{\Delta E}{E} = \sum (\text{IRE})$

$$\frac{\Delta E}{E} = \frac{\Delta m}{m} + \frac{\Delta p}{p} + \frac{\Delta C_g}{c_g} + \frac{\Delta V_r}{V_r} + \frac{\Delta E_d}{E_d} + \frac{\Delta E_{Hm}}{E_{Hm}}$$

Total Relative Error, $\frac{\Delta E}{E} = 0.01 + 0.014 + 0.005 + 0.025 + 0.002 + 0.025$

$$\frac{\Delta E}{E} = 0.081$$

Hence, % $\left(\frac{\Delta E}{E}, \text{ hybrid mixture}\right) = 8.1\%$

Table C. 5: Probability of ignition for propane gas and dusts based on the capacitor and ignition energy

Dust Sample	Propane gas concentration (vol%)	Capacitance (pF)	Ignition energy (mJ)	Total no. of ignition trials	Ignition event	Probability of ignition
Wheat flour	1.7	100	19.86	10	8	0.8
		50	12.74	10	6	0.6
		25	7.4	10	3	0.3
	1	200	28.01	10	7	0.7
		100	20.52	10	6	0.6
		75	15.85	10	4	0.4
	0.6	200	28.98	10	5	0.5
		100	21.94	10	3	0.3
		75	14.38	10	0	0
Protein	1.7	100	19.86	10	8	0.8
		50	13.73	10	5	0.5
		25	10.89	10	3	0.3
	1	300	36.65	10	9	0.9
		100	19.21	10	6	0.6
		75	14.75	10	4	0.4
	0.6	800	84.67	10	5	0.5
		600	63.6	10	3	0.3
		500	59.15	10	1	0.1
Polypropylene	1.7	100	16.04	10	6	0.6
		50	7.92	10	4	0.4
		25	5.64	10	1	0.1
	1.4	500	50.4	10	6	0.6
		200	22.71	10	4	0.4
		75	11.61	10	1	0.1
	0.6	800	58.82	10	4	0.4
		600	38.48	10	2	0.2
		400	29.85	10	1	0.1
Peat	1.7	100	18.55	10	9	0.9
		50	12.74	10	6	0.6
		25	8.46	10	3	0.3
	1.4	100	21.94	10	7	0.7
		50	12.74	10	3	0.3
		25	7.87	10	1	0.1
	0.6	500	50.4	10	5	0.5
		300	36.65	10	2	0.2
		100	21.47	10	0	0

C.3: Uncertainty and error analysis for both the minimum ignition temperature of hybrid mixture and single dust test

Based on the experimental work, detailed uncertainty and error analysis are discussed. The estimated uncertainties are based on all quantifiable errors, according to measured quantities and process control parameters. Table C.6 illustrates the error generation parameters, their uncertainties and measured values with regard to determination of the minimum ignition temperature of hybrid mixtures in the modified GG-furnace

Table C.6: Various parameter, their uncertainties and measured values

Parameters (error generation)	Uncertainties		Measured values	
	Symbol	Uncertainty	Symbols	Value of measurements
Mass measurement	Δm	0.001 g	m	0.3 g
Pressure measurement	ΔP	0.015 bar	p	0.7 bar
Input gas concentration/	ΔC_g	0.001 vol%	Cg	10 vol%
Input solvent concentration	ΔC_s	0.01 vol%	Cs	10 vol%
Furnace temperature	ΔT_F	20 K	T_F	700 K
Temperature interval	ΔT_{Hm}	5K	T_{Hm}	500K

Knowing uncertainties of the individual sources of error and the measured values, the relative error could be estimated. Table C.7 provides the calculated results for the individual relative errors.

$$\text{Individual relative error, (IRE)} = \frac{\text{Maximum error (uncertainties)}}{\text{measured value}} \quad (6.4.16)$$

Table C.7: Estimation of individual relative errors

Parameters (error generations)	Symbols	Calculated value
Mass measurement Error	$\Delta m / m$	0.003
Pressure measurement Error	$\Delta p / p$	0.024
Input gas concentration Error	$\Delta C_g / C_g$	0.0001
Input solvent concentration Error	$\Delta C_s / C_s$	0.0001
Furnace temperature Error	$\Delta T_F / T_F$	0.0285
Temperature interval	$\Delta T_{hm} / T_{hm}$	0.01

Hence the total relative error could be obtained by combining the individual relative errors.

Total Relative Error, $\frac{\Delta T}{T} = \sum (\text{IRE})$ eq. (5.4.17)

$$\frac{\Delta T}{T} (\text{hybrid mixture}) = \frac{\Delta m}{m} + \frac{\Delta p}{p} + \frac{\Delta C_g}{C_g} + \frac{\Delta C_s}{C_s} + \frac{\Delta T_F}{T_F} + \frac{\Delta T_{hm}}{T_{hm}} \quad (6.4.18)$$

$$\frac{\Delta T}{T} = 0.003 + 0.021 + 0.0001 + 0.0001 + 0.028 + 0.01$$

$$\frac{\Delta T}{T} = 0.063$$

$$\text{Hence, } \% \left(\frac{\Delta C}{C}, \text{ hybrid mixture test} \right) = 6.3\%$$

With respect to only dust test, eq. (6.4.18) could be modified by eliminating the errors resulting from input gas concentration or the input solvent concentration.

eq. (6.4.18) could be rewritten to eq. (6.4.19) below;

$$\frac{\Delta T}{T} (\text{only dust}) = \frac{\Delta m}{m} + \frac{\Delta p}{p} + \frac{RTF}{TF} + \frac{\Delta Thm}{Thm} \quad (6.4.19)$$

$$\frac{\Delta T}{T} (\text{only dust}) = 0.003 + 0.021 + 0.028 + 0.01$$

$$\frac{\Delta T}{T} (\text{only dust}) = 0.062$$

$$\text{Hence, } \% \left(\frac{\Delta T}{T} (\text{only dust}) \right) = 6.2\%$$

These estimated errors for only dust and hybrid mixture test will be considered in plotting error bars for various plots in the results and discussions.

Table C.8: Probability of ignition based on ignition temperature and different concentration of lycopodium

Probability of Ignition and No Ignition for Dust (Lycopodium) on different Temperatures and Concentrations									
Temperature (°C)	Concentration (g/m ³)								
	174			130			87		
	Explosion	No Explosion	Explosion Ratio	Explosion	No Explosion	Explosion Ratio	Explosion	No Explosion	Explosion Ratio
500	5	0	5:0	5	0	5:0	5	0	5:0
490	5	0	5:0	5	0	5:0	5	0	5:0
480	5	0	5:0	5	0	5:0	5	0	5:0
470	5	0	5:0	5	0	5:0	5	0	5:0
460	5	0	5:0	5	0	5:0	5	0	5:0
450	5	0	5:0	5	0	5:0	4	1	4:1
440	5	0	5:0	5	0	5:0	1	4	1:4
430	5	0	5:0	2	3	2:3	0	5	0:5
420	4	1	4:1	0	5	0:5	0	5	0:5
410	0	5	0:5	0	5	0:5	0	5	0:5

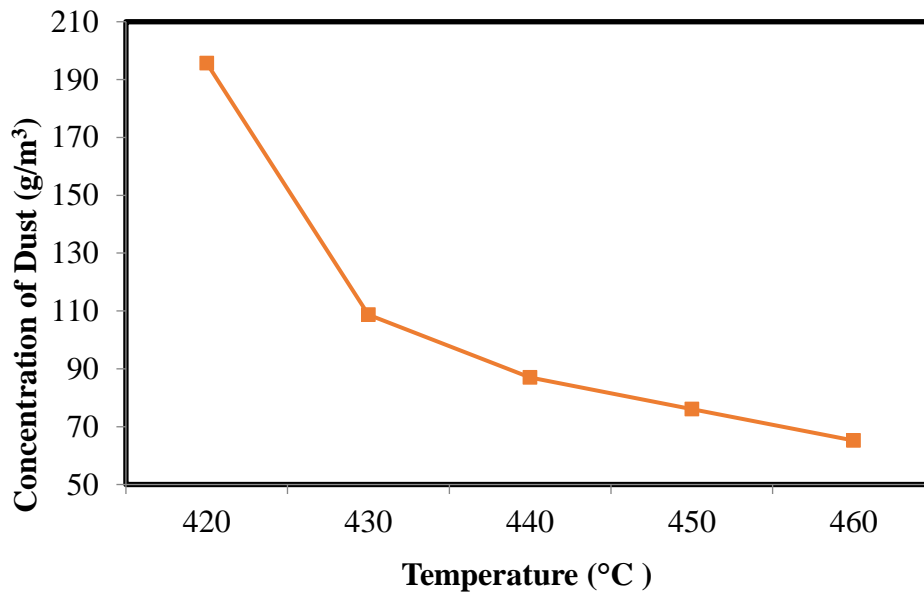


Figure C.1: Effect of concentration on the ignition temperature

8.4 Appendixes D: derivation of equations

D.1: Mathematical Model to estimate of the minimum ignition energy of hybrid mixture

The minimum ignition energy of decreases as the concentration of the added gas is increased. A general trend for this behavior is shown in Figure 68.4.D-1. The solid line indicates the results for the effect of adding a non-explosible gas (propane) concentration on the MIE of dust (polypropylene) while the dotted line represents a trend line with R^2 of 0.99.

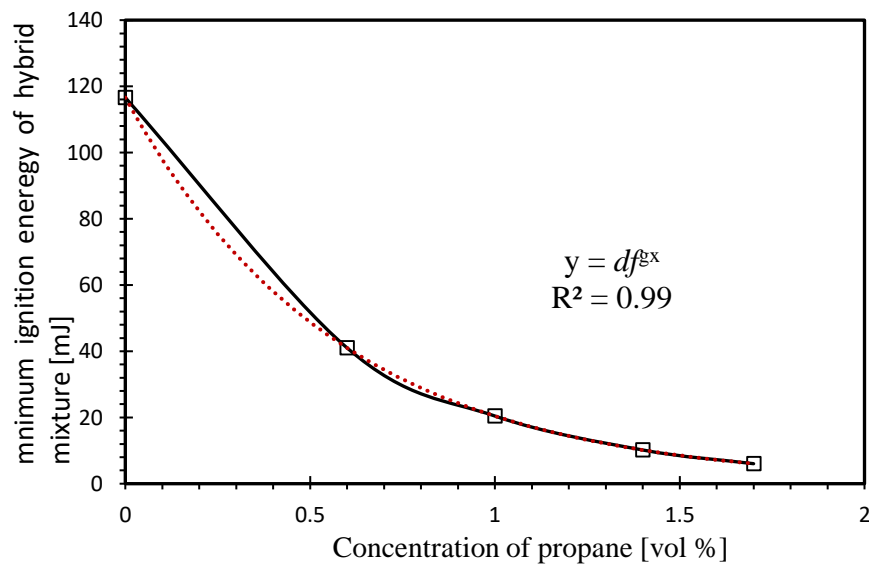


Figure 8.4.D-1: The trend of MIE of hybrid mixture of polypropylene and propane.

The general function gives a linear plot on the semi-logarithmic graph. This semi-logarithmic method to estimate the minimum ignition energy of hybrid mixtures was initially proposed by **Laurence Britton [185]**. A similar principle was adopted in this correlation.

$$y = df^{gx} \quad (8.4.1)$$

Here, d and f are positive constants and g is any constant.

eq. (8.4.1) can also be rewritten to produce eq. (8.4.2)

$$y = d(f^g)^x \quad (8.4.2)$$

Taking natural=log on both sides, eq. (8.4.3) could be obtained

$$\ln(y) = \ln(d) + (\ln f^g)^x \quad (8.4.3)$$

Suppose,

$$y_i = \ln(y), \quad a = \ln(d), \quad b = \ln(f^g)$$

And putting the value of y, a and b into eq. (5.3.3), eq. (5) could be obtained

$$y_i = a + bx \quad (8.4.4)$$

eq. (8.4.4) indicates a straight line with variables x and y_i with intercept a and slope b.

To solve eq. (8.4.4) for MIE of hybrid mixtures, two points on the Y-axis are needed, i.e. the MIE of the dust in air and the MIE of the gas in air. The first point on the X-axis corresponds to zero gas concentration, so x₁ = 0, and the second point x₂ to the optimum gas concentration. All the unknowns are experimental quantities.

From eq. (8.4.4), it was noticed that,

$$y_i = \ln y = a + bx \quad (8.4.5)$$

The values of a and b are unknown, and could be estimated according the following equation

For dust:

$$\ln(y_1) = a + bx_1$$

As for dust X₁=0, so

$$\ln(y_1) = a$$

For gas:

$$\ln(y_2) = a + bx_2$$

$$\ln(y_2) = \ln(y_1) + bx_2$$

$$\ln(y_2) - \ln(y_1) = bx_2$$

$$\frac{-\ln(y_1/y_2)}{x_2} = b$$

Putting the values of a and b into eq. (8.4.5), eq. (8.4.6) could be obtained

$$\ln y = \ln(y_1) - \frac{x}{x_2} \ln(y_1/y_2) \quad (8.4.6)$$

If y₁= MIE of dust, y₂ is the MIE at x=x₂=C₀ and x₂ = C₀, eq. (8.4.7) could be obtained

$$MIE_{hybrid} = \exp[\ln(MIE_{dust}) - (\frac{C}{C_0}) \cdot \ln(\frac{MIE_{dust}}{MIE_{gas}})] \quad (8.4.7)$$

eq. (8.4.7) could be rearranged and simplify to produce eq. (8.4.8)

$$MIE_{hybrid} = \exp\left[\ln(MIE_{dust}) - \ln\left(\frac{MIE_{dust}}{MIE_{gas}}\right)^{\frac{C}{C_0}}\right]$$

$$MIE_{hybrid} = \exp\left[\ln\left(\frac{MIE_{dust}}{(MIE_{dust}/MIE_{gas})^{\frac{C}{C_0}}}\right)\right]$$

$$MIE_{hybrid} = \frac{(MIE_{dust})}{(MIE_{dust}/MIE_{gas})^{\frac{C}{C_0}}} \quad (8.4.8)$$

Hence, the MIE of hybrid mixture MIE_{hybrid} could be estimated mathematically from eq. (8.4.8)

Where; C is the gas volume concentration (vol %), C_0 is the gas concentration (% vol) leading to the lowest MIE, MIE_{dust} and MIE_{gas} are minimum ignition energy of dust and gas respectively.

Note: this mathematical model is valid if, $C \leq C_0$.

D:2 Proposed model to estimate the minimum ignition temperature of hybrid mixtures

This model is based on the **Jaeckel model [191]** to predict the minimum and maximum explosible concentrations for dust clouds. A one-dimensional heat transfer from a plane flame front to the adjacent unburned layer of the dust cloud was assumed. According to Jaeckel, the minimum explosible concentration (MEC) is the minimum amount of dust per unit volume of the dust cloud, which by complete combustion liberates enough energy to heat the next unit volume of dust cloud to the ignition temperature. Jaeckel formulated the condition of self-sustained flame propagation through the dust cloud of concentration C_d , $mini < C_d, max$ at constant volume as:

$$Q_G = C_d H_d \quad (8.4.9)$$

$$Q_L = L + (T_{i,d} - T_0)(C_d c_d + \rho_{air} c_{air}) \quad (8.4.10)$$

According to the Jaeckel Model:

$$C_d H_d \geq L + (T_{i,d} - T_0)(C_d c_d + \rho_{air} c_{air}) \quad (8.4.11)$$

When $C_d = MEC$, by neglecting the heat loss by radiation and equating the two sides, after rearranging, the minimum ignition temperature can be derived:

$$\rho_d H_d \cdot MEC = (T_{i,d} - T_0)(\rho_d c_d \cdot MEC + \rho_{air} c_{air}) \quad (8.4.12)$$

Rearranging eq. (6.4.12) one obtains:

$$T_{i,d} = T_0 + \frac{MEC \cdot H_d}{MEC \cdot c_d + \rho_{air} c_{air}} \quad (8.4.13)$$

With respect to gases, eq. (6.4.12) could be rewritten to eq. (6.4.14), $C_g = LEL$

$$\rho_g H_g \cdot LEL = (T_{i,g} - T_0)(\rho_g c_g \cdot LEL + \rho_{air} c_{air}) \quad (8.4.14)$$

Rearranging eq. (6.4.14) one obtains:

$$T_{i,g} = T_0 + \frac{\rho_g H_g \cdot LEL}{\rho_g c_g \cdot LEL + \rho_{air} c_{air}} \quad (8.4.15)$$

In general, the MIT of hybrid mixtures decrease as the concentration of the fuel mixture increases [22]. A model to calculate the minimum ignition temperature of hybrid mixtures can be proposed based on an exponential relationship existing between the MIT of dust and gas as well as the concentrations of dust and gas of the mixture. The minimum ignition temperature of hybrid mixture decreases as the concentration of the added gas is increased. A general trend for this behavior is shown in Figure 8.4.D-2. The solid line indicates the results for the effect of adding a non-explosible methane concentration on the MIT of lycopodium dust while the dotted line represents a trend line with R^2 of 0.98.

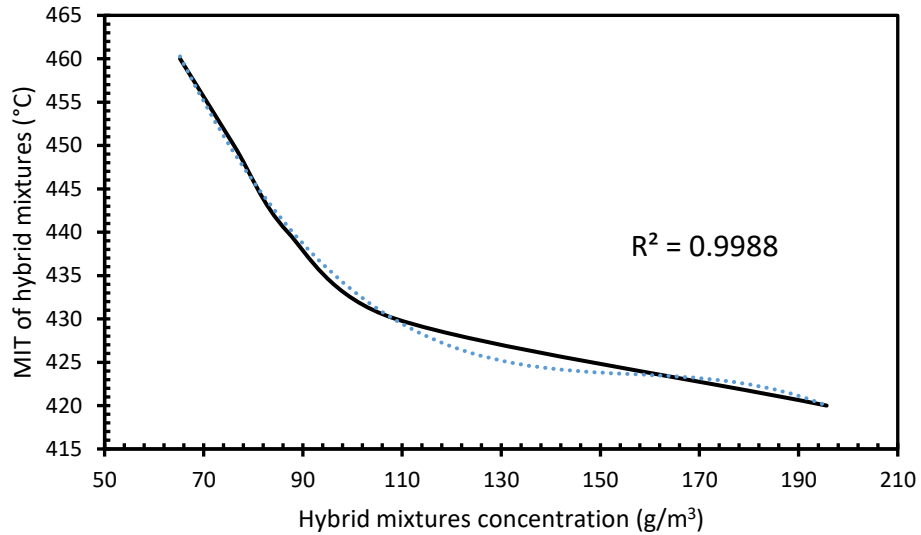


Figure 8.4.D-1: The trend of MIE of hybrid mixture of lycopodium dusts and methane gas

The general function gives a linear plot on the semi-logarithmic graph.

$$y = df^{gx} \quad (8.4.16)$$

Here, d and f are positive constants and g is any constant.

eq. (8.4.16) can also be rewritten to produce eq. (8.4.17)

$$y = d(f^g)^x \quad (8.4.17)$$

Taking natural=log on both sides, eq. (8.4.18) could be obtained

$$\ln(y) = \ln(d) + (\ln f^g)^x \quad (8.4.18)$$

Suppose,

$$yi = \ln(y), \quad a = \ln(d), \quad b = \ln(f^g)$$

And putting the value of y , a and b into eq. 8.4.18, eq. (8.4.19) could be obtained

$$yi = a + bx \quad (8.4.19)$$

eq. (8.4.19) indicates a straight line with variables x and yi with intercept a and slope b .

To solve eq. (8.4.19) for MIT of hybrid mixtures, two points on the Y-axis are needed, i.e. the MIT of the dust in air and the MIT of the gas in air. The first point on the X-axis corresponds to zero gas concentration,

so $x_1 = 0$, and the second point x_2 to the optimum gas concentration. All the unknowns are experimental quantities.

From eq. (8.4.19), it was noticed that,

$$y_i = \ln y = a + bx \quad (8.4.20)$$

The values of a and b are unknown, and could be estimated according the following equation
For dust:

$$\ln(y_1) = a + bx_1$$

As for dust $x_1=0$, so

$$\ln(y_1) = a$$

For gas:

$$\ln(y_2) = a + bx_2$$

$$\ln(y_2) = \ln(y_1) + bx_2$$

$$\ln(y_2) - \ln(y_1) = bx_2$$

$$\frac{-\ln(y_1/y_2)}{x_2} = b$$

Putting the values of a and b into eq. (8.4.20), eq. (8.4.21) could be obtained

$$\ln y = \ln(y_1) - \frac{x}{x_2} \ln(y_1/y_2) \quad (8.4.21)$$

If $y_1 = \text{MIT of dust } (T_{i,d})$, $y_2 = \text{MIT of gas } (T_{i,g})$ which at $x=x_2=C = C_g$ and $x_2 = C_g$ and inserting $T_{i,d}$ and $T_{i,g}$ from eq. (8.4.13) and eq. (8.4.15) respectively, into eq. (8.4.21), eq. (8.4.22) could be obtained

$$T_{i,\text{hybrid}} = \exp\left[\ln\left(T_0 + \frac{\text{MEC} \cdot H_d}{\text{MEC} \cdot c_d + \rho_{\text{air}} \cdot c_{\text{air}}}\right) - \left(\frac{C_g}{C_d}\right) \cdot \ln\left(\frac{T_0 + \frac{\text{MEC} \cdot H_d}{\text{MEC} \cdot c_d + \rho_{\text{air}} \cdot c_{\text{air}}}}{T_0 + \frac{\rho_g H_g \cdot \text{LEL}}{\rho_g C_g \cdot \text{LEL} + \rho_{\text{air}} \cdot c_{\text{air}}}}\right)\right] \quad (8.4.22)$$

eq. (8.4.22) could be rearranged and simplify to produce eq. (8.4.23)

$$T_{i,\text{hybrid}} = \exp\left[\ln\left(T_0 + \frac{\text{MEC} \cdot H_d}{\text{MEC} \cdot c_d + \rho_{\text{air}} \cdot c_{\text{air}}}\right) - \ln\left(\frac{T_0 + \frac{\text{MEC} \cdot H_d}{\text{MEC} \cdot c_d + \rho_{\text{air}} \cdot c_{\text{air}}}}{T_0 + \frac{\rho_g H_g \cdot \text{LEL}}{\rho_g C_g \cdot \text{LEL} + \rho_{\text{air}} \cdot c_{\text{air}}}}\right) \cdot \left(\frac{C_d}{C_g}\right)\right] \quad \text{eq. (8.4.23)}$$

Eq. (8.4.23) could then be simplified to (8.4.24) provided $T_{i,g}$ and $T_{i,d}$ are known

$$T_{i,\text{hybrid}} = T_{i,g} \cdot \exp\left[-\ln\left(\frac{T_{i,g}}{T_{i,d}}\right) \cdot \frac{C_g}{C_d}\right] \quad (8.4.24)$$

Mathematically, eq. (8.4.24) could further be re-formulated to:

$$T_{i,\text{hybrid}} = T_{i,g} \left(\frac{T_{i,d}}{T_{i,g}}\right)^{\frac{C_g}{C_d}} \quad (8.4.25)$$

The ignition temperature of a hybrid mixture can then be calculated from eq. (8.4.25):

Where $T_{i,g}$ is the MIT of gas [°C], $T_{i,d}$ is the MIT of dust [°C], C_g is the gas concentration in the mixture [g/m³], C_d is the dust concentration in the mixture [g/m³], ρ_g is the density of gas [g/m³], ρ_d is the density of dust [g/m³], c_g is the heat capacity of gas [kJ/kg.K], c_d is the heat capacity of dust [kJ/kg.K], c_{air} is the heat capacity of air [kJ/kg.K], L is the heat loss by radiation [KJ], H_g is the heat of combustion of dust [kJ/mol], H_d is the heat of combustion of dust [kJ/mol], LEL is the lower explosion limit of gas [vol%] and MEC is the minimum explosible concentration of dust [g/m³].

List of publications

Peer-review journal publications directly related to my Ph.D. thesis

- [1]. **Addai, E. K.**, Gabel, D., & Krause, U. (2016). Models to estimate the minimum ignition temperature of dusts and hybrid mixtures. *Journal of hazardous materials*, 304, 73-83.
- [2] **Addai, E. K.**, Gabel, D., & Krause, U. (2016). Experimental investigations of the minimum ignition energy and the minimum ignition temperature of inert and combustible dust cloud mixtures. *Journal of hazardous materials*, 307, 302-311.
- [3] **Addai, E. K.**, Gabel, D., & Krause, U. (2016). Lower explosion limit/minimum explosible concentration testing for hybrid mixtures in the Godbert-Greenwald furnace. *Process Safety Progress*. 35, 213-223
- [4] **Addai, E. K.**, Gabel, D., Kamal, M., & Krause, U. (2016). Minimum ignition energy of hybrid mixtures of combustible dusts and gases. *Process Safety and Environmental Protection*, 102, 503-512.
- [5] **Addai, E. K.**, Gabel, D., & Krause, U. (2016). Models to estimate the lower explosion limits of dusts, gases and hybrid mixtures. *Chemical engineering transactions*, 48, 313-318
- [6] Wang, C., Huang, F., **Addai, E. K.**, & Dong, X. (2016). Effect of concentration and obstacles on flame velocity and overpressure of methane-air mixture. *Journal of Loss Prevention in the Process Industries*, 43, 302-310.
- [7] **Addai, E. K.**, Gabel, D., & Krause, U. (2016). Experimental investigation on the minimum ignition temperature of hybrid mixtures of dusts and gases or solvents. *Journal of hazardous materials*, 301, 314-326.
- [8] **Addai, E. K.**, Gabel, D., Haider, A., & Krause, U. (2016). Minimum ignition temperature of dusts, gases and solvents hybrid mixtures. *Combustion Science and Technology*, 188, 1497-1504.

- [9] **Addai, E. K.**, Gabel, D., & Krause, U. (2016). Investigation of the minimum ignition temperature and lower explosion limit of multi-components hybrid mixtures. *Fire Technology Journal*, (**under review**).
- [10] **Addai, E. K.**, Gabel, D., & Krause, U. (2015). Explosion characteristics of three component hybrid mixtures. *Process Safety and Environmental Protection*, 98, 72-81.
- [11] **Addai, E. K.**, Gabel, D., & Krause, U. (2015). Lower explosion limit of hybrid mixtures of burnable gas and dust. *Journal of Loss Prevention in the Process Industries*, 36, 497-504.
- [12] **Addai, E. K.** (2015). Flame and explosion suppression using pyrobubbles. LAP LAMBERT Acad. Publ. (ed. 1) 68, ISBN 978-3-659-76630-5 (**book**).

Other peer-review journal publications within the time frame of my Ph.D. thesis

- [13] **Addai, E. K.**, Tulashie, S. K., Annan, J. S., & Yeboah, I. (2016). Trend of Fire Outbreaks in Ghana and Ways to Prevent These Incidents. *Safety and Health at Work*, 7, 1-9
- [14] **Addai, E. K.**, Acquah, F., Yeboah, I., & Addo, A. (2016). Reductive leaching of blended manganese carbonate and pyrolusite ores in sulphuric acid. *International Journal of Mining and Mineral Engineering*, 7(1), 18-36.
- [15] Tulashie, S. K., **Addai, E. K.**, & Annan, J. S. (2016). Exposure assessment, a preventive process in managing workplace safety and health, challenges in Ghana. *Safety Science*, 84, 210-215.
- [16] Annan, J. S., **Addai, E. K.**, & Tulashie, S. K. (2015). A call for action to improve occupational health and safety in Ghana and a critical look at the existing legal requirement and legislation. *Safety and health at work*, 6(2), 146-150.
- [17] Yeboah, I., **Addai, E.K.**, Acquah, F., Tulashie, S. K. (2014). A comparative study of the super cooling and carbonization processes of the gibbsitic Ghanaian Bauxite. *International journal of engineering, science and innovative technology*, 6, 76-85.

Conference publication with peer-reviews

- [18] **Addai, E. K.**, Gabel, D., & Krause, U. (2016). Investigation of the minimum ignition temperature and lower explosion limit of multi-components hybrid mixtures in the Godbert- Greenwald furnace. In Proceedings of the eleventh International Symposium of Hazards, Prevention, and Mitigation of Industrial Explosions (11th ISHPMIE), Dalian, China (24-29, 07-2016) paper # 128.
- [19] Krause, U., **Addai, E. K.**, & Gabel, D. (2016). Determination of the limiting oxygen concentration of dust/air and hybrid mixtures based on thermochemical properties. In Proceedings of the eleventh International Symposium of Hazards, Prevention, and Mitigation of Industrial Explosions (11th ISHPMIE), Dalian, China (24-29, 07-2016) paper # 167.
- [20] **Addai, E. K.**, & Krause, U. (2016). Experimental investigation and theoretical models to estimate the lower explosion limits of spray/dust and spray/gas hybrid mixtures. In 15th International Symposium on Loss Prevention and Safety Promotion in the Process Industries, 5-8th June, 2016, Freiburg-Germany.
- [21] Gabel, D., **Addai, E. K.**, & Krause, U. (2015). Explosionscharakteristiken von aerosolen hybriden Lösemittel/Staub-Gemischen. In Fachtagung Anlagen-, Arbeits- und Umweltsicherheit. Köthen, Germany, (5 -6, 11, 2015 ; Tagungsunterlagen. Hochschule Anhalt, insges. 2 S.
- [22] **Addai, E. K.**, Gabel, D., & Krause, U. (2015). Minimum Ignition Temperature of Hybrid Mixtures of dusts, solvents and gases. In Fachtagung Anlagen-, Arbeits- und Umweltsicherheit. Köthen, Germany, (5 -6, 11, 2015 ; Tagungsunterlagen. Hochschule Anhalt, insges. 2 S.
- [23] **Addai, E. K.**, Gabel, D., & Krause, U. (2015). Ignition and explosion behaviour of hybrid mixtures of two and three components. In 4th Magdeburger Brand- und Explosionsschutztag: am 26. und 27. März 2015. - Magdeburg, insges. 11 S. Kongress: Magdeburger Brand- und Explosionsschutztag; 4 (Magdeburg): 2015.03.26-27

- [24] **Addai, E. K.,** Gabel, D., & Krause, U. (2015). Minimum ignition temperature of hybrid mixtures of burnable dusts and gases. In: Proceedings of the 25th International Colloquium on the Dynamics of Explosions and Reactive Systems: 2-7 August 2015, Leeds, UK. – ICDERS.
- [25] **Addai, E. K.,** Gabel, D., & Krause, U. (2014). Lower explosion limit of hybrid mixtures in: Proceedings of the tenth International Symposium of Hazards, Prevention, and Mitigation of Industrial Explosions. - Bergen: GexCon AS; 2014, Paper 024, S. 995-1005; Congress: ISHPMIE; 10 (Bergen): 2014.06.10-14

Curriculum vitae

Emmanuel Kwasi Addai, Ph.D.

2234 west kemper Rd, Apt.1, 45240, Cincinnati, Ohio-USA. Mobile phone: Phone +15135576190

Email address: emmanueladdai41@yahoo.com, www.linkedin.com/in/emmanuel-kwasi-addai-73574156?trk

Professional summary: Process Safety and Environmental Engineering

Key Skills

- Experience in undertaking various explosibility testing, process hazard analysis and fire and explosion hazard identification, prevention and control
- Focused team leader, experience the field of fire and explosion safety professional, scheduling, budgets, estimates, progress reports, interpret plans and specifications.
- Skilled at designing and implementing safety programs, training personnel, accident investigation and Loss Control Programs.
- Ability to promote the professional development of Safety and Health within the work environment and exemplify a positive proactive attitude towards maintaining risk free working conditions.
- Very proficient in research and development in the field of fire and explosion prevention and protection. This reflects in more than twelve peer review publication in this field.

Professional Experience

10/2013 – 10/2016 Research Fellow in Process Safety Engineering at IAUT- Otto-von-Guericke-University •

- Undertake various explosibility testing such as minimum ignition temperature, minimum ignition energy, limiting oxygen concentration, lower explosion limits and explosion severity for dusts, gases, spray and hybrid mixtures.
- Supervise master thesis on fire and explosion prevention and protection
- Assist in teaching "plant design and process safety" course for masters' students.
- Undertake students' laboratory work
- Process hazard analysis and dust explosion hazard identification
- Design of preventive and mitigation safety measures for dust, gas and hybrid mixture explosion
- Hazardous area classification, ignition source identification
- Incident investigation and root cause analysis
- Quantitative and qualitative risk assessments in powder handling facilities
- Plan and execute experimental test programs
- Write technical reports, prepare and present technical results in international conference

- 02/2013-09/2013 Research Assistant in the fire and explosion laboratory at IAUT- Otto-von-Guericke-University**
- Undertake students' laboratory work
 - Undertake various explosibility testing such as minimum ignition temperature, minimum ignition energy, limiting oxygen concentration, lower explosion limits and explosion severity for dusts, gases, spray and hybrid mixtures.
- 06/2011- 9/2012 Safety and Environment Management at SGS Ghana**
- Health, Safety and Environmental Management consultant
 - Undertake the following activities: Environmental and social impact assessment, stack emission monitoring, ambient air monitoring, dust and noise monitoring, water quality analysis
 - Suggest proactive measurements that prevent incidents before they manifest as accidents
 - Coordinate environment health and safety aspects of project
 - Draft environment health and safety plans and verify any existing or proposed plans
 - Comply with all relevant HSE regulations and requirements
 - Ensure the health and safety of workers, decrease accident risks and improve onsite productivity
 - Give expert advice and recommendations for future safety maintenance and create a long-term safety culture
 - Consulted in different Africa countries such as: Mali, Cote d'Ivoire, Togo, Guinea
- 03/2010 - 08/2010 Process engineer (intern) at Newmont Ghana Gold Limited**
- Development and review Standard Operating Procedure (SOP)
 - Assist field operators, data analysis, safety presentations, monitor process flow.
- 01/2010 - 03/2010 Process chemist (intern) at SGS-Ghana- Ahafo Assay Laboratory**
- Undertook the following activities: Fire assaying, preparation of geological samples from the mines
 - Operations of spectrophotometry and atomic absorption spectroscopy for metals determination.
- 06/2009 - 08/2009 Process engineer and chemist at Tema, Lube Oil Company Limited**
- Undertook the following activities: Blending of lubricants, analyzing blended products (Lubricants) for its quality, determination of metals in the blended products,
 - Operations of spectrophotometer to determine metals in the blended products.
- 03/2009 - 05/2009 Research Assistance (intern) at Ghana Atomic Energy Commission**
- Operating Atomic Absorption Spectroscopy, Flame Photometer and Spectrophotometer,
 - Water Quality analysis and determination of Metals in soil.
- 06/2008 - 08/2008 Laboratory assistance- at Ghana Standard Board (3 months)**
- Operation of Atomic Absorption Spectrometer to determine metals in food substances,
 - Determination of: ash, moisture, alcohol, free fatty acids, protein, carbohydrate, and other laboratory analysis in food substance.
- 11/2005 - 06/2007 Junior high school teacher at Pentecost Preparatory School**
- Taught integrated science and mathematics in the junior high school

Education

- 10/2013 – Present** **Doctor of Philosophy in Process Safety Engineering at Otto-von-Guericke-University**
- Thesis topic: Experimental and theoretical investigation of explosion characteristics of multiphase mixtures
- 08/2012 - 09/2013** **Master of Science in Quality, Safety and Environmental Engineering at Otto-von-Guericke-University**
- Thesis topic: Flame and explosion suppression using pyrobubbles
- 08/2007 - 06/2011** **Bachelor of Science in Industrial Chemistry at University of Cape Coast**
- Bachelor thesis: Redox process technology of leaching of pyrolusite using low grade manganese carbonate ore in sulphuric acid

Professional Certificates

- 03/2016** **CPR, AED & First Aid Training at SaveALifeX**, (online learning initiative of SaveALifeX through edX)
- 01/2014 - 02-2014** **Certificate in project management at University of applied science Magdeburg**
- 10/2013 - 03/2014** **Certificate in health and society at Harvard University** (online course through edX)
- 09/2013 - 11/2013** **Certificate in Introduction to Water Treatment at Delft University of Technology**
(online course through edX)
- 05/2013 - 09/2013** **Certificate in Human Health and Global Environmental Change at Harvard University**
(online course through edX)
- 03/2013 - 05/2013** **Certificate in Occupational Safety and Health Management at OSHAcademy**
- 03/2011 - 05/2011** **Certificate in Oil and Gas processing at SIMA-University of Cape Coast**

Relevant Skills

- Strong communication skills with people both written and verbal
- Fantastic ability to learn new things quickly and adapt to changes in the environment
- uncommon ability to work independent and as part of team in solving complex quality, safety, environment and process engineering problems, ability to maintain a reliable and methodical approach to support and documentation

- Competence in computer: excel, word, power point, basic Mat-lab, origin-pro, python, Latex and basic C++ computational fluid dynamic (CFD)
 - A proven record of reliability, the ability to perform under time constraints, and good judgement under pressure
 - Ability to work under critical time deadlines and to re-evaluate priorities while exercising discretion, diplomacy, and good judgment
 - Ability to take ownership of projects and multi-task
 - Excellent interpersonal skills, including the ability to maintain effective working relationships
- Ability to interact with consultants and staff at all levels as well as with clients and business contacts

Professional Affiliations

- The International Association for Fire Safety Science (IAFSS)
 - German Association of Engineers (VDI)
 - German Association of safety Engineers (VDSI)
 - DECHEMA
 - Process-net (process safety)
 - Ghana Chemical society
-